The Causes and Implications of Microstructures in Glacial Sediments

Andrew John Evans
July 1998

Submitted in accordance with the requirements for the degree of
Doctor of Philosophy

The University of Leeds
School of Geography

The candidate confirms that the work submitted is his own and that appropriate credit has been given where reference has been made to the work of others.

Abstract

This thesis examines how microstructures in glaciogenic sediments reflect the processes forming them, and how these microstructures then affect the conditions around them, through a series of field studies, laboratory tests, models, and statistical analyses. Following literature reviews, a deformational chronology is developed for diamictons at Criccieth, North Wales, and their microstructures are used to indicate the stress, hydraulic, and environmental changes the materials have undergone. Microstructures of the lowest diamict indicate clast lodgement. The processes reflected in the microstructures of this lowest diamict are built into a quantitative model that estimates its residual strength (20 - 50 kPa) and the ice velocity during lodgement (20 - 50 m a^{-1}). The response of sediment to glacial stress is further examined by triaxial testing of diamict from Yorkshire, and the subsequent examination of its micromorphology. Shears in the material are disrupted by clasts, and this may be responsible for work hardening seen during the tests. Fabric compression, and the development of immobilised shears or hydraulic fractures buffer pore fluid pressure to ~470 kPa. The information from previous chapters is then used to analyse other material from the Yorkshire coast. This analysis confirms the presence in the area of meltout tills that have undergone low strain, as well as providing evidence for the decoupling of the ice and sediment in this region, and the nature of drainage systems within and above the diamicts during glaciation. Overall this thesis details the processes forming three 'classic' microstructures found in glacial sediments; omnisepic fabrics, lattisepic fabrics, and melanges, and provides evidence for the processes involved in forming diamict pebbles and skelsepic fabrics. In addition this thesis details how such structures reflect coupling and decoupling processes between glaciers and their beds, and examines the manner in which microstructures affect the response of a subglacial sediment body to stress and hydraulic conditions.

Acknowledgements

This thesis is completed with grateful thanks to the following people, who had a significant effect on its production.

Dr.Tavi Murray, who first suggested the modelling approach used in Chapter Five, and kept it from deviating into the impossible, as well as providing hours of fruitful discussion and continually indicating the difference between standard English and whatever it is I write.

Dr. Alex Maltman, who volunteered the use of the laboratories at Aberystwyth University, and organised the production of the thin sections used in this research. Thanks also go to Alex for his continually good humoured interest, and help with removing the linguistic tortuosity from this thesis.

Tommy Ridgeway, who produced all the thin sections used in this thesis and provided a considerable amount of aid in interpreting features caused during their preparation. Thanks are due in particular for the very high skill and 'above the call of duty' effort put into preparing thin sections from some extremely testing materials, and for his good humour in the face of my continual stream of sediments.

Al Bolton, Ben Clennell, and Malcom Peters, for their help in using the triaxial equipment and for freeing up the equipment for use in running the experiments. Thanks must go in particular to Ben for his continual interest in this project and for sharing his considerable knowledge of sedimentary rheology.

On a more personal note, thanks go to the following people.

My family, for their support and love.

Sarah P., for ordering the first vegetable tandoori pizza, and much, much, more besides.

Tavi for all the efforts she has made to keep me on the straight and narrow.

Gus, John, Matt, and Hester for their friendship and, sometimes literal, support.

Nicola, Andy, and Kathy, for humouring me, and for warding off the demons.

Sarah C., for providing me with an interesting, if !Hagasfell! summer of ‘97 and for preventing me from reverting to a feral state.

Stuart M^{c}C., for helping me to reach a feral state the first time round.

Kurt G. and Alfred J.A., for their help with my maths.

Brian, for reminding me of my idea of fun.

Mike and Anne, for their love, and bearing with me.

Logic, Jeremy and William B., for providing all the conversations that have changed my life.

Debbie H., for more than I can ever hope to repay.

and Phil, with love.

Tommy Ridgeway, without whom...

John Davies, who suggested to an impressionable 15 year old he do research, and taught me much in addition to introducing me to glaciology. Keep fighting the good fight...

The 100 cattle who died so that this thesis could live.

This thesis is dedicated to

Contents

1. Introduction

For almost two hundred and seventy five years it has been suggested that some lowland sediments may reflect processes occurring within glaciers (Scheuchzer, 1723, quoted in translation by North, 1943). Large scale features, such as diamict beds, uniform clast orientations, folds, and shears have been explained as the result of either glacial deposition and deformation, and have given us much information on the processes obscured under ice masses. The research in this thesis aims to refine the interpretation of glaciogenic structures, but at a much smaller scale.

The study of small scale (µm to cm size) structures in glacial sediments began in the 1950s. This followed the development of resin-impregnation techniques to produce soil thin sections. Plastic resin is drawn into the sediments by a vacuum, and allowed to harden. The material is then sawn up, set on glass slides, polished, and examined under an optical or electron microscope. As with soil science and hard rock geology, it was discovered that glacial sediments that appear homogeneous on a larger scale display complex depositional and deformational structures under a microscope. It was quickly realised that such structures reflect the mode of the sediments formation. However, it was only after advances in other soft sediment fields that it was recently realised the structures will also have affected the materials bulk properties. These property changes may have affected the glacial dynamics. It is hoped that the results of this Ph.D. research add to the understanding of how specific microstructures both reflect and affect the conditions in which they are produced.

The principle aim of this Ph.D. research is to examine the place of microscopic structures in the response of glaciogenic sediments to the ice and surrounding conditions. However, it is also hoped that this research indicates a number of new ways of using micromorphological data, as well as utilising recently developed techniques, such as dynamic permeability testing in triaxial rigs. Larger scale information is only rarely brought into this discussion, principally to explain the background to each region studied, and also, occasionally, to enlarge upon, or back up, interpretations derived from the micromorphology.

The structure of this thesis.

Chapter Two introduces previous studies of microscopic structures from glacial sediments and reviews their conclusions. These conclusions largely centre upon how the microstructures may have been produced, and how this production reflects the environments they formed in.

Chapter Three introduces work from other studies of sediment microstructures, continuing the theme of the origin of the structures, but also examining work that looks at how microstructures may have gone on to affect the response of the sediment to stress and fluid throughflow after their formation. This information will be used throughout this thesis, and also reveals a number of conclusions pertinent to other glacial studies.

Chapter Four examines a deposit in North Wales, using the information reviewed in the previous chapters to analyse the simplest case of glaciogenic sediment development; the passive response of sediments to changing conditions. The development of the sediment's micromorphology is used to form a chronology of events which the material has experienced, and to indicate how conditions changed during these events in a qualitative manner. The changes in the material are not thought to have fed back to change the local glacial dynamics.

Chapter Five determines new information on the development of a suite of micromorphological structures which reflect a situation where the ice and subglacial bed are actively affecting one another; the ploughing and lodgement of a clast. Here the micromorphology is still largely a passive reflection of conditions, however, a more complex analysis is undertaken which allows us to quantify the rheology of the sediment using the micromorphology.

Chapter Six examines the active response of till to glacial stress and hydraulic conditions using laboratory tests. The problems with moving from laboratory tests to a generalised till rheology are discussed, and a model of till rheology for specific areas of deforming sediments is developed. The areas of this model which are uncertain are outlined in preparation for their examination in Chapter Seven.

Chapter Seven looks at the micromorphology of the test samples, and indicates how the development of micromorphological features in the till contributes to the bulk responses seen in the laboratory tests. The micromorphology of the test samples also shows how a number of the 'classic' glaciogenic microstructures develop.

Chapter Eight examines the active and passive response of glacial sediments from a number of field sites using information from the previous chapters. The information from these sediments is used to build up a picture of the basal conditions of the Late Devensian glacier responsible for their development.

Chapter Nine draws together the most important results of the previous chapters and outlines the directions future work will follow.

Thus, it is hoped that this thesis provides information on the active and passive interaction between the microstructure of sediments and their surrounding conditions, and indicates the wealth of information locked in the small scale structure of glaciogenic materials.

2. Previous studies of microscopic glacial sediment structures

2.1 The problems involved in interpreting glacial sediments

The particles in granular materials can align during their deposition or deformation to form structures. Such structures reflect the processes forming them and, inevitably, effect the bulk properties of the materials. Considerable progress has been achieved in understanding in an holistic manner the way in which structures are caused and go on to affect the physical properties of soils, soft sediments and 'hard' rocks. It is only recently, however, that this holistic approach has been applied to glacial geology (Murray, 1990; Murray and Dowdeswell, 1992; and to a smaller extent Menzies, 1986; Talbot and von Brunn, 1987; Hooke and Iverson, 1995).

Much of glacial geology is occupied with the interpretation of the origins of sediments that may be glacial, and this is particularly true of glacial geology conducted at the visual, as opposed to regional or microscopic scales. Such studies have aimed to define sediment types on the basis of their origins, and to place sediments within this taxonomy. The taxonomy determined by the International Union for Quaternary Research (INQUA) Commission on Genesis and Lithology of Glacial Deposits is that of Dreimanis (1988) (See *Table 2.1* for the most common till types).

Till type	Short definition
Lodgement till	Deposited by plastering of glacial debris from the sliding base of a moving glacier by pressure melting and/or other mechanical processes.
Meltout till	Deposited by a slow release of glacial debris from ice that is not sliding or deforming internally.
Flow till	Derived from any glacial debris...in direct association with ice [redeposited by] gravitational slope processes, mainly by gravity flow, or by squeeze flow, [taking] place ice marginally, supraglacially, or subglacially, and subaerially or subaquatically.

Table 2.1 INQUA till definitions of common till types from Dreimanis (1988).

However, the failure of this scheme to separately define both deformation tills and glacitectonites lead to its partial abandonment in the late 1980's, when the importance of these till types became realised. In the absence of a reasonable standard taxonomy, this thesis follows a broadly processed based definition scheme. Lodgement is defined following

Dreimanis (1988), as is flow till, though the *subglacial* flows of Dreimanis are not included. In agreement with common practice these subglacially reworked materials are divided into glacitectonites, using the definition of Benn and Evans (1998) as being 'rock or sediment that has been deformed by subglacial shearing but retains some of the structural characteristics of the parent material', and deformation tills, which are the same, except that they have lost their primary structure. Meltout till, is here defined on purely processed based terms as a till derived from the meltout of debris from ice. This definition has in common with all others the fact that meltout till overlaps a number of other categories. The largest difference when compared with other definitions is that the meltout need not be from a stagnant glacier. This is to accommodate materials that are shown in Chapters Five and Eight of this thesis to have been deposited by meltout from *moving* ice, but have not been changed by the movement of ice over them. Such sediments do not fit comfortably in other taxonomies. Where reference is made to the interpretations of other authors it may be assumed that stagnant ice is responsible.

Tills interpreted on the visual scale are generally placed in the defined classes by a combination of their structure, fabric orientation, sediment type, and associations with other sediments, both in terms of their stratigraphy and associations into landforms (Benn and Evans, 1998). Much of the problems of the field relate to the ambiguous nature of this evidence. For example, shears may form both subglacially and in glaciomarine sediment flows. The evidence used in glacial micromorphology is largely identical to that used at the larger scale, and micromorphological evidence is chiefly used as a supplement to regional and visual scale studies. However, in other subject areas micromorphology is more process-orientated; each feature is taken in a much more explicit fashion to represent the mechanics of the material, and an environment is then derived from those that could account for the mechanics. Micromorphology is notably useful because it gives insights into the processes that are acting outside the assumptions of continuum mechanics. There is a vast body of work in material science and geology that can be exploited by glacial micromorphology to deal with the ambiguity of glacial sediments on a larger scale (see Chapter Three). For example, shear micromorphology gives a semi-quantitative estimate of the pressure on the material as it deformed, and such evidence is usually present even when the material appears to have deformed in a ductile 'continuum' manner on a larger scale.

The study of microscopic glaciogenic structures is still in its infancy, so it is perhaps unsurprising to find that most of the work dealing exclusively with micromorphology has so far been descriptive and taxonomic. The majority of studies that use micromorphology in conjunction with outcrop scale features do so to describe localised deposits; often to delineate sediment units (for example, Gravenor and Meneley, 1958; Madgett and Catt, 1978; van der Meer, 1987a), though sometimes with a view to describing the origin of the sediments as well (for example, Kluiving *et al*., 1991; Evans *et al*., 1995).

The aim of many studies has been the assignment of features to families that characterise different environments, and processes, of deposition and alteration (for example, van der Meer, 1993, subglacial deformation; Harrison, 1957, meltout from stagnant ice; Owen and Derbyshire, 1988, deposition from proglacial mudflows) using two methods. One method takes larger scale features for which we know the formational *processes*, and uses them as metaphors for similar small-scale features (see, van der Meer *et al*., 1985; van der Meer, 1987b; Talbot and von Brunn, 1987). For example, grain-size gradients suggest sediments settled through standing water (van der Meer, 1987b). Of course, there is the danger that the same processes are not acting in both cases; there may be small-scale subglacial processes we have never seen. In the case of graded material, strain gradients or illuviation may have sorted the grains (Lowe, 1975; Cowan, 1982; Menzies, 1986). A tectonic mechanism is also given in Chapter Five. Studies verifying the origin of features by creating them in the lab are rare (though see Menzies and Maltman 1992, and the related studies quoted therein; Murray, 1990; Murray and Dowdeswell, 1992). Even these studies can only suggest *one* process for the formation of each feature.

In the second method, deposits of a known formational *environment* are sampled (for example, van der Meer, 1993; Owen and Derbyshire, 1988). While generally more reliable, this assumes that the microstructures have formed in their present environment or the environment indicated by their macroscale form. More importantly, materials forming today are hard to sample without deforming them. There is always doubt over the environment in which stiffer palaeodeposits formed. Even with this method the *causes* of individual features are still only estimated by the first technique; although the processes that could have acted are restricted by the environmental conditions.

2.2 The results of previous studies: an introduction to the structures

The following review will first introduce the microscopic scale fabrics found by glacial geologists. Some of these fabrics are shown in Figure 2.1. The orientation of particles, their spatial distribution, grain size and chemical alteration have suggested processes acting to form some features, and these are therefore also reviewed. Following this the attribution of these structures to facies characterising different depositional environments is outlined.

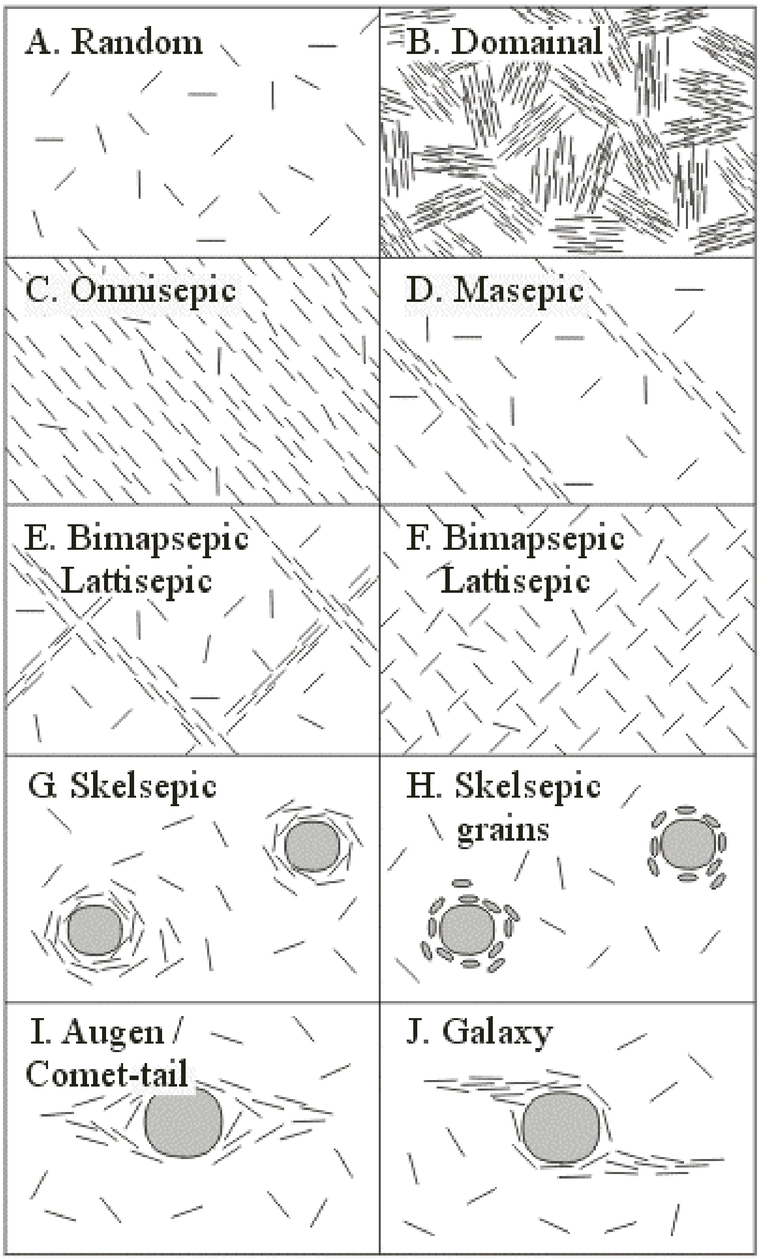

Figure 2.1 Common types of grain fabrics seen in microscope investigations of glaciogenic sediments. Such fabrics are also seen at scales up to the point at which the 'grains' are tens of centimetres long.

2.2.1 Grain size and shape

Grains' sizes may reflect the processes involved in forming them. Comminution has been suggested as a proxy for transport distance, though this approximation is limited by the production processes and grain mineralogy (Clark, 1987). Recent work on the fractal nature of fault gouges (Sammis *et al*., 1987) and tills (Hooke and Iverson, 1995) has suggested that the that size distribution in tills is due to grain-grain chipping. The scratching of grains is characteristic of glacial sediments (Whalley, 1996). The chemical environments the grains have passed through can also be estimated, for example by surface solution hollows (May, 1980).

2.2.2 Horizontal unidirectional, random and domainal fabrics

Just as the clast content of glaciogenic deposits may be strongly orientated on a metre scale, so may the sediment grains on a millimetre scale. Grain orientation occurs in silt and sand-sized material, however, the platy nature of clays means that orientation is particularly well seen in microscope studies of argillaceous material.

The grains of undeformed sediments are usually found with either a random (*Figure 2.1a*) or single direction orientation (*Figure 2.1c*). Random fabrics are rarely attributed a cause. In glaciology a single orientation has been termed 'omnisepic' by van der Meer (1987b; 1993) following Brewer (1976; similarly for all '-sepic' nomenclature following). When fabrics are horizontal they are often attributed to consolidation by a force perpendicular to the alignment, or settling through fluids. Van der Meer *et al*. (1985) note fluvial fabrics are weak compared with glacial processes (below) and the same has been found in other fields in the case of consolidation (Chapter Three).

Because clays are electrostaticly charged they can form patches with an internal alignment while settling and under consolidation. These 'domains' may be randomly aligned with respect to each other (*Figure 2.1b*), or lie all in one direction (See Rieke and Chilingarian, 1974, and Chapter Three for discussions on domains in undeformed sediments). In glacial sediments, however, these domains are rare. They are most likely in material deposited in saline situations, but are strongly dependent on the clay type involved. Their absence in glacial sediments suggests that if they ever exist in the glacial environment then they are easily removed. Menzies and Maltman (1992) have described a fabric consisting of isolated patches of orientated material in a generally random matrix. This is too discontinuous, however, to be defined as domainal. They associated the fabric with differential pore water movement and, as such, indicative of a meltout till.

2.2.3 Non-horizontal unidirectional fabrics

Commonly the orientation of omnisepic fabrics is not horizontal (*Figure 2.1c*). Gravenor and Meneley (1958) found grains with dips of up to 30°, which were taken as a proxy for larger clast orientation. Given our present ignorance of subglacial deformation this correlation appears optimistic. However, the correlation is backed up by Harrison (1957), Ostry and Deane (1963), Korina and Faustova (1964) and Evenson (1971), all of who found a good match between grain and clast orientation in till deposits. Various explanations have been put forward for these findings. Harrison suggested direct deposition by meltout was responsible for both grain and clast orientation, with alignment being developed in up-glacier dipping shears and between ice crystals. Evenson (1971) and Sitler and Chapman (1955) suggested reorientation in shears as well, but during sediment deformation under the ice. Seifert, in 1954 (translated in part in Harrison, 1957), found that microfabric orientations varied from ice flow transverse to ice flow parallel near outcrop scale "shear layers". Pervasive subglacial deformation may also occur as the diminishing velocity of the sediment with depth (Boulton and Hindmarsh, 1987) revolves particles into new orientations (van der Meer, 1993).

On the basis of outcrop scale structures and the similarity to folding, Kluiving *et al*. (1991) have attributed crenulated fabric in a till to regional compression of the sediment. This would appear a reasonable interpretation, however, investigation is needed into the spread of kinking fabrics (localised crenulation) associated with shear (Chapter Three) so it seems wise to use large scale indicators to confirm compression where crenulation is seen.

2.2.4 Lattisepic, bimasepic and masepic fabrics

Diamicts sampled by Korina and Faustova (1964) showed a complex clay fabric, in which the clay minerals were arranged in a 'lattisepic' fabric (*Figure 2.1e*). This consists of two sets of thin, linear areas, each with a single, length-parallel, internal orientation, arranged at around 90° to each other, though the term is also used to describe a more pervasive mix of grains in two directions (*Figure 2.1f*). The lattisepic fabric is a particular case of the more general 'bimasepic' fabric in which the angle varies between the two sets of bands (or more, tri-, quad- etc.) (for example, Sitler and Chapman, 1955; van der Meer, 1987b).

Korina and Faustova suggested that lattisepic orientation is due to the meltout of clays that were aligned between ice crystals in debris-rich ice. It seems unlikely that the ice between aligned bands would have been replaced by more sediment without disrupting the bands. Paul and Eyles (1990) have shown that the fabric of sediments in ice can only survive meltout in very limited circumstances. An alternative is that lattisepic fabrics form after the sediments are deposited. Shrink-and-swell clays can produce lattisepic orientations, however, these will be weak (van der Meer, 1987b; 1993). The subglacial rotation of sediment blocks under shear has been suggested as one cause of the fabric (van der Meer, 1987b; 1993). Girdle fabrics, where particles are orientated in planes, are the three dimensional equivalent of lattisepic fabrics. Lafeber (1964) has implicitly suggested that girdle fabrics form between two close, rotating, clasts. An alternative explanation; that the fabric develops through the constraint of shears, is examined in Chapter Three, Seven and Eight.

In a 'masepic' sample there is only *one* set of bands, all pointing in the same direction, and each with a single, length-parallel, internal fabric (*Figure 2.1d*). Various mechanisms have been suggested to account for masepic fabrics (Korina and Faustova, 1964; Sitler and Chapman, 1955). It is now accepted that most of these structures are caused by syn- or post-depositional shearing (Menzies and Maltman, 1992; van der Meer 1993). As grain reorientation strengthens the material, masepic areas *may* appear as fractures or erosion resistant bands in the field, especially in palaeodeposits (but see cautionary notes in Chapter Eight). It has been suggested that masepic areas develop into wholesale omnisepic fabrics with greater shear (van der Meer, 1993). While shear zones often develop in several directions in one shear event, and bimasepic fabrics can often be seen to be shear zones, the conditions for the development of masepic and bimasepic fabrics are probably different, particularly in terms of stress.

2.2.5 Skelsepic fabric and astronomical curiosities

The alignment of particles parallel to the sides of large grains (skelsepic fabric) is a common micromorphological feature of glaciogenic sediments (*Figure 2.1g*). Seeing skelsepic fabrics is more difficult where they have developed around areas of matrix, whether local or exotic. Van der Meer (1993) hypothesised that such matrix areas were stiffer and possibly dryer than the rest of the material and the fabric was formed by rotation. Lafeber (in figure 5 of Lafeber,

1964) suggests that skelsepic fabrics form through the interaction of large grains. It may be that skelsepic and bimasepic fabrics are interrelated (van der Meer, 1993, and references therein). However, such associations are based on the juxtaposition of the two fabrics in thin sections, and these may display features from multiple events. Consolidation has also been suggested as an origin for skelsepic fabrics (Harrison, 1957). Clay swelling has also been put forward as a possible cause (van der Meer, 1987b).

Orientation of big silt and sand grains around larger grains can occur with or without an associated skelsepic clay fabric (van der Meer, 1993) (*Figure 2.1h*). Van der Meer has suggested that the absence of a clay orientation in these situations indicates a ‘flow’ (pure shear?) rather than a ‘shearing’ (simple shear?) origin. That a pure shear geometry produces some of these features has also been put forward by Menzies and Maltman (1992). They found 'comet [tail] like structures' associated with grains (see figure 4e of Menzies and Maltman, 1992) (*Figure 2.1i*). These, they suggested, may result from pure shear in a confined horizon. Alternatively they suggest they may be due to pore water winnowing of the finer sediments (see Clarke, 1987 for a theoretical basis). The equivalent features under simple shear are the ‘galaxies’ of material strung out in opposing directions at the base and apex of soft clasts (van der Meer, 1993) (*Figure 2.1j*). Van der Meer (1993) suggests these may develop into augen-shaped areas akin to those seen in metamorphic geology (though note that these form by recrystalization; for a review see Simpson and Schmid, 1983). Further rotation, he notes, might be responsible for the development of the classic grain and skelsepic fabric orientation around large grains. It is not obvious why Van der Meer considers the *lack* of a skelsepic clay fabric allows for the introduction of pure shear as a condition in the formation of grain skelsepic fabrics, as discussed above.

Distinct pebbles of material may often be found in the matrix. The pebbles may be of local material (van der Meer, 1987b), implying deposition and then brecciation, or reworked from older sediment (Menzies and Maltman, 1992; van der Meer, 1993). Pebbles have been classified by van der Meer (1993) into types based on a mix of form and possible origin.

Type I) Composed of local till with no internal fabric. Recognisable by surrounding voids, [possibly] formed by slight deformation.

Type II) Composed of local till with an internal fabric, [possibly] formed by 'plastic deformation'.

Type III) Composed of till or fines with an internal fabric, formed by brecciation.

A more consistently genetic classification could be based on Cowan (1985). The environments so far examined in the literature give little indication as to the processes forming the pebbles. They are found in areas both with (van der Meer, 1993) and without (van der Meer, 1987b) shear fabrics. Neither need reflect the origin of pebbles, as the pebbles could have been inherited in these situations (see Chapter Eight for evidence of one formational environment). Type I pebbles have been attributed to the freeze-thaw creation of voids by Sole-Benet *et al*. (1964) in a Mediterranean environment. Van der Meer (1993) found Type I pebbles displaying an upwards dissipation and rounding at one site, and this was taken to indicate a strain origin through rotational movement with a downwards reduction in strain. However, it is possible such a velocity gradient could be responsible for the morphology of the pebbles without being active in their initial formation. Equally, such strain may be periglacial rather than subglacial.

2.2.6 Pores, fissures and structures associated with hydrology

Very little work has been completed in the important area of fabrics associated with fluid throughflow. Menzies and Maltman (1992) have suggested that patches with a single fabric orientation in a otherwise random matrix are representative of fluid throughflow in meltout (*Figure 2.2a*). They also suggest diffusely sheared sediment with ripped up pieces of more coherent sediment may be from an area of pervasive movement in a slurry piping event (*Figure 2.2b*).

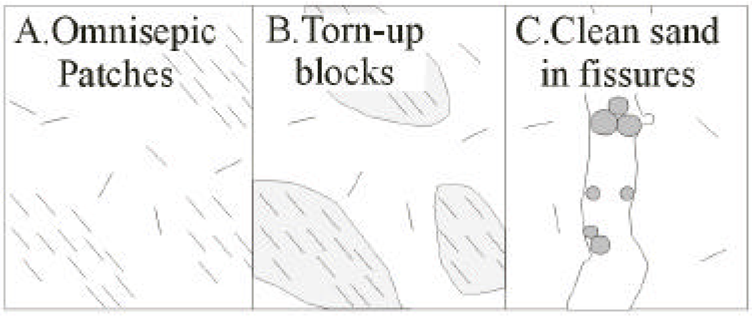

Figure 2.2 Microscopic fabrics caused by the interaction of water and grains in glaciogenic sediments. A)Broad patches of grains with one orientation (Menzies and Maltman, 1992). B) Blocks of local or exotic sediment torn-up by pipe flow (Menzies and Maltman, 1992). C)Clean sand washed into fissures. The fissures may be caused by water flow (van der Meer, 1987b).

Silt injection pillars may have been formed by high fluid-pressure sediment translocation (van der Meer, 1987b). Van der Meer (1987b) has noted the occurrence in several samples of linear but discontinuous pores forming a 'fissile' fabric, often highlighted by the presence of iron and/or manganese precipitates. This fissility is unrelated to the grain orientation. Clean skeletal grains and translocated silts in the fissures suggesting they were formed by, or at least were a path for, water (van der Meer, 1987b) (*Figure 2.2c*). Work by Murray (Murray, 1990; Murray and Dowdeswell, 1992) suggests that deformational features such as shears and dilatant areas, common in till thin sections, are extremely efficient drainage paths (Chapter Three). Probably the most significant indicator of pore fluid conditions is the form of deformational features (Menzies and Maltman, 1992). However, the relationship is complex, for high fluid contents may simultaneously act to weaken fabrics while encouraging greater strains.

Air-filled pores may also be a significant component of any thin section. Harrison (1957) and van der Meer (1993) suggest that high porosity indicates subaerial mass movements, during which air has been trapped.

2.3 The results of previous studies: attribution of microstructures to glacial environments

The above structures have, piecemeal, been attributed to various broad glacial environments. This attribution suggests that such environments have characteristic suites of microstructures. In order to critically assess this notion, the next section draws these associations together, giving the predicted microscopic components of glaciogenic facies. Some of the environments that will be discussed below are outlined in Figure 2.3.

2.3.1 Stagnant ice meltout environment

Two sets of features *could* be present in unaltered meltout till, if such a sediment exists. These are structures inherited from when the sediment was trapped in the ice, and structures formed during the meltout period. Bell (1981), Harrison (1957), Korina and Faustova (1964) and (implicitly) Gravenor and Meneley (1958) have suggested inheritance is responsible for all the micromorphology of till bodies not reworked by proglacial mass movements (*Figure 2.3a*). This suggestion seems unlikely, however, for even the situations where large-scale features may be inherited are limited (Paul and Eyles, 1990). Such conditions will be more stringent for microstructures, for which even small strains result in total disruption. If the ice is in contact with the subglacial sediment, and meltout material does not have to fall across a gap at the interface, vertical grain-grain support inevitably develops (Iverson and Semmens, 1995). This support implies considerable consolidation and reorientation in materials with a wide grain-size distribution. Given these factors, inheritance of structures from the ice seems implausible. Much *more* likely is the presence of features formed during the meltout process, such as winnowed beds or consolidation structures.

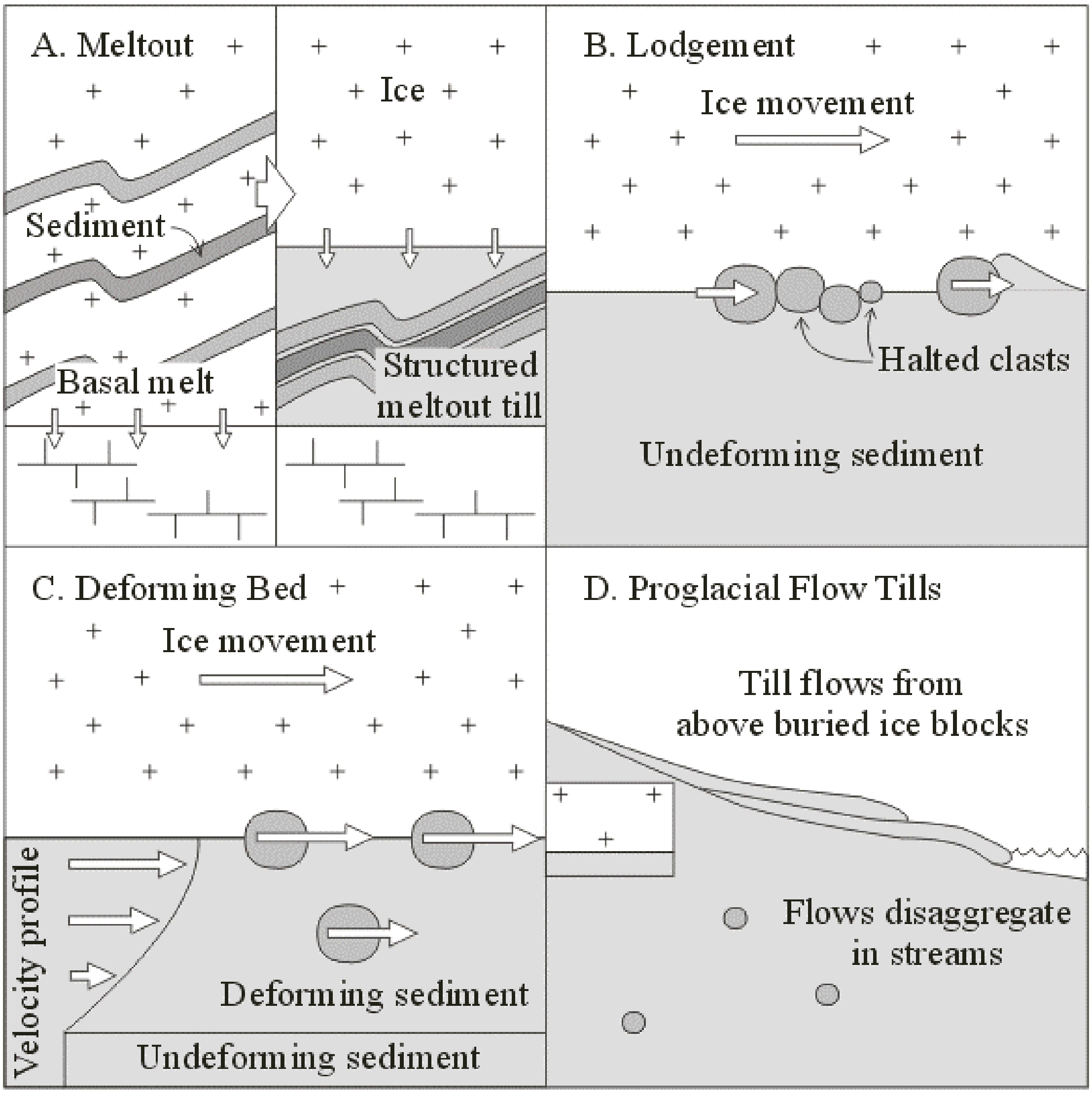

Figure 2.3 Frequently quoted situations in which glaciogenic sediments form. A) Structures coherently melt out of the basal ice. B) Material in the base of the ice lodges in a stiff bed. C) The glacier deforms a soft bed incorporating material from below and within the ice. D) Material melts out of the ice and flows off the top of ice blocks into streams.

Paul and Eyles (1990) have shown that, in almost all situations, meltout materials shear and dewater as the build-up of fluid at the melt-front reduces the sediment strength. This work was at the metre scale, but necessarily holds for smaller scales. Such structures will only be absent where there is supraglacial meltout on to an absolutely horizontal surface or subglacial meltout into protected hollows far from the ice margin. The former will lack shear features, the latter will lack shear *and* dewatering features. These conclusions match those of recent micromorphological studies. Fluid throughflow features (*Table 2.2*) have been identified as potential indicators of meltout materials, based on the hypothesis that the fluid pressures will be higher than normal. However, in most ice models homogeneous subglacial sediments rapidly become saturated, so low effective pressures may also occur under normal subglacial conditions.

Feature	Notes	Author
High number of voids	c.f. flow tills (below)	Van der Meer (1993)
'Patchy' orientation	From piping and throughflow	Menzies and Maltman (1992)
Load structures	Will depend on increasingly high pore fluid pressures as grain size decreases	After Paul and Eyles (1990)

Table 2.2 Microscale indicators of high water pressures (low effective pressures) in glaciogenic sediments.

Harrison (1957) and Korina and Faustova (1964) suggest that *sand* grains and large clasts show the same orientation when deposited by meltout. This fabric may be specific to passive meltout environments. The fabric seems unlikely in other glacial environments, where clasts would rotate or plough and alter the local stress field responsible for the alignment of the sand grains. However, Korina and Faustova give no indication of how widespread such a fabric is at their site, or the relationship between their sample positions and the measured clasts. These relationships are of paramount importance in deciding if the fabric is reliable, as the orientation could be produced by shear at a distance from the clasts. Van der Meer (1987b) suggests graded beds combined with an absence of dropstone fabrics are indicative of melt deposition into thin subglacial cavities. However, such fabrics can also be found in *proglacial* rhythmites (Chapter Eight). It is suggested that the beds in question would have to be very thin to show grain size dropstone deformation.

The above discussion shows that there are no reliable criteria for recognising meltout from stagnant ice. Details of structures indicative of meltout are given in Chapters Five and Eight. However, these structures are associated with the specific cases of meltout associated with lodgement and a specific local water system respectively. One hypothesised criteria that has not been discussed before is the presence of ice-collapse areas in material deposited through shallow water layers. Fluvial deposition into standing water *may* be identifiable by a light omnisepic fabric and the absence of infinite strain deformational structures. A collapse fabric in such material has not, as of yet, been observed, and mineral solution may produce a similar fabric. However, Harrison (1957) and Ronnert and Mickelson (1992) have suggested that porosity in some tills may be 'fossil' and represent areas of sediment previously filled by ice.

2.3.2 Glacier moving by sliding over a soft bed (lodgement)

There have been no attempts to define till lodgement structures (*Figure 2.3b*) separately from those structures associated with general till deformation (*Figure 2.3c*). It might be that lodgement only produces finite strain features in sediments (that is, ones in which we can calculate the strain). However, *finite* shear need not be *exclusive* to lodgement. For example, such strain is to be expected in meltout material that flows a short distance. Subglacial sediments might also be reset after infinite deformation by fluid throughflow. *If* small-scale grain alignment matches clast alignment on an outcrop scale (Gravenor and Meneley, 1958; Korina and Faustova, 1964) lodgement may be reflected in grain orientations, as has been suggested for larger clasts (Glen, Donner and West, 1957; Dowdeswell and Sharp, 1986; Hart, 1994). However, despite the start made by Hart (1994), there has been insufficient work to confirm this suggestion on the larger scale. At present there is insufficient understanding of the processes involved in clast orientation to warrant an investigation of smaller-scale grain alignment. A set of structures associated with lodgement under specific circumstances is given in Chapter Five, and these can be used as criteria for lodgement except in cases where there is subsequent infinite strain.

2.3.3 Glacier moving by soft bed deformation

Van der Meer (1993) has hypothesised that the following sequence of glacial microstructures exists (*Table 2.3*), based on the deformational model of Boulton and Hindmarsh (1987) (*Figure 2.3c*).

Place in sequence	**Feature**
Upper pervasive deformation zone	Omnisepic fabric generally
	Discrete shears
	Type I pebbles (*in situ* with no internal fabric)
	Type II pebbles (*in situ* with internal fabric)
	Skelsepic fabric
Middle pervasive deformation zone	Lattisepic fabric generally
	Discrete shears
	Type I pebbles (*in situ* with no internal fabric)
	Pressure shadows
	Masepic fabric
Lower pervasive deformation zone	Skelsepic fabric generally
	Discrete shears
	Type I pebbles (*in situ* with no internal fabric)
	Type III pebbles (reworked)
	Kinking fabric
Upper brittle deformation zone	Discrete shears
	Type I pebbles (*in situ* with no internal fabric)
	Discretely sheared soft clasts
	Crushed grains
	Dewatering and escape structures (presumably involving downwards escape)
	Kinking fabric

Table 2.3 Hypothesised position of microscale features in a deforming bed with a vertical decrease in velocity down from the ice-sediment interface (extracted from van der Meer, 1993).

None of these structures would appear restricted to formation by subglacial deformation. However, if such a sequence is located it would be strong confirmation of van der Meer's hypothesis that the amount and type of pervasive deformation can be delimited using these structures.

Shear zones are formed by deformation and, as such, are an indication of strain. However, there has been little discussion, even in van der Meer (1993), of the extent to which deformation till can be distinguished from small movements during meltout, lodgement, or consolidation. The presence of till pebbles has been implicitly suggested to indicate significant till movement ('reworking', van der Meer, 1987b; 1993), though to what extent this transport is in the ice or till is not clear. Skelsepic fabric development seems a likely candidate for recording large strains, if rotation is part of that development. The formation of bimasepic, skelsepic and till pebble fabrics needs investigation before their morphology can be used as an indicator of infinite strain. A start on such an investigation is made in Chapters Seven and Eight.

2.3.4 Proglacial / stagnant ice terrain

In an environment of proglacial ice blocks, we expect supraglacial till combined with flow and meltout tills (*Figure 2.3d*). The difference between till reworked by proglacial mass movements ('flow till') and tills deformed subglacially will be slight as they both deform internally. The two are probably more easily distinguished on the outcrop scale (for example, Boulton, 1977; Kemmis, 1981). Even then there is considerable controversy (B.G.R.G. Subglacial Working Group Workshop, Isle of Man, 1996; Saunders 1968; Boulton, 1977; Kemmis, 1981). Both subglacially deformed tills and flow tills could include areas of shear, reworked till pebbles, and skelsepic fabric. Pure shear geometries may also occur in both tills. Two possible criteria for recognising flow tills are their consolidation state, and the related porosity.

Fabrics indicative of high pressure consolidation are not expected in flow tills as they have not been overridden by ice. However, clay and silt fabrics *have* been found in suspected flow tills by van der Meer (1993), and patches of material consolidated subglacially may survive reworking. More doubt is cast on consolidation as a criteria as it varies considerably in subglacial tills (Boulton and Dobbie, 1993), and could be disrupted by throughflow. Dewatering disruption can occur in both proglacial and subglacial environments (Paul and Eyles, 1990). Either way, pre-consolidation is easier to assess in the laboratory by examining the loss of porosity under restressing (Boulton and Dobbie, 1993) than by looking for consolidation fabrics in the micromorphology of samples.

Air-filled pores may be indicative of the subaerial entrapment of air, and are common in flow tills (van der Meer, 1993; Owen and Derbyshire, 1988; Harrison, 1957). Such pores should be discontinuous to indicate that they are not formed by fluid. Pores caused by water may be associated with weak sediment fabrics, and could lead to confusion. However, dead end pores *have* been found to form during sediment consolidation (Lowe, 1975). Thus, the examination of consolidation and porosity in sediment thin sections does not appear to give reliable enough information to assess the difference between proglacial flow and subglacial deformation.

2.3.5 Glaciomarine/glaciolacustrine environments

Glaciomarine/glaciolacustrine materials are deposited into large water bodies at, or near, the ice front, and usually include a large amount of sediment from the ice mass. The chief indicators of such environments are fossils. These are usually calcareous exoskeletons, though fish remains have been interpreted as having been trapped in near-glacial marine pools by sea ice (Bell, 1981). Fossils may, of course, be reworked from prior marine deposits. Microfossils are less likely to survive the rigors of the subglacial environment, suggesting whole specimens might be a reliable sign of glaciomarine deposition. However, whole shells are found in terrestrial deposits in limestone areas. Derived fossils can be determined by the presence of limestone erratics and secondary calcite in shell chambers.

Loading and dewatering structures caused by density variations in the sediments may also indicate lacustrine or marine conditions. However, none of these features are exclusive to the glaciomarine environment. Dropstone fabrics, where pebbles indent lower beds and are draped over by later deposits, may be more characteristic. However, in deforming till, grain-grain contacts could conceivably push particles into laminae, causing the traditional drop-stone flexure of the underlying sediment.

Random fabrics are likely in glaciomarine deposits, but occur elsewhere as well (see above). In a detailed four-dimensional analysis of a hand specimen Talbot and von Brunn (1987) suggest that in proglacial glaciomarine environments, sediment and fluid can be tidally pumped through tills by the glacier resulting in microscopic diapirs. All that is necessary is that pore fluid pressures are high enough to dilate channels, and then small-scale faults are used as pathways. Again, though, diapirism is not confined to the glaciomarine environment, and very localised subglacial pressure changes (Blake, 1992; Jansson, 1995) could be envisioned to have the same effect. For practical purposes a number of features in combination must be present to reliably define these sediments. Hart and Roberts (1994) suggest the following suite of structures, that might be found on a microscopic scale, as indicative of glaciomarine sediments:

1) Laterally continuous, ungraded rhythmic alterations of fine and coarse laminae with low shearing.

2) Whole shells.

3) Onlapping beds.

4) Loading/water escape structures.

5) Internally intact blocks that have slumped under gravity.

6) Highly variable fabric directions dependent on water content.

7) Sedimentary, rather than tectonic, boundaries.

8) Localised deformation.

2.3.6 Non-glacial overlays

Finally, to add to all this exasperating uncertainty, glacial sediments may record previous depositional environments (Menzies and Maltman, 1992) and subsequent environmental superimpositions - notably from periglacial and pedogenic processes.

Pedogenesis is, largely, easier to spot than periglacial alteration. This partly reflects the maturity of pedology as a science compared with glacial micromorphology, and partly reflects the fact that major pedological changes are more or less limited to the soil horizons obvious on an outcrop scale (see, Mücher, 1985; Kemp, 1995; Kemp *et al*., 1995, on microstructures associated with palaeosols, as well as Fitzpatrick, 1984 for a detailed discussion of soil microstructures). A number of processes *do* act at levels not identifiable on the outcrop scale. All are associated with the transport of materials by soil pore waters (for example, see Madgett and Catt, 1978; Bouma *et al*., 1989).

Clays deposited by postdepositional translocation are often visible as cutans (clay drapes) on grains in tills and around pores (Fitzpatrick, 1984). Clay translocation may also occur subglacially producing sandy areas in till (van der Meer, 1993; Clarke, 1989). Translocated chemicals can highlight boundaries and give information on the relative ages of events (Chapter Four), but staining can interfere with the identification of fine structures and grain size changes using fabric birefringence under cross polarised light. Voids with a drab of impurities may indicate the dissolution of limestone postglacially. These voids may later collapse leaving just the deformed drab (van der Meer, 1987b). Carbonate may be deposited in pores and crystal growth move grains. Silicate dissolution has been associated with the embayment of quartz grains the subsequent local disturbance of fabrics (May, 1980).

Small scale periglacial structures are less well understood. Slope processes such as slumping will produce structural suites which also will form in other environments. Freeze-thaw can produce voids around material which are less ambiguous (Sole-Benet *et al*., 1964), however solifluxion could produce a pebble structure from these. Other features formed in this environment are shown in Table 2.4.

Feature	**Cause**	**Author**
Millimetre scale flame like intrusions of lower material	Gravity	Sole-Benet *et al*. (1964)
Horizontal planar pores	Freeze thaw	Sole-Benet *et al*. (1964)
Domains	Freeze-thaw	Sole-Benet *et al*. (1964)
Cracks and shears	Freeze thaw and solifluxion	Coutard and Mücher, (1985)
Sand grain orientations in flows	Injection of soft material between frozen blocks (take 15 to 23 cycles of freeze-thaw to develop)	Sole-Benet *et al*. (1964)
Silt intrusions	Translocation of silt into silt lenses resulting from the formation of segregation ice lenses	Coutard and Mücher, (1985)
Clay coatings	Illuviation	Bouma *et al*. (1989)

Table 2.4 Microscopic fabrics associated with periglacial activity.

2.4 Conclusions

The assignment of sediments to different glacial environments or processes is fraught with difficulties, compounded in glacial micromorphology by working at a scale that is at odds with daily experience. In the real world, sediments undoubtedly result from a mix of depositional processes that cross environmental boundaries in a most inconvenient way. A process based perspective, concentrating on how features form and how they change under different stress and hydraulic conditions will aid in the reconstruction of environmental information, and put us in the best position for looking at how the sediments affect the surrounding conditions. While this thesis makes no claims for adhering to this policy completely, it is hoped a process-based approach is discernible within some of the following chapters.

The next chapter examines what can be learnt about the causes and effects of microscopic structures from other subject areas that include the deformation of soft sediments in their remit. The separation of 'macro' and 'micro' scale processes is essentially one of viewing equipment.

Morgenstern and Tchalenko (1967) define 'microstructures' as 'those structural features which require the resolving power of at least an optical microscope for their study'. Given that this is anthropogenic anyway, a more appropriate division is probably between the models of structures that include the effect of individual grains and those taking grain-grain effects in bulk and the sediment as a continuum. The scale independence of structures like shear zones (Tchalenko, 1970) down to the grain-grain level suggests this is reasonable. The fact that the smallest shear zone size may be fixed at 8-16 times the mean grain diameter (Mühlhaus and Vardoulakis, 1987; Bardet and Proubet, 1992) prevents the arbitrary scaling of such features below this level and suggests this division may be objective in some situations. Plainly grain-grain interactions should ideally be taken into account in all situations, continuum mechanics being a non-ideal representation of bulk grain-grain effects. The division is a monument to our own inabilities rather than any real situation. Because the structures seen in thin section *can* be scaled in this way to outcrop size, and models exist for such large features, the discussion in the next chapter does not exclude larger structures.

3. The development and effect of microscopic deformational structures

3.1 Introduction

Because glaciologists are interested in very large scale models they tend to generalise proglacial and subglacial sediments as homogenous continua. In other subject areas, however, small scale structures in the sediment have been shown to have a profound effect on the dynamics of the material as a whole. Such structures form through the sediments' grains varying in size and orientation. Two properties are considered to alter with the development of grain orientation in sediment; the sediment's drainage and its strength. In continuum models these two have been related via water pressure (which is often controlled by drainage) for example in the classic Mohr-Coulomb equation for sediment strength,

$$t^* = c + P_e \tan f \qquad \textit{...Equation 3.1}$$

where t^* is the maximum shear stress supported by the sediment (or 'yield strength'), c is the cohesion of the sediment, P_e is the effective pressure on the sediment, and f is the angle of internal friction for the sediment. In glaciology P_e is usually the ice pressure minus the pore fluid pressure in the sediment. Cohesion is the deviatoric stress that the sediment supports at zero effective pressure. This is often visualised as the force necessary to overcome the electrostatic attraction of sediment grains. The internal friction of the sediment is calculated from the rate at which the yield strength of the sediment changes with effective pressure (for a review see, Price and Cosgrove, 1990). It is often visualised as being determined by the force needed to mechanically move grains up and over each other (Hooke and Iverson, 1995).

Creep prior to the sediment yielding is usually ignored. Following yield, strain rate is usually modelled through equations relating it to the shear stress and effective pressure. Therefore, because they are part of the effective pressure, the pore-fluid pressure and ice overburden pressure affect the yield strength of the sediment *and* its post-yield strain.

The pore fluid pressure of homogeneous sediment is dependent on the ability of the sediment to drain. For homogeneous sediments drainage is usually modelled in two dimensional terms by Darcy's law,

$$\frac{Q}{A} = K\frac{\mathrm{d}H}{\mathrm{d}l} \qquad \textit{...Equation 3.2}$$

where Q is the discharge, A is the drainage area transverse to flow, dH/dl is the fluid pressure gradient, and K is a material-specific constant known as the hydraulic conductivity. Hydraulic conductivity varies from 10^{-8} to 10^{-16} for clay sediments. Discharge may also be represented in terms of permeability (k), which is related to hydraulic conductivity by

$$K = \frac{krg}{h} \qquad \textit{...Equation 3.3}$$

where r is the density of water, g is the gravitational acceleration, and h is the viscosity of water. The permeability is chiefly dependent on the size of pores in the sediment. In turn, the pore size is partially determined by the effective pressure on the sediment, so that drainage reduces the pore size and reduces the permeability. Pore space is often represented in terms of the ratio between pore volume and the volume of the grains (the 'void ratio'). Mesri and Olson (1971) showed that permeability is a log-linear function of void ratio from ratios of 0.7 to 4.0. Permeability is likely to also be affected by mineralogy, grain size, cementation, water chemistry, and particle packing (Brown *et al*., in press). However, Mesri and Olson's work gives some indication of the considered importance of small porosity changes to fluid flow and, subsequently, the effective pressure acting on the sediment and the sediment's strain response.

Changes in permeability may also occur through changes in the path length or 'tortuosity' of the sediment (Arch, 1988), and changes in the electrostatic response of sediment grains (Mesri and Olson, 1971). The tortuosity is defined as the true path length across a chosen region divided by the length across the region in the absence of sediment grains. This will be dependant on the length-to-width ratio of the sediment grains and their alignment. Arch and Maltman (Arch, 1988; Arch and Maltman, 1990) give the following variant of the Kozeny-

Carman model of permeability for representing the control of permeability by tortuosity, pore shape, and size,

$$k = \frac{Cm^2}{BT^2} \qquad \textit{...Equation 3.4}$$

where k is permeability (m^2), B is a shape factor, as is C which relates to flow at an angle to pores treated as pipes of a shape determined by B, m is the ratio of the pipe volume to its surface area in contact with the fluid, and T is the tortuosity.

This chapter examines work on the development of microstructures and their effect on the ideal models outlined above. Much of this information will be used in a glacial context in future chapters, however, a number of novel conclusions on the causes and effects of glacial microstructures are presented at the end of this review. The treatment of the structures will progress from depositional forms, to simple consolidation structures, through bodies intruding into sediments, to the complexities of shear deformational features. Some of these features are presented in Figure 3.1.

The geometrically simplest alteration a sediment can undergo is a bulk reduction of its pore space. This is commonly caused by electro-chemical processes or consolidation of the material under stress.

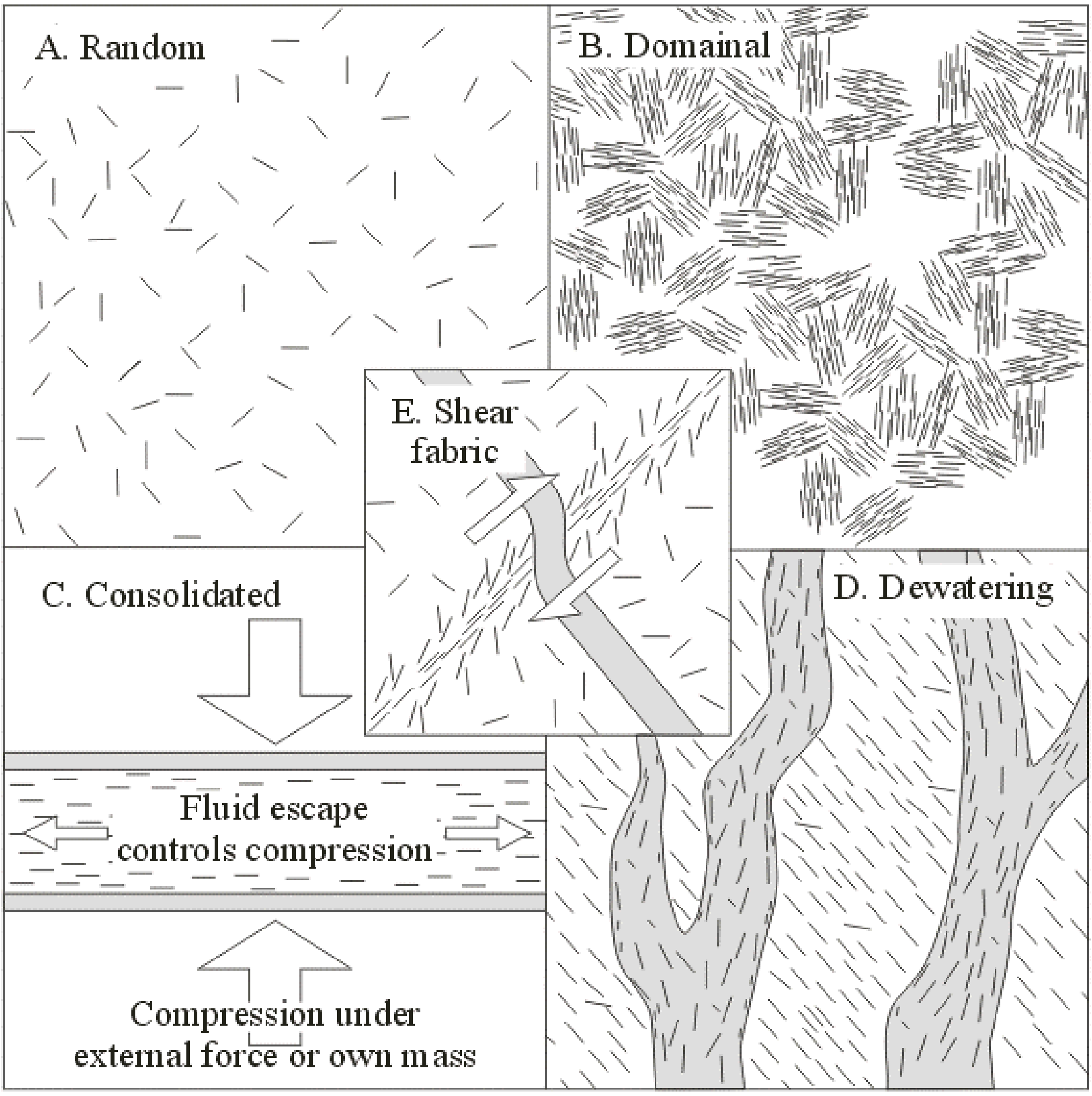

Figure 3.1 Some common soft sediment fabrics and microstructures: a) random orientation b) domains c) omnisepic fabric d) dewatering fabric e) shear fabric.

3.2 Depositional forms - The electro-chemical reduction of porosity

Unsatisfied charges on the surface of clays mean that structures can form through the attraction and repulsion of grains when sediments settle out of fluid suspension. The chemistry of fluid flowing through clays alters their permeability by changing the fluid viscosity, the clay structure and distribution, and thickness of water layers bound to the grains. Lower electrolyte concentrations lead to greater grain dispersion but the effect will be strongly dependent on the clay type (Mesri and Olson, 1971). Thus, in the glacial situation, the permeability may be dependent in part on the fluid's source and how far it has moved through the sediment already picking up solutes.

The classic electro-chemical structure is the domain (*Figure 3.1b*). These are randomly oriented patches, some 50 μm to 1 mm square, of aligned particles (though note the term is also used in reference to broader areas, such as shear zones by some authors, for example, Morgenstern and Tchalenko, 1967; McConnachie, 1974). As domains form through electrostatic attraction the porosity will be lower than in clays with random grain alignments. This reduction would suggest a decrease in the sample permeability. However, the tortuosity of randomly aligned domains will be less than a sediment which is totally random. Large pores may also develop between the aggregates (Mesri and Olson, 1971). Flow is generally increased through domainal sediments by the latter two processes, but this is dependent on the effective pressure on the sediment (Mesri and Olson, 1971). That domainal structures are rare in glacial sediments suggests that the pore fluid chemistry is not suitable, or the features are destroyed after formation.

Substantial subglacial solution of grains can occur (May, 1980). The characteristic embayment of grains affected by this process has been seen in tills from the Yorkshire coast, the micromorphology of which is examined in Chapter Seven. Possible glacial iron deposits found in Criccieth in Wales are examined in Chapter Four. It seems possible that the solution and redeposition of minerals may also significantly alter the permeability of glacial sediments.

3.3 Consolidation

Consolidation is the reduction of a sediment's porosity under its own mass or external forces. It is usually taken to refer to gravitational coaxial strain, that is, a vertical length change. Rates of consolidation are modelled using the stress and the rate at which fluid is expelled from the reducing pore space; the 'diffusivity'. The diffusivity is dependent on the permeability, the friction, and cohesion of the sediment as well as the pore fluid (see Rieke and Chilingarian, 1974, and Murray, in press, for a comprehensive review). The porosity of sediments is often in equilibrium with the effective pressure they are under. Such sediments are said to be normally consolidated. Where more porosity has been retained than is normal, the sediments are said to be underconsolidated for the present pressure or the maximum they have experienced *in situ*. (the latter is also known as overpressuring). When there is less porosity than expected for the present situation or a past maximum pressure the sediments are known as overconsolidated.

Under loading particles become strongly aligned perpendicular to the compressive stress (*Figure 3.1c*) (Delage and Lefebvre, 1984; Dewhurst *et al*., in press). However, alignment is in the direction of the maximum strain where this direction differs from that of maximum stress because of heterogeneous deformation (Baker *et al*., 1993). Alignment is strongly dependant on the material (Dewhurst *et al*., in press). Where domains form under progressive loading, the sediment first develops grain clusters which break down between 200-500 kPa to be replaced by domains and smaller pores (Dewhurst *et al*., in press; Brown *et al*., in press). Most porosity is then lost through the reduction of large inter-aggregate pores despite the internal deformation of the domains (Delage and Lefebvre, 1984). Domain deformation may be constrained by loading thresholds (M^{c}Connachie, 1974). Inter-domainal pores may elongate before they collapse (Delage and Lefebvre, 1984) potentially leading to increased horizontal permeability without a change in vertical permeability.

Alignment of grains and pores under consolidation produces an anisotropic permeability in sediments (Al-Tabbaa and Wood, 1987; Znidarcic and Aiban, 1988; Dewhurst *et al*., in press; Brown *et al*., in press). For kaolinite and calcium montmorillonite Brown *et al*. found that the horizontal drainage was greater than the vertical (horizontal to vertical ratios of 1.7 and 8 at void ratios of 0.7 and 1.6). This result matches Dewhurst *et al*.'s similar findings. The effect was attributed to increases in the vertical tortuosity (perpendicular to fabric). However, these ratios are not as great as those expected from the Kozeny-Carmen model (*Equation 3.4*). It was suggested that domains, shears caused by uneven consolidation, and other heterogeneities, reduce the effect of the alignment. The permeability response of glacial material might be expected to fall between that of Brown *et al*.'s (in press) mixed clay material and their silt-clay mix. The ratio between horizontal and vertical permeability would thus range between five and zero if only gravitational consolidation took place.

It should be noted that glacial clays have been reported which have suffered no consolidation. Meltout till might maintain 'fossil' porosities of 40%+ from ice filled 'pores' in the basal ice (Ronnert and Mickelson, 1992). In addition, the consolidation alignment of fabrics is thought strongly dependent on the depositional fabric. Lateral pressures can also cause consolidation. The widespread glaciotectonic alignment of particles under horizontal compression was reported by Kluiving *et al*. (1991).

Consolidation may be represented by more complex features than horizontal alignment. Even sediments that have undergone no obvious tectonic event can contain deformational features formed in the process of consolidation. Though Paul and Eyles (1990) pointed out the process on the visible scale, this fact has been too often ignored in glacial micromorphology. Many of the classic signs of tectonic deformation (for example shears, *Figure 3.1e*) can be found in material that has suffered only local vertical stresses (Arch *et al.*, 1988; Brown *et al*., in press). Such features are produced by differential compaction. This strain difference results from varying diffusivity in heterogeneous sediments (Athy, 1930), fluid pressure gradients set up by drainage in homogeneous material (Roscoe, 1970; Al-Tabbaa and Muir Wood, 1991), and sub-sediment topography (Athy, 1930). In the first two cases, the material will eventually appear to have consolidated evenly on a large scale.

Consolidation may also produce dewatering fabrics (Cowan, 1982) (*Figure 3.1d*) when the force from expelled fluids exceeds the sediment strength and the force needed to transport the particles (Lowe, 1975; Paul and Eyles, 1990).

3.4 Localised bodies of altered porosity

The intrusion of exotic sediments, localised sorting, or comminution will alter the porosity and drainage potential of sediments (Athy, 1930; Barron, 1948; Åmark, 1986; Boulton and Dobbie, 1993; McCabe and Dardis, 1994). Structures showing such variation include dewatering paths (fine sediments winnowed out and deposited elsewhere), load-failure structures between two beds (sediments move up or down into another bed), brittle fracture fills, drag-folds, channel fills, and soft clasts which are strung out by deformation. The effect of such structures will depend on the drainage potential of the material around them and the areas they link with. Often it is implicit in such structures that they link areas of different permeability. For example, gravity structures (Lowe, 1975; Allen, 1977), stop dropping into sediments when the resistance of the surrounding material becomes too great. Such resistance is intimately tied to sediment porosity and permeability through the fluid pressure and friction. The drainage effects on the bulk sediment containing the structures will control the ability of the external material to deform both locally and at a considerable distance (for quantified examples see, Athy, 1930, Barron, 1948, Al-Tabbaa and Muir Wood, 1991).

An example of these drainage processes may be the clay brecciation seen around sand intraclasts by Menzies (1990). While Menzies attributes this to the drawing of water onto freezing fronts on the clast surfaces, the clasts could equally maintain a low pressure in the impermeable till for long enough for the brecciation to form (implied in Menzies and Maltman, 1992). Heterogeneities in drainage may provide the initial stiffness responsible for drumlins (Boulton, 1987; McCabe and Dardis, 1994) or even tougher "sticky-spots" controlling glacier velocity (Kamb, 1991; Fischer, 1992).

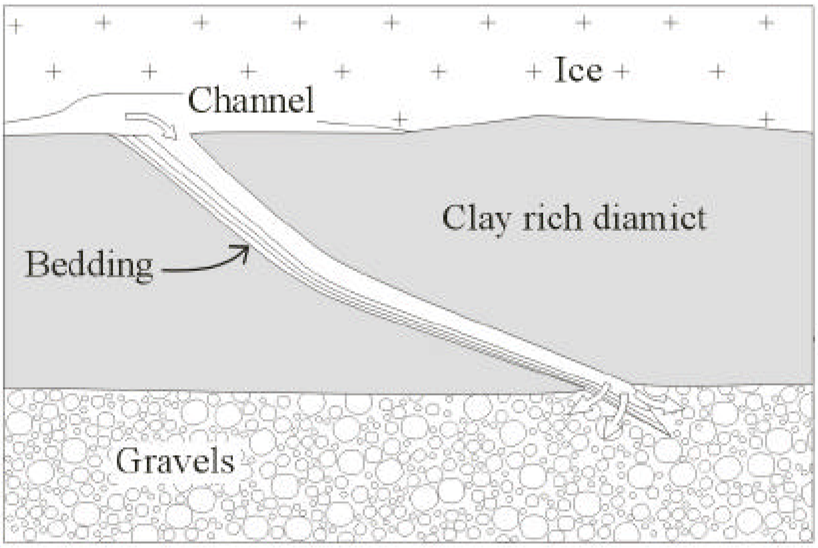

Figure 3.2 Diagrammatic representation of one of Åmark's (1986) clastic dykes. The dykes link the glacial bed to highly permeable gravels through an aquitard of till.

As an example of this, Åmark (1986) found clastic dykes linking the ice interface to a lower gravel unit through a clay-rich diamict bed (*Figure 3.2*). The bedding inside the dykes suggests the fluid depositing the beds drained easily into the gravels. As the dykes filled with material that is coarser than the clay-rich bed it seems likely the dykes continued to act as drainage conduits after they filled. Boulton and Hindmarsh (1987) have argued that one would need a thickness of 1.5 million metres of till at the terminus of a warm bedded glacier to evacuate its meltwater by throughflow. However, one would need only 150m of sandy till (as in the dykes) and only 15 cm of coarse gravel such as that under the diamict at Åmark's site. Thus, the dykes (up to 2.5m across) control the flow between the top of an aquitard and the highly permeable gravels. This drainage may explain the low strain after their formation. A similar situation could be envisioned for the coarse material filling a large-scale pipe recorded by Kluiving (1994). This was interpreted as having been implaced into a frozen fine-grained body. Paré *et al*. (1984) found till with a hydraulic conductivity anisotropy of 10 to 20 (horizontal to vertical ratio) at the base of dams in Northern Québec. This anisotropy was attributed to sand body orientation. The orientation of glacial sand bodies seen at the microscale has also been shown to control larger-scale flow anisotropies (Barron, 1948; Nyborg, 1989).

All this makes for a problematic reconstruction of the hydrology of any palaeoglacier in three dimensions and across time, however, it should not be viewed as impossible. M^cCabe and Dardis (1994) have shown the qualitative possibilities for such work, and researchers in soil science and civil engineering tackling similar problems have devised methodologies that simplify the problems from a quantitative viewpoint. Unique solutions are possible for individual features and stress fields (for example, Barron, 1948; Al-Tabbaa and Muir Wood, 1991), however, generalisations of features can successfully represent their effects (Nyborg, 1989; Paré *et al*., 1984). Estimates of bulk hydraulic properties can be made from field samples (Bouma *et al*., 1989; Ahuja *et al*., 1989), and these approaches may make possible the interpolation of till hydraulic characteristics from borehole data, micromorphology, and outcrop samples.

3.5 Shear zones

It is becoming increasingly accepted that many of the fabrics found in glaciogenic sediments are formed in pure and simple shear situations (Chapter Two). Measurements of subglacial deformation imply that simple shear, and possibly pure shear, geometries exist subglacially (Boulton and Hindmarsh, 1987; Blake, 1992; Porter, 1997). It is a possibility that the shear fabrics found in glaciogenic sediments are due to such subglacial deformation. Alternative causes are proglacial flow, low strain because of the meltout from basal or buried ice, or heterogeneous consolidation shearing. Large-scale shear structures can have a controlling influence on the dynamics of sediment bodies (Moore, 1989; Maltman *et al*., 1993b). Such macroscale shear *zones* may be formed from a mass of microscopic shears (*Figure 3.3*) (Maltman *et al*, 1993a). Glacial studies have shown macroscale shear features in the proglacial zone (Hart, 1989; Hart *et al.*, 1990; Thomas, 1984; van der Wateren, 1986;

Kluiving, 1994), and in frozen subglacial sediments (Echelmeyer and Zhongxiang, 1987). However work on the development of subglacial shears has largely been hypothetical (Harrison, 1957; Evenson, 1971; Menzies, 1986; Boulton and Hindmarsh, 1987).

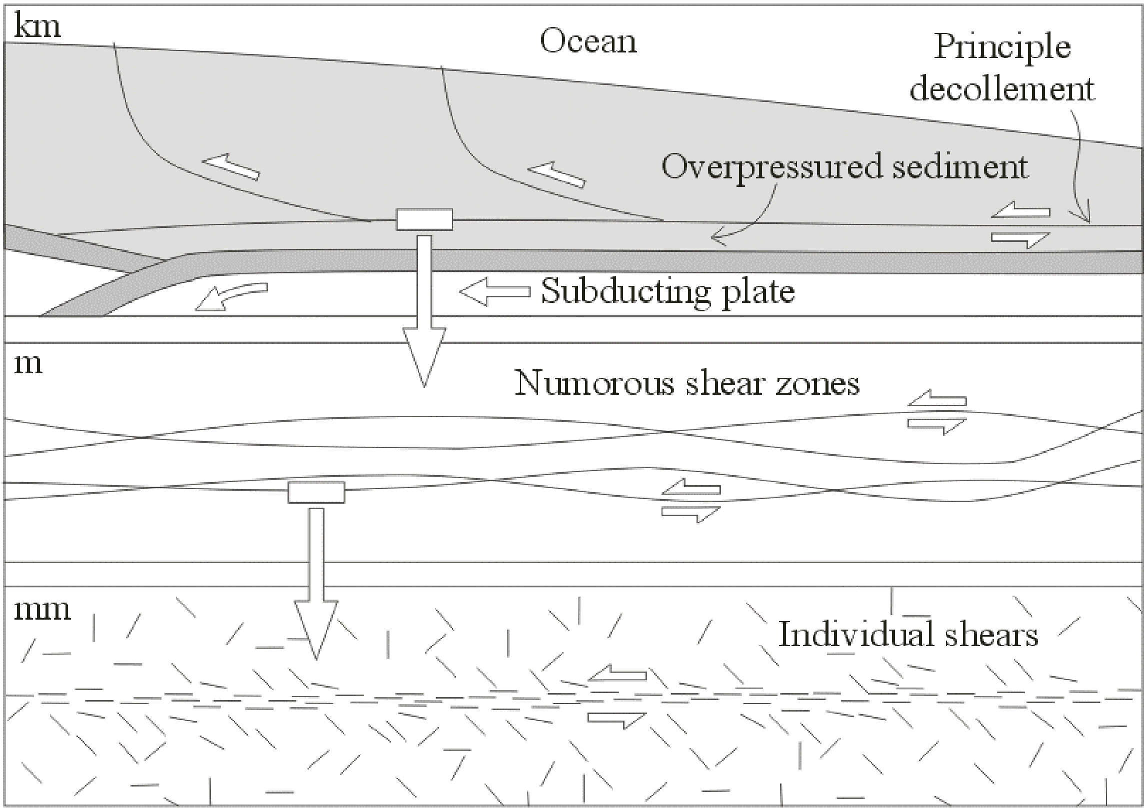

Figure 3.3 Diagram of the structure of the Nankai Prism, East of Japan, showing the décollement at different scales. After Maltman et al., 1993a/b.

The next sections examine the development of shear zones, and the effect they have on the hydrology and strength of the sediments they form in.

3.5.1 The development of shear zones

Shears are thought to develop at localised stress concentrations or material heterogeneities when the ability of material to maintain higher and higher stresses through compaction is exceeded (White *et al*., 1980). Early work showed that shear in soft sediments produces a complex morphology of structures (Tchalenko, 1968; 1970; Morgenstern and Tchalenko, 1967). This shear zone morphology develops in the following order (*Figure 3.4*).

1) The material undergoes particle realignment and strain before yield. This appears pervasive, but is partly due to microscopic shearing (Maltman, 1987; Arch, 1988) (*Figure 3.4a*).

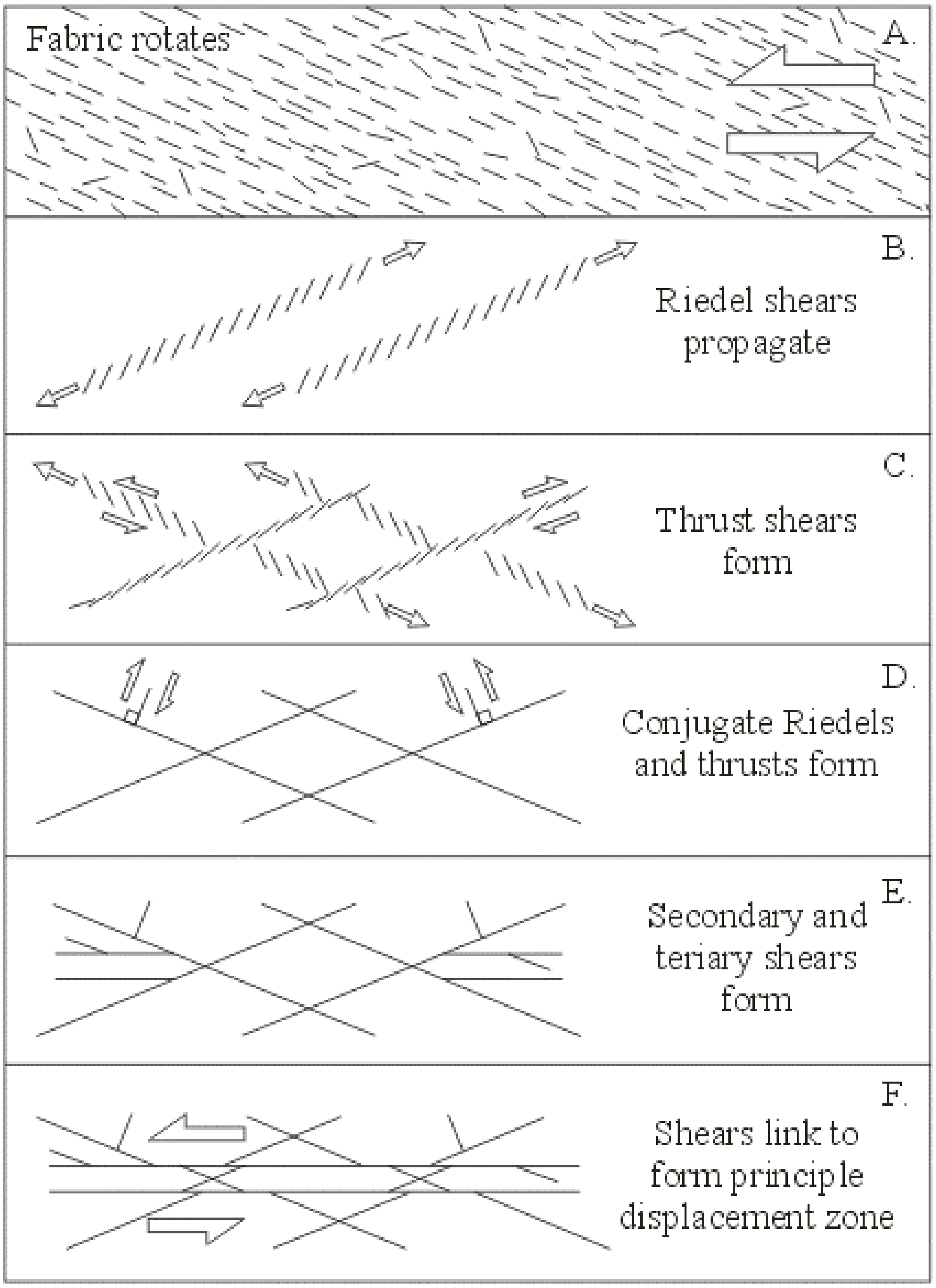

Figure 3.4 The development of shear zones (after Morgenstern and Tchalenko, 1967; Moore et al., 1986, p.42; Rutter et al., 1986; Tchalenko, 1968; 1970; Arch, 1988).

2) At the yield strength of the sediment (i.e. when the maximum stress is supported) yield at weak spots or stress concentrations transfers stress to nearby areas causing catastrophic propagation (Byerlee *et al*., 1978). Propagation may be further aided by the pumping of fluid from collapsing areas of the shear into areas which then dilate (Arch, 1988). 'Riedel' shears form at an acute angle (a) to the major principle stress (*Figure 3.4b*), modelled by

$$a = 45° - \frac{f}{2} \qquad \text{...Equation 3.5}$$

where f is the internal friction of the sediment. Atkinson and Richardson (1987) show there is a maximum a of 45° from the applied stress, which is also the figure when there is no bulk drainage from the sample

3) Riedel shears represent only small strain, being arranged at an orientation not conducive to large amounts of sliding in the direction of shear. As the material softens with strain, 'Thrust' shears form, mirroring the Riedel shears (with respect to a line perpendicular to the major principle strain direction) (*Figure 3.4c*) and conjugate Riedels form (*Figure 3.4d*). Conjugate Riedels form at higher pore water pressures in unconstrained simple shear experiments (Tchalenko, 1970). When their internal fabric is sub-perpendicular to their shear direction, the conjugate Riedels form structures known as kink bands (*Figure 3.5*) (Tchalenko, 1970).

4) The residual strength of the material is the stress supported as the material undergoes steady state infinite strain. This state occurs when the shears form a long 'Principle Displacement Zone' (PDZ) through the development of new shears in the Riedel and Thrust angles to the old shears (*Figure 3.4e*). The PDZs form parallel to the shear strain direction in simple shear experiments (*Figure 3.4f*), and along the Riedel shears in triaxial experiments. These shears may then undergo infinite strain without change.

The PDZs often bound lenses of undeformed material in cataclastic zones (Rutter *et al*., 1986). A similar situation may occur in glaciogenic sediments (Seifert, in 1954, quoted in translation by Harrison, 1957). Thus it is essential that low strain thin sections are not taken as indicative of bulk finite strain without the boundaries and any resistant layers in outcrops being sampled. Often the lens fabric reorientates normal to the major principle stress (*Figure 3.5*). The grains rotate until the shear stress on the grains is zero (Tchalenko, 1968). Such reorientation can represent considerable strain (Morgenstern and Tchalenko, 1967; Tchalenko, 1968).

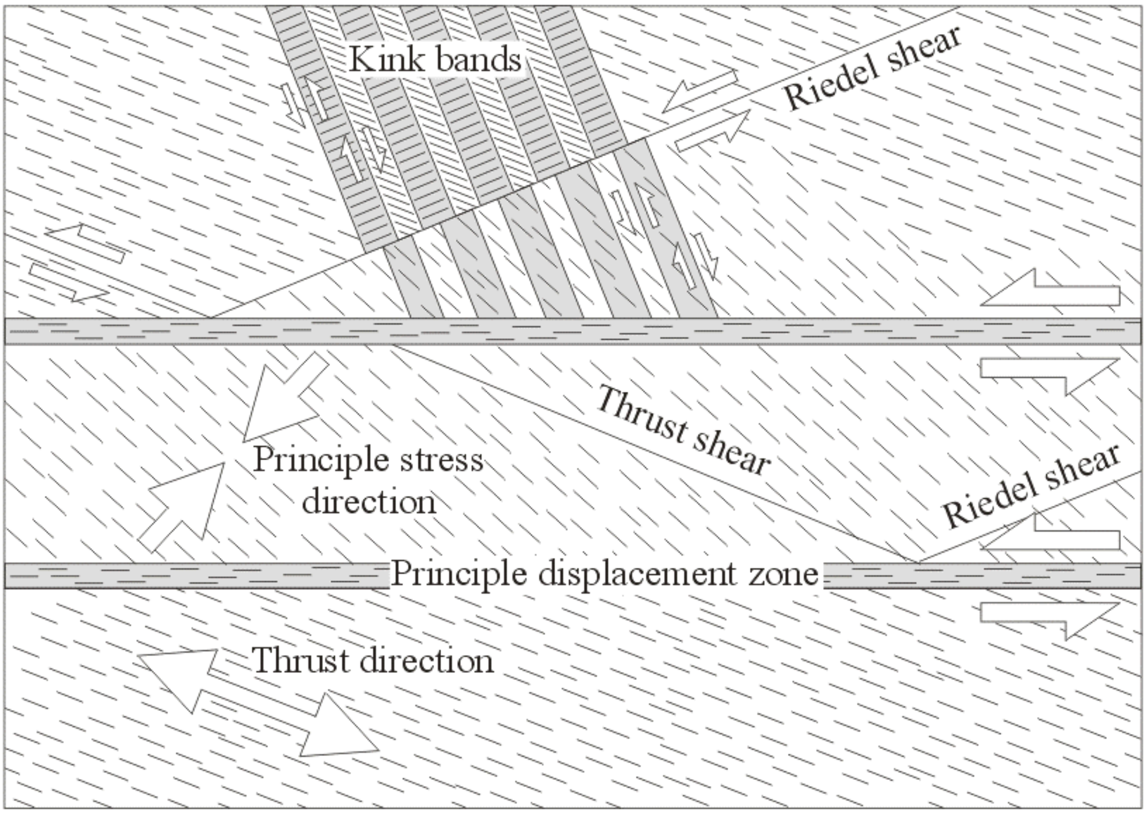

Figure 3.5 The orientation of fabrics in kink bands and lenses bound by Principle Displacement Shears (after Tchalenko, 1968; 1970).

A mix of primary fabric and a single PDZ could both represent infinite shear and give information about the final principle stress direction. Van der Meer (1993) has described broad zones of fault bounded lenses in glaciogenic deposits. However, increased shear may lead to more shears, rather than a development of individual PDZs (Maltman, 1987). It should be noted that local reorientation around shears occurs prior to yield. In *overconsolidated* samples (contrast with Rutter *et al*. (1986), above) the fabric in the area where the shear zone will develop rotates to *a* prior to peak strength (Tchalenko, 1968); when not overconsolidated the fabric is in the Thrust shear direction.

Interaction of shears may lead to strain hardening, and Riedel and Thrust shears that have developed in the absence of a PDZ (bimasepic or lattisepic fabrics) may imply this stiffening has occurred (Rutter *et al*., 1986). It has been suggested that shear zone thickening compensates for local hardening on the shears (Rutter *et al*., 1986). However, it is impossible to tell from geometrically constrained lab tests whether such widening of a lattisepic fabric fully compensates for hardening when the thickness of the fabric zone is not limited.

Kink bands are rare in triaxial tests, and have only been found in samples with water contents greater than 30% (Maltman *et al*., 1993a; 1993b). However, such features have been found in nature in conjugate sets (Maltman *et al*., 1993b), and in the absence of other shear forms (Maltman, 1977; Maltman *et al*., 1993a). In the latter the unusual breadth of the features suggests they may be associated with conditions in which shear stress is not released through the normal shear mechanism. Byrne *et al.* (1993) showed that kink bands can narrow and become shears, suggesting they are low strain forms of normal shears. Maltman *et al*. (1993a) suggest kinking arises from compression associated with the volumetric problem of moving sediment along shears while there is no movement occurring at the propagating tips. Kink bands can be both extensional and compressive features dependent on their throw. Whatever their cause, it would appear that kink bands represent strain prior to the sediment yielding *locally*. It may, however, be that sufficient stress could be supported by the residual strength of a Principle Displacement Zone to cause such behaviour in its periphery. Kink band formation can only be taken to represent pre-yield creep if there are no PDZs.

Repeated, close spaced kink banding forms ‘crenulations’ parallel to the principle displacement shear. Massive crenulation in glaciogenic sediments has been attributed to regional compression by Kluiving *et al*. (1991). In thin sections kinking can be so intense that there is the potential for misinterpreting the stress field and strain response responsible for it.

Factors affecting formation

It has been noted that shear *zones* may contain several sets of each geometry of shear outlined above. The orientation, number, and length of different shears is controlled by the skeletal and hydraulic properties of the sediment under deformation, and the strain. Thus, the geometry of the shear zones can give information about the sediment and the conditions under which deformation occurs. The general form (Riedels, Thrusts etc.) is not controlled by the material as it appears in a wide variety of geologies. This overall form must relate to strain/stress application (Logan *et al*., 1992), or the development of material anisotropy (Rutter *et al*., 1986). The response of shear geometry to changing several important conditions is given in Table 3.1.

Condition	Response	Authors
Effective pressure increases.	Work hardening of sediment.	Feeser, 1988
	The increased *deviatoric* stress resulting from increased loading leads to acceleration of the evolution of shears, the material reaching the residual strength faster.	Simamoto and Logan, 1981; Maltman, 1987; Logan *et al*., 1992; Parry, presented by Roscoe, 1970
	Riedels are shorter, more numerous, and inclined at higher angles to the Principle Displacement zone.	Byerlee *et al*., 1978; Logan *et al*., 1992
	Higher angle between the confining stress and shear, some dry specimens having an angle greater than the theoretical maximum of 45 degrees	Arch *et al*., 1988
	Principle Displacement shears are less frequent and longer (cf. Riedel shears, above). Strain concentrates in a few Principle Displacement shears.	Maltman, 1987; Arch *et al*., 1988.
	For water contents <25% shear zones are narrow, and with >25% they become more complex.	Arch *et al*., 1988; Logan *et al*., 1992
Increased depth of material available to shear.	Displacement needed to produce the same shear zone geometry increases. Because shear geometry is related to the shear stress supported at any time, it follows that a higher shear stress is needed to deform thicker zones over an equal displacement to thin ones	Logan *et al*., 1992
Change in material.	In unimodal sediments the form is roughly constant whatever the material.	Maltman, 1987; Logan *et al*., 1992
A fabric exists prior to deformation (for example, because of depositional processes or due to changes in glacial thermal and stress regimes as the glaciers advance).	The reorientation fabrics in mylonites theoretically induces considerable hardening	White *et al*., 1980
	If the initial fabric is close enough (<15°) to the expected shear angle, shears develop along the primary fabric because the high shear stress on grain boundaries at an angle close to that of the shear direction preferentially rotates these grains. At higher angles shears become pervasive or anastomosing.	Arch, 1988; Arch *et al*., 1988; Platt and Vissers, 1980; Stephenson *et al*., in press

Table 3.1 The response of sediment shearing and shear geometry to changing effective pressure, material thickness, constitution and fabric.

The relationship between shear geometry and effective pressure will relate to the number of stress concentrations on the shears from which subsequent shears propagate, the ease of realignment under different porosities (Maltman, 1987), and the ease of fluid movement within the shears, which will control the ease of propagation (Arch, 1988). The conflicting signatures of PDZs (get longer and less numerous with increased effective pressures) and Riedels (get shorter and more numerous) plainly demands a great deal more experimental work, particularly as one may become the other. However, the geometry of shears can broadly be used to qualitatively estimate the effective pressure.

The effect of potential shear zone depth is important in till, where shear zone size may be nominally unlimited. The only controls on shear zone width are fluid diffusivity and the stress-strain relationship of the sediment, both of which are controlled in part by shear zone development. There are, thus, two alternatives for thick glacial tills; either it takes a great deal more stress to produce less and less strain as the initial thickness of the sediment grows, or the deforming thickness reaches a threshold after which it is internally controlled. Thick tills may develop Riedels without PDZs up to considerable displacements, maintaining a high strength. However, PDZs do develop on a larger scale in other unconstrained environments (Tchalenko, 1970).

The relationship between shear form and material is also complex under glaciers, where the sediments are often multimodal. It was suggested in Chapter Two that bimasepic fabrics may be shear zones constrained by larger grains, and such constraints could act at an outcrop scale. This hypothesis is backed up by Rutter *et al*. (1986) who found that in natural and experimental fault gouges, Riedel and conjugate Riedel development was constrained to areas between clasts rather than expelling them. The shears developed preferentially next to clasts because of stress or strain heterogeneities associated with their surfaces. It is possible that clast expulsion from the shears will also occur. Alternatively, soft clasts may break up through slip on Riedel and Thrust shears (Rutter *et al*., 1986), giving the strung-out ‘tails’ of material seen in glacial sediments. This explanation suggests that pervasive flow is not necessary to form these features.

In much of the above, it can be seen that the water pressure is an important factor in determining the form of shears and, therefore, their strength and effects. Thus it is worth examining in greater detail the ways fluid in sediments and deformation interact. Despite the fact that many sediments act as though pervasively deforming up to failure at ~8 to 12% strain (Arch *et al*., 1988), true pervasive deformation is rare, and shears form rapidly in sediments with pore water volumes of up to 60% (Maltman, 1987). Equally, even in so-called 'undrained' lab tests samples are locally drained by shear zones (Atkinson and Richardson, 1987), and their strength is controlled by this process. Thus, an examination of water movement in sediments is largely an examination of fluid interactions with shear zones. Following such a study, the effect of shear development on strength will be reviewed.

3.5.2 Hydrological effect

There are two viewpoints from which the interaction of shears and fluid flow can be examined. Shears can be considered as static objects which affect permeability, or more rarely, they can be considered as evolving structures interacting with, and being affected by, fluid flow. In both cases the shears will affect the consolidation of surrounding material, and this will affect the shear's development (Moore, 1989).

Shears as static structures

Large-scale shears may act as dewatering paths (Moore, 1989; Maltman *et al.*, 1992; Maltman, 1988; Byrne *et al.*, 1993). Dilatant shears will have a higher porosity than the surrounding material, however, increases in permeability have also been seen in clay materials in which the platy grains in the dilatant areas may be expected to collapse and porosity be reduced. Arch and Maltman (1990) quote shearing as reducing porosity from 30% to 10%. They found that the permeability of samples increased as shear zones developed, if the fluid flow and shear were aligned, and decreased if they were perpendicular (Arch, 1988; Arch and Maltman, 1990). As porosity should have been the same in each case tortuosity was invoked to account for the variation (*Equation 3.4*).

It has already been noted that Equation 3.4 overestimates the effect of tortuosity by an order of magnitude for consolidation structures because of heterogeneities along the structures formed by alignment (Dewhurst *et al.*, in press). Brown *et al*. (in press) compared the permeability of consolidated kaolinite to consolidated kaolinite sheared in a ring shear rig.

They show that shear zone behaviour can be reasonably predicted with the equation, although only in the vertical direction.

Brown *et al*. (in press) found the greatest permeability was horizontally through vertically consolidated samples. Horizontal drainage for the material that was both consolidated and sheared was identical to the vertical drainage in a sample that had simply been consolidated. The two samples had the same overall void ratio. For the authors these results indicate particle alignment cannot increase permeability, though greater tortuosity may *decrease* it. However, they tested bulk samples, not individual shears, and it should be remembered that there is a logarithmic relationship between void ratio and permeability. Shear specific effects like tortuosity will be swamped by bulk effects.

The lowest permeability found by Brown *et al*. was the vertical drainage through the sheared sample, with a horizontal to vertical ratio of 25 at a void ratio of 0.85. This is in line with Equation 3.4. Brown *et al*. suggest that the tests reflect porosity decreases under shear. The situation is further complicated by shears being preferential areas for the flow of fluidized sediments, forming sediment dykes (Talbot and Brunn, 1987; Maltman, 1988; Menzies, 1990).

Long horizontal pores may form in consolidating material as the grains align (Delage and Lefebvre, 1984; Dewhurst *et al*., in press). The fact that, despite lab work, natural shears *do* appear to act as enhanced fluid flow paths led Dewhurst *et al*. (unpub.) to suggest that these pores were causing enhanced horizontal permeability (B.Clennell, pers. comm., 1996). Such pores may only form when there is an increase in the pore fluid pressure after grain alignment (Delage and Lefebvre, 1984). It is this propensity to open under reduced effective pressure which may be responsible for hydraulic anisotropy (B.Clennell, pers. comm., 1996). In traditional fracture mechanics it is presumed that there is a grading between tension cracks to shears (Price and Cosgrove, 1990). With the possible localisation of fluids in shears subglacially there is no reason why this should not be so. Freeze-thaw cycles can rapidly lead to horizontal macrochannels (mm+) in unsheared soils (Sole-Benet *et al*., 1964), and may form similarly under glaciers, closing as the effective pressure increases. Other features larger than the grain-grain scale that will effect permeability are slickenlines and broad undulations parallel to the movement direction (seen by Bryne *et al*., 1993; Maltman, 1987; van der Meer, 1993) which will affect the tortuosity of shears.

There are a number of conditions which significantly alter the permeability response of the sediment to shear strain. The nature of the material itself has an effect. For example, Bryne *et al*. (1993) found that in a sand/kaolinite mix permeability increased with strain (unlike kaolinite on its own), particularly at yield, the permeability then dropping with greater strain. This response is very similar to mixed sediments reported on in this thesis (Chapter Six). If we presume a mixed grain size distribution causes shear zone disruption it seems hard to explain why the permeability increases with greater pervasive movement. Large grains may preserve dilated areas in the manner suggested by Murray (1990).

The second major control on the permeability response is the sediment consolidation history. Consolidation itself introduces a hydraulic anisotropy (above). However, shear is much more efficient. Brown *et al*. (in press) found that it took twice as high an effective pressure to consolidate samples down to a 0.85 void ratio as it did to shear them to this ratio. Consolidation affects the development of shears. Stephenson *et al*. (in press) found that under-consolidated and normally-consolidated sediments decrease permeability with strain because the fabric compresses, whereas over-consolidated sediments increase in permeability because they dilate to strain. Some lightly consolidated sediments vary in a complex fashion during deformation, while decreasing in permeability over all. Such complexity develops as the peak strength is reached and shears develop. Stephenson *et al*. (in press) worked in terms of ‘dynamic’ permeability, which is the effective permeability measured during continuous deformation and therefore includes fluid movements forced by deformation. This viewpoint provides a more realistic understanding of active systems, such as those likely under deforming-bed glaciers. Therefore, the next section examines the dynamic considerations which such authors have revealed.

Shears as dynamic structures

When an individual shear zone forms, particles must realign. In normal and overconsolidated sediments this realignment will include some element of dilation as the grains must move up and over their neighbours. In underconsolidated and some pre-aligned normally consolidated sediments this is unnecessary and alignment occurs by compaction in the shear zone (Stephenson *et al*., in press). In saturated sediments at low stresses fluid is drawn into the shear zones as they form. If these zones then collapse this fluid is expelled (Stephenson *et al*., in press).

Such fluid movements will affect the porosity of nearby sediments (Boulton and Hindmarsh, 1987; Moore, 1989; Brown *et al*., in press), dilation possibly draining the surrounding material and inducing brittle behaviour. This is recognisable in *anisotropic* hard rocks by the development of reverse drag (*Figure 3.6*) (Platt and Vissers, 1980). In the case of glaciogenic sediments this process may be expected below a depth determined by the overburden and the fluid pressure. The latter is presently thought to decrease with depth in homogeneous sediments (Boulton and Hindmarsh, 1987; Clarke and Murray, 1991). The increase of such reverse drag with depth would be a strong indicator that such a fluid pressure regime existed in a sediment body.

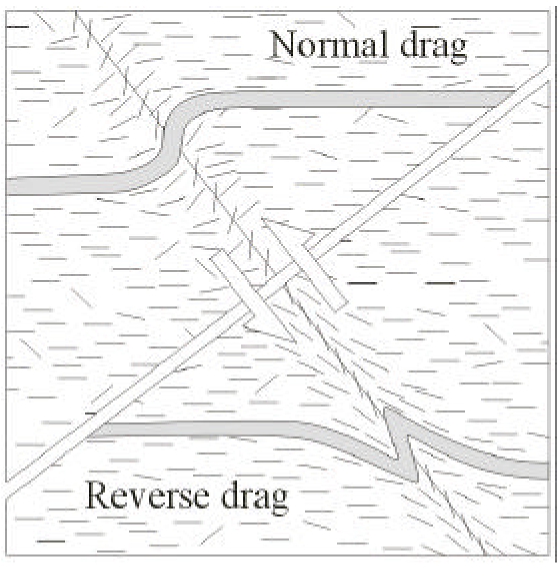

Figure 3.6 Reverse and normal shear in anisotropic rocks. Solid shaded band is a marker horizon that has no effect on material properties of rock.

3.5.3 Strength effects

The form and, therefore, strength of shears will be determined in part by the consolidation history of the sediment. The strength of overconsolidated soils is shear controlled. The shears dilate and soften, allowing further softening in these areas, dilating until they reach a stable porosity and strength (the 'critical state') (Atkinson and Richardson, 1987). Underconsolidated soils deform by compression so shears are less likely (Atkinson and Richardson, 1987), however, at some point there is a balance between the two processes. For steady state deformation the critical state is, ideally, the same for a soil tested in normal and overconsolidated states, that is, both have the same final porosity (Roscoe, 1970). The residual strength is unaffected by the initial consolidation state, though the overconsolidated sample will have supported a yield stress greater than this around yield. In reality this behaviour is only found in truly undrained situations, and shears cause local drainage (Atkinson and Richardson, 1987). Thus, we cannot say that normally consolidated glacial sediments and any overridden material that is pre-consolidated will act similarly given enough time.

Particle alignment is a crucial factor in bringing a sediment to its residual strength (Early, 1964, quoted without source by Tchalenko, 1968; Tchalenko, 1968; Maltman, 1987). However, what is equally important is the form the alignment takes. Changes in the rheology and drainage potential of shear zones are likely to be strongly dependent on the shears' overall form. The overall form of such features controls the angle the aligned grains make to the direction of the stress application and the fluid throughflow. It also controls the interconnectivity of such zones. One can only compare the response of similar geometries. Because of this fact, response to varied stress can only be compared after the development of Principle Displacement Zones (Logan *et al*., 1992). Once this point has been reached, the residual strength of the material may be constant (Brown *et al*., in press), although at high strains PDZs develop new Riedels and conjugate Riedels between them (Logan *et al*., 1992). This suggests that a balance may be reached between the residual strength of the sediment and continued shear zone formation.

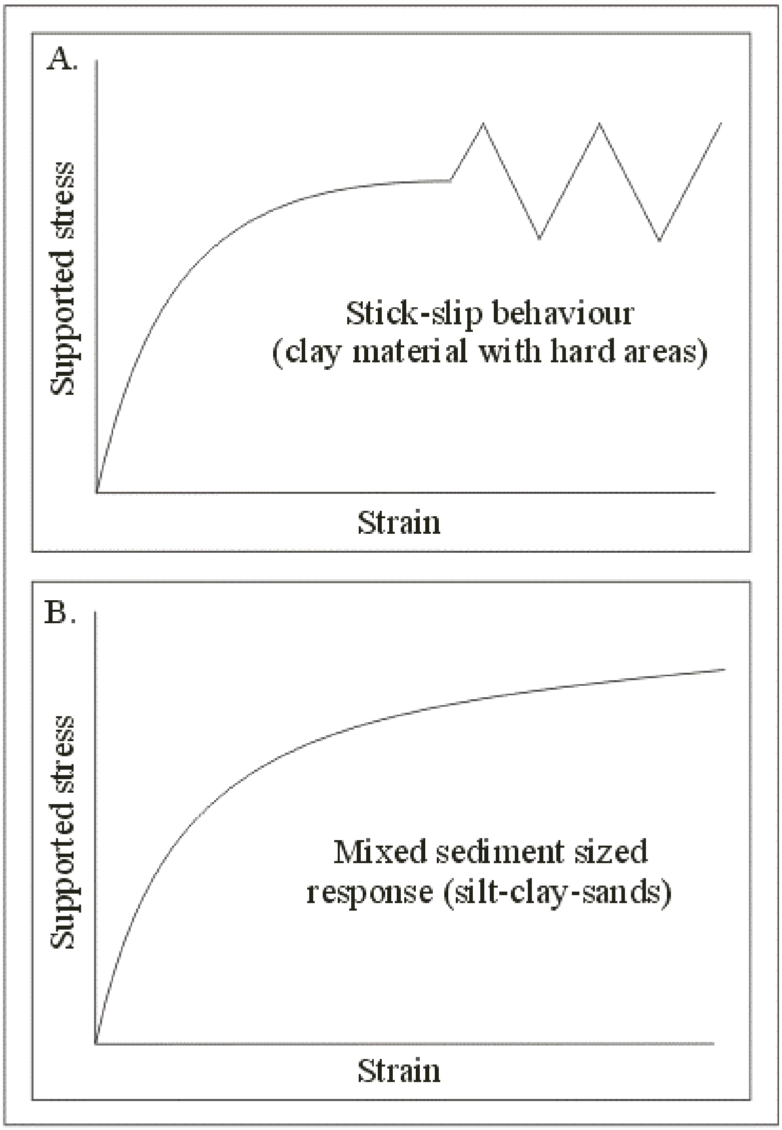

Figure 3.7 Idealised stress strain relationships: a) stick-slip behaviour b) response of mixed silt-clay-sand sediments (after Maltman, 1987, figure 1C).

In laboratory tests, both saw-cut and gouge-filled rock faults (normally consolidated) can develop stick-slip strain after a few percent of smooth movement (~3%-5.5%, Logan *et al.*, 1992). During this behaviour supported stress oscillates between high and low values (*Figure 3.7a*). The stress variation amplitude reduces with increased gouge thickness. There is no accepted explanation for this effect. It may be that lenses in the faults are strain hardening while the shears soften (Logan *et al.*, 1992), however, this would still necessitate an unexplained synchronisation of shear development. Gouge material includes fragments on the scale of the shear zone width, therefore, such stick-slip behaviour could be grain fracture events (Summers and Byerlee, 1977). This suggestion is backed up by the fact that soft materials do not display such behaviour (Simamoto and Logan, 1981). Such behaviour only develops in soft gouges at confinement pressures greater than 50 MPa (Logan *et al*., 1992), which is far higher than expected for glacial tills. However Simamoto and Logan (1981) found two important features of the behaviour:

a) it may be the presence of material compacted to rock strength in the gouge that is causing stick-slip.
b) the thicker the gouge, the more confining pressure is necessary to initiate stick-slip in fine grained material.

Both suggest that the interaction of hard areas and shears may be responsible for stick-slip behaviour, and that the confining pressure effect largely reflects the pressure necessary to produce hard patches. Such behaviour can then be imagined to occur at much lower stresses in till, where the hard areas are already present in the form of clasts. Indeed, if such a response was seen in tills under low pressures, this would be additional evidence for the effect being caused by hard patches. Such a response is tentatively outlined in Chapter Six.

Slickenlines or broad undulations parallel to shears are common in soft sediments. Slickenlines will strongly influence the friction across the shear zone as unorganised material is pushed out of the way by particles to make the grooves. Slickenlines will be highly significant in the heterogeneous diamicts under ice. In the situation where undulations develop they increase the surface area of the shear, presumably increasing the total frictional resistance (though other effects may lead to overall strain softening).

3.5.4 Disruption of shear under glaciers

Permeability and strength effects will combine to give a complex rheological response to the sediment under glaciers. The nearest analogue may be the movement of oceanic accretionary prisms (*Figure 3.3a*). The shear zone at the base of the actively moving area of the Nankai prism (East of Japan) is thought to determine the dynamics of much of the material above. This décollement affects the hydrology of the prism, raising the fluid pressure below the shear zone. The problem in the Nankai prism (one reflective of shears in general) is that the décollement is both dense enough to prevent fluid flow from below yet is weak enough that it deforms and no stress is transferred across it, that is, it is a 'dynamic seal'. One possibility is that particle alignment allows weakness along the shear zone, while preventing the flow of fluid across the zone. However, there is evidence that the shear zones act as drainage paths (Moore, 1989; Maltman *et al*., 1992). There is some controversy about the effect of particle alignment along shear zones (see above), and this has cast doubt on tortuosity as an explanation allowing both deformation and overpressuring. The present hypothesis is a cyclic change from overpressuring to movement (Bryne *et al*., 1993; Moore, 1989; Maltman *et al*., 1993b) controlled by hydrofracturing as the overpressuring below builds. In the case of glacial sediments under ice the overpressuring will probably be above the décollement, but otherwise the same problems hold if movement is on a shear zone. Equally impermeable shears may form early in the deformational history, raising the pore pressure and strain rate in the material above (Murray and Dowdeswell, 1992).

The Nankai sediments may decrease in porosity with each overpressuring cycle, increasing the chance of overpressuring (Bryne *et al*., 1993). Steady-state views of shears may also be poor for glacial sediments. In opposition to this process, healing processes could reset fault zones in 'slack' periods of movement (Logan *et al*., 1992); glacial effective pressure/water system changes for example (Menzies and Maltman, 1992). Equally subglacial shear zones may be disrupted by clasts, particularly if they move down through soft till during deformation (Clark, 1991).

Even clasts with neutral buoyancy could cause disruption if trapped and rotating in wide shear zones, leading to an increased residual strength. However, the effect of reducing drainage along disturbed shear zones would be softening of the material. Sediments of a wide size distribution have broader, anastomosing, shears (Maltman, 1987) and strain harden, displaying no distinct yield strength (*Figure 3.7b*) (Maltman, 1987, figure 1C; Chapter Six). Shear zones may expel clasts, however, in thick tills it would take a great deal of shear for this to occur. Rutter *et al*. (1986) have shown how shear stress is supported on clasts in clay-bearing gouges as their concentrations increase and the possibility of expulsion is reduced. Under their (high) pressures the grains fracture, rather than exiting the shear zones easily. Strings of material extending from soft clasts in till show that such clasts supported a force sufficient to cause them to yield, even though they were in a ductile matrix. It may be possible to quantify till residual strength from such clasts.

Clast comminution may also radically change strain patterns (Aydin, 1978; Logan *et al*., 1992). Shear could provide a mechanism for comminution in till (Boulton *et al.*, 1974; Hooke and Iverson, 1995; Iverson et al., 1996). Fractured grains are found in till, though this may be due to freeze-thaw processes. It is likely that tills become finer grained down-glacier and over time, causing more fluid to be retained and the till to become softer, with the possibility that the ice becomes thinner than expected on a hard bed. Laboratory tests show that the difference in properties between remixed comminuted material and harder surfaces leads to shears initially being concentrated at the interface between the two, then moving deeper into the sediment during work hardening (Logan *et al*., 1992; Maltman, 1987). This may explain the layered bed described from under Breiðamurkurjökull (Boulton and Hindmarsh, 1987; Benn, 1995), where there is a layer of pervasive mixing, dilatancy and high strain next to the ice, and more distinct shears deeper in the sequence.

3.6 Conclusions

The principle aim of this review has been to outline the work on the development and effect of a number of microstructures. These microstructures have been located in glacial sediments, but little significance has been attributed to them in glaciology. This review has been undertaken so that it may be referenced during the rest of this study, however, it also allows us to draw a number of novel conclusions in two areas. The first is using micromorphology to recognise glacial processes. Secondly, we can also hypothesise a number of processes that may occur glacially, but need further testing. To conclude this chapter, these conclusions are drawn out in the next section.

3.6.1 Test criteria for glacial processes

Initial deposition processes. The rarity of large domains in glaciogenic sediments so far thin sectioned suggests that the conditions necessary for their formation (low effective stresses and/or, the correct pore fluid solutes) did not occur after the structures that *are* seen were deposited. Sediments that have undergone no obvious tectonic event may display significant strain markers formed in the process of consolidation.

Pre-yield Creep. Kink banding without Principle Displacement Zones may represent pre-yield creep. Kinking can be so intense that it is mistakenly interpreted as forming under a uniaxial compression stress field, therefore it is essential the presence or absence of larger scale compressive features is included in any interpretation.

Bed deformation. Large-scale shears form in a sufficiently varied set of stress and hydrological conditions that it seems likely that they could form subglacially. The pervasive/discrete shear layering of some subglacial sediments may result from the progression of shears away from the interface between two differing materials. Infinite strain shears often bound lenses of undeformed material. Thus, low strain thin sections should not be taken as indicative of bulk finite strain without the boundaries and any resistant layers in outcrops being sampled. A non-horizontal primary fabric with Principle Displacement Zones could represent infinite shear and give information about the principle stress direction.

Deformation with a high residual strength. Thicker material requires a greater absolute shear distance to induce the same post-yield features and residual strength. In the absence of numerous Principle Displacement Zones it is possible that a high proportion of shears in the Riedel orientation represents the early deformation of a thick till deposit with a high residual strength. Thus, such microstructures would not seem to be implicit of steady-state glacial conditions. Bimasepic fabrics may develop when shear zones are constrained between, and initiated by, clasts. Soft clasts may break up through slip on Riedel and Thrust shears giving 'tails' without 'pervasive' flow.

Hydraulic conditions in deforming till. If developing shears in glacial sediments drain the surrounding material sufficiently it is possible that they may induce brittle behaviour in the local sediment recognisable through the presence of reverse drag features. A depth-dependant variation in these structures would be strong proof of a hydraulic gradient in glacial sediments. At high confining pressures Riedel shears are short, numerous, and at a high angle to the Principle Displacement Zone. Large numbers of anastomosing Principle Displacement shears may represent low effective pressures, with water contents above >25%.

3.6.2 Potential glacial situations

Changes in till permeability. Till permeability is likely to be dependent on the origin of the fluid flowing through it and the sediment. Such variation will be enhanced by the solution and redeposition of till constituents. The reduction of large inter-aggregate pores is the main change in porosity in aggregated sediments. This is likely to occur early through shear in proglacial or subglacial material. If glacial consolidation occurs, the ratio between horizontal and vertical permeability would range between five and zero. Small heterogeneities in sediment bodies may have a large drainage effect as well. On a larger scale, it is implicit in the formation of injection and gravity instability features that they bridge between two differing sets of drainage potential. The production of microchannels and slickensides during subglacial shear may alter permeability.

Sediment deformation processes. Stick-slip motion has been found in very thin cataclastic laboratory specimens of material similar to glacial sediments, and clast interactions may be responsible for such behaviour. Permeability and strength effects may combine to give complex rheological responses under glaciers, with dynamic seals developing across shear zones, or shears simply inhibiting the depth of deformation. Equally possible is that effective pressure/water system changes might ‘reset’ the sediment, clearing features. Similar resetting could be completed by clasts falling through soft sediments or caught in shear zones. The presence of ‘tails’ from soft clasts shows that they supported stresses up to their yield strength, even though they were imbedded in a ductile medium. Comminution of such material will affect glacial deformation. It is likely that the stress field changes considerably, both temporally and spatially during a glacial period. It is possible that the necessary reorientation of shears induces some shear hardening.

The rest of this thesis will examine a series of thin sections from various sites around the British Isles and laboratory tests. The information in this chapter will be used in the next two chapters to reconstruct the history of one site in North Wales. At this site there are examples of sediment that has responded to surrounding conditions passively, but also material that shows signs of having controlled the movement of the glacier over it. The former case is explored in the first of the next two chapters.

4. Historical reconstruction from micromorphology: a case study from the Lleyn Peninsula, Wales

4.1 Introduction

Understanding the causes of microstructures (Chapters Two, Three) and recognising their spatial relationships allows us to reconstruct the environmental history of deposits. In this chapter the environmental history of a deposit at Criccieth, North Wales (*Figure 4.1*), is reconstructed in more detail than is possible using macroscale features. Such studies are all too rare, partly because of our ignorance as to the causes of microstructures, and partly because of a lack of confidence in microstructural homogeneity on a larger scale. Both views can be attributed to the youth of microstructural research. Such interpretations are, in fact, reasonable - if care is taken over their application. While it is essential that further studies are made of heterogeneity within small areas of outcropping glaciogenic sediments, it should be remembered that the same scale differences are encountered in other branches of geology.

The Quaternary deposits of the Lleyn peninsula, in North Wales, have been the source of much controversy. Past discussions centred on the number of terrestrial glaciations in the area (Saunders, 1968 vs. Boulton, 1977). However, present interest in the peninsula stems from an older debate; that between the supporters of terrestrial glaciations and glaciomarine floods. Eyles and McCabe (1989) have split workers by suggesting that the Irish Sea deposits are glaciomarine (*Figure 4.1*). This origin would add weight to the theory that the last major deglaciation ($\delta^{18}0$ Stage $2 \rightarrow 1$) was so rapid because the edge of the major ice sheets were floated from their beds (Broecker and Denton, 1990). With this in mind, it has been realised the Lleyn may represent a perfect laboratory for glaciologists to determine the controls acting to produce major deglaciations.

Naturally, the two debates have become mixed for much of the peninsula. Many areas that were once interpreted as recording two glaciations have been reinterpreted as a lodgement sequence overlain by glaciomarine material (Eyles and McCabe, 1989). However, the debate has also become mixed on a more unconscious level. Traditionally the peninsula has been divided into two regions; the west/north, which was overridden once or more by Irish Sea ice, and the east/south, overridden once or more by Welsh ice from South Snowdonia (*Figure 4.1*). As the glaciomarine reinterpretation has focused on the Irish Sea deposits in Ireland, the same deposits have been studied on the Lleyn (Eyles and McCabe, 1989; McCarroll and Harris, 1992; B.G.R.G. Subglacial Working Group meeting, 1995). The east/south are still regarded as terrestrial, despite the fact that any marine transgression associated with the Irish Sea Ice is likely to have also affected the area only a matter of kilometres to the south west.

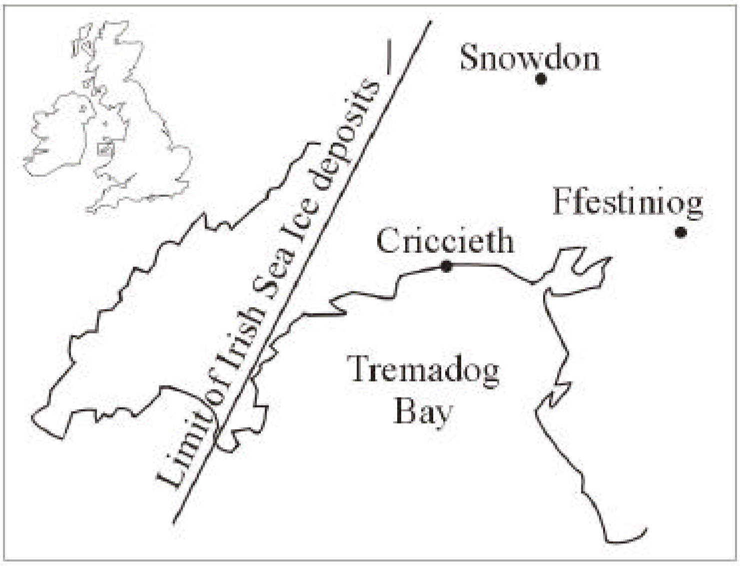

Figure 4.1 The Lleyn Peninsula, North Wales, showing the eastern limit of material deposited by Irish Sea ice in $d^{18}O$ stage 2 (position within United Kingdom and Eire inset).

With this background in mind a site in the south west of the Lleyn was picked for an assessment of the use of micromorphology in distinguishing the environmental history of glaciogenic sediments, in particular a deposit which may have undergone a 'passive' reaction to the stress and hydrological changes it experienced (rather than affecting them). The mechanical response of such a sediment should be simpler to interpret in terms of the surrounding conditions than a sediment that has actively fed back to affect those conditions. Such more complex situations will be dealt with in future chapters.

The deposits around Criccieth on the south coast of the Lleyn have been the subject of discussion for almost a century. They have variously been described as representing one (Boulton, 1977), two (Fearnsides, 1910) and three (Saunders, 1968) terrestrial glaciations. This chapter first attempts to collate and correlate in one place the information on the macroscale sedimentology of the area; more specifically the sedimentology of the microstructural sample site. This information is then compared with a detailed outcrop and microscale study to determine the nature of the deposits. This study uses two techniques. Understanding the *processes* involved in the formation of the microstructures allows us to bracket the likely conditions in which the deposits formed. The *spatial relationships* of the microstructures then allow us to reconstruct the temporal progression through the suites of possible environments in a way that gives considerably more detailed information than previous macrostructural studies of the area.

4.2 The deposits and their relative chronology on the basis of outcrop scale sedimentology

The outcrop in question lies to the East of Criccieth on the South coast of the Lleyn Peninsula, between the town and the sea cliffs (SH507381, *Figure 4.2*) (for details of the surrounding areas see Saunders, 1968; Matley, 1936; Boulton, 1977). The deposit will be referred to here as the 'bay middle' deposit. The two dimensional form of the outcrop is stratigraphically and topographically similar to outcrops locally described by Boulton (1977) as drumlins buried by flow material (*Figure 4.3*). However, the internal structure of the deposit is unusual, and does not match the topographic inversion seen by Boulton.

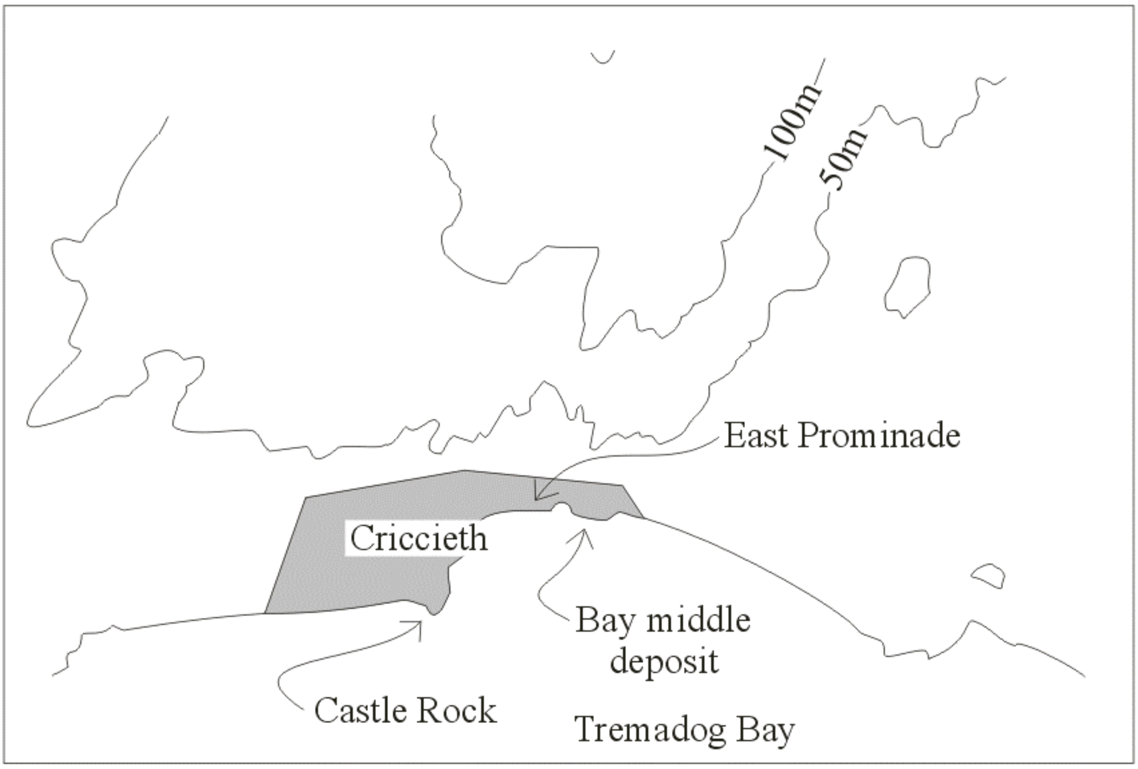

Figure 4.2 Locations around Criccieth, North Wales, showing the position of the 'bay middle' deposit examined in the text.

At present, the deposit is lobate, rising above the level of the surrounding bay. The broad upper surface gently slopes inland, joining the hill rising under the eastern outskirts of Criccieth (*Figure 4.2*). The three dimensional form is unknown below the surface. The two dimensional outcrop consisting of several lithofacies in an anticlinal form, at least in the case of the upper three lithofacies and the lower blue grey diamict (*Figure 4.3*). However, the general anticlinal form belies considerable complexity both within and between lithofacies, particularly between lithofacies D and E.

4.2.1 The sediments

Figure 4.3 shows the sedimentary character of the feature. A near complete cross section above sea level was available during fieldwork in 1993 and 1994.

The outcrop scale sedimentology is;

Lithofacies A: fine silt/sand layer with localised disturbance.

Lithofacies B: clast supported diamict of slate, which fills a frost wedge in lithofacies C and has an involuted boundary with lithofacies A.

Lithofacies C: massive matrix-supported but clast-rich diamict yellow in colour. Clast fabric is random (Grant, 1990).

Lithofacies D: massive matrix-supported but clast-rich light yellow diamict with an weak clast fabric (Grant, 1990).

Iron stained boundary

Lithofacies E: massive blue clay-rich matrix-supported diamict.

The same sequence is seen west of the Castle Rock (SH500377) in Criccieth and as far as Glanllynau (*Figure 4.2*). However, on the eastern side of Castle Rock the sequence is reduced to 25 m of lithofacies C/D, with no other visible beds (though bedrock cannot be seen). Houses are situated on the edge of this small outcrop so it is possible lithofacies A and B were removed before foundations were laid here, being both structurally unsound and horticulturally poor. Further towards the outcrop studied here, the sequence under the town's east promenade (*Figure 4.2*) was revealed by deep foundation placement in 1994. Though the material is certainly glacial, the deposition could be glacial, proglacial, or from the construction of the promenade;

Lithofacies X: dark grey clay without clasts (2m).

Sharp boundary with 2m boulder embedded between the clay and diamict.

Blue dark grey massive matrix supported diamict (2m).

Gravely yellow clast rich, though possibly matrix supported, diamict (2m +).

It was impossible to sample the sediments therefore a visual comparison only can be used. This suggests that the section revealed lithofacies E and D/C, but that they were inverted, and that lithofacies X is astratigraphic and anthropogenic. Stratigraphic inversion is seen elsewhere in the sequence (below). It should be noted that the surface of the blue diamict thus represents an erosional boundary and could not be expected to contain the features associated with boulders in Chapter Five.

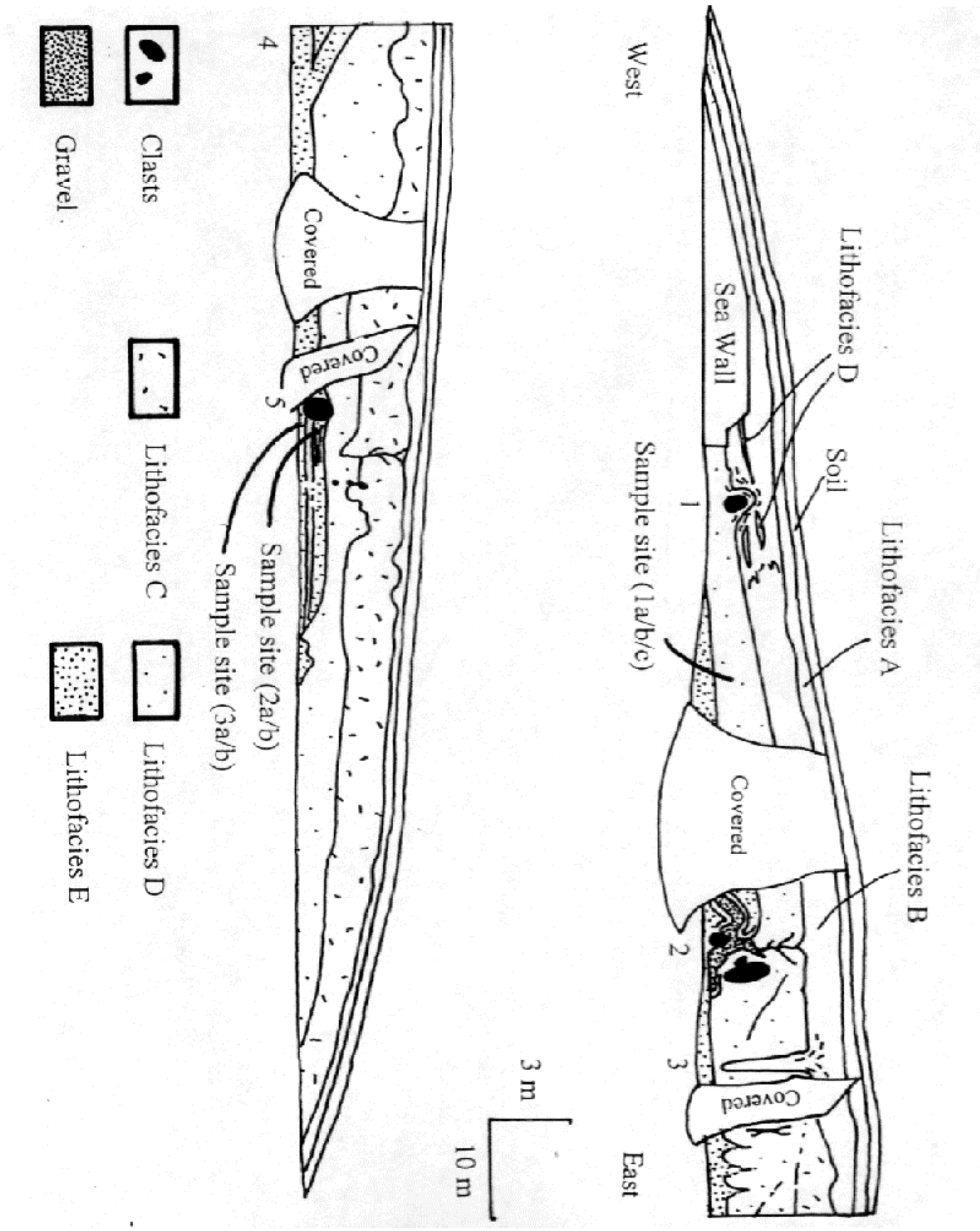

Figure 4.3 Outcrop profile for the 'bay middle' deposit at Criccieth, North Wales.

4.2.2 Previous interpretations

The area has been studied and interpreted by other authors. However, the variation in descriptive techniques means it is difficult to reconcile the 'bay middle' sequence with any of the accounts. Saunders' (1968) sequence describes similar sediments, but with additional stratigraphic layers. Grant's (1990) sequence has a similar stratigraphy, but differs in sediment description, despite using the same scheme (Eyles *et al.*, 1983).

The specific location described by Saunders at Afon Wen is now covered, however, 300m to the east the laminated outwash sands and gravels he describes *can* be seen. These coarse deposits can be correlated with Grant's laminated silts and gravels further east at Glanllynau. The correlation is only tentative, and should be contrasted with Matley's (1936) claim that both areas are included in a 50 ft (13.9 m) terrace. Matley suggests the terrace is formed from gravels *above* glacial sediments, making the correlation of the gravels untenable. Matley's claim is, however, based on the continuity of this landform rather than stratigraphy. If the correlation outlined above *is* accepted the regional stratigraphy given in

Table 4.1 is gained.

The sedimentological conditions described by Boulton (1977) are considerably more complex, but the complexity is wholly local.

Afon Wen Saunders	**Glanllynau Grant**	**Criccieth Grant (probably East of Castle Rock)**	**Criccieth Saunders (probably West of Castle Rock)**	***Figure 4.3***
Peat + Gyttja			soil	soil
				lithofacies A: fine silt / sand
	Dcm			lithofacies B: + Dcm slates
		erosion surface		frost wedge forms
upper gravely till	Dcm	Dcm	upper gravely till	lithofacies C: Dmm - yellow clast rich random diamict
				lithofacies D: Dmm - clast rich light yellow diamict
gravel + sands	gravel + silt			
weathering horizon + frost wedges		erosion surface	weathering horizon	Fe staining + deformation structures
blue grey slatey till	Dmm	Dmm	blue grey slatey till	lithofacies E: Dmm - blue grey diamict
			head	lithofacies F: unfound
			soliflucted till	lithofacies G: unfound
			head	lithofacies H: unfound

Table 4.1 Regional correlation of sediments described in different studies carried out in the Southern Lleyn Peninsula.

Table 4.1 can be shown to give a regional stratigraphy that is in line with Boulton's three-dimensional mapping whatever ultimate interpretation is applied to it. It seems likely that the sequence observed by Grant and the 'bay middle' deposits are one and the same. As bedrock is not visible in the middle of the bay, nor is likely to have been in the past, it seems reasonable to suppose Saunders' exposure was to the west of Criccieth where a similar sequence to the bay middle deposits exists. Here there are no bedrock outcrops, but vegetated inactive cliffs may be obscuring the section. Fearnsides (1910) records the sequence on both sides of Castle Rock as boulder clay resting on angular unworn talus with "a scree-like stratification", under which is a wavecut platform a few feet above the present tide. This description matches Saunders' sequence. Both sides of Castle Rock are now covered with sea defences.

Lithofacies	**Possible environments**	**Reasoning and caveats**
A	Periglacial loess	A micromorphological study would probably not confirm this, the less permeable materials below having encouraged subsurface flow illuviation and particle reorientation. These processes will have removed delicate aeolian structures.
B	Periglacial solifluction material	Evidence of mass movements and small (~1m) stream deposition. Fills frost wedge (3; Fig. 4.3) without slumping structures and the material involuted at surface. The material is draped over, rather than around the large clast at '1' (Fig. 4.3) suggesting mass movement deposition rather than the deposition of individual clasts in a fluvial environment. West of Castle Rock lithofacies B contains boulders and occasional sand lenses (~1m length) suggesting a highly active environment of streams and mass movements, a hypothesis in line with Boulton's (1977) reconstruction of the area further west at Glanllynau.
C	Periglacial cryoturbation of lithofacies B and D.	Present only where B is absent and D is reduced. Cryoturbated fabric with a high angular slate content. Frost wedge at 3 (Fig. 4.3) suggests depth for periglacial action. West of Castle Rock the boundary with E has clast concentration suggesting fluidization of D or a fluvial event.
E	Glaciogenic sediment flow (Boulton, 1977; Grant, 1990) or Lodgement till (Saunders, 1968), or flows under lake / marine conditions (Matley, 1936).	Clast orientation eigenvectors cover the first two possibilities (Grant, 1990). See text for further discussion.
F	Subglacial till (Grant, 1990; this chapter, Chapter Five)	It seems unlikely given the exposure of the site that this formed under a pre-Dimlington stadial (δ^{18}OStage 2). See text for further discussion.

Table 4.2 Potential environments represented by the Southern Lleyn sediments

Given this correlation, Table 4.2 is an outline of the possible environment each lithofacies represents.

Interpretative clashes involving the sediments revolve around both the environments and history they represent. These arguments are compared below.

Lithofacies D : yellow, clast rich, matrix supported, massive diamict

Lithofacies D has a weak southerly dipping fabric, with eigenvectors suggesting glaciogenic sediment flow, deformed or undeformed lodgement till (Grant 1990). Grant suggests that the material is a series of flow deposits formed on top of margin-parallel buried ice ridges, in line with Boulton (1977). Saunders (1968) suggests a lodgement till, and provides evidence that for some of the area covered by lithofacies D, glacial retreat was active rather than by stagnation as suggested by Boulton (1977). The layer is continuous over much of the south eastern Lleyn, with a fabric which sweeps from north-south at Glanllynau to a 080-260° fabric at Afon Wen (Saunders, 1968) (*Figure 4.4*). To fit the Boulton/Grant model, the deposit at Afon Wen would have to infer a change in the orientation of stranded ice ridges to 080-260°. If the ridges reflect the orientation of the ice margin, as Boulton suggests, this change in orientation may indicate a late-glacial piedmont glacier spreading into Tremadog Bay during deglaciation.

An alternative explanation is a lobe of material flowing from the high ground to the north of Criccieth. Matley's (1936) stratigraphy is impossible to relate to any local sequence, but he suggests all the material above a basal boulder clay (lithofacies E) was deposited in an ice-marginal freshwater lake during the last deglaciation. Such an interpretation must also include the glaciomarine option. Such deep water origins could plausibly explain the deformed internal nature of the sediments (through slumping) and the regular surface expression of the deposits. Whatever the explanation, it must also account for the claim by Saunders that the layer exists at Crugan 10 kms further west than Afon Wen.

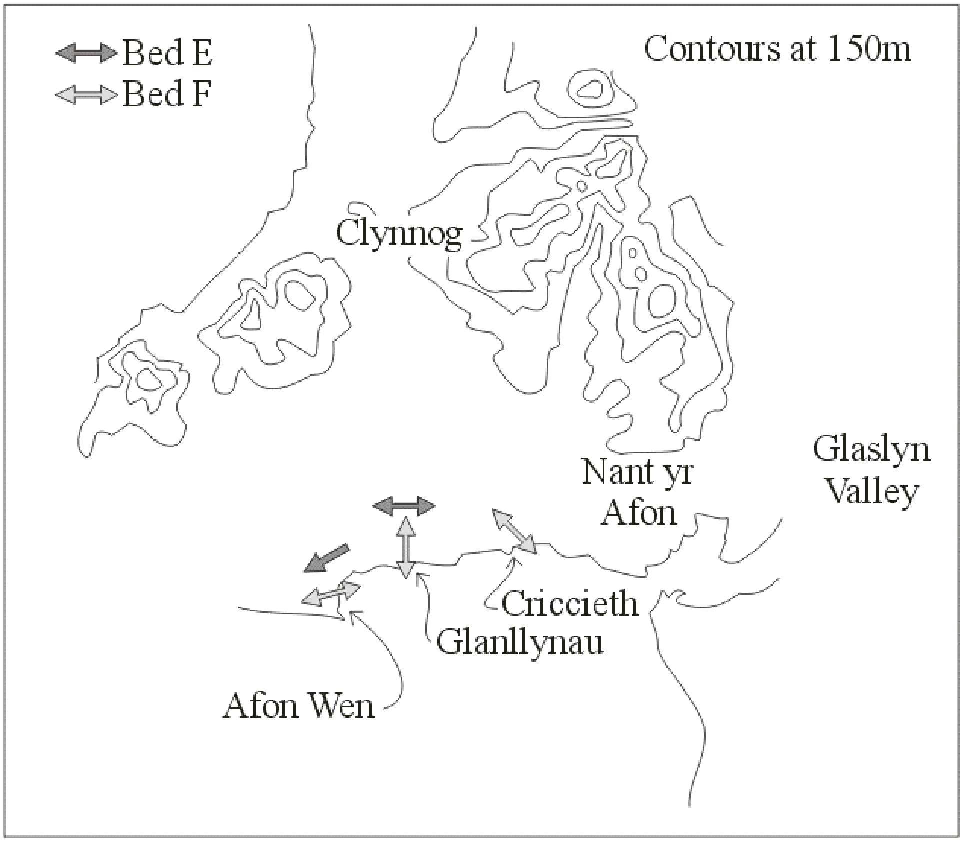

Figure 4.4 Eastern Lleyn Peninsula showing direction of pebble fabrics in lithofacies D and E described by Saunders, 1968, Boulton 1977, and Grant, 1990.

The deposits' identification as a subglacial deposit formed in a glaciation after that depositing lithofacies E (Saunders, 1968) relies on two lines of evidence. Firstly, the presence of frost wedges in the sequence (lost beneath 'Butlin's') at Afon Wen (Saunders 1968) and Glanllynau (D. Evans, *pers.comm*., 1995). These features are said to represent a significant time period between the two diamicts D and E. However, in contrast to Saunders' claim this period does not have to be a full interglacial. In addition, the frost wedges at Glanllynau are similar in form to a possible fold feature that will be discussed below. The second line of evidence for an interglacial is a proposed iron stained 'weathering' layer at the top of the lower diamict (Saunders 1968). It will be shown in the micromorphological study below that such layers could also have formed either subglacially or in a short periglacial period. The 'outwash' gravels and sands/silts in the sequence provide no useful information in this context. They are on the southern margin of the deposition area associated with a col to the far north in Clynnog (SH450480, *Figure 4.4*). Ice must have abutted the northern hills at the time the sands were deposited in the ice-free South. Such a situation is in line with the glaciomarine theory, in which ice retreats north-south in the Irish Sea, however, casts little light on the nature of the lithofacies D.

Lithofacies E: stiff blue-grey matrix supported, massive diamict

At Criccieth, this diamict is at least *partially* a glacitectonite derived from laminated muds (D.Evans, *pers,.comm*., 1997). It has generally been recorded as massive, however, very fresh, storm erroded, sections are needed to see any laminations (D.Evans, *pers,.comm*., 1997). The diamict has a varying clast orientation along the coast from NNW-SSE east of Criccieth to E-W at Glanllynau to movement from the NE in Afon Wen (Saunders, 1968; Boulton 1977; Grant, 1990) (*Figure 4.4*). All the fabrics measured in the literature are more strongly clustered than in the higher diamict. The regional orientation change could be reconciled with the traditional picture of ice moving out of the Ffestiniog Vale and splaying into Tremadog Bay (*Figure 4.1*) by considering ice movement onto the coast at Criccieth, and its deflection along the present coastal plain at Glanllynau and Afon Wen by the topography immediately inland. Alternatively, Fearnsides (1910) suggested the material was deposited by western ice that had passed over the Lleyn and was forced inland from Tremadog Bay. This position should be respected given the author’s extensive knowledge of the area’s geology, however, it seems more likely that the northern material was reworked from glaciofluvial deposits. Boulton (1977) has also suggested ice flowing from the north. Both views are repudiated by Fearnsides’ own work which suggests a considerable ice thickness in the Glaslyn Valley and over Nant yr Afon valley (SH550400, *Figure 4.4*). Striations and erratics suggest the ice moved down the Glaslyn Valley from Snowdon (*Figure 4.1*), and stopped ice moving from the north at Criccieth.

The diamict contains heavily weathered erratics which Saunders (1968) took as evidence for the deposit including glacial material older than itself. Such a boulder is seen at point 5 on Figure 4.3. Here weathering is continuous across striations, suggesting weathering occurred after the glaciation associated with the deposit. The hypothesis that the deposit itself is older than the last glaciation seems unlikely in such an exposed area, though the sediments could have been protected from the Late Devensian ice by the gravel deposits of Matley (1936). This would make his terrace surface of Ipswichian (δ^{18}O Stage 5) age.

In conclusion, it is impossible to gain any satisfactory origin for the deposits from the macroscale sedimentology, the literature, or the implications of the information contained within it. Thus, in the next section outcrop and microscale structural evidence is presented with the aim of elucidating this controversial area.

4.3 The macrostructure

4.3.1 Folding

Description

At point '2' on Figure 4.3 lithofacies E overlies lithofacies D, either as a sheared off block or a nappe (see *Figure 4.5* and *Figure 4.6*). In section the feature appears to originate to the north west. After, or as a part of this deformation, the lithofacies have been folded into an open parallel form (*Figure 4.5*). Neither compressional event is represented elsewhere in the Southern peninsula, with the possible exception of under the East Promenade at Criccieth (see above).

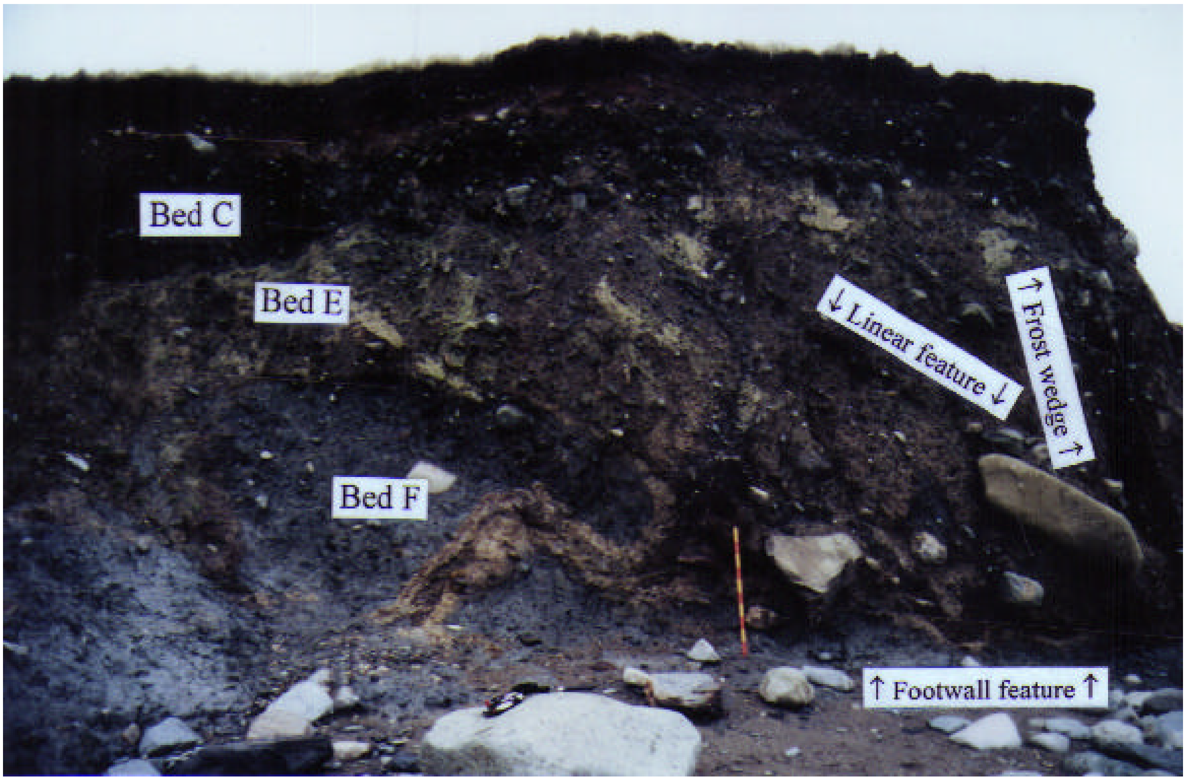

Figure 4.5 Features in the Criccieth 'Bay middle' deposit. Note what appears to be a recumbent fold of blue diamict (lithofacies E) in the centre of the picture. The centre of the fold is filled with darker clastic material in a light envelope. Similar material can be seen in a smaller structure just above lithofacies E to the right of the photograph. A dark frost wedge extends through the sequence in the far right of the picture.

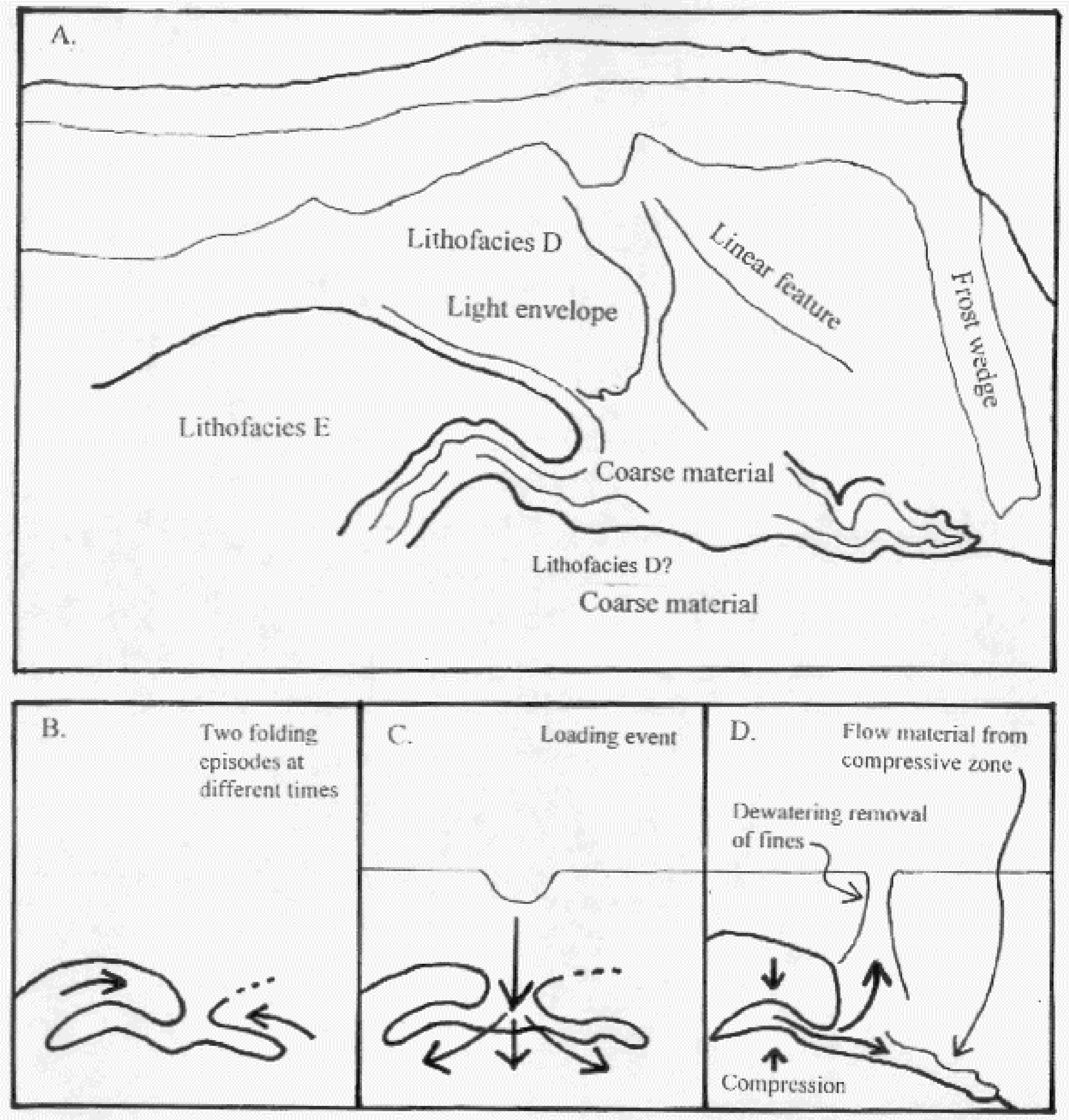

Figure 4.6 a) The main features of the 'fold' structure. Possible explanations: b) two folding episodes, c) loading, d) slump complex.

The ‘fold’ is unusual, in that the fold interior, which one would expect to be filled by lithofacies D, is composed of iron stained clastic material surrounded by an envelope of light material around 15 cm thick. This clastic layer spreads up out of the fold, through lithofacies D, thinning and arboressing until the boundary with the overlying slate lithofacies B (though this example has proved hard to photograph, an equivalent is shown in *Figure 4.7*). A second strange feature of this ‘fold’ suite is the small fold-like structure lying on the surface of the footwall of lithofacies E. The nose of this faces south east (in outcrop) and it has a similar internal sedimentology to that of the main fold.

Figure 4.7 Part of an arborescent clast concentration in lithofacies D.

Interpretation

The combination of clastic material and light envelope matches descriptions of frost-wedges elsewhere (Saunders, 1968). However, this interpretation cannot account for the absence of the light layer elsewhere in the section. Nor can it account for the extension of the clastic material up through lithofacies D. The frost-wedge interpretation of these features is also in doubt at present (D.Evans, *pers.comm*., 1997).

The structural suite could be a double fold, though the change in stress direction necessary to form the small footwall ‘fold’ would demand explanation. Equally, the whole suite of structures could represent a cross section through a loading structure, with the clastic material moving into lithofacies E in two directions while it was weak. However, neither explanation satisfactorily accounts for the arborescent structure of the clastic material in lithofacies D. A more complete explanation interprets the major fold as having supplied dewatering fluid during the folding strain. This fluid dewatered upwards to form an arborescent dewatering channel. Some fines were probably removed from this channel during the deformation, while the remainder were removed more recently by water percolating through this porous zone.

Under this interpretation the clastic material left in the fold interior represents a fluid-supplying gravel bed within lithofacies D (which explains the localised deformation), or material from either lithofacies with the fines washed out. The smaller ‘fold’ is interpreted as clastic material that has flowed out of the larger fold and down the sloping footwall of lithofacies E. The consistencies of the materials involved demands that the light layer around the clastic fold interiors is a postdeformational weathering 'rind' around the highly permeable clastic material. The envelope cannot be translocated fines as the clastic material flowing to form the second ‘fold’ would have sunk through such material.

The consistencies of the materials also demand that the feature formed under gravity. lithofacies E must have been hard enough to fold rather than move more pervasively. lithofacies D must have been weak enough to allow material to move out of the fold interior and down the footwall (ie. probably extremely saturated and easily fluidized). However, if the strain was caused by lithofacies D overriding lithofacies E, lithofacies D must also have been strong enough to maintain the stress necessary to cause the fold. The stress problem becomes redundant if the original nappe/sheared block formed under gravity as a slope deposit, overriding the clastic material. The most obvious situation these conditions could occur in is a deep-water environment. It seems unlikely that such a feature could be produced under the force of the proglacial flows proposed by Boulton (1977) to account for lithofacies D.

The simplest explanation for this complex feature is therefore a fold episode associated with a landslip and weathering. It is interesting to note, as a further complication, that there may be a boundary in the yellow diamict dipping at ~45° in the same direction as the fold, starting just east of the top of the arborescent structure (we are not able to gain a chronology as the two do not interfere). The boundary is marked by large boulders, or possibly suggested by their coincidental positioning. Exploited boundaries *are* seen in lithofacies D to the west of Criccieth castle. These dip in 3D towards the beach at 40° (south) and may be related to Grant's weak lithofacies D southerly fabric. Note, also, that Grant’s NNW-SSE fabric for lithofacies E matches (is explained by?) the fold direction. The fold thus contradicts the suspected ice flow east of Criccieth for lithofacies E from Glaslyn Valley, but it does not contradict the regional flow of lithofacies D, suggesting it is post-glacial.

4.3.2 Contacts between lithofacies.

Description

At area ‘4’ on Figure 4.3 lithofacies E appears to rise and merge with lithofacies D in a ramp of matrix supported material which has a recent landslide base as its upper surface and has been undercut at its base to reveal lithofacies E.

The boundary between lithofacies C and lithofacies D varies considerably around area ‘5’ on Figure 4.3. There is an unusual step in the boundary down to the East. Along this step runs a vertical anastomosing pebble fabric similar to that attributed to dewatering with respect to the fold above (*Figure 4.7*). The fabric leaves the stepped boundary and continues up to, and fans out at, the base of lithofacies B. Downwards, the fabric splays at the base of the step where it meets lithofacies E.

Interpretation

Difficulty in mapping due to landslips make an accurate assessment of Area ‘4’ on Figure 4.3 difficult, they particually obscure the boundary between the ramp and lithofacies E. It is possible the ramp material is lithofacies D after weathering.

Area ‘5’ on Figure 4.3 appears to confirm the periglacial mixing hypothesis for the origin of lithofacies C (note the depth of post-depositional frost wedge at '3'). The inclination would be to attribute the variations of the boundary to buried ice melt following Boulton (1977) and Grant (1990). However, the fabric may be associated with the consolidation dewatering of coarse material deposited at the top of lithofacies E below this step. This coarse material is further described in Chapter Five.

In conclusion, the deposits are very complex on a small spatial, and probably temporal, scale. Many of the section's structures have never been recognised in other deposits, or have been recognised but misinterpreted or passed over. It seems likely that more detailed structural and sediment mapping will reveal the solution to a number of the problems posed above. However, the most promising technique available, which has never been used in the area, is the micromorphological study of the features and sediments. As this remit of this thesis is micromorphology, it is to this technique we now turn.

4.4 The micromorphology of lithofacies D and E

4.4.1 Sampling and methods

A hand-sample was taken from lithofacies D (location *Figure 4.3*). All sample material in this thesis was taken after between 50 to 100 cm of material was removed from the outcrops in question to limit recent damage. The sample was of a fine, yellow, silt with no visible structure. The sample was sectioned orthogonally to gain two orientated thin sections. The poor thickness of one sample led to a second thin section being cut despite the adequate quality of the former section for fabric analysis. Thus three thin sections were examined to see if they could cast any light on the controversial nature lithofacies D. One section is orientated north west to south east (section 1a) and two are orientated north east to south west (sections 1b and 1c). There were no clasts larger than the final thin sections within 20 cm of the sample site. Thus, it might be suggested that any clast effects on the thin sections would be characteristic of the whole sediment. Any local effects from small clasts would grade across the thin sections. Such gradients were not found and the samples are therefore regarded as representative.

A hand-sample was also taken from lithofacies E (location *Figure 4.3*). The sample was of blue-grey clay silt, with no visible structure, and sectioned orthogonally to gain two orientated thin sections. One section is orientated east-west (section 2a) and the other north-south (section 2b). While these samples were taken to prove a prediction outlined about a specific feature in lithofacies E discussed in Chapter Five, they reflect on the general sedimentology of this lithofacies too, and are discussed in this context in this chapter.

All the thin sections in this thesis were prepared by T.Ridgeway, in the Institute of Earth Studies, University of Wales, Aberystwyth, with (limited) assistance from the author. A close approximation to the preparation process used has been given by Awadallah (1991). The production of slides follows six stages.

1) The hand-specimens are trimmed down to rectangular prisms with sides of ~2 cm with a sharp knife attempting to minimise disturbance by avoiding stressing larger clasts and pulling material away from the prism's faces, rather than 'slicing' (in this case this work was undertaken by the author).
2) The material is placed into containers that extend above their tops, which are marked with the sample orientations determined in the field. These are then covered with epoxy based resin ('Epo-thin', supplied by Buehler Ltd, University of Warwick Science Park, Coventry, is recommended, but the resin used in this thesis varied), and placed in a vacuum oven at ~30°C. This oven draws air out of the samples, which become impregnated with the resin. This resin then cures over the course of a day.
3) The samples are cut down to the approximate size of a microscopy slide and the top 2 to 3 mm of one side of the sediment trimmed off using a oil lubricated cutting wheel (water based systems as used in hard rock sectioning are unsuitable for use with resin impregnated samples).
4) The trimmed face of the slide is examined, reimpregnated if necessary (ie. if there are patches that have not taken up resin), retrimmed if necessary, and polished on a diamond paper polishing wheel. This face is then stuck to a microscopy slide with epoxy resin and clamped while it cures at room temperature to ensure temperature changes do not crack the glass.
5) The sample is then trimmed down to ~ 2 mm thick with a cutting wheel and hand ground to 1 to 2 grains thickness on oiled diamond paper of increasingly fine grains. During this process the slide is continually checked.
6) Finally, a cover slide is stuck to the slide with epoxy resin, again clamped at room temperature.

Preparation-induced features of the thin sections include;

a) resin discoloration;

b) sample cracking;

c) the removal of grains during coarse trimming (which may then spin locally within the sample causing damage);

d) air bubbles;

e) trimming disturbance prior to impregnation.

All are rare, with the exception of (e), which is seen around the edge of samples. All are also easily recognised and discounted.

The samples in this thesis were examined using a petrographic microscope (Olympus B201), unpolarized, plain polarized, and cross-polarized light and cross-polarized light with a 'tint' or '$^1/_4$ wavelength' plate. The latter splits the mixed wavelength light that passes out of most minerals under cross-polarised conditions such that finer colour distinctions can be made, that is, slides appear to be highly coloured, rather than the more typical grey-scale. These 'birefingence colours' allow mineral identification and assessment of grain alignments. Grains orientated in a single fabric direction all change colour at the same time as the slide is rotated within the polarized light. Once such an area has been located, the grain orientation can be assessed by examining the individual grains at a higher magnification.

The synchronous colour change of such aligned areas allows us to recognise simple patterns of alignment within sediments. Plainly, our ability to recognise patterns will be partly determined by our previous experience (in a cultural rather than an individual sense). A review of the problems of pattern recognition is beyond the remit of this thesis, and the reader is recommended Bruce and Green (1990) for a full review. Lengths and population numbers in this thesis are determined by 100 random point counts where possible. In the cases where several slides were taken from one site, the slides were described 'blind', that is, without knowledge of their position within the sequence, though additional measurements were made after a hypothesis was put forward involving the sediments if necessary.

4.4.2 Description (lithofacies D)

Section 1a (see *Figure 4.3* for sample site) has a strong omnisepic fabric with an apparent dip 45° down to the north west (*Figure 4.8*). This fabric fills all the spaces between other fabrics, and areas of stronger fabric within it are split and shifted by later shear events. The fabric is therefore presumed to precede all other fabrics seen in the material. The event forming this fabric is denoted as the Primary Fabric Event. There is a strong and discrete shear fabric developed with an apparent dip orthogonal to the primary fabric, in which the fabric has reoriented so that mineral grains are approximately vertical (Shear Event One) (*Figure 4.8*). This fabric suggests sinistral displacement and this interpretation is backed up by the movement of the slight heterogeneities in the primary fabric. These shears are further displaced by discrete linear zones of strong primary fabric alignment (Shear Event Two) suggesting later dextral shear in the primary fabric direction.

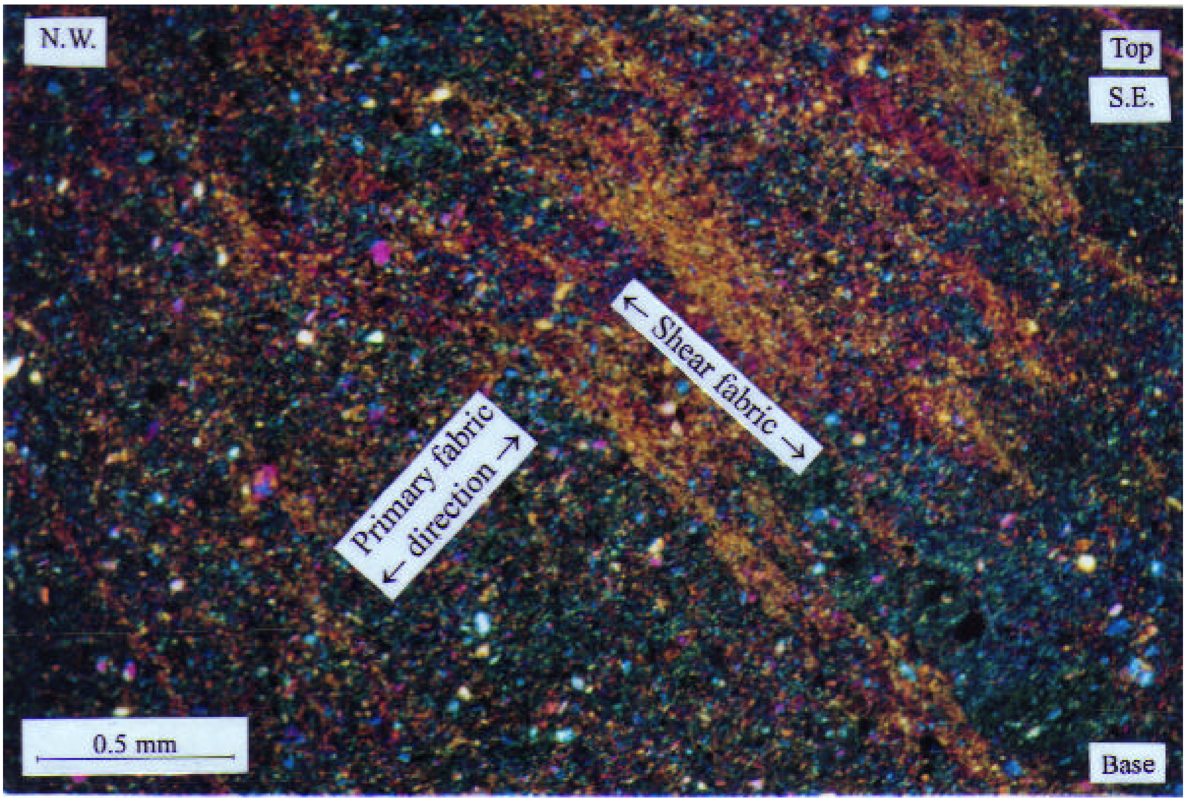

Figure 4.8 Tinted polarized micrograph of section 1a (vertical section from north-west to south east) showing strong north-west dipping primary fabric (blue-green) and a shear fabric dipping south-east (yellow).

Iron staining is present in Section 1a. This is not unusual in Quaternary thin sections which will have suffered some pedogenesis (Chapter Two). However, as shall be shown, in this sample staining is of chronological significance. In section 1a, the staining shows an intensity gradient building up to a boundary, below which there is no staining. This pattern is as expected, iron being deposited along very mild fluid restricting layers or at the limit of travel by capillary action or under a pressure gradient. However, the boundary often has gaps, after which the boundary gradient is reversed to below the boundary (*Figure 4.9*). Figure 4.10a shows the boundary orientations across the slide.

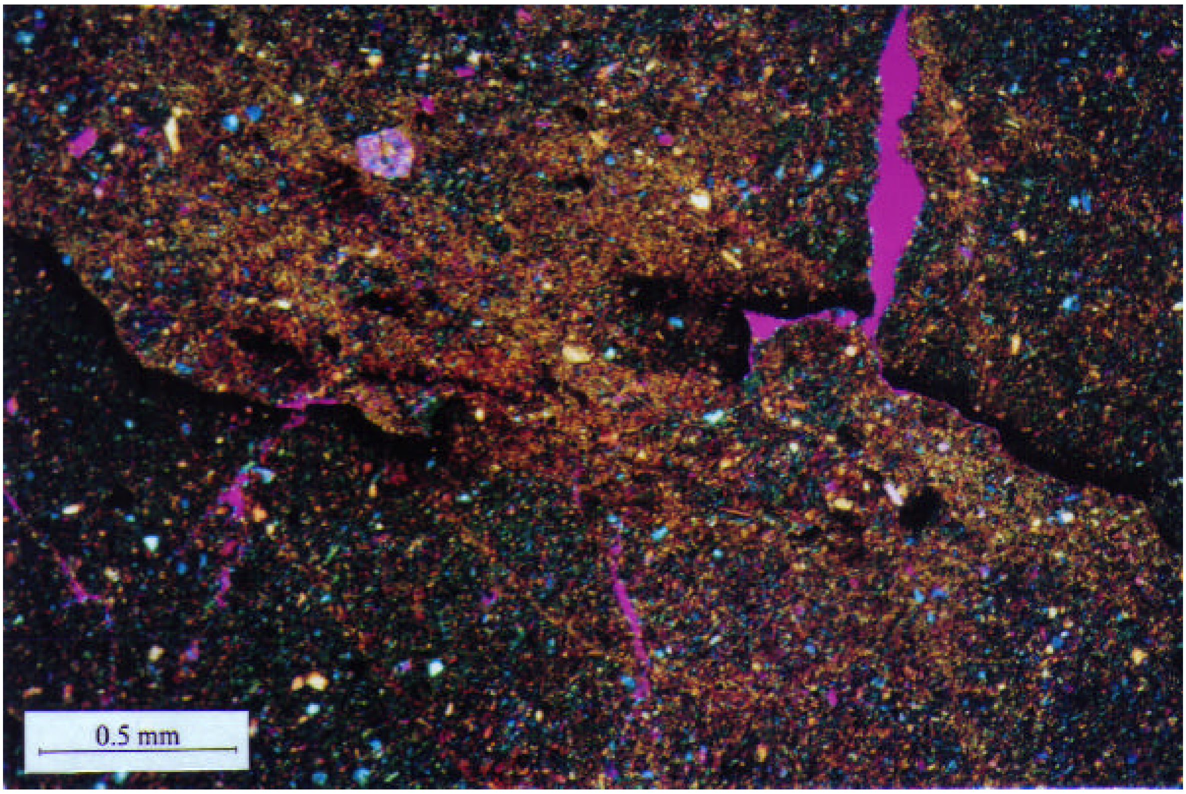

Figure 4.9 Tinted polarized micrograph showing part of the iron stained boundary (brown-black) in section 1a (vertical section from north-west to south east).

Sections 1b and 1c (see *Figure 4.3* for sample site) are broadly similar to each other, as would be expected. The upper sixty percent of the slides are formed of blocks with a single direction internal fabric or random fabric material. These blocks are separated by shears in numerous directions. The lower forty percent of the slides consist of areas below a strong iron stained boundary (*Figure 4.11*) which have strong single direction fabrics with an apparent dip 45° south west. These areas are cut by two shear zone sets (*Figure 4.13*). It is presumed the primary fabric formed in the same Primary Fabric Event as that seen in Section 1a.

The first shear zones have an apparent dip orthogonal to the primary fabric with sinistral *and* dextral displacement. The second shears displace these shears dextrally and are orientated horizontally. Internally, the first shears have grains aligned along the zone, the second have an apparently random internal fabric. It is assumed that the first shears are those formed in Shear Event One and the second those formed in Shear Event Two. There is no evidence of the second shears being truncated by the first, however, there is a variation in the displacements of the first shears along one of the second shears. This variation may suggest Shear Events One and Two were simultaneous, though it may be due to different levels of movement along/ductile accommodation around the shear. The fact that the Event One shears with less displacement along Event Two Shears were formed more vertically suggests a rotation of the primary stress direction with time. This may be a result of a change in the load application direction under strain along the Event Two shears. Alternatively, the rotation may be a result of a change in the fluid conditions. If the shears were formed synchronously this increase in angle might represent drying conditions (Chapter Three).

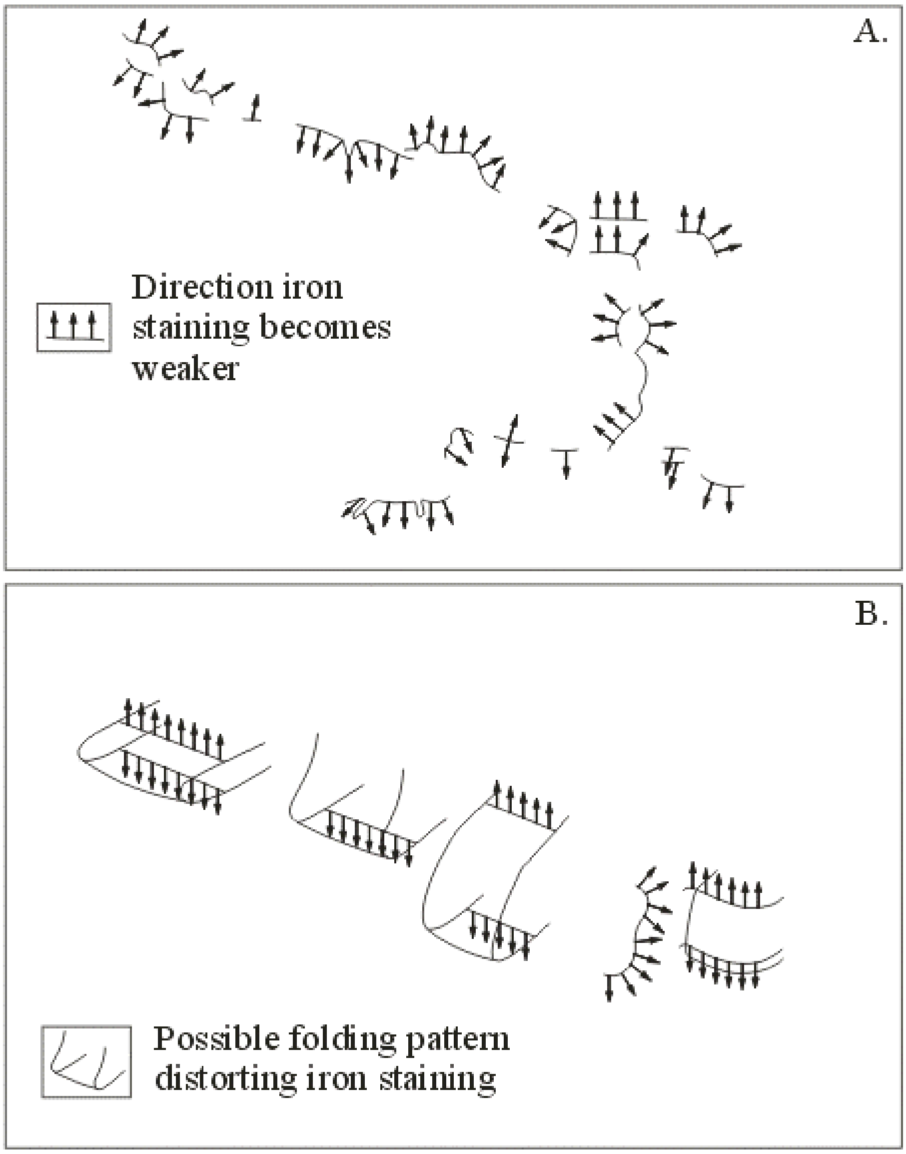

Figure 4.10 a) The Iron staining in section 1a (vertical section from north-west to south east). b) Diagrammatic representation of the possible folding responsible.

Iron staining is found bounding the blocks on at least one side, rather than being inside the blocks. This positioning indicates the staining strengthened the material prior to block formation (*Figure 4.14*). In places dewatering deformation can be seen to have occurred (*Figure 4.15*) after or during block emplacement. Dewatering is also seen at the boundary between the upper and lower areas (*Figure 4.11*). Shears from Shear Event One can be seen crossing the dewatering areas indicating that dewatering occurred before this event. Some of the blocks in the upper area contain shear zones of both Shear Events dictating that the blocks were moved after these events. There are, therefore, traces of *two* dewatering periods.

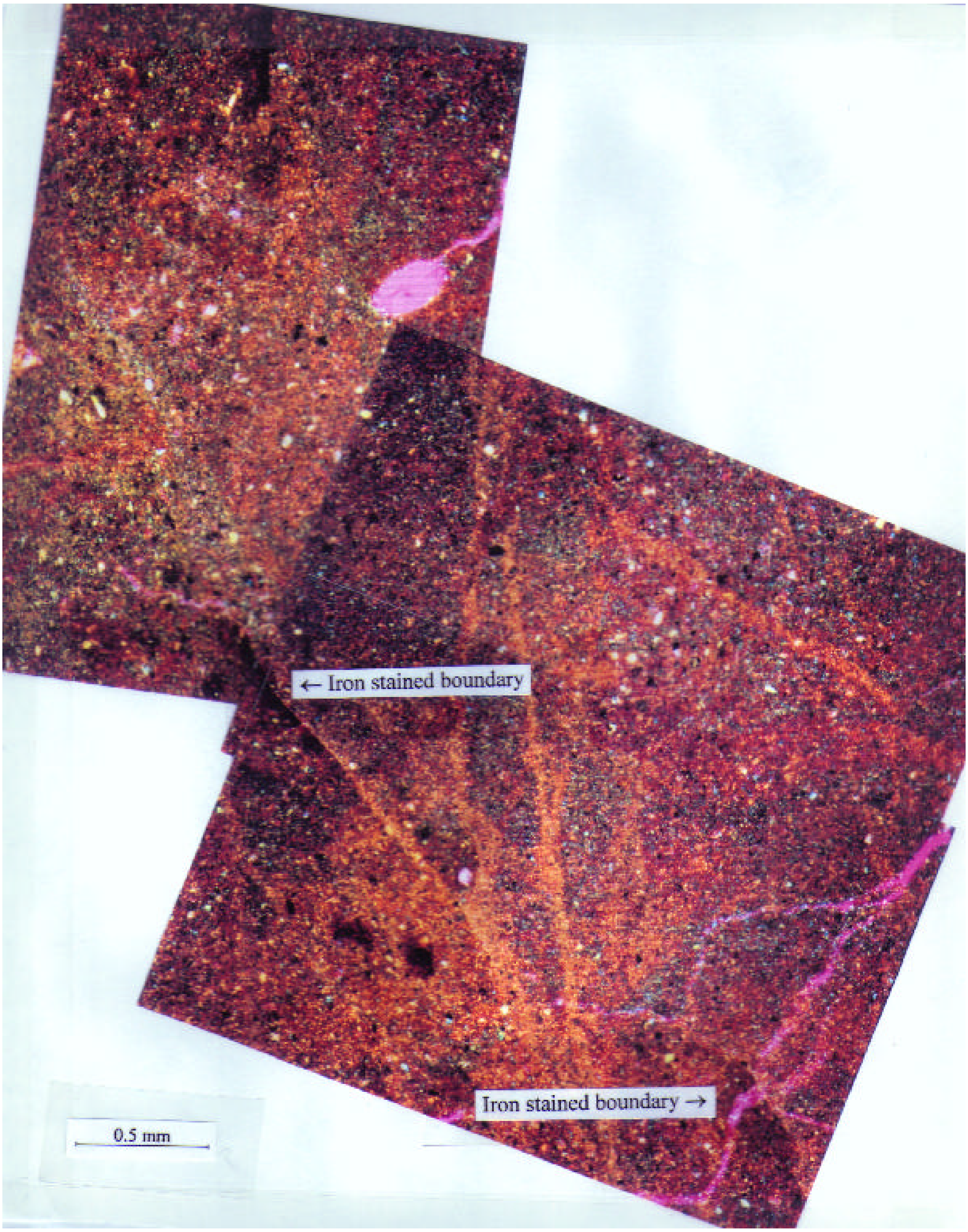

Figure 4.11 Tinted polarized micrograph showing the boundary between the two areas of Sections 1b/c (vertical sections from north east to south west). Above the boundary the material is formed from rotated blocks, each with its own primary fabric direction. Below the boundary the material has a single primary fabric.

4.4.3 Description (lithofacies E)

Sections 2a and b have similar micromorphologies. Each is formed from clays and silts with conformable silt sized material layers of various lengths up to 5 mm, and various widths up to 0.4 mm (*Figure 4.12*). These layers are truncated and rotated by shear bands in a wide variety of orientations. The shears have a high strain morphology (*Figure 4.12*, and Chapter Three) and where a previous fabric can be seen, the dislocation across the shear is often infinite. Both the layers and the matrix surrounding them have single internal fabric orientations between the sets of shears, through deformation occasionally has destroyed the fabric completely. This suggests an original primary fabric that has been deformed, though to no consistent final orientation (*Figure 4.12*).

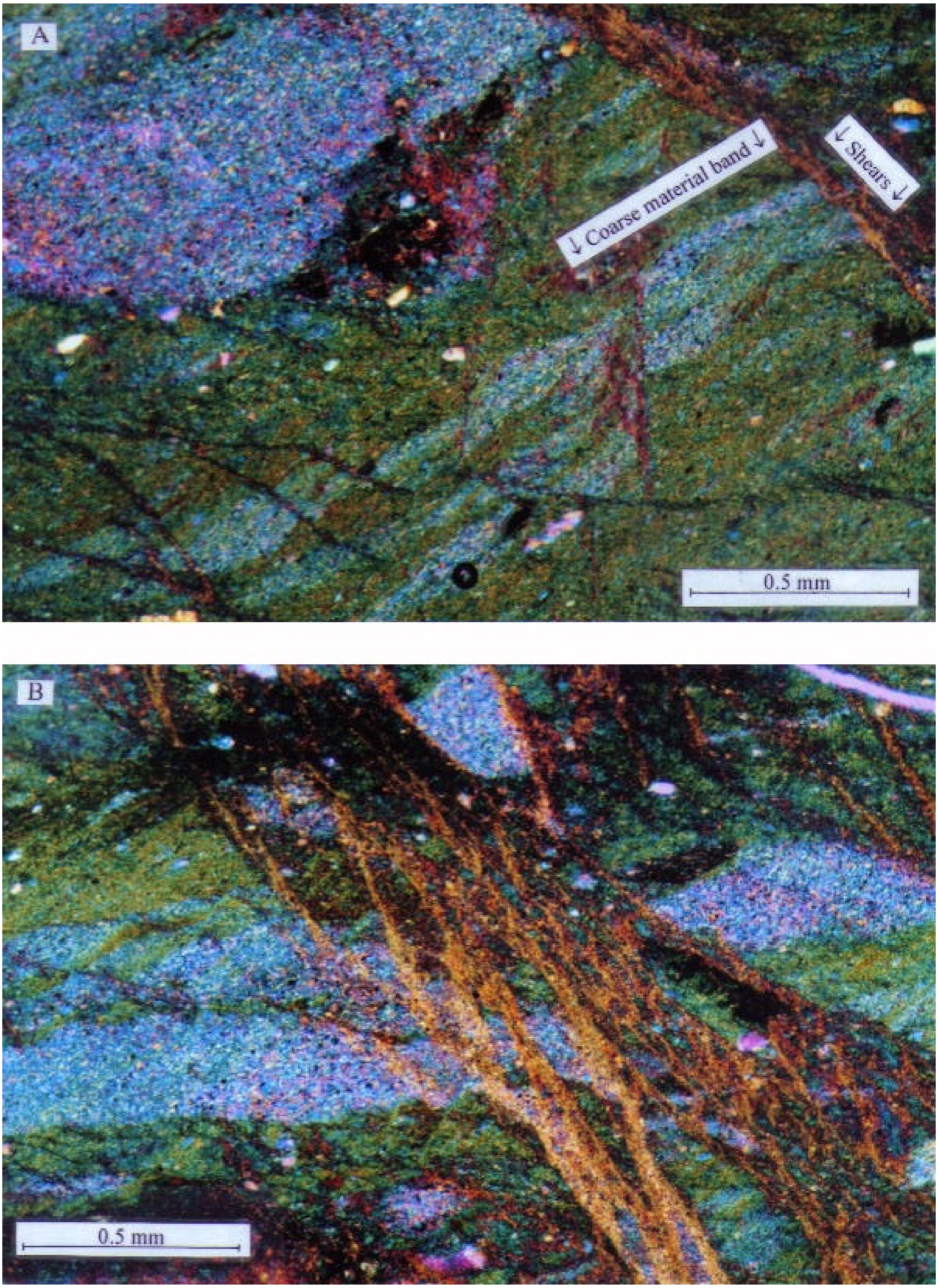

Figure 4.12a/b Sections from lithofacies E (sample 2a). Cross polarized light with tint plate. West-east vertical plane.

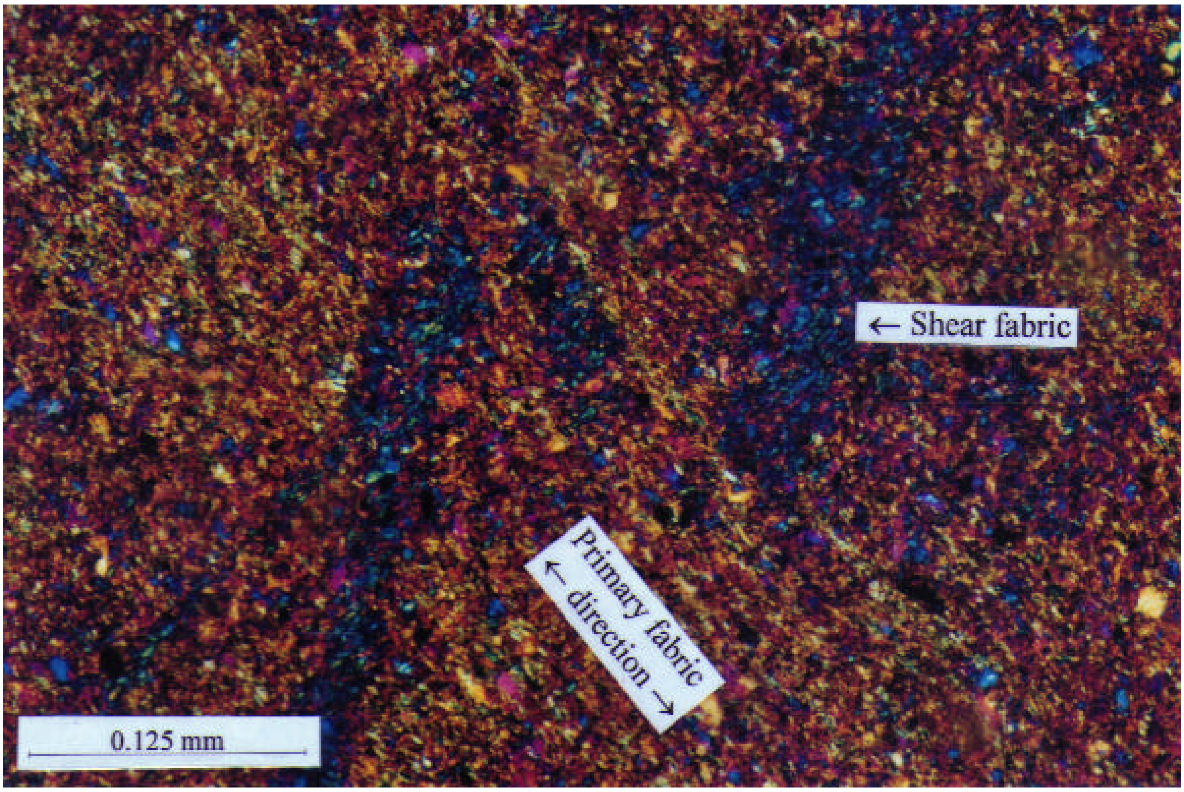

Figure 4.13 Tinted polarized micrograph showing shear fabrics in section 1b / c (vertical sections from north east to south west). Primary fabric (yellow) dips south west. Shears formed in Shear Event One (blue) dip north east, and are displaced by shears in the primary fabric direction (yellow as well).

4.4.4 Interpretation (lithofacies D)

The displacement across the shears formed in Shear Event One and Two may indicate they were the result of a single compressive deformation, or tensile conditions at a flow-nose (following Menzies and Maltman, 1992, sample M2). In this case the compressive stress would be approximately horizontal, and tectonic, rather than by vertical loading (as found by Menzies and Maltman). As such, the features could not be due to consolidation (Chapter Three). However, there is no evidence for the second shears being truncated by the shears of Shear Event One. Their simultaneous development is speculation based on the likely environments of formation. Two temporally disparate, opposing, stresses producing a single shear set each are less likely than a single compressive force. The features are unlikely to have formed under a simple shear geometry. The development of simple shear fabrics includes the development of secondary shears (thrust shears and conjugate Riedels) after the initial (Riedel) shears (Morgenstern and Tchalenko, 1967, see Chapter Three). However, the progressive development of the fabric on increasingly large scales during shear means the two sets of shears *are* truncated by each other in simple shear geometries. Thus, the fabric seen here is unlikely to represent a simple shear geometry. This leaves a pure shear geometry, or more complex strain conditions as possible. One possible explanation is that the movement on the first set of shears was eventually prevented on a larger scale than the thin sectioned area, and the second shear set activated to relieve stress. Such a sequence has been suggested for the larger scale back-thrusting of the Bride Moraine on the Isle of Man (G. Thomas, *pers.comm.*, 1996).

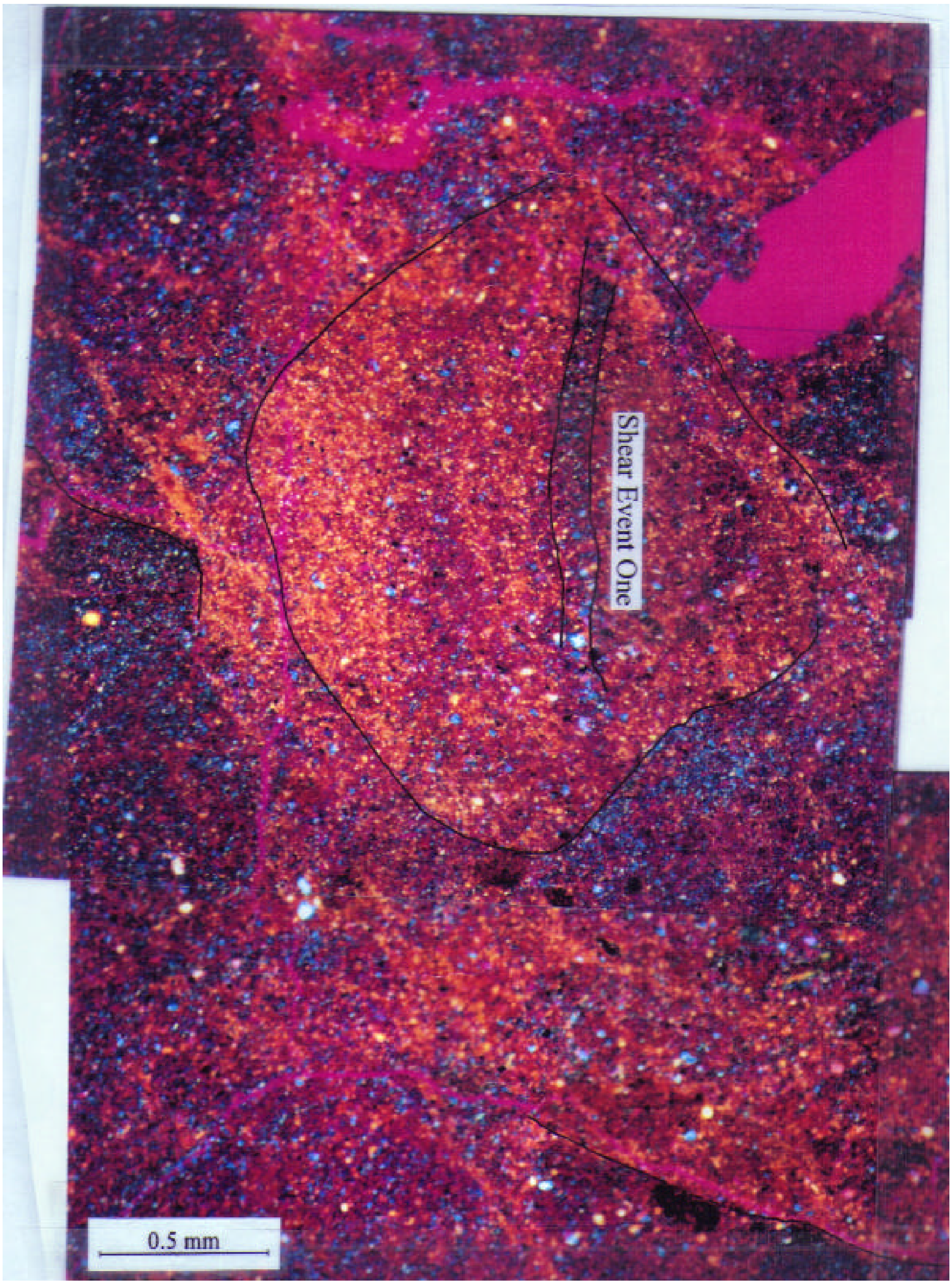

Figure 4.14 Tinted polarized micrograph showing an iron stained block in the upper part of section 1b (vertical section from north east to south west).

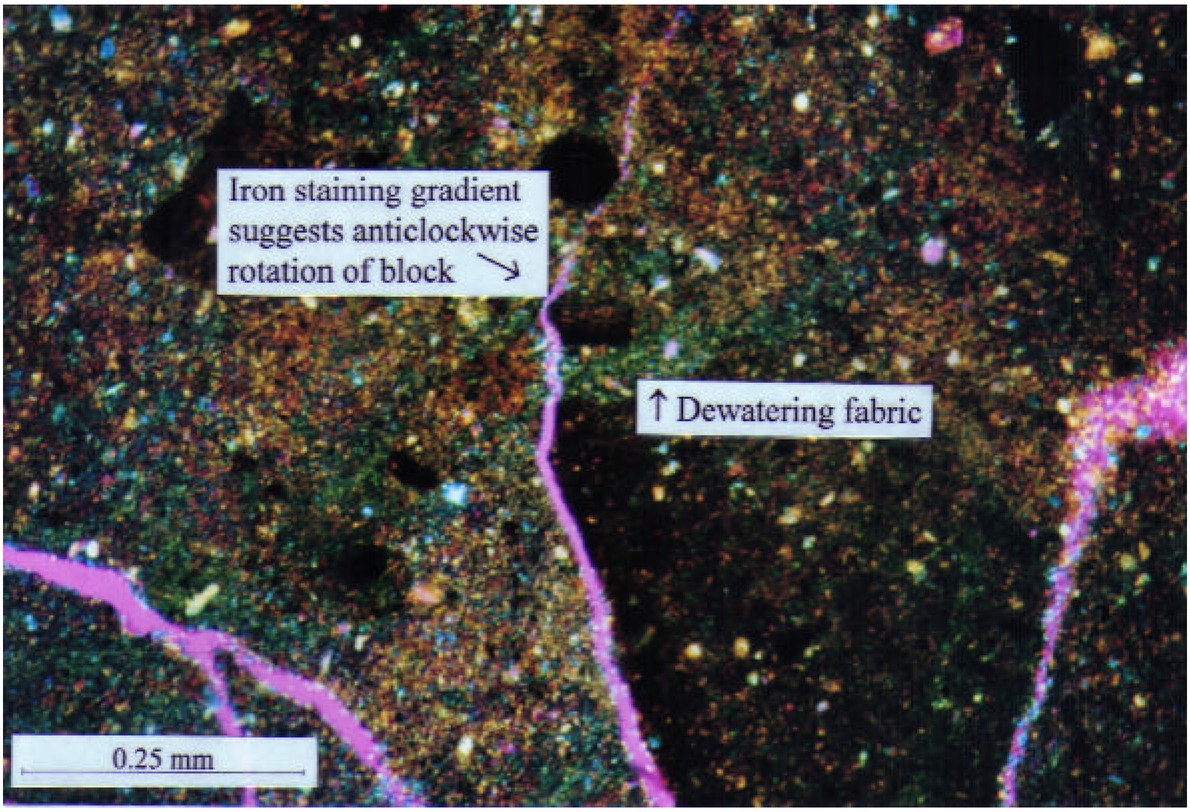

Figure 4.15 Tinted polarized micrograph showing a dewatering fabric destroying a block in section 1b (vertical section from north east to south west).

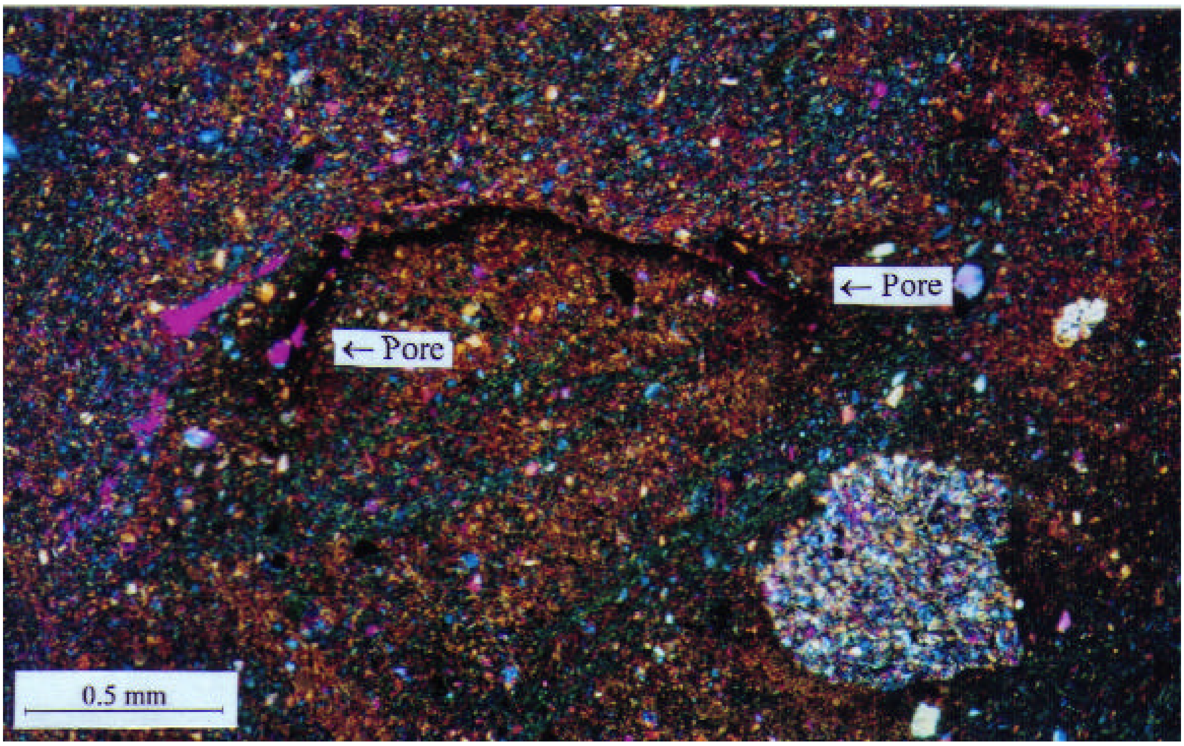

Figure 4.16 Tinted polarized micrograph showing iron staining around pores in section 1a (vertical section from north west to south east).

The complexity of the iron stained boundary in slide 1a. (*Figure 4.10a*) indicates one of two possibilities.

a) The water carrying the iron did not flow simply from top to bottom of the slide. Instead it moved by capillary action or under a fluid pressure gradient against gravity, such that staining occurred at flow barriers from both above and below. There is evidence for such heterogeneous movement in the form of iron staining around large pores (*Figure 4.16*). That these *are* pores and not sampling and preparation cracks is suggested by their location in the hardest part of the sediment; the iron stains. Deposition of iron from bulk through-flow is unlikely *after* an efficient pore system developed, therefore the throughflow would have to be earlier than the pores. There is no need to resort to subglacially pumped meltwater to explain the pressure gradient necessary for heterogeneous through-flow. If saturated sediments are slightly heterogeneous (as seen in the primary fabric) they are likely to develop heterogeneous fluid movement as they drain. The deposition of impervious iron layers would have led to the development of a pore system as they would allow the head to built up, however, it is equally possible the head build-up was externally induced. Pore systems rarely develop in iron-pans in soils, however, the potential head in thin soils is much smaller. The presence of the primary fabric and its lack of a consistent staining gradient direction suggests the heterogeneous flow was not due to ice growth in the material.

b) The boundaries were implaced and subsequently deformed as in Figure 4.10b.
The primary fabric inside the bound areas has been disturbed so that it is largely random, though horizontal bands of primary fabric broken up by shears (in the relative orientation of Event One shears) are found within this. The horizontal bands could be indicative of the folding of the sediment. If so, then this folding represents another deformational event (Fold Event One).

The randomness of the fabric fits either explanation as such randomness may constitute a flow barrier. The folding disruption may therefore have occurred prior to the iron emplacement.

4.4.5 Interpretation (lithofacies E)

The micromorphology of samples 2a/b is wholly consistent with the interpretation of the lithofacies as a glacitectonite of laminated sediments, made on the basis of ephemeral outcrop scale evidence (see above; D.Evans, *pers.comm.*, 1997). Given the area over which lithofacies E is found it is likely that the original material was deposited in a marine or lacustrine situation. The fine lamination suggests the body of water was associated with an ice mass that had a water system that could transport coarse sediment into the proglacial environment (ie., a warm bedded ice mass). Any primary fabric is likely to have been formed subglacially, as deposition through water does not produce strong fabrics (Chapter Three). The well developed nature of the shears and the often completely reworked fabric of the matrix suggests considerable strain which points towards a subglacial origin for the deformation as well. We will see further evidence for the subglacial deformation of this material when we examine one particular feature that is present near the surface of lithofacies E (Chapter Five deals with this particular feature separately from this general discussion of the sedimentology of lithofacies E, largely to spare the reader a set of arguments unrelated to the general sedimentology, but also because the methodology for handling the evidence is very different).

4.5 Summary and Synthesis

To summarise the analysis given above a timeline may be constructed, thus,

Lithofacies E formed

a) Laminated sediments deposited in a lacustrine or marine situation from warm bedded ice.

b) Laminated sediments deformed subglacially.

Lithofacies D formed

c) Primary Fabric Event forms a fabric with a maximum true dip of 35° down to the west. This alignment is either due to compression orthogonal to the fabric (suggesting flow or subglacial consolidation under an overburden and pure shear stress) or pervasive shear (which may be subglacial). The development of such fabrics is examined in Chapter Seven.

d) The iron stains may have been deposited.

e) Fold Event One distorts the iron stain boundaries. The fold direction is complex.

f) The iron stains may have been deposited.

g) The sediment dewaters. This drying may explain the change from the pervasive deformation of (c), to the discrete shear of the two following events.

h) Shear Event One produces a shear plane with a maximum true dip 35° down to the east. Note that the ice in the area moved east to west.

i) Shear Event Two produces a shear plane with a maximum true dip 45° down to the north west. These shears may have developed late in Shear Event One, and therefore represent the Principle Displacement Zones (Chapter Three).

j) Blocks seen in the upper parts of sections 1b and 1c move. This movement appears to be by pervasive deformation, with the flow of material carrying the blocks. However, the large number of differently orientated shear zones in the upper area may suggest some movement by discrete shear. These shears may also have developed late in Shear Event Two; more vertical shears may have formed later in this event. These shears survived in the lower, 'unblocked', areas of 1b and 1c where they were protected from break-up by the iron boundary. The return to pervasive shear may imply a lower effective pressure than during the shear events.

k) The sediment dewaters.

There is no evidence in the sediments that any of the events from 'c' onwards took place subglacially, except the moderately high strains which must have been involved in 'c'. The timeline is by no means certain as some features seem to be formed diachronously. There are instances of Shear Event One shears stopping at dewatering fabrics. However, these tend to be small and this truncation may be attributed to the extra strain needed to orientate the more random fabric. More serious is the identification of dewatering fabrics which appear to have been formed after block emplacement. These fabrics may suggest either events (g) to (j) occurred simultaneously (which would explain the shears associated with the blocks) or that there was a second dewatering event (k). If the second is the true interpretation it would certainly match a lower effective pressure in event (j) associated with more pervasive movement (Chapter Three).

One of the most important inferences that can be drawn from the thin sections is the simple fact that the iron staining at the boundary between the upper and lower diamicts is not indicative of an interglacial or interstadial period, as some researchers have suggested. This timeline suggests that the iron staining occurred prior to the last deformation though possibly after the primary fabric formation. Thus, at the longest estimation, iron deposition occurred sometime between the start of the last glaciation and the end of periglacial activity (under cold climate conditions). There is no reason to suppose the iron staining at the boundary between the two diamicts is not from the same event, concentrated by the permeability change to the heavy, consolidated, clayey, lithofacies E.

Permeability change alone, however, is not a sufficient reason for the chemical precipitation of iron; there must be a chemical environment change. In soils and between lithofacies D and E, where water levels and material vary vertically, it is not hard to produce vertical chemical changes. However, subglacial or flow tills would be expected to be saturated throughout and it is hard to envision chemical changes vertically in lithofacies D.

Figure 4.17 gives the environments in which different iron minerals are stable (Baas-Becking *et al.*, 1960, Garrels and Christ, 1965). Iron is only commonly a solute in anoxic marine/lake sediments and in acidic peaty soils. Outside of these environments iron movement is rare. Ice thicknesses dictate that upland peats did not survive the glaciation of this area. The iron supply was, therefore, the sediment itself, or its source rock. This hypothesis matches the large amount of ‘primary’ iron minerals in the thin sections. This hypothesis is also backed up by the depth the sample was taken from. It is unlikely that washed-in iron would precipitate so widely throughout such a thick sediment if the precipitation was caused by the diamict’s chemistry.

Thus, the most likely explanation for the iron staining is that the sediments were at some stage submerged under anoxic deep-water conditions. The sequence of events involved in the iron deposition will be dependant on the mineralogy of the precipitate. The colour in thin section suggests the precipitate is hematite, however, the yellow staining of the deposit on a larger scale may point to greater pyrite precipitation. Further evidence in favour of pyrite is given by Grant (1990), who suggests that there is little hematite in the sediments on the basis of magnetic studies.

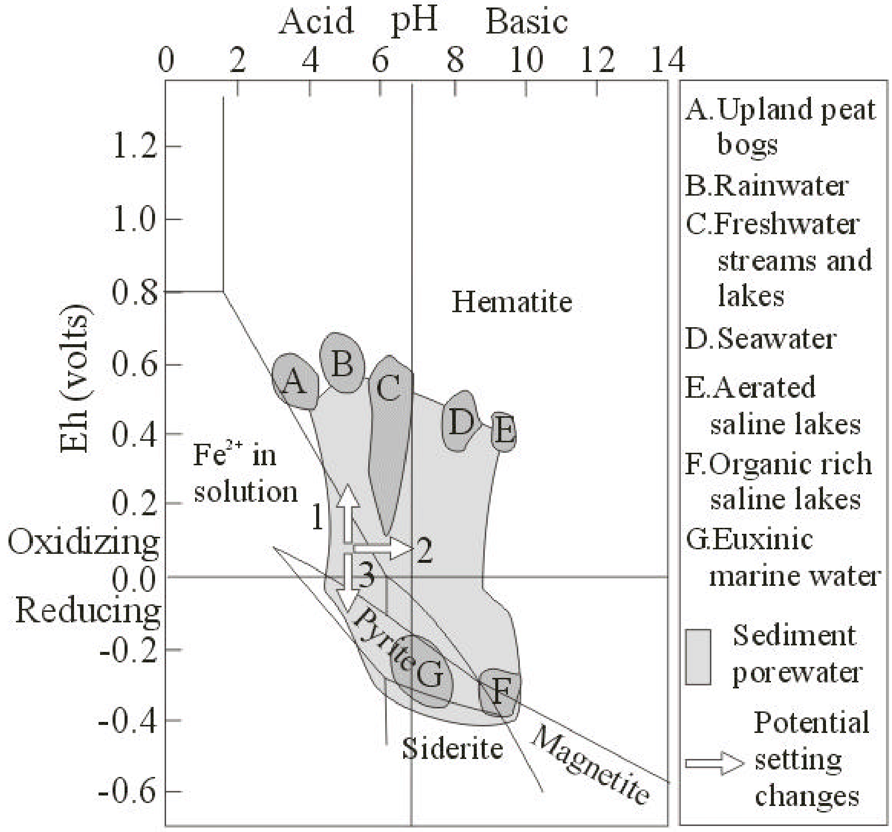

Figure 4.17 Different chemical conditions in natural environments (shaded with letters) and the iron minerals stable in them (lines and names). Arrows show the paths in pH and redox potential (Eh) space that possibly explain the presence of iron staining in lithofacies D. After Baas-Becking et al., 1960; Garrels and Christ, 1965; Tucker, 1991.

Figure 4.17 shows the three possible environmental changes that would have led to precipitation. Hematite could have been deposited in a change from anoxic to oxic water (Path 1) or from anoxic fresh water to anoxic saline water (Path 2). Pyrite could have been deposited in a change from oxic to anoxic marine conditions (Path 3). The redox potential of natural environments are chiefly controlled by bacterial action (Baas-Becking et al., 1960). It seems likely that the sediments were deposited in an environment too cold for rapid bacterial action on the scale of the precipitation seen here. It is possible that anoxic conditions could be produced chemically by non-seasonal capping of the deep water by ice or fesh water. However, the precipitation was probably induced by a change in pH. This limitation suggests Path 1 is most likely. The conflict between the most likely environment (hematite producing) and the likely mineralogy (pyrite) can only be resolved by a more detailed mineralogical examination.

Each path can be accommodated into the history given for the deposit. While we have no evidence that gives an absolute origin of lithofacies D, it is almost certainly 'glaciogenic' in the broadest sense of forming due to the presence of a glacier. What we *do* have evidence for in the sediment is its history *after* deposition. The sediment was deposited in a saturated state and deformed, the deformation being pervasive so as to remove the structures associated with deposition and form the primary fabric (event c). This deformation could have occurred subglacially, proglacially, or periglacially. Iron deposition occurred in the diamict at some point after this in a proglacial lacustrine / glaciomarine setting caused by the trapping of water against the hills to the North, or by isostatic depression in front of the ice, respectively. The throughflow was either heterogeneous or the iron stains were deformed in the same environment after iron deposition (f). Outcrop-scale folding may also have occurred in this environment. The sediment then dewatered as the external water level fell (g) and was subsequently deformed by shear (h,i) and pervasive movement (j). The shears are not suitably orientated for them to have been associated with consolidation, and the low strain recorded in the shears renders them unlikely to have been formed subglacially, as does the evidence for a previous deep water environment. The change from discrete to pervasive shear may have been due to a change in water phase (for example, the change from permafrost to solifluction in a periglacial area), between two environments, or in one, seasonally variable, environment. Alternatively it may have been associated with the extrusion of fluid from areas of discrete deformation. Such an extrusion was seen in the formation of outcrop scale folding, which may also be synchronous with the deformation seen here.

4.6 Conclusions

The micromorphological study above shows that the iron staining between lithofacies D and E was formed after the start of the last glacial period. This chronology removes one line of evidence that was used in the argument for two glaciations in the area. The identification of the ‘fold’ structure seen in outcrop as a deformational feature throws doubt on the similar ‘frost-wedges’ used as the other line of evidence in the argument.

The microstructural analysis suggests lithofacies E formed in glaciomarine or lacustrine conditions, and was then overridden and deformed. However, the evidence gives little information as to the absolute origin of lithofacies D. Boulton’s (1977) evidence from Glanllynau indicates that lithofacies D was probably deposited proglacially from supraglacial meltout material. However, the microstructural study *does* allow us to see that much of the outcrop scale structural evidence is almost certainly postglacial in origin at Criccieth, and that lithofacies A to D cannot be described by ‘broad brush’ terms such as ‘terrestrial’ or 'glaciomarine' at this location, as they have been altered and remobilised in both a proglacial, and possibly a deep-water, environment.

That the sediment passed through a deep-water environment after initial deposition is suggested by its deformational and chemical character seen at the micro- and outcrop scales. These attributes give contradictory evidence for the size of such a water body. A *local* ice-marginal lake would explain the absence of structures seen in this deposit in material west of Castle rock, however the iron staining of lithofacies D is regional. This regional staining suggests the *structures* at Criccieth are limited to this location by local topography, and the absence of the ice-wasting conditions invoked by Boulton (1977) further along the coast. Following the period of chemical precipitation associated with a subaqueous environment, there was a period of disturbance. The presence of lithofacies C and a large frost wedge in sequence indicates a period of periglaciation, including considerable cryoturbation.

To conclude, lithofacies E formed through the deformation of laminated water-lain sediments. The microstructures in lithofacies D cannot give an absolute origin for the material, however, they do provide evidence for the postglacial history of the material (a summary of this history is given in *Figure 4.18*), and show that much of the remaining structural record of the sediments is postglacial.

This study has revealed considerably greater environmental detail than is possible using outcrop scale features through the use of sub-millimetre scale structures. Such details allow us to reconstruct the environmental history of the deposit with greater accuracy. The following chapter, in contrast, concentrates on a unique event, and aims at a more detailed reconstruction of the processes acting during the glacial formation of lithofacies E. This reconstruction allows us to accurately detail aspects of glacier dynamics.

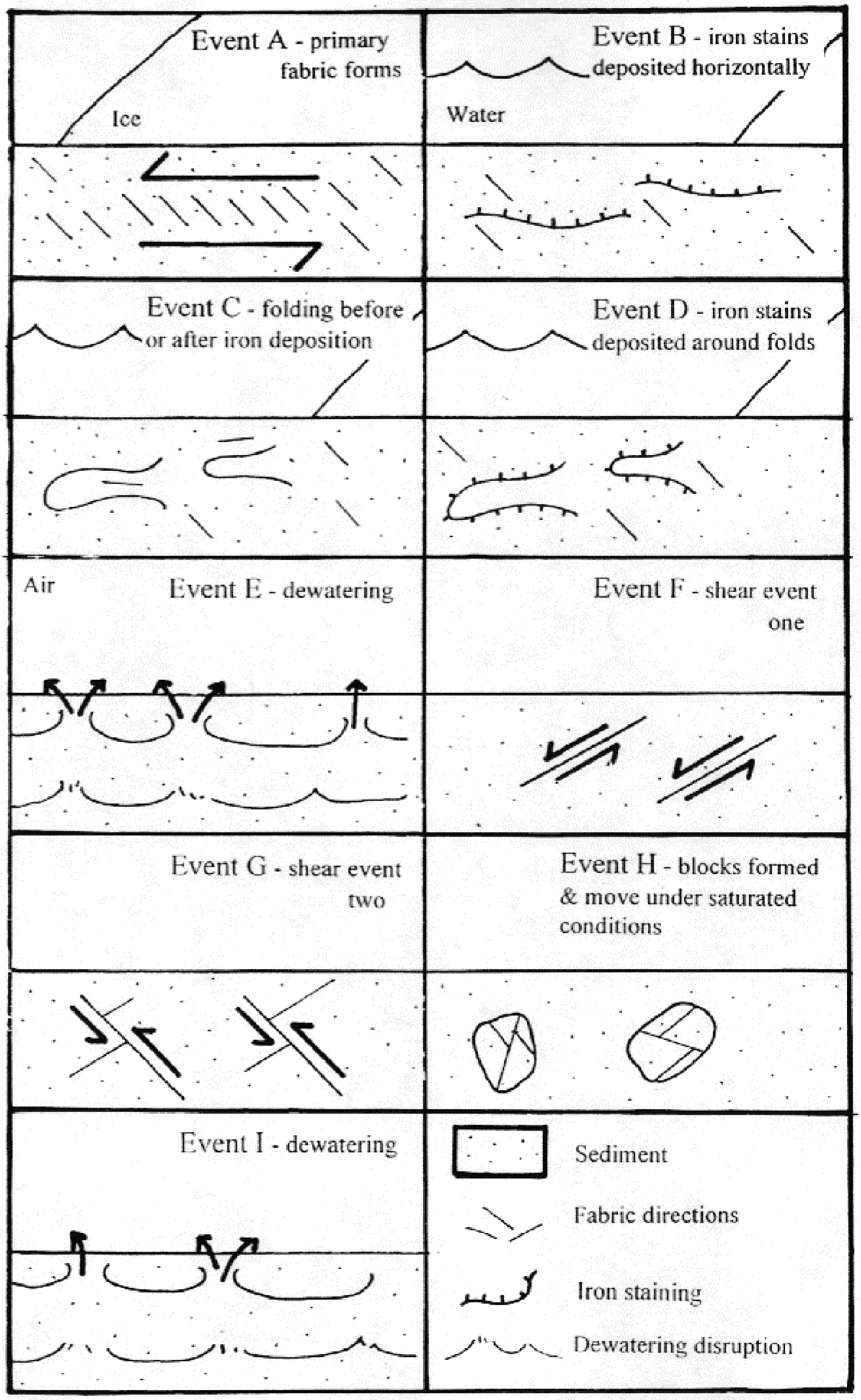

Figure 4.18 The postglacial history of the deposit at Criccieth.

5. The Ploughing and Lodgement of Clasts: a field based case study and theoretical model

5.1 Introduction

Subglacial till is assumed to form by the deformation of pre-existing deposits, meltout of sediment from the ice, and the lodgement of sediment trapped in the base of the ice that is ploughing through the top of the till. The mechanism by which ploughing material becomes lodged is only poorly understood, chiefly because the rheology of till is uncertain. The present qualitative hypothesis for lodgement is that it occurs by the development of a prow of sediment in front of the ploughing object or by collision with other clasts (Boulton *et al*., 1974). There is evidence to suggest that prows *do* develop (Clark and Hansel, 1989; and references therein). However, as subglacial effective pressures are usually considered low, and till easily deformed, it is not clear how prow development acts to lodge clasts, particularly where clast density is low and collisions are therefore infrequent.

Present quantitative models of lodgement assume it occurs once the force on a clast drops below that needed to cause Mohr-Coulomb failure in the down stream sediment (*Equation 3.1*) (Brown *et al*., 1987). Such models do not provide a *steady state* method for the development of lodgement till, and assume the rheology of the sediment to be perfectly plastic. It has been shown that such models tend to lead to a pervasively deforming bed (Alley, 1989), indeed, it is implicit in some models that the stress necessary to cause deformation is transferred by ploughing (Alley, 1989). Deforming beds are often considered to have a low friction at the ice-sediment interface (implicit in Alley, 1989), and to be weakened by the low effective pressures acting on them (Boulton and Hindmarsh, 1987). Under such conditions basal frictional melting will be reduced, and it is unclear how a thick deforming till bed builds up. Under such models till thickness is limited to the height of the largest clast in it which can remain fixed relative to the ice and cause the regelation deposition of fine material. Such thin layers are at odds with the great till plains of the Northern Hemisphere.

This chapter will focus on a suite of micromorphological structures associated with the ploughing and lodgement of a clast, with the processes these structures suggest being built into a quantitative model of clast lodgement. The first half of this chapter will examine the microstructural evidence of ploughing and provide a suite of process-related features that can be used for the determination of lodgement in specific circumstances. The second half of the chapter puts forward a model of the processes to examine their implications, investigate their relative importance, and quantify the subglacial conditions necessary for their action.

The clast in question has lodged into the up ice ('stoss') side of a shallow, Devensian, subglacial ridge or hummock located near the town of Criccieth on the Lleyn Peninsula, Wales (*Figure 5.1*). The outcrop scale sedimentology of the feature has been discussed in detail in Chapter Four, however, an extensive discussion of some aspects of the lithofacies containing the clast (lithofacies E, see last chapter) has been left until this chapter because the techniques used in the following analysis are both considerably different from those used in the last chapter, and better served by being presented with the data they are developed from because of their complexity and length. The sediments discussed in this chapter are also not representative of the sediment of lithofacies E as a whole. A summary of the environmental interpretations discussed in the last chapter is repeated in Table 5.1. The following section indicates the stratigraphic position of thin section samples within the sediments. The sedimentology allows an estimation of the post-glacial alteration of any small-scale structures. These alterations need to be assessed before one can investigate glacial effects. The following section therefore also details such an assessment.

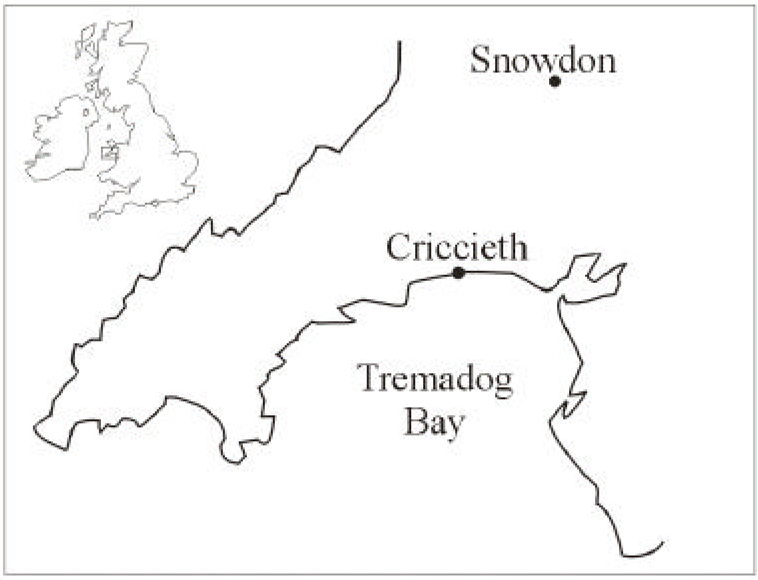

Figure 5.1 The Lleyn Peninsula, North Wales (inset of the UK).

5.2 The samples and their possible post-glacial disturbance

The exposure scale sedimentology of the area is given in Chapter Four, and is repeated in Table 5.1 for convenience.

Lithofacies	Possible origins	Reasoning and caveats
A	Periglacial loess	A micromorphological study would probably not confirm this, the less permeable materials below having encouraged subsurface flow illuviation and particle reorientation.
B	Periglacial solifluction material	Evidence of mass movements and small (~1m wide) stream deposition. Fills frost wedge (3, Figure 4.3) and is involuted at surface.
C	Periglacial cryoturbation of lithofacies B and D.	Random fabric with increased angular slate content. Frost wedge at 3 of fig.4.3 suggests depth for periglacial action. West of Castle Rock, the boundary with D has clast concentration suggesting fluidization of C or a fluvial event.
D	Glaciogenic sediment flow (Boulton, 1977; Grant, 1990) or lodgement till (Saunders, 1968), or flows under lake/marine conditions (Matley, 1936).	Clast orientation eigenvectors cover the first two possibilities (Grant, 1990). See Chapter Four for further discussion.
E	Subglacial till (Grant, 1990; this chapter)	It seems unlikely given the exposure of the site that this formed in a pre-Dimlington stadial (pre-δ^{18}O Stage 2). See Chapter Four and below for further discussion.

Table 5.1 Sedimentology of Criccieth bay middle deposit (see Chapter Four for further details).

The thin sections were taken from an area where the cliff trends sub-parallel to the lithofacies E clast orientation of 135-315 (Grant, 1990) (Area 5 on Figure 4.3). The samples were taken from the boundary between lithofacies E and lithofacies D, immediately up-ice of a large boulder (shown in black on the figure). At this point the blue grey lithofacies E alternates with sand lenses (~1 x ~5 cm) and a light yellow diamict in thin (<5 cm) bands. This alternation occurs in a zone approximately 50 cm thick (*Figure 5.3*) which becomes a wave-resistant band (30 cm thick) in the up-ice direction (*Figure 5.2*). This band runs approximately 20 cm below the surface of the blue grey diamict and extends some 15 m up-ice, disappearing under the beach with the blue grey diamict. A land-slip made extensive mapping to the west impossible, but immediately west of the boulder homogeneous blue till leaves the top of the erratic and drops to the west. This suggests the interbedded sediments do not extend to the west of the boulder.

Figure 5.3 Interbedded sample area from the Criccieth deposit. Material is a mix of yellow and blue silts and clays, interbedded with short (~50 mm) sand lenses. Object in centre is a food tin lid ~7 cm.

Figure 5.2 Sampled feature. Note the blue diamict at beach level and the large boulder within the blue diamict to the left of the picture. Material was sampled from interbedded material 1m right of the boulder, and from the blue diamict just below.

Thin section samples were taken from the interbedded material and from lithofacies E. On the microscale, it will be shown that this deposit represents the trace of the boulder as it ploughed. Given the environmental attribution outlined in Chapter Four, it is possible to indicate the potential postglacial alteration of the sectioned material.

The possible *postglacial* disturbances to the samples include periglacial cryoturbation, deep-water alteration and mass movements, and compression (Chapter Four). There is evidence at Criccieth that lithofacies E is partly a glacitectonized laminated mud (*D.Evans, pers.comm., 1997,* see also Chapter Four). However, the latter three processes can probably be discounted for the *postglacial* period here, as the samples are taken from an area of lithofacies E that includes interbedding which could only be formed subglacially (see analysis below) and which has not been disturbed. Cryoturbation can also be discounted as the uncryoturbated lithofacies D overlies the sampled area. Microscale periglacial changes that have been reported elsewhere (Chapter Two) are not seen here. It seems likely that such microstructures as *are* found could not have formed if the ground was frozen as they require free water. They are, therefore, extremely unlikely in a sediment mass undergoing permanent permafrost conditions.

5.3 The microstructure

5.3.1 Thin section description

Two thin sections were prepared from the interbedded zone immediately up-ice of the large boulder, from the west-east vertical plane (samples 3a/b). Two thin sections were also later prepared from lithofacies E to test the model suggested here. These have also been discussed in terms of the general sedimentology of lithofacies E in Chapter Four. The sections 3a and 3b show that the alternating banding seen in outcrop was a result of the interbedding of three sedimentary types.

1) Sands (100 point-count average length of ~0.3 mm) of schistose material. This is found in bands with clean pores constituting 45% of the sediment (*Figure 5.4*).

2) Silts in unimodal, graded, and melange units of various sizes (including some clays) and internal fabrics. These silts form the blue and yellow bands seen in hand-samples (*Figure 5.5*).

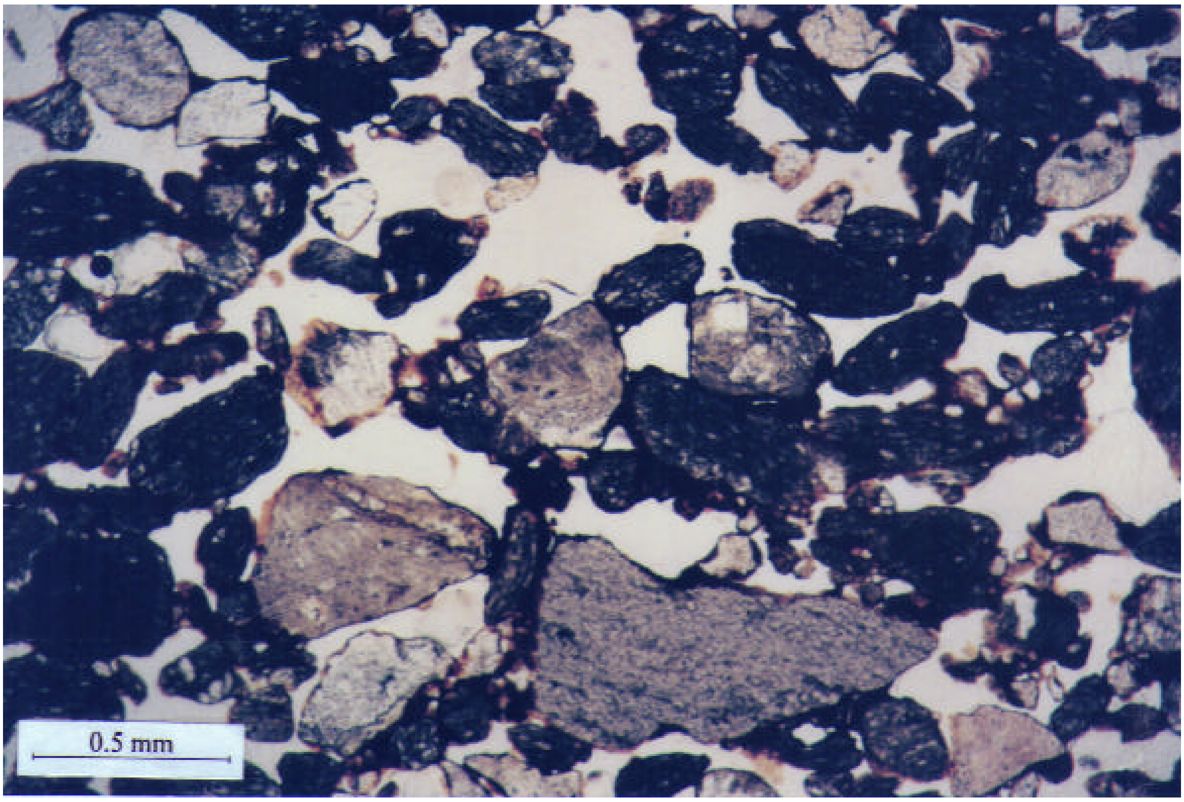

Figure 5.4 Photomicrograph of a sand layer from the base of section 3a. Unpolarized light. West-east vertical plane.

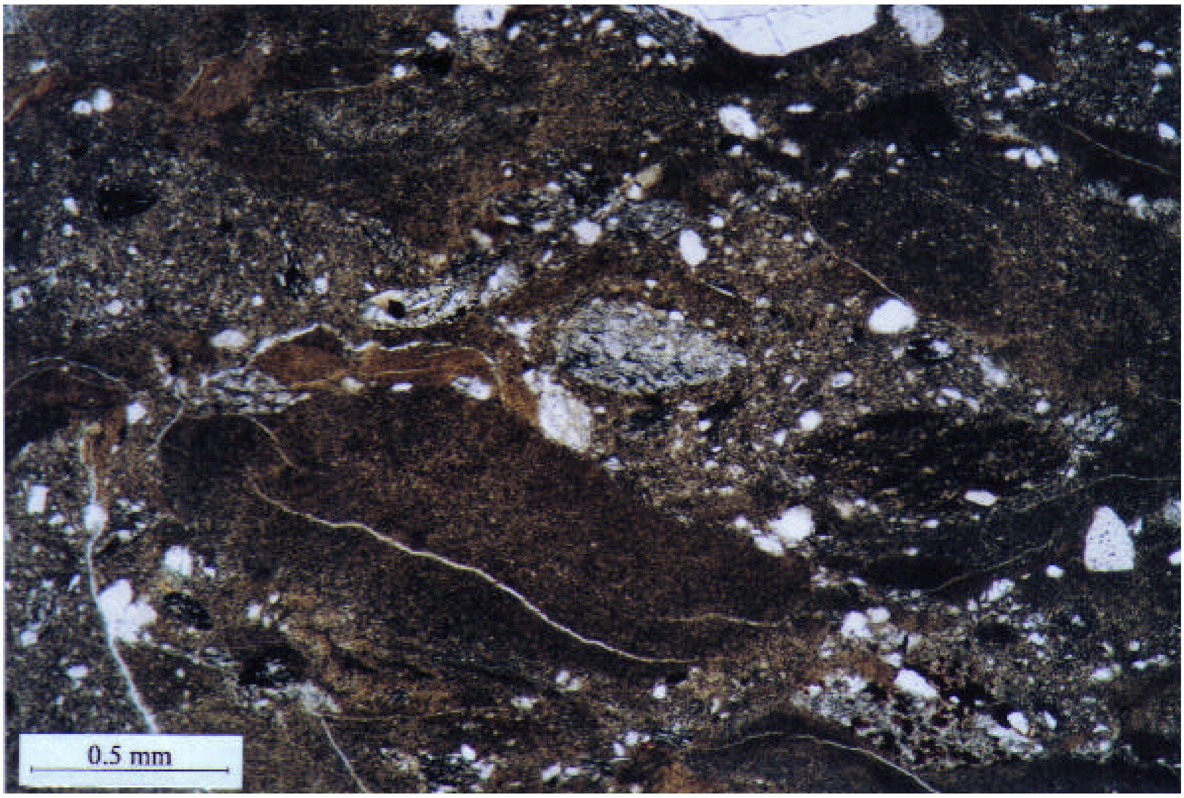

Figure 5.5 Photomicrograph of a melange of silts of various sizes mixed with larger quartz grains. From section 3a; unpolarized light conditions, west-east vertical plane.

3) Quartz grains (~0.1 mm) in separate masses and as units between/in other layers (*Figure 5.6*).

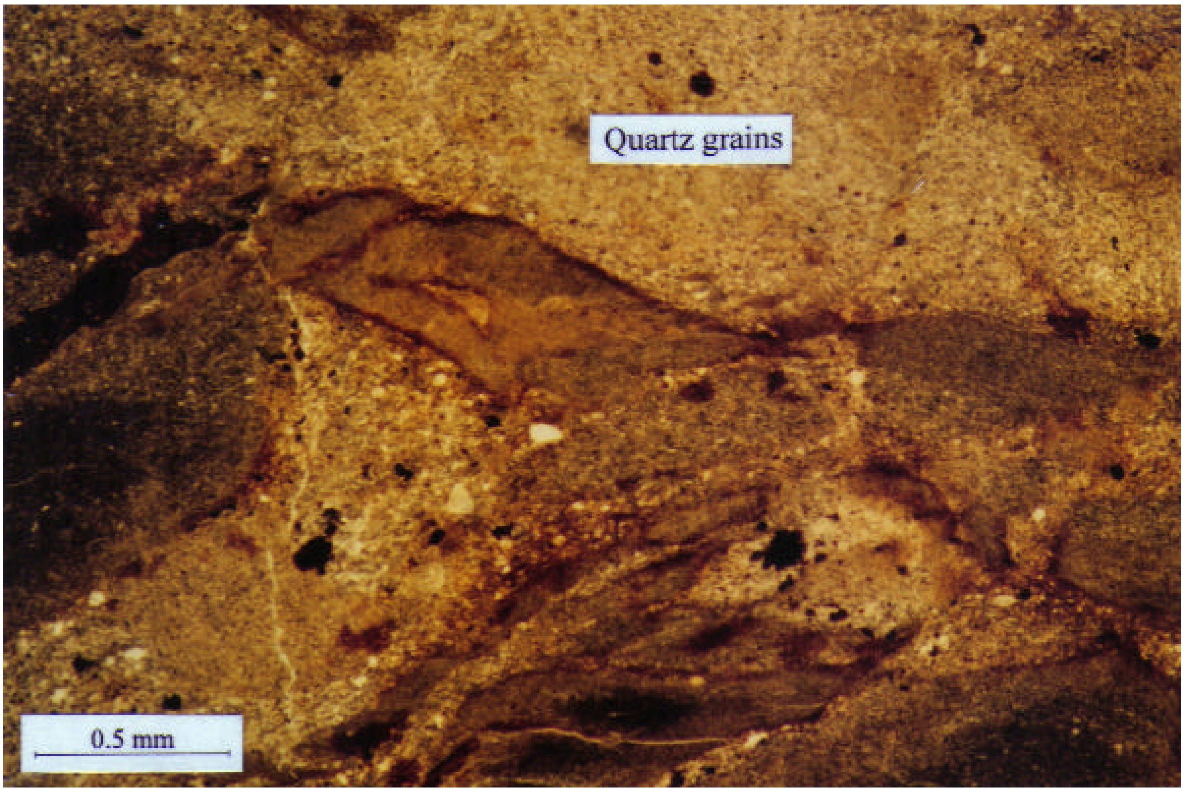

Figure 5.6 Photomicrograph of a quartz grain unit from section 3a (lower third of photo). Unpolarized light. West-east vertical plane.

The boundaries between the different bodies are discontinuities but are not formed by post-depositional shear; instead they are deep undulations. There *are* shear fabrics extending from some boundary irregularities at the top of these undulations, however, in most areas the material moves into the topography of lower sediment bodies. In places the boundaries undulate in response to the intrusion of discrete sediment units from above, suggesting deposition by displacement in semi-coherent flows (*Figure 5.7a*).

The sands were deposited in bands with little or no silts in the pore spaces (*Figure 5.4*). The sands are also weakly aligned horizontally. In one place the sands are overridden by silts, the two units being mixed together in a 4.3 mm zone indicating that the clean pores are probably due to washing of water rather than protection by ice fills during deposition. In places in this mixed-zone, slugs of silt are armoured with sand grains indicating the edge of flow units (*Figure 5.7b*). While it is impossible to determine the true flow direction of these features, it is apparent from the associated extensional features (*Figure 5.7b*) that they did not move east-west.

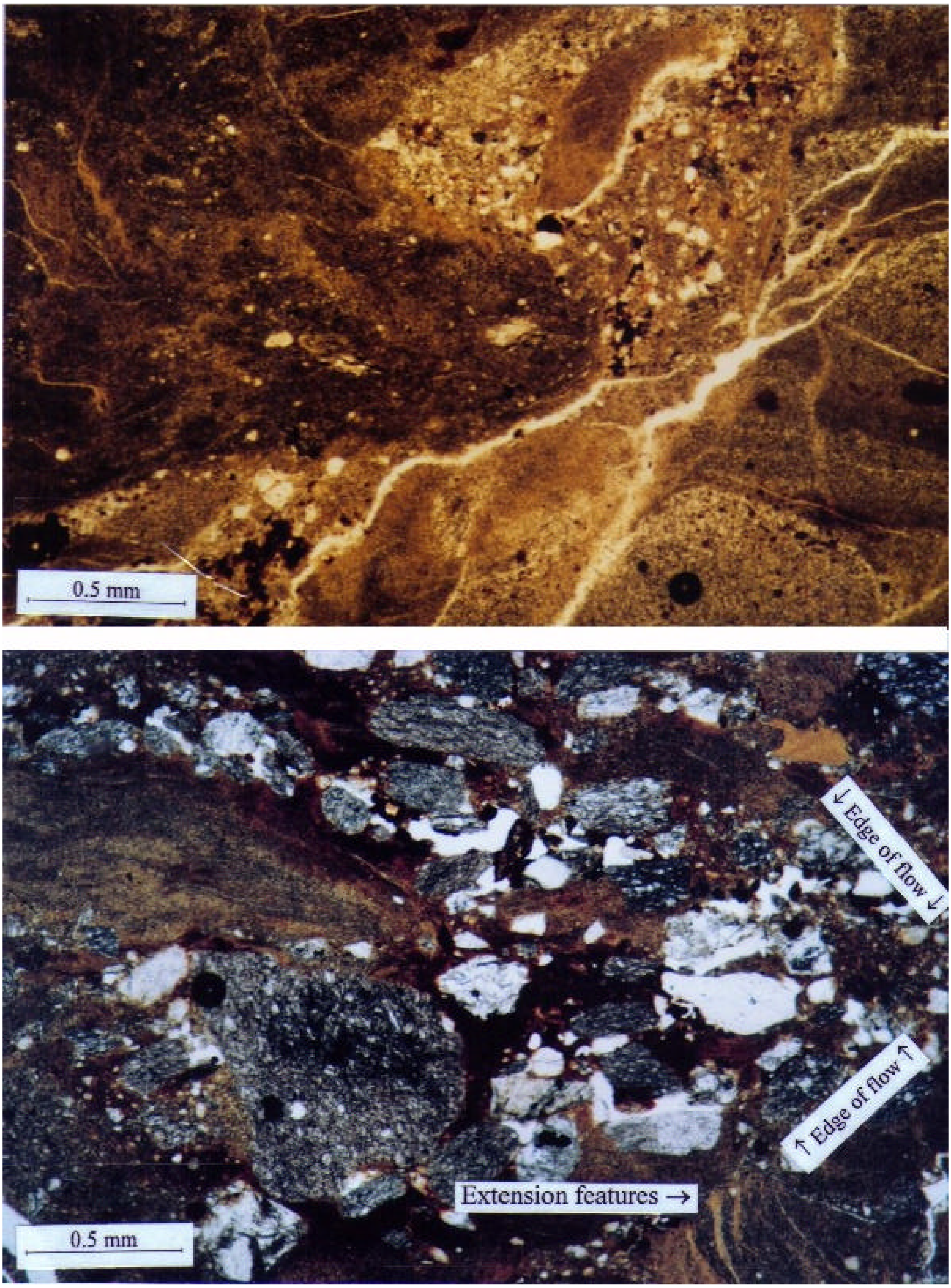

Figure 5.7 A. Photomicrograph of a silt unit that has moved into a quartz rich unit from section 3a. Unpolarized light, west-east vertical plane. B. Photomicrograph of a silt slug nose, armoured with sand grains, from section 3a; unpolarized light conditions, west-east vertical plane. Tension cracks, filled with light yellow, fine, material can be seen defining the lower forward edge of the nose.

The quartz grains were found throughout all the other sediment types except the sands, suggesting they may have winnowed out of the sands in a water body. The quartz grains are especially prevalent at the boundaries of sediment bodies indicating fallout deposition between mass movement events (*Figure 5.8*). However, the quartz grains also form units that moved with the surrounding mass movements and filled dewatering veins.

The silts can be subdivided into three types of bodies.

a) 'Typical' melanges consisting of blocks of coherent sediment within a groundmass of deformed material (*Figure 5.5*). Neither the blocks nor the 'matrix' are of one specific silt size. The rotated and varying fabrics in these bodies suggest the material did not suffer glacial consolidation after deposition (*Figure 5.5*). However, the strong internal fabrics of many of the blocks suggest overburden or shear alignment of individual grains *prior* to the melange formation. It is possible that the strong pre-deposition fabric was resistant to reorientation, and that these pre-orientated areas protected the weaker matrix. Thus, prior consolidation is certain, but post-depositional conditions suitable for consolidation cannot be ruled out.

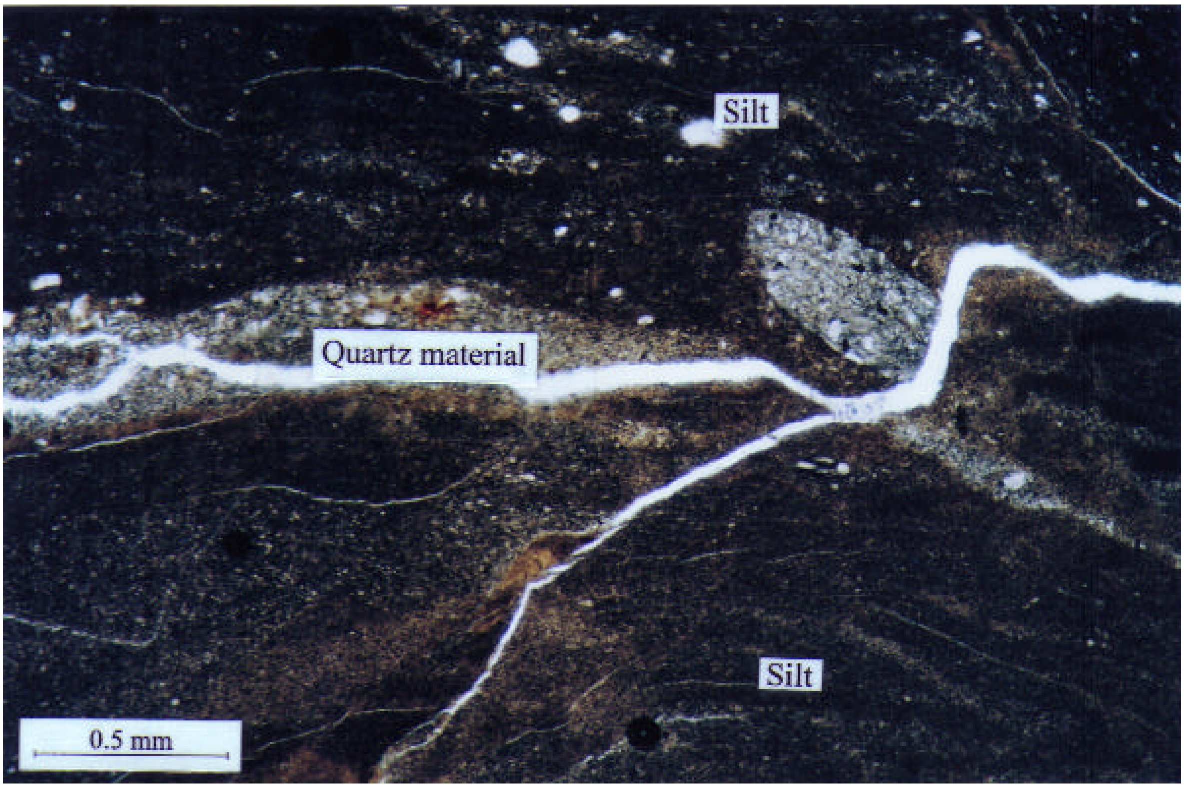

Figure 5.8 Photomicrograph of two silt slugs (blue in hand specimen) with an attenuated quartz layer between them, from section 3a; unpolarized light conditions, west-east vertical plane

b) Flow bodies with a unidirectional internal fabric. Between these flow bodies are, coarse grained quartz units which have been extended by shear by the moving units (*Figure 5.8*).

c) Graded units in overlapping lenses. These units have sharp boundaries between the coarse material of one lens and the fine material of the one above (*Figure 5.9*). The fine material has a single fabric orientation which is also weakly present in the coarse material.

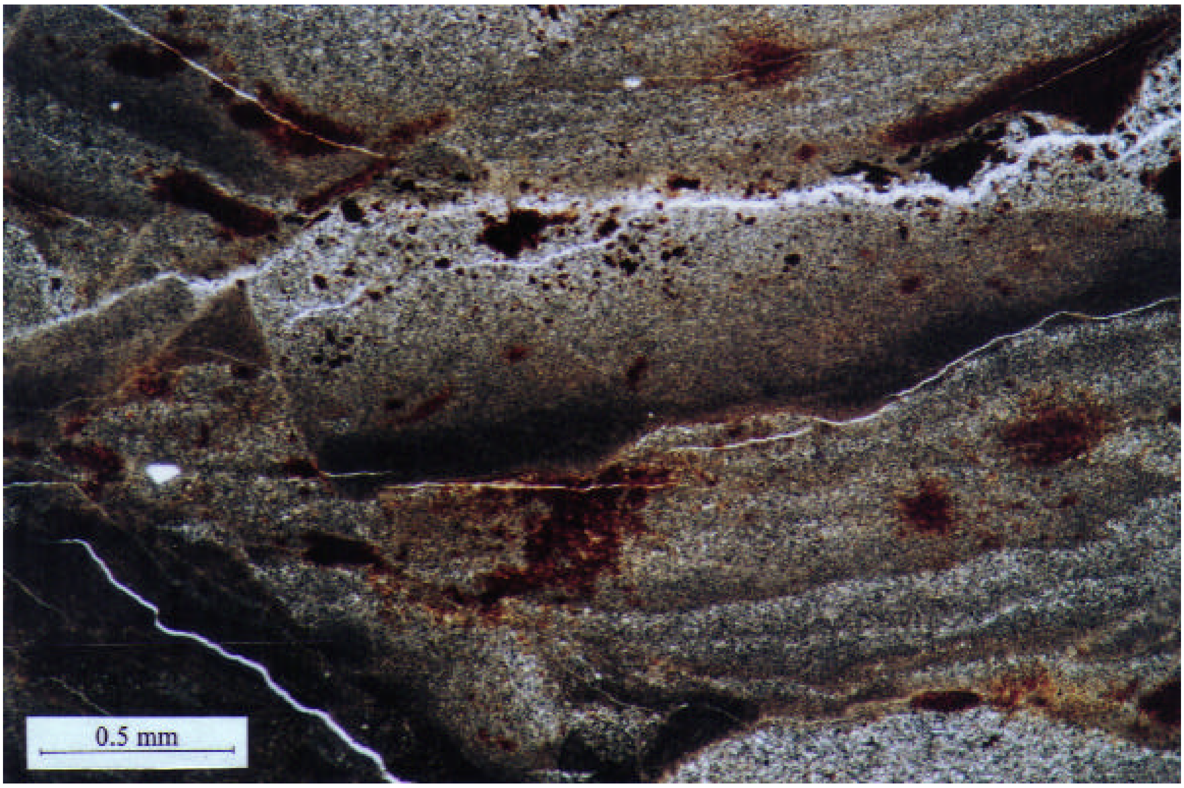

Figure 5.9 Photomicrograph of graded units from section 3a; unpolarized light conditions, west-east vertical plane.

5.3.2 Discussion of microstructural study

The fact that the larger grain sizes are *above* the fine silts in each graded silt 'unit' suggests these are not water-sorted features, most of which have fine material above the coarse, particularly in glacial environments where seasonal stratification leads to the long suspension of fines in the water column. While it is possible to suggest that the units were inverted in transport or the larger grains were expelled as the bodies were emplaced, a progression can be found which supports a deformational origin for these features. Figure 5.10a shows low strain fracturing of a coarse unit (fine-grained sand quartz unit) into lenses along listric faults. In the more developed features, shears can be seen to bound the lense-like areas (*Figure*

5.10b). This faulting and imbrication process causes the observed juxtaposition of fine and coarse material in lenses.

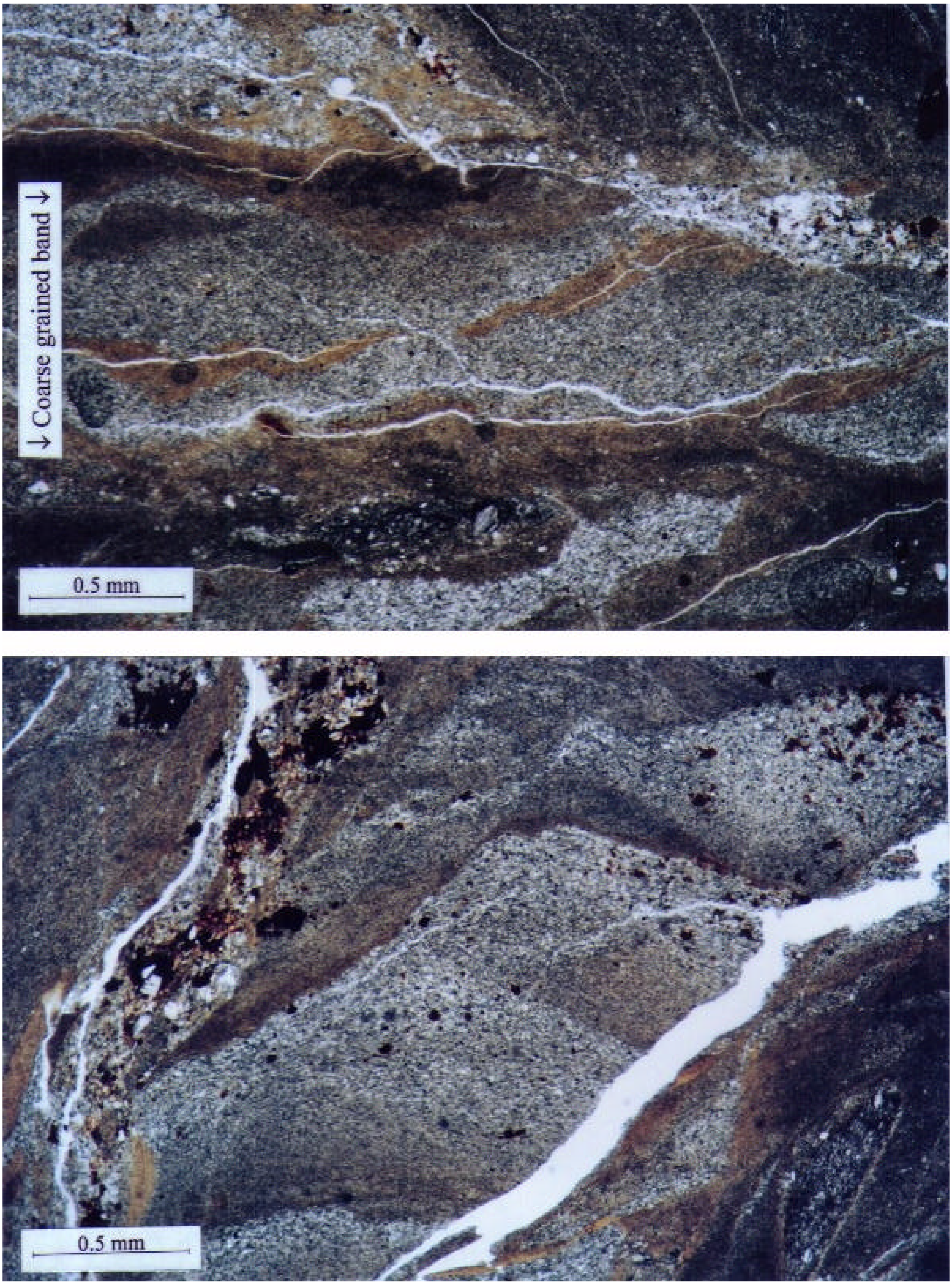

Figure 5.10 A. Photomicrograph of a coarse band of material breaking up. B. Photomicrograph of the same band as in (A), only here showing greater deformation. Listric shears have developed and the band has been compressed. The listric shears give a lens-like appearance to the coarse material. Both photos are taken under unpolarized light in west-east vertical planes.

It can be suggested that free water movement through the coarse units as the listric areas dilate and collapse allows sharp faults to form. In the post-faulting situation, the juxtaposed fine sediments restrict the fluid flow. This may lead to a reduced effective pressure close to shearing areas, and more pervasive movement. This pervasive movement would provide the mixing necessary to give the units' 'graded' appearance.

There are a number of other important features of the sediment that require explanation:

1) melanges of silt blocks with prior developed fabrics;

2) clean areas of sands;

3) quartz grain bands that may have suffered winnowing;

4) the movement of coherent sediment bodies into each other by small scale displacements.

There are a two possible situations accounting for these features.

1) Lodging clast gouging, and lodgement induced melt-out (*Figure 5.11*).

a) The boulder immediately in the down stream ice direction from the sediments described above (see *Figure 5.2*) gouges through pre-existing diamict.

b) Diamict moving from in front of the clast is joined by diamict flows from the sides of the gouge. These processes go some way to forming the 20 cm of blue-grey diamict above the 15 m + of harder material extending up-ice from the boulder.

c) The clast starts to lodge as material piles up in front.

d) The pressure of the ice on the clast causes pressure melting and water fills some of the gouge behind the clast. Meltout debris intermittently mixes with the reworked lower diamict. Smaller quartz grains rain out more slowly.

e) Lodgement of the till continues. As the large boulder is covered, normal ice flow can resume, with all the above processes acting, but on smaller particles. The particle size means that this later sediment is less protected and, thus, more mixed. This gives a homogeneous till which then suffered shear consolidation.

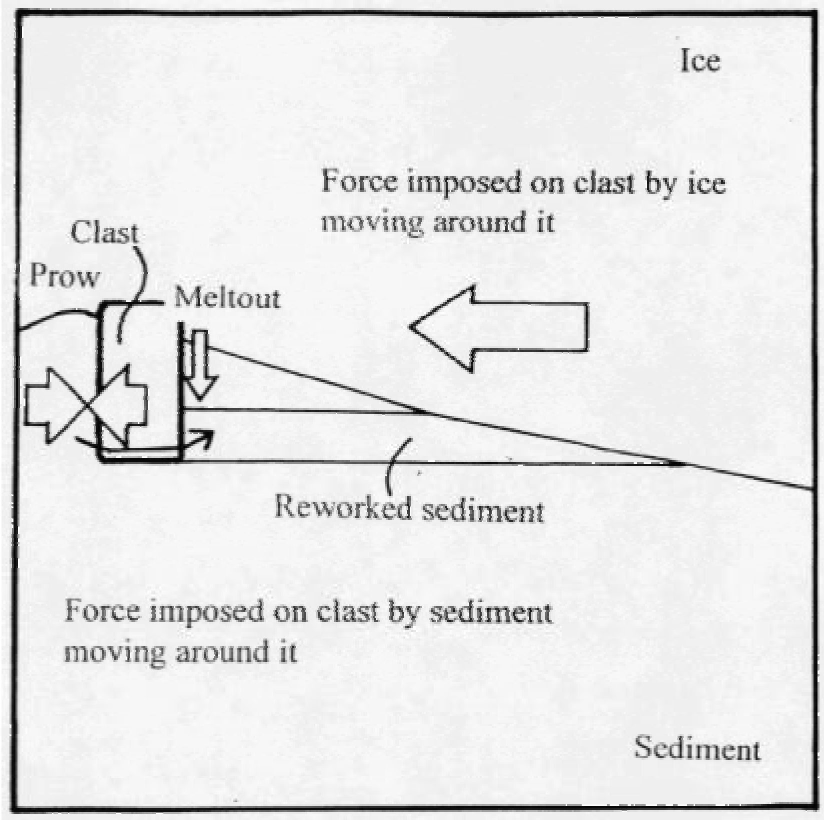

Figure 5.11 Processes involved in the lodgement model.

2) Pressure pumping of sediments.

a) Water pressure variations in distant till pump material from the upper diamict down shear zones and into the lower diamict or the ice (for mechanism see Talbot and von Brunn, 1987).

b) This mix of basal till and ice melts. High discharge meltwater moves preferentially through the diamct concentrating sands and washing them. Quartz grains represent till bodies with fines removed where escape could not occur through sands. These unimodal units may also have been deposited as such from the ice.

It is the macroscale form of the deposits which allows the attribution of the microscale features to process (1) with greater probability than process (2). The amount of meltout material in (1) would be expected to increase as the clast became lodged. The resistant layer seen in Figure 5.2 widens up and becomes more sandy towards the clast, so that the geometry strongly supports hypothesis (1). It is possible that the resistance of the layer is partly caused by consolidation under the lower part of the ploughing clast. The ice pushed the clast west and lodged it against a massive till prow, with meltout thickening the mixed zone only in the very last stages. It should be noted that the micromorphology of the sediments indicates a 'warm' (unfrozen) bed at the sample point, however, the inclusion of the silts with a prior fabric, and the general form of the feature on a macroscale indicate that it did not form through simple 'meltout' *alone*.

The ploughing hypothesis allows a prediction of the nature of lithofacies E under the resistant layer. The material is expected to show;

1) a generally homogeneous mix of material from clay to sand sizes;
2) strong shear fabrics.

Under the glacier pumping hypothesis we would expect to still see some injection features and areas of fabric disruption which may develop prior to throughflow winnowing. We may alternatively see a very heterogeneous meltout sediment under this model.

Two orthogonal, vertical samples (2a/b) were taken to compare with these predictions. They showed homogeneous material, though largely without sand-sized material, and a very strong shear fabric (*Figure 5.12a/b*) with no evidence of sediment intrusion. The evidence for lodgement is therefore good, though the sand sized material must probably be regarded as exotic.

It seems likely that the extreme size of the boulder in question meant that sufficient sediments were produced to survive further, limited, overriding. The low post-depositional reworking suggests the deforming layer at this time was thin and/or the deposition was towards the end of the glaciation. Model evidence (below) suggests the till was weak, which may indicate a thin deforming layer due to very low effective pressures and/or the low clast concentration of the original till. The material examined above may also have been protected by the introduced sand-sized material (which has a higher angle of friction). It is equally possible that the unaligned silt and clay material seen in the thin sections of the interbedded material was more resistant to shear. Indeed, it is interesting to speculate that there is a feedback here which could mildly enhance the further lodgement of clasts.

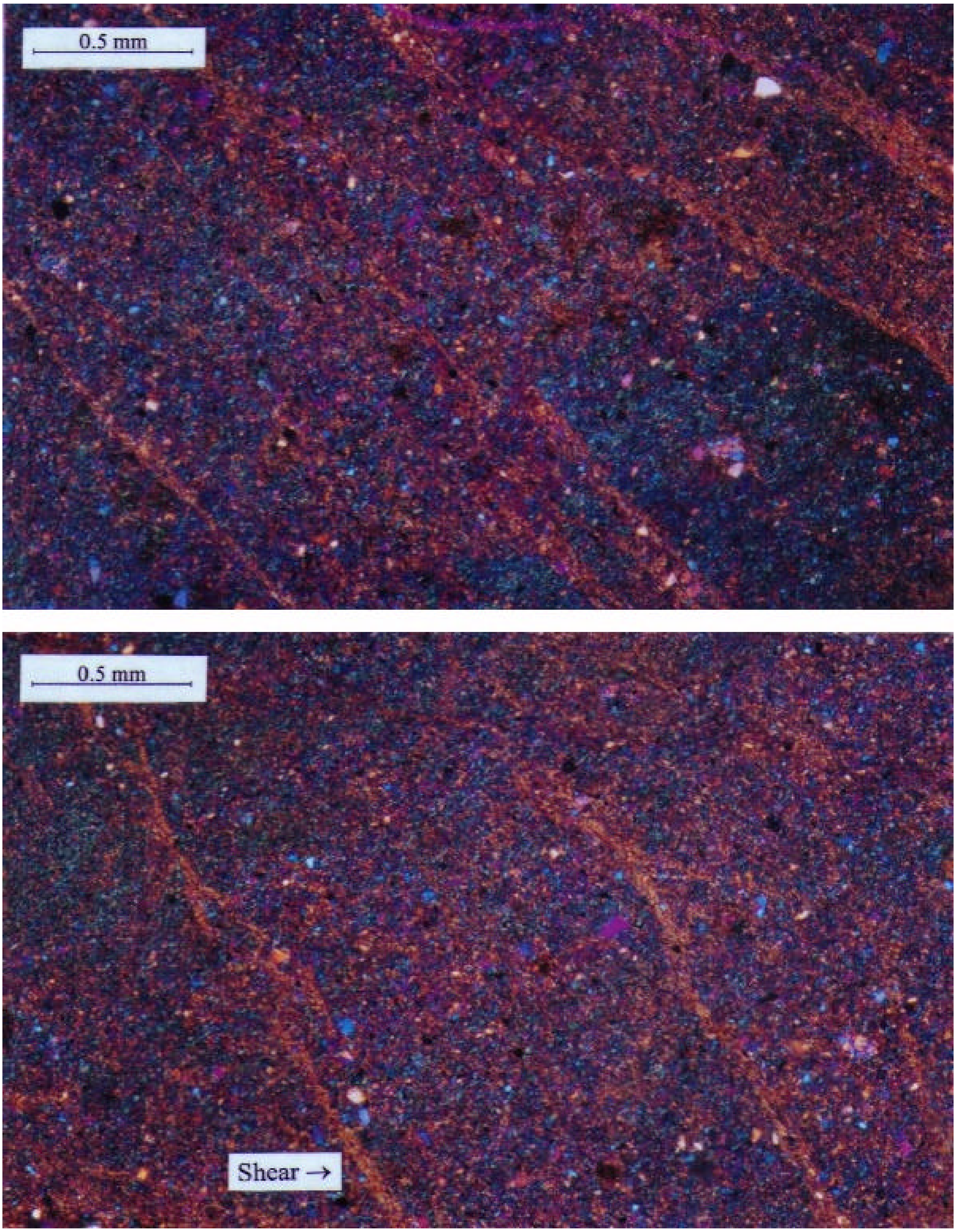

Figure 5.12a/b Sections from lithofacies E below the interbedded material (Sample 2a). Cross-polarized light with tint plate. West-east vertical plane.

The strong macroscale clast fabric makes it unlikely that simple meltout without reworking was a significant factor in the deposition of the whole of the two diamicts (Grant, 1990, see also Boulton, 1977). While similar areas of interbedded material *are* found elsewhere on the ice-upstream side of the outcrop, they are rare and discontinuous. This picture is in line with explanation (1) though localised simple meltout may also have produced some of these interbedded sediments (see Boulton, 1977). It is suggested that the microstructures seen here *are* associable with simple meltout, with the important exception of the pre-aligned slugs of silts and clays. These indicate the reworking of material that has already been deposited. It is possible such alignment occurred in the sediment while trapped in the ice. While shear occurs in sediment trapped in ice (for example, Echelmeyer and Zhongxiang, 1987), we have no knowledge of such sediment's microscale alignment. It seems likely that in the case of stagnant meltout, the sediment will lack cohesion and mix to form more homogeneous deposits (Paul and Eyles, 1990). A fluvial origin for the material can be dismissed as such a situation is unlikely to produce cohesive sediments horizontally juxtaposed with clean sand bodies and substantially winnowed material. Each sediment type suggests a differing fluid flow rate and sediment concentration. One must also remember that this feature is inextricably included in the lower diamict.

If the ploughing boulder interpretation (*Figure 5.11*) is taken as correct, it may greatly elucidate the process of clast lodgement. The inferences that can be drawn from the work so far, and avenues of further research, are outlined below.

5.4 Modelling

5.4.1 The qualitative model

There are four important stages to the clast lodgement process implied by the till flow and pressure meltout-induced microstructures discussed above. The potential contribution to the process from other meltout is discussed in the model assumptions (below).

1) The clast initially moves with the ice. As there is no velocity difference between the two, there is no longitudinal stress imposed on the clast by the ice. Thus, there is no horizontal net pressure gradient across the clast and no pressure melting ('regelation') or pressure-enhanced creep associated with the boulder (contrast with Weertman, 1957). Provided

there is some decoupling between the ice and the lithofacies E (which is anticlinal in section - *Figure 5.2*) the ice creep over the anticlinal hummock will probably be at a maximum at the hummock's top in the same manner as the 'streaming' effect around obstacles seen by Boulton (1979) (uncertainty is introduced by our ignorance of the three dimensional form). The thinning of any debris-rich ice with velocity increases the chance of vertical clast-clast collisions. These collisions may push clasts up into the ice and down into the stoss side of the soft till hummock. That is, clasts will plough horizontally into the forms because of the enhanced creep around the obstacle. This hypothesis of horizontal clast release is within the constraint on the release of clasts found by Iverson and Semmens (1995). Iverson and Semmens showed that meltout of clasts from ice will only occur if there is clast-clast contact bridging a determinable thickness of basal ice. This constraint needs to be satisfied in some manner before the model can be used as a flat-bed analogy (below, see also Philip, 1980; Iverson, 1990; Hallet, 1979; 1981; and Shoemaker, 1988, for the arguments leading to the development of this constraint).

2) The clast moves partially into the sediment. The difference between the flow of the till around the ploughing clast and the ice velocity will cause a stress to be imposed on the clast. This stress will result in regelation and ice creep around the clast. These processes produce the microstructures seen above. There is a problem here, in that we would expect till to be much softer than the ice and lodgement to be unlikely. Several factors may increase the till resistance. These are discussed further below.

3) As the till resistance increases the clast will start to lodge and the stress on the clast will increase. The till flow into the gouge behind the clast will be combined with meltwater and meltout material produced by regelation. This is in line with the regelation production of diamict matrix suggested by Kemmis (1981). At this point it is still considered that the ice-gouge interface could have a geometry such that the ice is fully in contact with the back of the clast having partly filled the gouge. However, the sediments filling the gouge will restrict the up-ice contact area between the ice and clast. This will increase the stress at this contact, in turn resulting in an acceleration of the pressure meltout. At the same time the clast-till contact area will be increasing, reducing the force per unit area on the yielding sediment in front, making lodgement more likely.

4) Meltout will continue to accelerate until meltout till and slumped out material from the gouge edges fills the gouge. At some point the melt and creep around the clast will equal the ice velocity, or the meltout material will cover the clast. At this point lodgement will have occurred. Normal ice flow will then take over. Lodgement of the till will continue, with all the above processes acting to produce the same mix of reworked matrix and meltout sediment, but on other, in this case much smaller, particles. With more numerous smaller particles, there is a greater chance of another small clast obliterating all the sedimentary signatures of the processes. Thus, the sediment is more mixed and homogeneous. This material is then shear consolidated during the remaining glaciation.

As mentioned above, it is difficult to explain lodgement in till which is assumed softer than the ice. Stress acting on the till will partly result in the flow of the till from in front of the clast into the gouged area behind. Under the present understanding of tills it is expected that this flow will be accentuated by the compressive stress in front of the clast temporarily increasing the water pressure in the till. Pore pressure in front of the clast will increase until the sediment yields pervasively or on shears. This increased pore fluid-induced weakening will continue until a balance is reached between clast advance and Darcian flow or discrete dewatering, with the fluid pressure reaching a steady state. It is possible that this weakening is catastrophic, however, we know that clasts do lodge, suggesting that processes that are more powerful are acting to increase resistance. Four processes are suggested as potential ways of increasing the effective till viscosity locally to the clast, all are feasible under our present understanding of the subglacial environment.

a) To maintain pressure induced regelation, melt must be balanced by freezing somewhere else to provide the energy for melting (Weertman, 1957). Freezing may be occurring in the sediment around the clast, the material becoming stiffer and increasing the clast's effective size in the till. By comparison with similar sediments we can reasonably expect the till to have a residual strength, that is, even when deforming, there will be some stress transferred across the clast, from the till, to the ice. This stress will initiate the regelation cycle. Freezing of water in the sediment rather than on to the ice (as in traditional regelation) would be dictated by the geometry of ploughing into a slope, and for the development of a prow in front of the boulder.

b) The residual strength of the till may cause a cavity to open down-ice of the clast as the clast slows in the sediment. The excess pore fluid pressure may be released into this cavity, with the excess meltwater from up-ice of the clast. Cavities downstream of clasts have been suggested by Boulton *et al.*, (1974) and have been seen by Boulton (1979). However, there is an observational bias towards marginal ice regions where the movement of ice into such features would be slow. The rate of ice creep closure and regelation refreezing in such a cavity would have to be less than the creep due to the fluid pressure increase keeping it open. The opening of such a cavity seems unlikely to initiate slowing when it is considered that a process has to be found that produces considerable slowing in order to develop a cavity. Thus, while cavitation may play a late-lodgement function, regelation refreezing in the till seems more likely to cause early clast deceleration. The relative importance of the two will relate to clast size.

c) A cavity opens in front of the clast, as above, and the soft till moves up into the space. This causes a flute as suggested by Boulton (1976) and the cavity re-forms further and further upstream, the flute acting as an extension of the clast. Thus, the area of dewatering and softened sediment is moved away from the clast, and stiff till forms just in front of the boulder. The same problem holds for initiating such a cavity as in (b). Prow size may provide detailed information on the relative till-ice rheologies, however, this chapter does not deal with this interesting avenue.

d) The chief mechanism of lodgement involves changes in the contact areas of ice and till due simply to the geometry of ploughing into a slope, or the development of a prow on a flat bed. This development will affect the stress transferred from the ice to the deforming till down-ice of the clast. The difference between this situation and that of the flute in (c) is that this geometrical change does not need to be initiated by the clast slowing relative to the ice, though this may well be a result of the change.

In this lodgement model, the clast slowly decouples from the ice, undergoes a transition period, and then becomes coupled to the till. This process of transitional decoupling may be a major process inducing deformation in the sediment and slowing the ice. It has been assumed in the above that the sediment has no effect on ice velocity. This may be the case for the small deposit at Criccieth, however, under more general conditions the process will feedback to link the till and ice velocities. It will be the ease of ploughing (the length of the decoupling transition) which determines the effect sediment has on reducing the ice-bed friction and increasing the velocity of the ice with respect to hard beds. It seems wise to construct a quantitative model of the proposed processes to test and explore their complex implications. A quantitative model will also allow us to determine whether these implications are consistent with our present knowledge of the subglacial environment.

5.4.2 The quantitative model

Initial caveat

Ideally we should model the till rheology as non-linear. Such an attempt is far from trivial. If the till were shown to be of a low effective viscosity in relation to the ice, the sediment could be modelled as deforming to release all the stress after a residual stress. This would remove the difficulties of non-linear modelling, while allowing the till to impose some stress on the clast, that is, giving the till a residual strength.

The effective viscosity of ice flowing around a clast can be calculated using the equations quoted by Weertman (1957; 1964; 1979). In Weertman's model the ice flow around an object of equal height and width transverse to flow and a given length is equal to the sum of the creep and regelation around it.

To set up the regelation component we assume there is a force difference (s) across a boulder of width and depth (w) and height (h) resisting ice flow. The stress is split between an upstream, compressive, component and a downstream, extensional, component, each with a value of $s\ /\ 2wh$. The stress difference across the boulder can be converted into an equivalent change in the melting point of the ice, $C\ (s\ /\ wh)$ where C is a constant equal to 7.42x10^{-5} K kPa^{-1} (Weertman, 1957). This causes ice to melt upstream and refreeze downstream. Following Weertman's derivation we gain the total volume of ice melted per unit time (m) by a longitudinal stress as given by

$$m = \frac{a\,s\,Ch_i K}{Hr} \qquad \textit{...Equation 5.1}$$

giving the melt rate per unit area of clast ($\dot{m}$) as

$$\dot{m} = \frac{a s CK}{Hrw} \qquad \text{...Equation 5.2}$$

where h_i is the height of clast out of sediment, K is the conductivity of the rock (taken as 0.1194229 J °C s^{-1} cm^{-1} following Weertman, 1957), H is the heat of fusion of ice, r is the density of ice, a is a constant dependent on loss of heat into the ice rather than the rock.

To set up the ice creep component we assume the stress causes the creep of ice around the resisting boulder at a rate ($\dot{c}$) determined by a variant of Glen's flow law, the original form of which is,

$$\dot{c} = Bs^{\,n} \qquad \text{...Equation 5.3}$$

where B is taken (for 0°C and 50-130 kPa stress range) as 5.5 x $10^{-15}s^{-1}$ kPa^{-3} (table 3.2 of Paterson, 1981) and n is 3 or 4.

Weertman suggests the creep of the ice around the obstacle/boulder per unit area per unit time $\dot{c}$ is given by the variant of Glen's flow law,

$$\dot{c} = \frac{2}{9} Bds^{\,n} \qquad \text{...Equation 5.4}$$

where d is Weertman's 'distance of action', taken here as one clast width in line with Weertman. The constant arises from the uniaxial nature of the force application (see p.32 of Paterson, 1981, for the assumptions involved).

The total velocity of ice past the clast (v) is thus the creep and melt rate combined. The equation for total velocity can then be used to calculate the effective viscosity (h_e) from

$$h_e = \frac{F}{v} \qquad \text{...Equation 5.5}$$

This value can be compared with the effective viscosity for a sphere moving through a non-regelating Newtonian fluid (the till), calculated using Stoke's equation,

$$F = 12 p h_t Rv \qquad \text{...Equation 5.6}$$

where h_t is the viscosity of the till. Figure 5.13 shows the till viscosities at which movement around, and force on, a clast moving through till is equal to that around and on a clast of the same size moving through ice. This rather complicated set of values is taken to represent the till viscosities at which non-linear till rheology effects will start to become very apparent during lodgement. It is considered that if the viscosities of tills found in the field fall higher than these values the present model is a less suitable model of till behaviour. Plainly this comparison has no absolute mathematical basis as the two models are unrelatable for reasonable values.

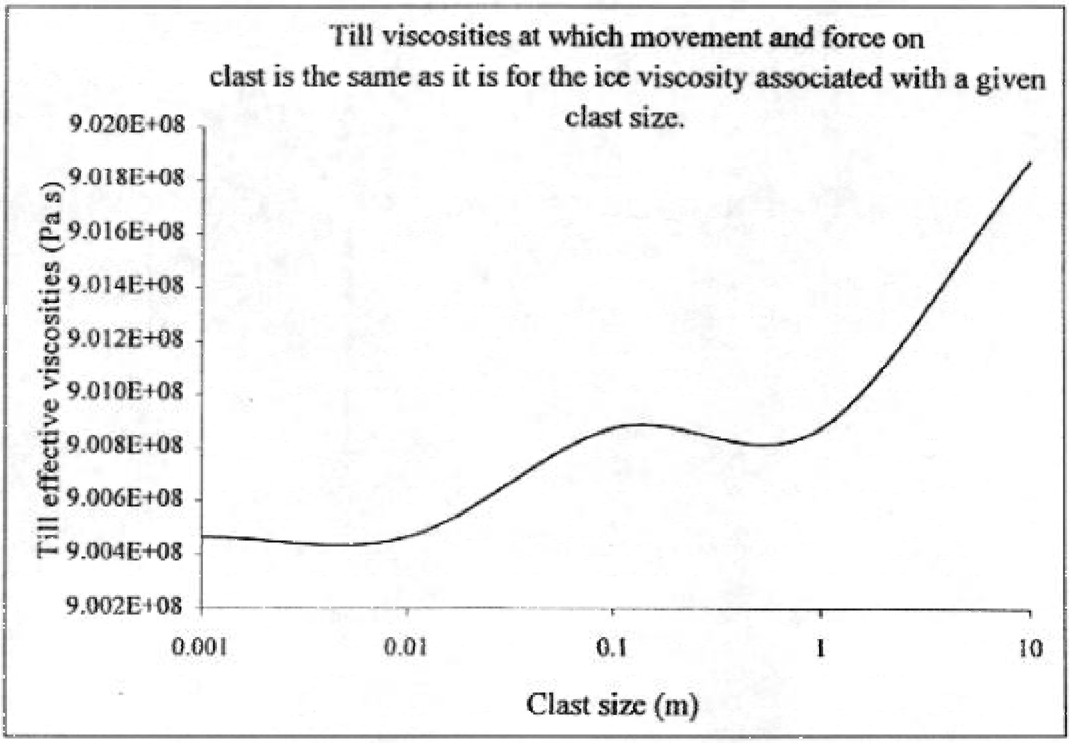

Figure 5.13 Till viscosities at which deformation is equal to ice deformation dependant on clast size for various ice viscosities.

Till viscosities measured in the field range from extremes of 10^8 to 10^{11} (Paterson, 1994). Thus, it can be seen that the model is a poor representation of reality for all but the weakest, least viscose tills. It is not a simple matter to calculate the stress supported on the clast in a non-linear viscose material. It must be accepted that the model presented here is the simpler end member of a continuum also dependant on the influence of sediment in the basal ice on the ice rheology. However, the model results suggest that in *this* case, the till has a low residual strength, and its low clast density may make it act in a manner closer to that of the model (these ideas will be enlarged upon in later chapters).

Assumptions

A number of important assumptions will be made in the model of ploughing into a slope that can be utilised to produce a flat bed analogue at a later date.

The forces on the clast are simplified here such that the clast is driven horizontally into a slope. There are two components of this simplification that may need to be altered in order to produce a model corresponding to other real situations. Firstly, the local slope may be different, indeed, may be horizontal. Secondly, the clast may be driven into the slope at a different angle. Taking the local slope first; it should be remembered that the primary process suggested for the lodgement of clasts is the resistance offered by a sediment prow. Even if the slope is horizontal, it has been seen that prows can develop (Clark and Hansel, 1989). The development of such a prow is determined by the sediment hydraulic diffusivity, internal friction, the clast size, and the stress acting on the sediment.

As a simplification it is presumed that the strength of the material is affected little by being pushed into a prow. Triaxial experiments presented in Chapter Six suggest work-hardening in sheared till at low total strains. The limited plough-meter evidence from under modern glaciers (Porter *et al*., 1997) shows force increasing as objects trapped in the ice move through sediment. However, this is usually interpreted as ice velocity changes rather than the development of resistance. It seems wise at this stage to take the simplest model and assume there is no hardening dependent on large strains. This assumption is easily remedied later as it can be handled with a variable in the calculation for the residual strength of the till. The stress build-up is therefore controlled by the changing contact area of till to clast including the prow effect, and may be calculated geometrically. The prow can reasonably be approximated as a slope angle local to the clast, provided the material is not allowed to flow into the gouge behind the clast. Thus, even on a horizontal bed, ploughed into horizontally, there will be a local change in contact heights that can be visualised as a slope.

Moving on to the direction the clast ploughs in; this angle is determined by the velocity parallel to the local sediment slope surface and the velocity normal to the slope. Slope-parallel movement is the enhanced creep rate minus the gravitational pull of the clast in the opposing direction. Slope-normal movement is the melt rate local to the slope, plus the gravitational movement in this direction, minus the regelation of the ice downwards around the clast normal to the slope (Hallet, 1979; 1981; Shoemaker, 1988; Iverson and Semmens, 1995). The resultant velocity can be assumed to be horizontal in the case considered here for the simple reason that there is empirical evidence for this situation. Iverson and Semmens (1995) suggest that thick sequences of clast supported sediments are necessary for clast expulsion. This criterion is satisfied at Criccieth because of the size of the clast, and the greater clast-clast contact caused by the enhanced flow of the ice over the mound, as discussed above. Any evidence for a slope-wide rapid melt rate will have been mixed into the till by later deformation.

A more general approach to the model would be to first calculate the direction of the resultant movement and include this in the slope calculation, along with regional slope and prow slope. It should be noted that the regelation that is calculated in the model should alter the driving force direction. Therefore, the entrance angle would vary as the model proceeded if it were not assumed to be constant on the basis of the ploughing trace seen in the field (*Figure 5.2*). Indeed, assuming a horizontal resultant velocity assumes an increase in the average melt rate over the slope to counteract this effect. This is the only non-steady-state assumption of this model.

Ideally, a more general solution is needed, showing the effect of many clasts on bed stresses. Kamb and Echelmeyer (1986) have produced a rigorous determination of hard-bed shear stress by including longitudinal stress and decoupling length terms. One way of getting from this investigatory *single* clast model to a more general solution may be to relate the decoupling lengths determined here to those of Kamb and Echelmeyer.

Model components

The release of stress caused by ice flow against a lodging clast is separated into the component removed by the ice moving around the clast, and that removed by the flow of till from in front of the clast.

Taking Weertman's (1957; 1964; 1979) model, which works reasonably for a rectangular prism, the flow of ice around the boulder is modelled as due to regelation and creep (*Equation 5.2* and *5.4*).

The till is assumed to yield to relieve all the stress above a residual stress supported by the material. This residual stress is transferred across the clast to cause regelation and enhanced creep in the ice. The movement of the ice past the clast is then totalled and removed from the ice velocity to give the resultant movement rate of the clast through the till. The shear stress that is traditionally used to drive regelation and creep is included by using the ice velocity. The residual strength of till cannot be related well to the Mohr-Coulomb equation, therefore empirical estimates are used when necessary (see below).

The till is assumed incompressible in the model, and the effective pressure is maintained as a constant. There is no freezing in the sediment. The empirical evidence suggests some of these factors *are* varying, however, they are not well understood. The compressibility and effective pressure are related, but not enough is known about the rheology of tills to calculate the effect yet. The same problem holds for the effect of freezing in the sediment. Therefore, these processes are assumed equal and opposite (which they will be for one particular clast size) and neglected here. When more information is available, these processes can be included in the calculation for the residual strength. The forces acting in the model are distributed over areas calculated geometrically.

Because the gouge fills with material, the height of the clast is not a measure of h_i the contact height between the clast and the ice. This is calculated assuming

$$h_i = h_b - f\left(\frac{Md}{w}\right) - T \qquad \text{...Equation 5.7}$$

where h_b is the total clast height, w is the clast width, M is the total meltwater volume, d is the volume of debris in the ice divided by the fluid equivalent volume of the ice containing it, and T is the till inflow height, which is the average height of the till flowing around the clast. The value of d is taken as 0.2 for the ice at Criccieth. Values of d in modern glaciers range from 0.0002 to 0.74 (Kirkbride, 1995). A value of 0.2 is slightly above average, and is based on Boulton's (1977) contention that lithofacies D at Criccieth is stagnant meltout material. The method of calculating the debris height is difficult, however, it is suggested that a reasonable model is to proceed thus,

a) distribute the sediment as a ramp extending from the clast, where the angle of the slope is equal to the angle of internal friction of the sediment. Calculate the average height of this ramp,
b) calculate the area of the last increment's meltout that is covered by the base of the ramp and the volume of the last increment's meltout in that area,
c) add the overlapped material to the average over the new increment's base area.

The sediment is largely clay sized material with some silts. There are only low levels of sand sized clasts (above). Thus the angle of internal friction for the sediment is taken as 22°.

The clast-till contact height can be calculated from simple geometric considerations based on the following lengths;

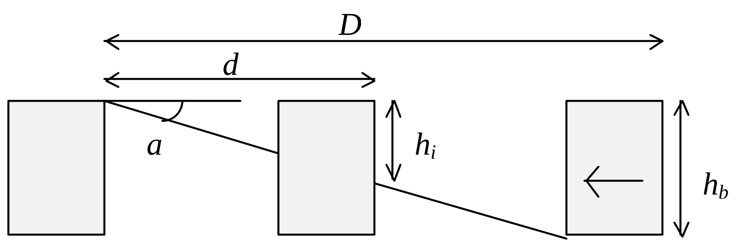

Where d is the distance to complete burial (h_i tan$a$), D' is the total distance to burial, a is the slope angle, and h_i and h_b are the upstream height of the boulder in the ice and the absolute clast height respectively.

The model has two implicit states,

$$\dot{e} = v_i \,, F_c = 0$$
$$\dot{e} = 0 \,, F_c \geq F_v \qquad \textit{...Equation 5.8}$$

where $\dot{e}$ is the strain rate in the till i.e. represents movement of the clast, v_i is the ice velocity minus the flow of ice around the clast, F_c is the force acting on the clast due to the residual strength of the till, and F_v is the viscous drag force of the ice around the clast when it is unmoving. The force terms will vary with clast exposure. Thus, F_c can be compared with F_v at each stage of a model run and the point at which they are equal will be that at which there is no clast movement through the till. The Weertman (1957) equations are used to calculate F_c. These equations give a cubic solution for force in terms of total ice velocity. Over the clast widths used in this study (below) the discriminant of this solution suggests there is only one real and positive root as required by the physical basis of the model (the other root being complex). The roots can therefore be gained using the Tartaglia / Cardano method (Daintith and Nelson, 1989).

Data used in model runs

Two sets of model runs were completed. In one set the ice velocity and residual strength were given and the lodgement characteristics calculated, in the other the residual strength was calculated for a number of velocities on the basis of the ploughing length at Criccieth. The ice velocity, when controlled, was taken as 20 ma^{-1}. Although there is no evidence that this velocity is suitable, there is no evidence for any other velocity, and it is both mathematically convenient and reasonably representative for a glacier. The bed slope local to the ploughing boulder is 5°. The residual strengths for the till, when required, are set to vary over three orders of magnitude from 0.5 kPa to 50 kPa, which covers field estimates (Table 8.1 of Paterson, 1994). Initial runs used clast sizes ranging over three orders of magnitude. Cubes of side 0.01m and 0.11m (the transition size assumed in all abrasion studies, following work quoted by Hallet, 1979; 1981) were used, and a boulder 1m height by 1.75m width and depth - the size of the clast discussed above at Criccieth. The code for the models can be found in Appendix B.

5.4.3 Results

Figure 5.14 shows the distance ploughed before lodgement by different sized clasts over time through tills of various residual strengths. The fact that in one case (0.5 kPa residual strength till) the model clast the same size as the Criccieth clast (1.75 m x 1.0 m) ploughs a similar distance (11.08 m) to that seen in the field (~10 to 11 m) strengthens our interpretation. This is further backed by the height of meltout associated with this clast size (*Figure 5.15*), which is close to the field estimates of ~0.5 m just before lodgement (note that the model does not include meltout after lodgement, or frictional/geothermal meltout, so the model results are a minimum estimate). The force supported by the clasts over time is given in Figure 5.16.

If the ice velocity and till strength are allowed to vary in steps of 10 m a^{-1} and 1 kPa respectively over 0 to 2000 m a^{-1} and 0 to 50 kPa, we can estimate the till strength for various velocities at the Criccieth site by searching for those clasts that plough the same distance as that suspected to have occurred in Criccieth (between 10 and 11 m). The potential residual strengths are given in Figure 5.17. In reality these values will form a continuous field of potential strengths, surrounded by a strength-velocity field which could *not* account for the feature at Criccieth. The total meltout fill for these cases is given in Figure 5.18 and the maximum force supported by these clasts is given in Figure 5.19. The thin sections suggest that lodgement is partly occurring because of the till flowing around the clast. This is allowed to fill the gouge in the model, pushing the ice off the clast back. This material would not flow into the clast gouge in the case where the local slope is being used as an analogue of prow development. If the model is run without this inflow to simulate this material having no effect, the potential residual strengths for the till and ice velocities are more limited (*Figure 5.20*), the meltout volumes are higher (*Figure 5.21*), and the supported forces for any given velocity are larger (*Figure 5.22*).

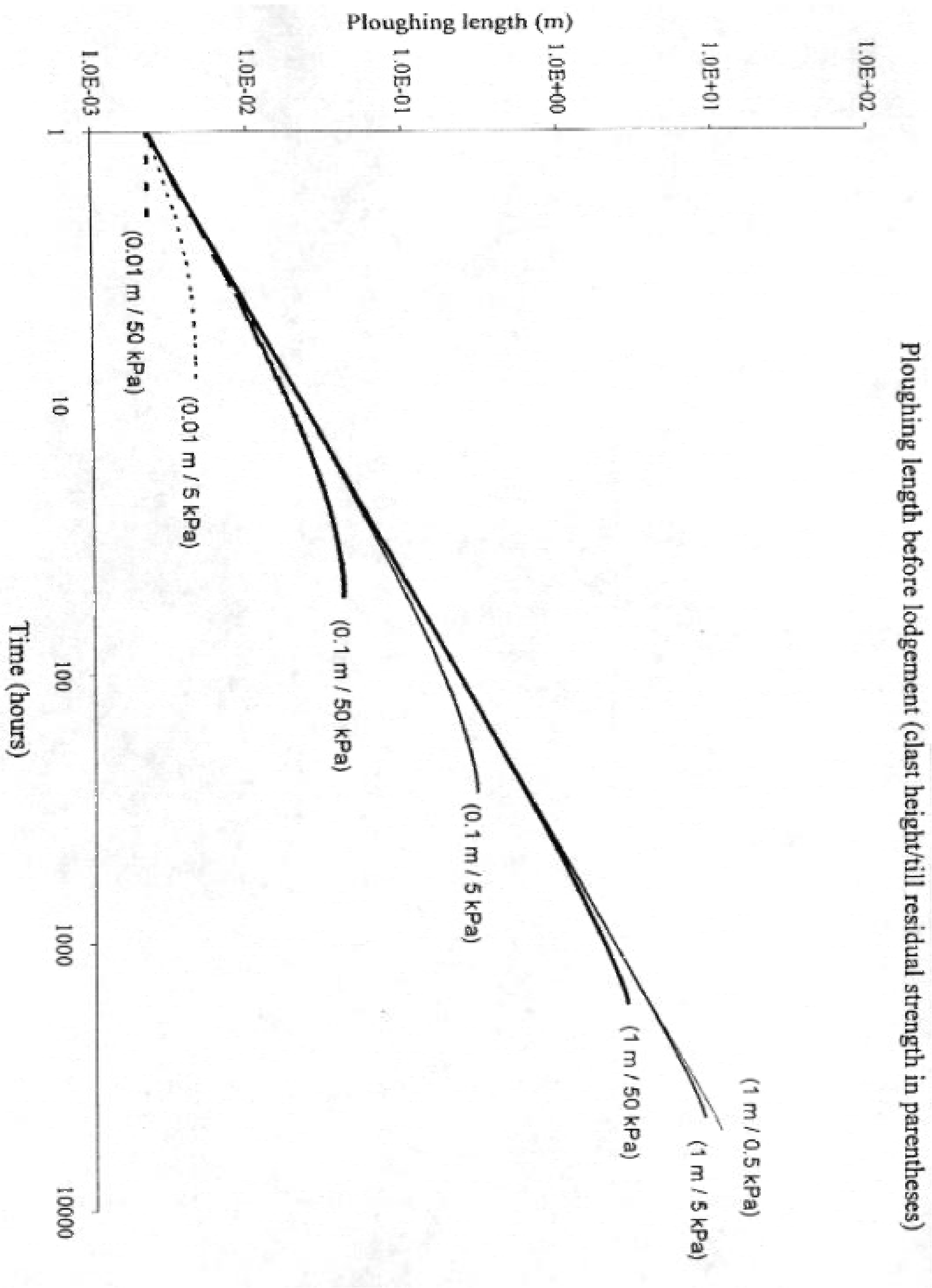

Figure 5.14 Distance travelled over time by different sized clasts through tills of various residual strengths up to lodgement when the model terminates (infill behind the ploughing clast by regelation and slumping allowed).

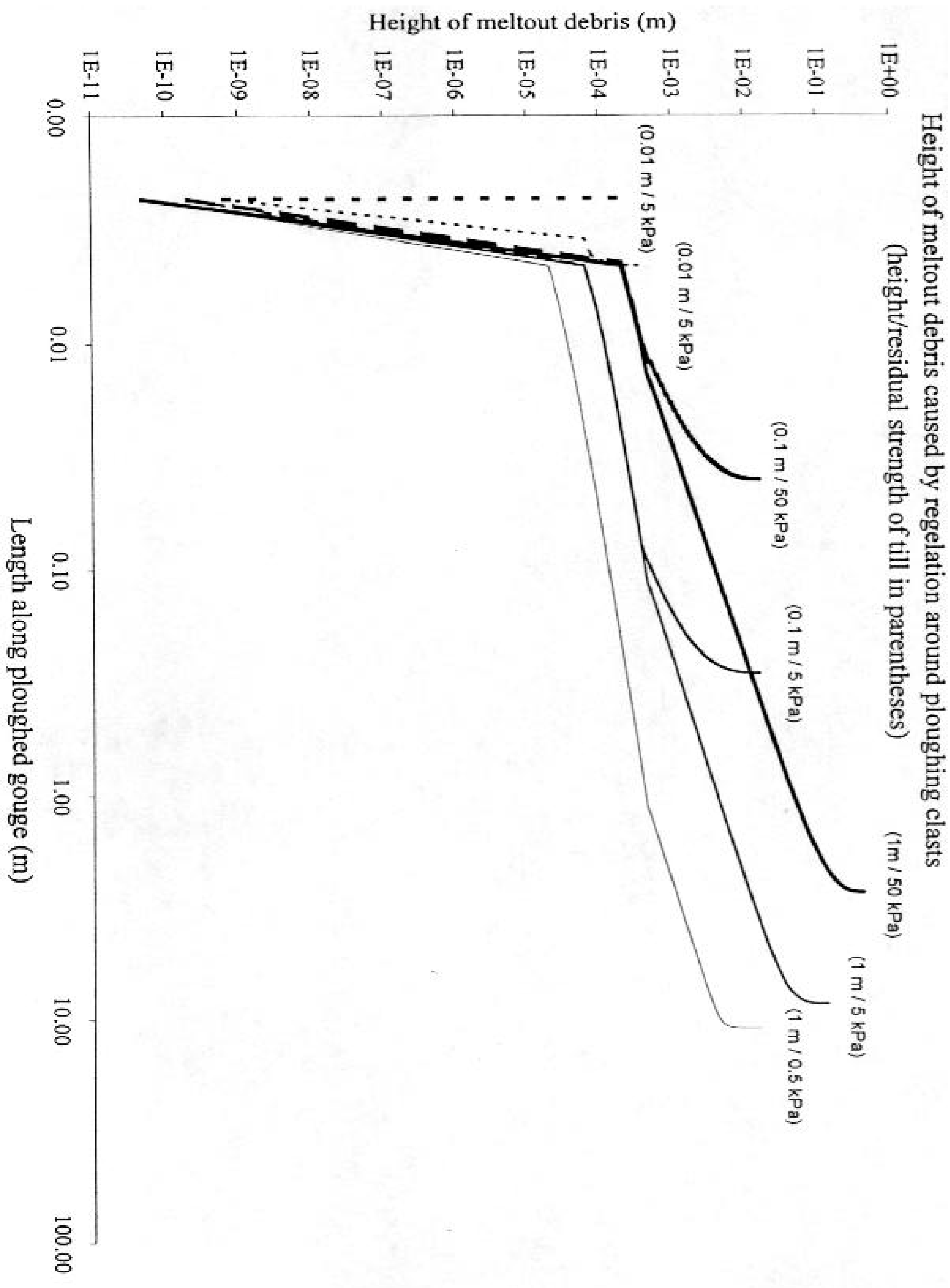

Figure 5.15 Meltout produced over the ploughed distance by the ploughing of different sized clasts through tills of various residual strengths (infill behind the clasts also allowed by slumping of the trench walls).Note that meltout production is halted in the model when lodgement occurs and frictional/geothermal meltout is not included, making these values minimum estimates.

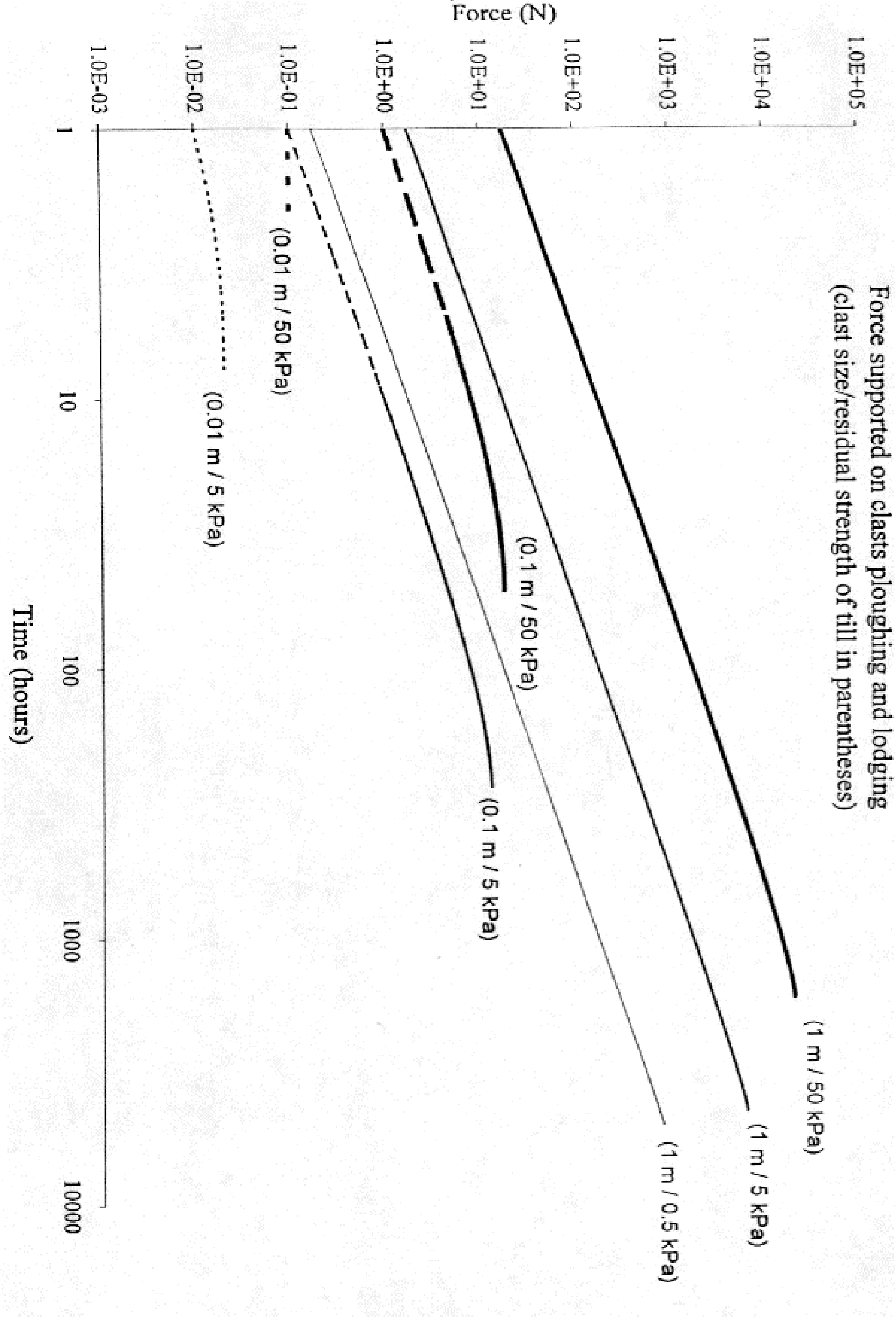

Figure 5.16 Force resisting ice flow over time up until lodgement, caused by clasts of various sizes ploughing through tills of various residual strengths (infilling by meltout and slumping of the trench walls allowed). The model terminates at lodgement.

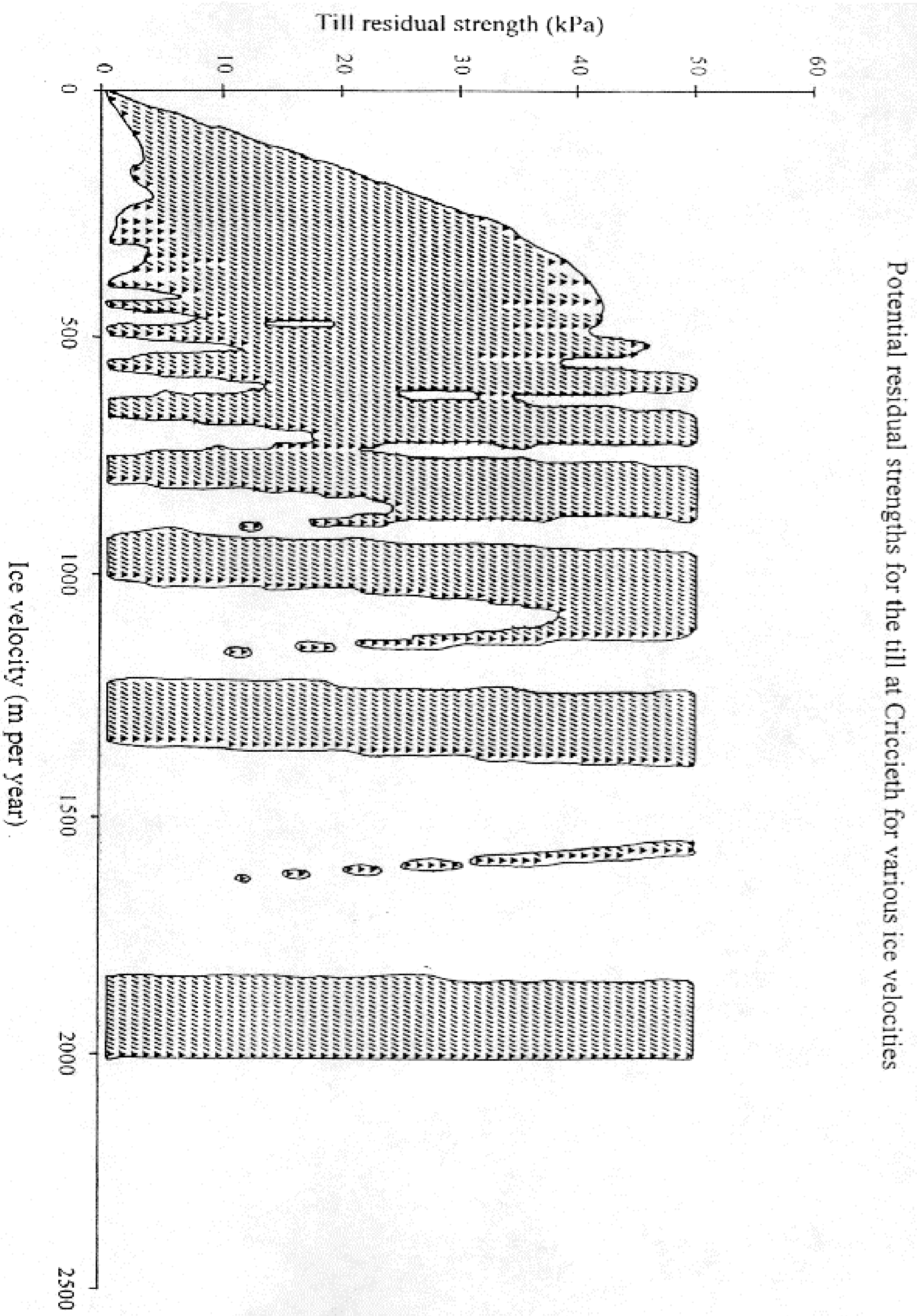

Figure 5.17 Potential residual strengths of the lithofacies E till at Criccieth for various ice velocities based on the length of the ploughing trace (infilling behind the ploughing clast by regelation and trench slumping allowed).The till strength was allowed to vary between 1 and 50 kPa in 1 kPa steps, the ice velocity was allowed to vary between 1 and 2000 m a^{-1} in steps of 10 m a^{-1}. Ploughing lengths were then compared with the length seen in the field and only those conditions producing this length accepted as likely.

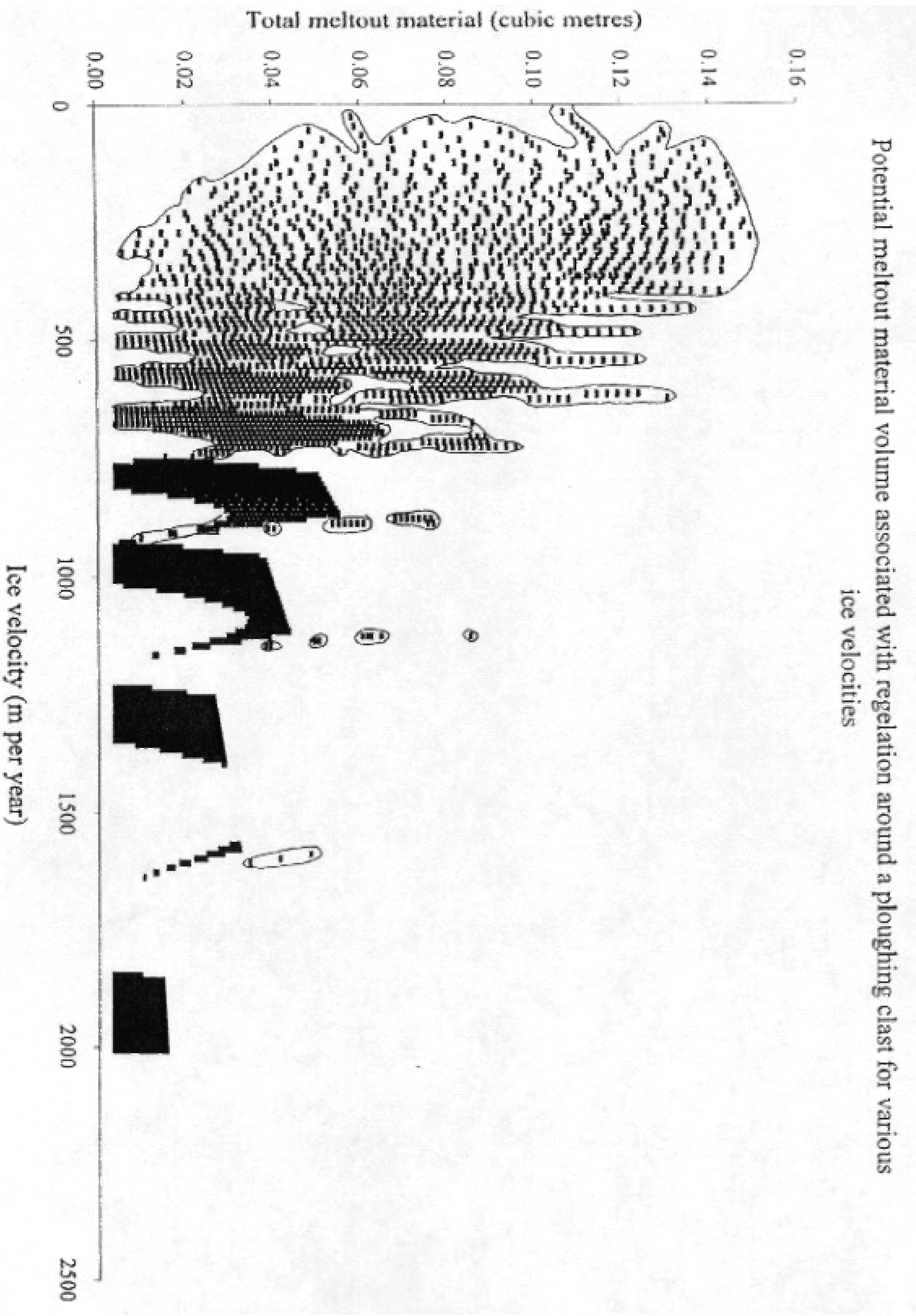

Figure 5.18 Meltout material associated with the potential residual strength estimations for various ice velocities based on the length of the ploughing trace (infilling behind the ploughing clast also allowed by trench slumping).

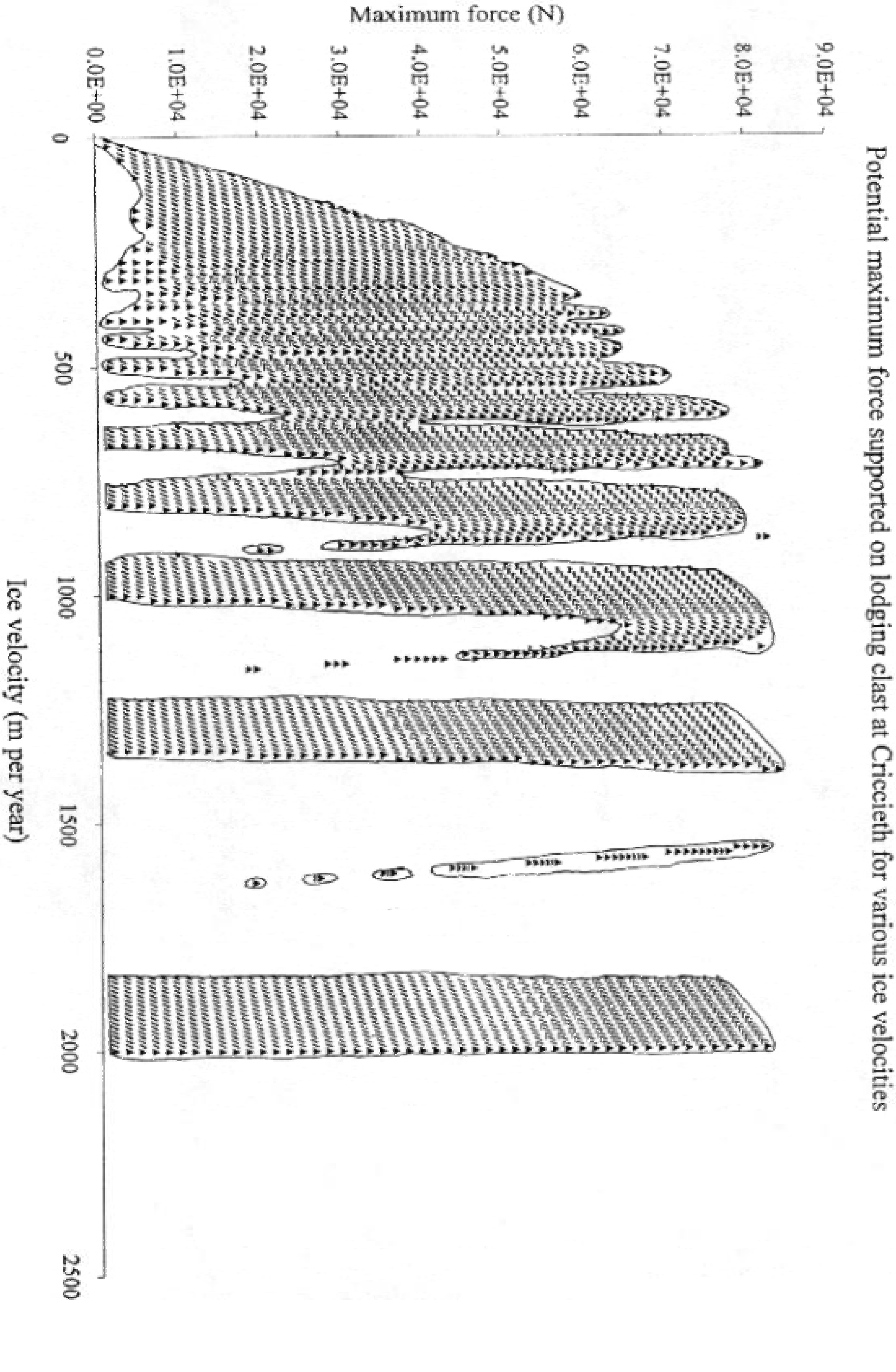

Figure 5.19 Maximum force resisting ice flow associated with the residual strength estimates for various ice velocities based on the length of the ploughing trace at Criccieth (infilling behind the ploughing clasts by meltout and slumping allowed).

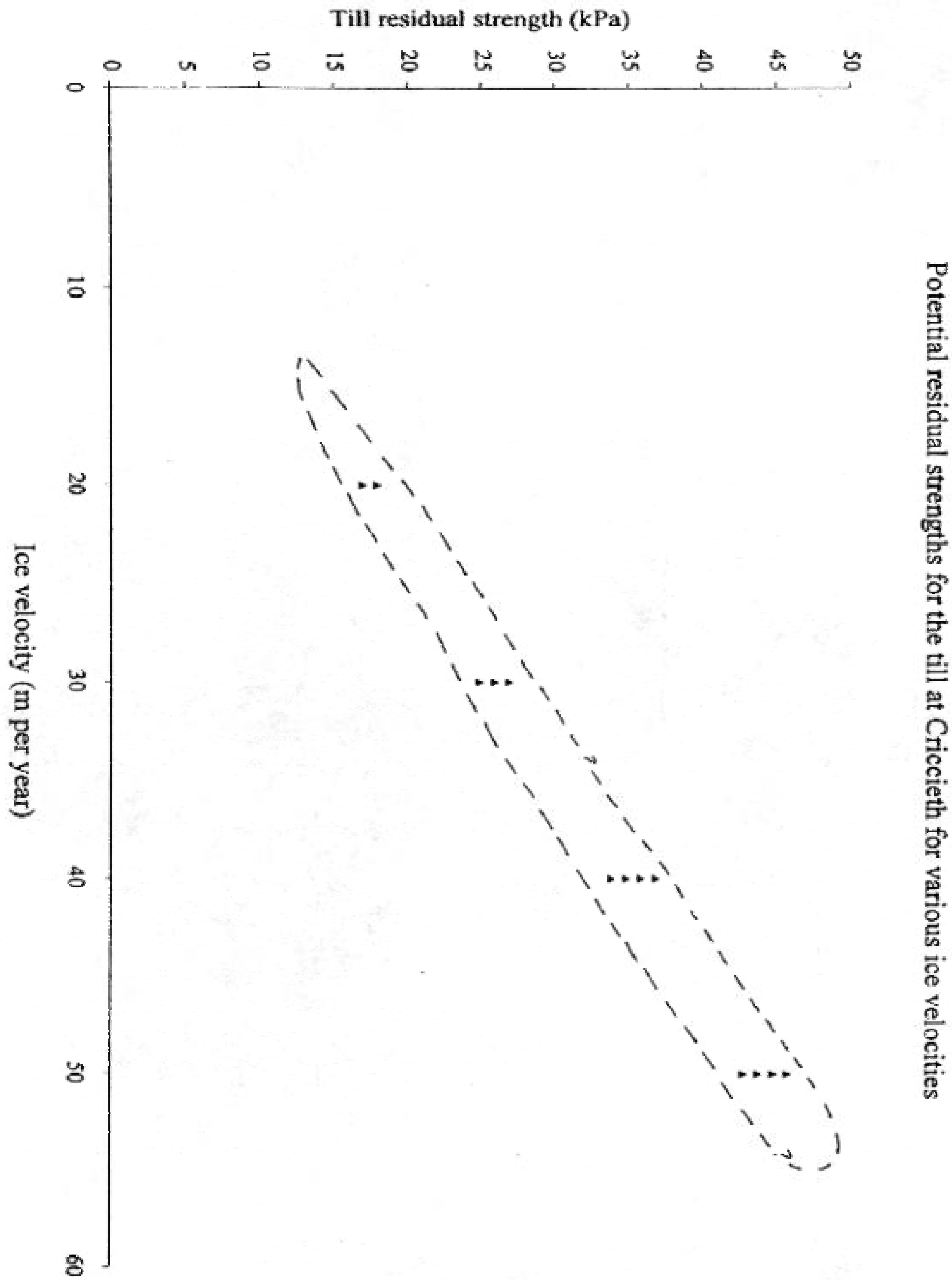

Figure 5.20 Potential residual strengths for lithofacies E at Criccieth for various ice velocities based on the length of the ploughing trace (infilling behind the clast not allowed).Note that the residual strength was allowed to vary between 1 and 50 kPa in steps of 1 kPa, and the ice velocity was allowed to vary between 1 and 2000 m a^{-1} in steps of 10 m a^{-1}, thus the values are not continuous. In reality the values would fall in a continuous field of potential strength-velocity combinations. The values seen here are the only ones found reasonable in the quoted ranges based on the criteria that the ploughing length should be that seen in the field.

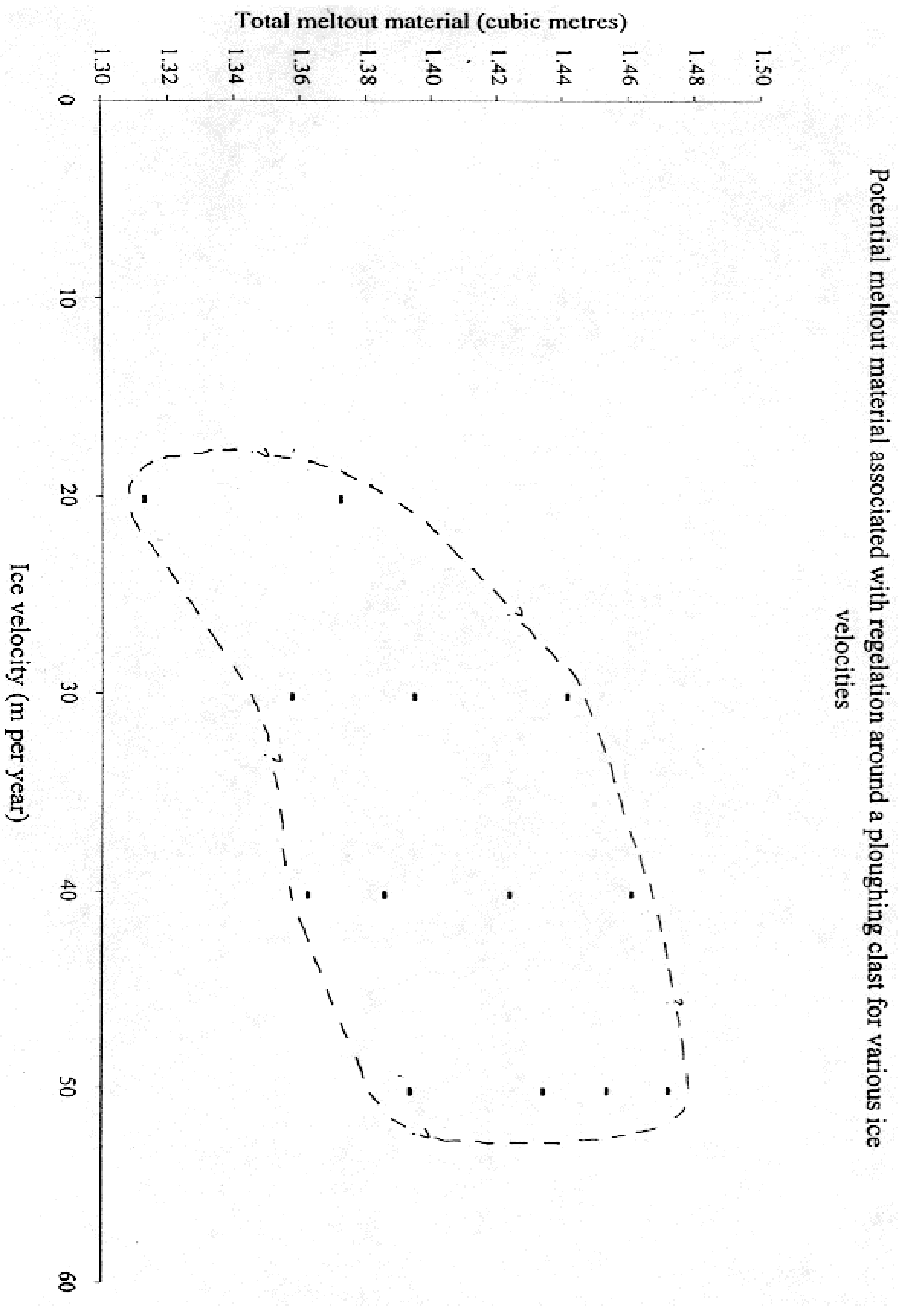

Figure 5.21 Meltout associated with the estimates of till residual strength for various ice velocities (infilling not allowed).

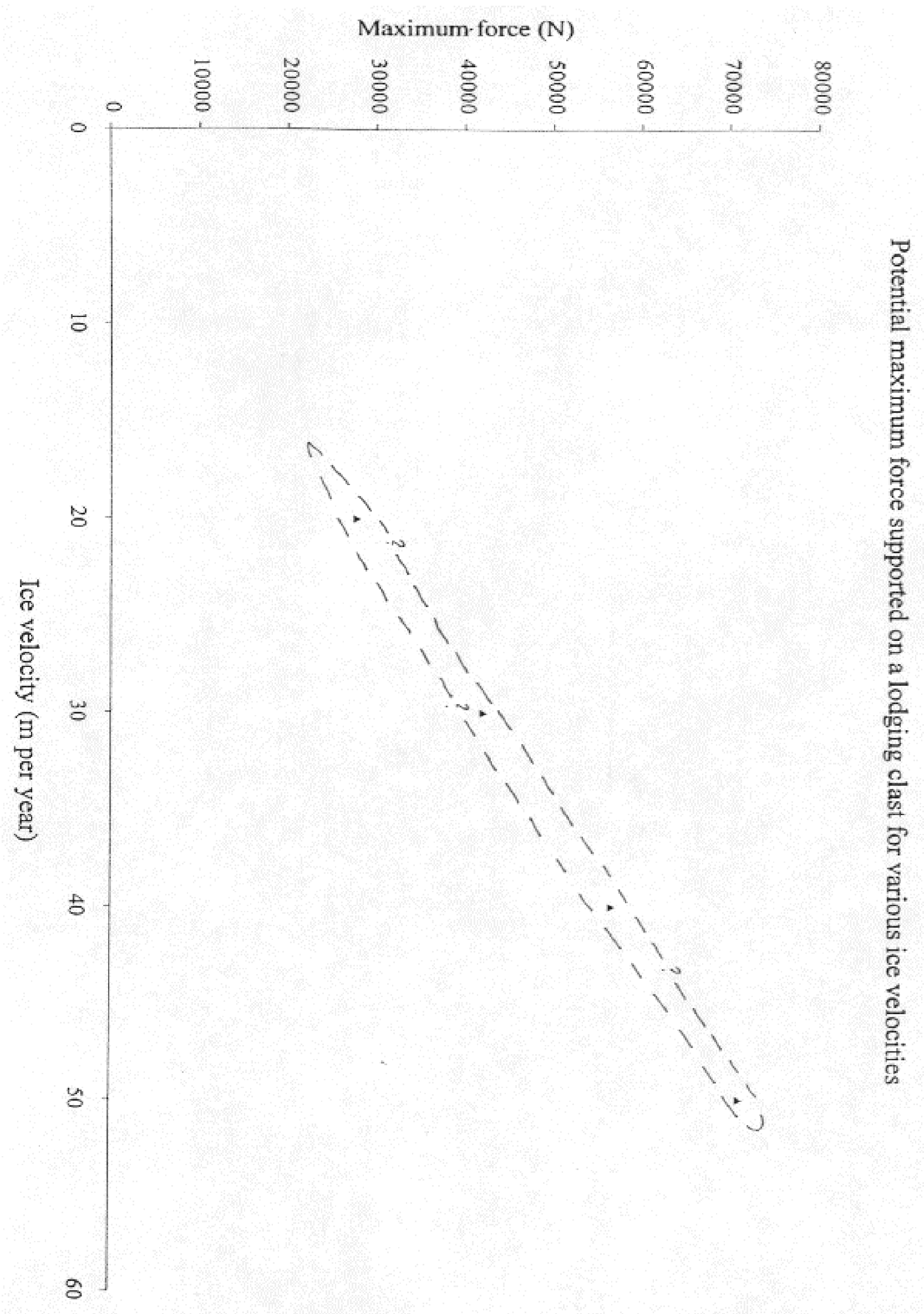

Figure 5.22 Maximum force supported on a ploughing clast for various potential till residual strengths associated with various potential ice velocities (infilling behind ploughing clast not allowed).

5.4.4 Discussion of the model results

The model which allows inflow of till from in front of the boulder gives convincing residual strengths for the till at Criccieth for ice velocities of 0-200 ma^{-1} (*Figure 5.17*), though does not give minimum values at higher velocities. This is because till inflow into the ploughed gouge will inevitably swamp the clast if allowed. In reality the micromorphology suggests periods of slack water in the gouge during which winnowed material could settle. This points to less till inflow than the model produces. Thus, we might expect the residual strength to fall between the values associated with till inflow (*Figure 5.17*), and those produced when the inflow is turned off (*Figure 5.20*). This would put the residual strength of the till between 1 and 10 kPa for ~20 m a^{-1} ice velocity. This matches other estimates well, though is on the lower end of observations (Paterson, 1994).

Such a low residual strength suggests a low effective pressure / high pore water pressure. This matches both the fluid-depositional nature of the micromorphology and the subsequent low deformation, which also possibly indicates a thin deformation layer. Free surface water nearby may explain the sand concentrations in the micromorphology and their apparent absence deeper in lithofacies E. Conditions at Criccieth may well have matched those under Ice Stream B today, where low effective pressures are associated with a thin deforming layer (M.Jackson, *pers.comm.*, 1996) and low residual strength (Kamb, 1991) (though the deposit is considered too small to have effected the ice velocity at Criccieth). The low residual strength of the material does not match the high strength of till from Yorkshire examined in Chapter Six. However, the Criccieth material is clay-rich, with few sand sized particles in the till as a whole (*Figure 5.12a*). This absence of sands will have allowed greater shear development (for confirmation of this shearing see *Figure 5.12b*), and easier deformation. This theme of a sediment's strength being related to its size distribution will be enlarged upon in the next two chapters.

One future improvement to the model will be to limit the potential residual strengths at Criccieth on the basis of the proportion of meltout material produced as well as the ploughing length. This may give an even greater accuracy to the potential strengths, and limit the potential ice velocities further.

5.5 Conclusions

1) One situation microscopic melanges may form in is in the ploughing trace of boulders (*Figure 5.23*). In the case of normal meltout there is no evidence to suggest that material should be preconsolidated to the extent seen here prior to deposition. Normal meltout material will lack cohesion and form more homogeneous deposits. In fluvial situations, large amounts of cohesive sediments would not be found on a microscopic scale horizontally juxtaposed with clean sand bodies and substantially winnowed material.

2) Until alternatives are found, the preconsolidated melanges should *sceptically* be taken as indicative of the ploughing of a boulder. The processes forming such melanges do not necessarily result in lodgement, therefore it is possible that these processes are responsible even if there are no clasts in the sediments. The melanges may be taken as indicative of a stress transfer between ice and till. It is likely that such diamicts will be found only at the top of till units, or in rare areas of intra-unit protection where they cannot be destroyed. In this case, lodgement was into the upstream side of a hummock as the last till deposition was occurring, and the preservation may partly have been a result of the particle size of the melt out.

3) The mechanism of ploughing discussed here can provide both the clasts and the matrix of diamictic tills. It is possible that the random alignment of the melanges in the till would slightly stiffen the deposit to make lodgement more likely, and facilitate the till deposition. The evidence for ploughing and lodgement discussed in this chapter strengthens the argument put forward in Chapter Four that lithofacies E was deformed subglacially, and the lodgement model explains how once laminated sediments contain large pebbles without the need to invoke ice rafting.

4) The model of the suggested processes (*Figure 5.23*) gives low residual strengths for the till (1 to 10 kPa) for reasonable velocities, and these match values from tills under present day glaciers (Paterson, 1994). The low values found here may reflect the fine grained nature of the till, and suggest a high pore fluid pressure environment matching the suggested deposition of the micromorphology through water.

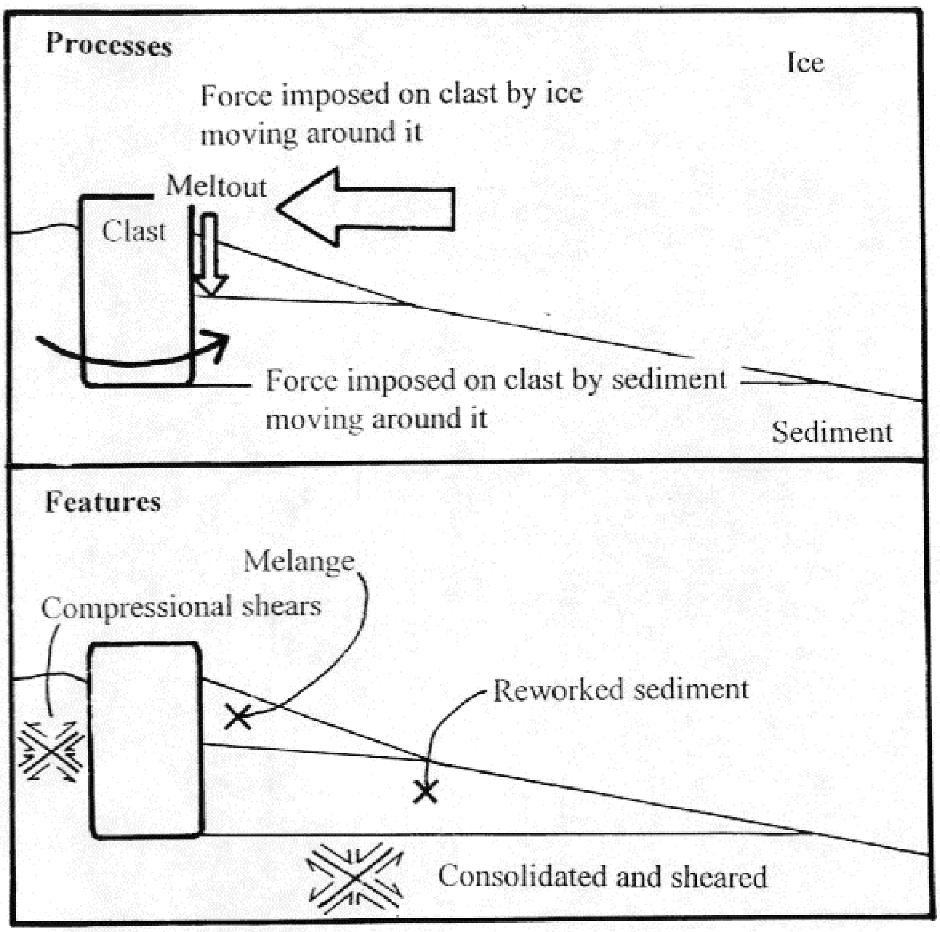

Figure 5.23 Processes and features associated with the ploughing and lodgement of clasts

6. Till Deformation with Clasts: laboratory experiments

6.1 Introduction

6.1.1 Overview

When the first models of the basal movement of glaciers were being devised it was realised that the problem with modelling motion over a hard bed was not how movement could develop, for ice should move unrealistically fast on a smooth bed. Rather the problem was how to model reasonable, slower, glacier speeds while still allowing any movement at all (Weertman, 1957). A similar problem has been posed with regards more recent soft bed models. Movement over a *deforming* bed of till may give high glacier velocities (Boulton *et al*., 1974; Boulton and Jones, 1979). However, Kamb (1991) has shown that the vital problem with the soft bed model is, again, that the velocities produced may be far *too* high to be realistic.

Subglacial till deformation has been modelled as a viscose material (Boulton and Hindmarsh, 1987; Clarke 1987; Alley 1991)

$$\dot{e} = a t^{n} P_e^{m} \qquad \textit{...Equation 6.1}$$

where t is the effective basal shear stress, P_e is the basal effective normal stress, $\dot{e}$ is the strain rate, and a, n, and m are empirically derived constants. The potential for non-linear behaviour is given by n and m.

Fitting this model to field data, Boulton and Hindmarsh (1987) suggest $n \approx 1$. Clarke (1987) also uses a linear stress response. Kamb (1991), however, suggests $n \approx 100$ on the basis of laboratory experiments.

6.1.2 Kamb's shear box analogue

Kamb (1991) ran shear box tests (Bolton, 1979) (*Figure 6.1*) on sediment from the base of Ice Stream B in Antarctica. Clasts ≥ 10 mm were removed from the sample. Under constant stress tests a threshold stress was identified between low stress work-hardening and high stress catastrophic work-softening. All movement occurred across a thin shear zone. The terms work-hardening and work-softening are used here to indicate a lowering or raising of the shear rate with strain at a constant shear stress. They are also used to indicate an increase or decrease of the supported stress with strain at a constant shear strain rate. The ideal terms for this behaviour ‘strain hardening and strain softening’ are already in use to describe changes in behaviour with initial shear strain rate.

Using constant strain rate tests the stress threshold was found to match the residual strength of the material. The sediment showed a typical silt strain response, undergoing work-hardening at a decelerating rate until a constant ‘residual’ stress was supported (for example, *Figure 3.7*). There was no peak supported stress which could be identified as a failure or ‘yield’ point, therefore ‘residual stress’ is used in preference to Kamb’s ‘yield strength’. A coincidence of residual and yield strengths is not unusual for reformed sediments. Kamb’s conclusions for glacial dynamics are intimately connected with his nomenclature.

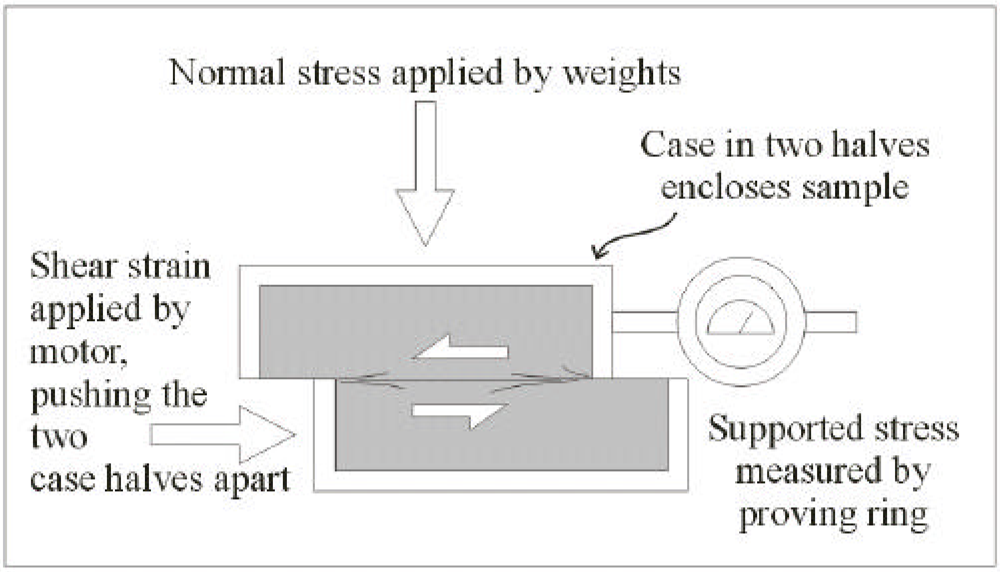

Figure 6.1 The simple shear box method. Sample shears at a point between the two halves of the containing box, forced by the box geometry.

Kamb described the catastrophic work-softening of the material as a highly non-linear response to shear stress, so non-linear in fact, that it could be considered as instantaneous and modelled by $n \approx 100$ in Equation 6.1. This is a reasonable, though unrepresentative, model of this behaviour. The non-linear viscose model describes a change in strain rate with stress. Kamb found a change in the strain rate as strain progressed, but with a stress threshold. This substitution is reasonable as long as the rate of work-hardening/softening is rapid. Given such non-linear behaviour, Kamb proposed that there could be no bed friction under a soft-bedded glacier with a basal shear stress greater than the threshold value. This includes most glaciers, therefore, another mechanism must be controlling glacial velocities (Boulton and Jones, 1979, use a similar model, but with a higher threshold).

However, a corollary of this model is the glacial shear-stress would be wholly released across a thin shear zone. Thus, there could be no transferral of stress deeper into the sediment (contrast with field work in Boulton and Hindmarsh, 1987), and no vertically extending deformation structures in palaeo-tills, only meltout features from deformed debris-rich ice (contrast with Paul and Eyles, 1990). The model is therefore incomplete. The catastrophic failure of the sediment in Kamb's experiments is probably a consequence of the experimental technique. The simple-shear 'shear box' set-up used constrains the development of shear planes. These propagate from the interface between the two box halves rather than spreading through the sediment. In natural simple shear, shears form at an angle to the horizontal, interact, and then develop into a Principle Displacement Zone with a complex internal geometry (Chapter Three). In nature there will also be a complex interaction between the shear strain and hydrological response which is not accounted for in such undrained shear tests.

These shear development problems are exacerbated by the removal of clasts larger than 10 mm from the samples. With a shear box height of 25 mm, it is quite possible that the shears never included clasts in their plane, or that any clasts were expelled from the shears until they did not straddle the interface between the two boxes. If shears pervaded the sample they would be forced to interact with clasts as the density of both shears and clasts increased.

The ‘triaxial rig’ set-up (*Figure 6.2*) can counter the problems of grain size distribution to a greater extent, and allows free development of shear zones. However, the equipment is limited to strains below ~ 30%; the progression to infinite strain cannot be studied. ‘Ring-shear’ rigs, can produce infinite strains but have not yet been used to provide hydrologic information with sediments of a size range suitable for glaciology. Iverson *et al*. (1996) tested suitable material, and Brown *et al*. (in press) included hydrodynamics, but no one has tested both. Ring shear rigs also force shear zone geometries. Thus, a series of triaxial tests were run on material sampled from the Skipsea Till at Skipsea in Yorkshire (*Figure 6.3*). The next section outlines the reasoning behind the methods employed and the limitations on the specific situations that can be recreated. The section following this outlines the details of these methods and the test conditions used.

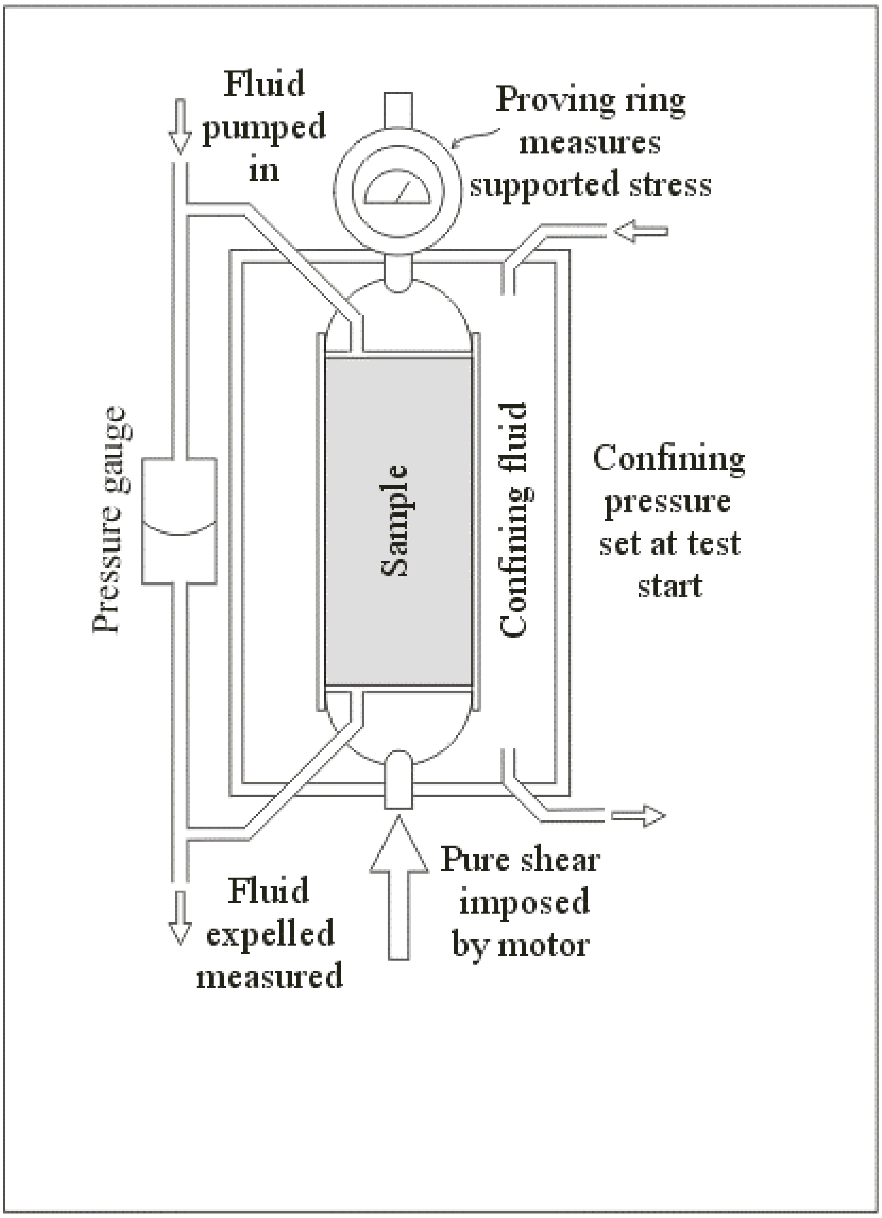

Figure 6.2 The triaxial deformation apparatus used in the experiments.

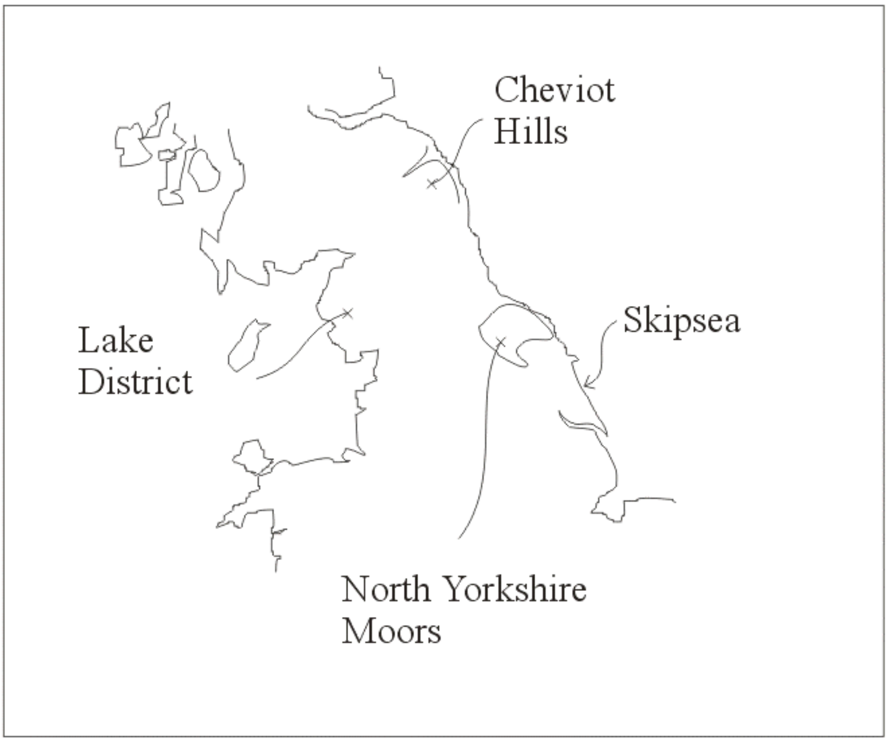

Figure 6.3 Location of sample site and sites discussed in the text.

6.2 Methods

6.2.1 Creating an analogue for subglacial deformation

It is an over-simplification to model subglacial deformation on the basis of one experimental set-up. Deformation is likely to be heterogeneous and dependant on the ice history, the ice-sediment interface, and the clast density in the sediment and basal ice. As well as steady state deformation, the deformation boundary may rise and fall during the glaciation (Hart *et al.*, 1990). The ice-sediment interface may be smooth (Clarke, 1987), the ice may move into the sediment (Boulton and Hindmarsh, 1987; Iverson and Semmens, 1995), or the stress may be transferred by an irregular ice base topography or clasts (implicit in Alley, 1989; also Chapter Five).

Clasts may bridge the deformation front or ice interface, and the stress conditions they impose will be dependant on their density and the sediment response. For example, a pure strain geometry will exist between two clasts trapped at different heights in a deforming layer where the velocity drops with depth (*Figure 7.3*). Where clast density is lower, there may be no depth overlap between clasts and it may be possible to approximate the sediment deformation as simple shear.

The response of deforming sediments is extremely sensitive to the imposed stress magnitude and direction. It is therefore essential in tests that the stress conditions, including the hydrological changes, are as close as possible to those found subglacially. It is also important to specify which subglacial situations are being recreated. Each set of equipment is an analogue for only certain situations (*Figure 6.4*). A general model of deformation will only be successful when the rheological response of several bed situations can be combined. Triaxial tests recreate two important situations.

1) The initial ploughing of boulders or irregular basal ice into undeformed sediment. Such sediment could be under a descending deformation front.
2) The deformation of sediment trapped between clasts. A clast trapped in the ice, or in higher strain rate sediment, will transfer stress through the sediment to downstream clasts on the same horizontal. If Kamb's shear-box experiments show the response of matrix without clasts, clast interactions may be the most important mechanism for the transfer of stress into soft-beds. The time over which the clasts interact will determine the period over which stress is transferred deeper into the sediment. Clast-clast interactions will also take place *within* triaxial samples.

The flow of material around clasts is a crucial addition to the stress transfer, thus it is unnecessary to run the tests under the zero lateral strain (sometimes known as K_0) conditions commonly sought for in other environmental reconstructions.

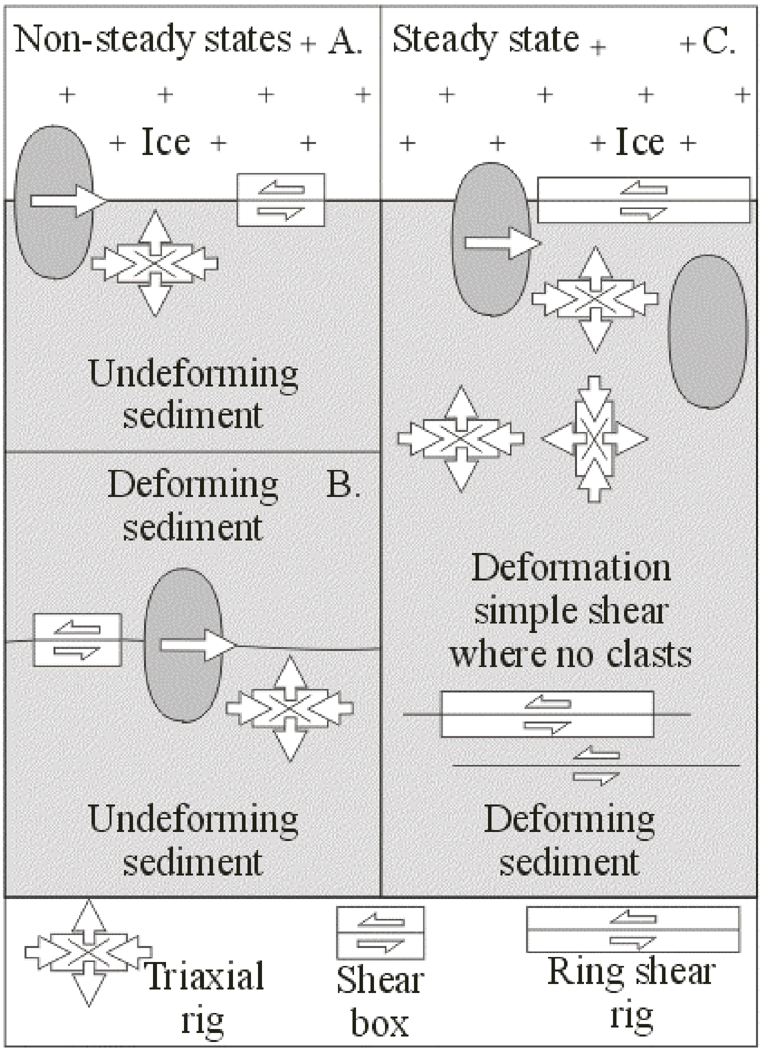

Figure 6.4 Subglacial situations for which different deformational equipment is analogous. A. Clast trapped in a smooth ice base ploughs through undeformed sediment. Conditions similar to those in a triaxial rig exist in front of the clast (arrows show force directions). Conditions similar to a shear box exist at the smooth ice-bed interface. B. Clast trapped in fast moving till ploughing through undeforming sediment. Conditions similar to those in a shear box exist at décollements within the sediment. C. In steady state deformation conditions similar to triaxial and shear box experiments exist, as well as conditions similar to ring shear rigs.

The subglacial conditions that must be recreated are;

1) applied confining stresses ranging between ~10’s m to 2000 m of ice.
2) pore fluid pressures ranging from zero to above the confining stress.
3) rates of water inflow (for warm bedded glaciers) such that a pore-fluid head will build-up if the sediment remains homogeneous (Boulton and Hindmarsh, 1987).
4) rates of compression in front of solid clasts locked in the ice from 0.00379 mm min^{-1} (2 m a^{-1}) to 3.79 mm min^{-1} (2000 m a^{-1}).

The most difficult condition to reproduce is the excess fluid inflow. The fluid influx from warm bedded glaciers rises above the discharge capacity of subglacial sediments both seasonally and diurnally. Seasonal variations are concentrated in areas that eventually pipe and become channelled as the meltwater flux increases (Boulton and Hindmarsh, 1987; Walder and Fowler, 1994). For a typical Alpine glacier and a range of likely sediments, the distance affected by high rainfall events around the channel may be between 5 and 80 m (Hubbard et al., 1995; A.Barrett and D.Collins, pers.comm., 1996). The rheology and size of the areas which do not pipe will be controlled by the drainage response of the sediment as the effective pressure moves towards zero. The drainage capacity is controlled by structures formed during deformation (Chapter Three).

Triaxial tests are usually run so that the sediments are either undrained (rapid tests) or fully drained (pore-pressures allowed to adjust by straining slowly compared to the drainage). These tests correspond to engineering situations relevant to the stability of constructions. The response of sediments to non-equilibrium conditions are rarely examined. The inflow in tests must be constrained such that leakage does not occur between the sleeve and the sample. In an effort to reproduce glacial levels of strain and inflow these restrictions were ignored. Fluid pressures were allowed to build up under the assumption that the record up to the point of sleeve leakage would more accurately reflect the natural development of the sediments. As it happens, internal changes in the sediment decrease the excess pressure prior to the leak point. The pore fluid pressure could have been raised manually during the tests, however, this would have obscured a number of interesting processes, for example, the relationship between yield fabric development and the fluid pressure.

6.2.2 Samples and equipment set-up

A till block was removed from the Skipsea till exposed at Skipsea on the Yorkshire coast (*Figure 6.5*). The sample was taken from a homogeneous cliff of diamict with no low strain features in it (including dilation or shear horizons such as described by Boulton and Hindmarsh, 1987). The area sampled was 500 m south of a set of canal deposits (D.Evans, *pers.comm.*, 1996, see also Walder and Fowler, 1994).

Approximately 1 km south of this position lie the Skipsea Mere deposits. These deposits are the remains of a lake system drained in medieval times that lies on the sub-Devensian topography of Anglian tunnel valleys (Sheppard, 1957). These tunnel valleys were undoubtedly low topographic points during subsequent glaciations and may well have been controlling the subglacial drainage layout. Thus, the sample area is in an area that may have experienced considerable subglacial fluid pressure fluctuations seasonally, and possibly diurnally, if the glacier was warm-bedded.

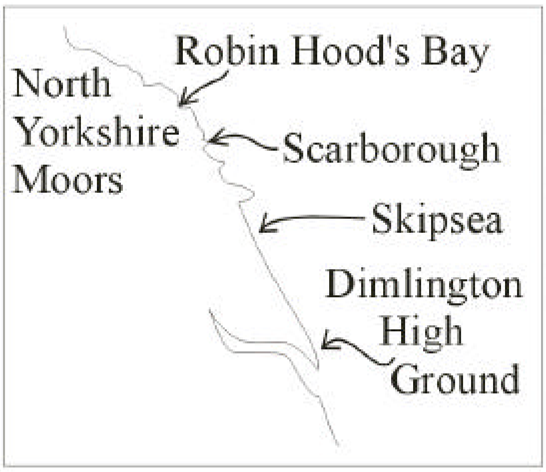

Figure 6.5 Locations around Skipsea

The block was removed 4 m below the cliff top after 1 m depth of till was removed from the cliff surface. The ambient stress conditions were not of interest, so the samples were allowed to dry under normal room temperature. Drying allowed cylinders of material to be cut from the block without disturbing their internal fabric. The block was cut into 50x50x120 mm sections with a wood saw, which were planed down to cylinders of 38 mm radius and 76 mm length using a knife. Clasts crossing the cylinder edges were trimmed flat to the sides with a hacksaw (if soft), or removed (if hard and could be removed without disturbing the surrounding material). Empty 'casts' were filled with a mix of wood glue and ground sample material as a hard, impermeable, and neutrally buoyant pebble replacement. If neither option was possible the sample was discarded. Samples frequently split along horizontal planes, suggesting a fabric in this direction. It was impossible to prepare cylinders with the original horizontal plane along the long axis of the cylinders, as the stress from the preparation techniques activated these weak planes. Typically samples took two days to prepare, with a failure to success ratio of 3.5:1. Table 6.1 summarises the mineralogy and grain size of the till.

Mean carbonate content (<2 mm fraction)	13.1%
Mean silt content	37.6% (32.8 to 42.4%)
Mean sand content	33.5% (22 to 45%)
Mean clay content	29% (21 to 37%)
Clay types	kaolinite, illite, vermiculite, smectite

Table 6.1 Mineralogy and grain size of the Skipsea Till (After Madgett and Catt, 1978; Goodyear, 1962) As will be shown in Chapter Seven, the size and mineral distribution of the material varies significantly on the scale of the triaxial samples.

Samples were tested in a triaxial rig in the Sediment Deformation Laboratory of the Institute of Earth Studies, University College of Wales, Aberystwyth. The triaxial rig (*Figure 6.2*) is of the standard type (for example, Vickers, 1983), with the exception of alterations to allow hydraulic measurements. The hydrology is determined by;

1) inflow into the top of the sample (computer controlled via an automated syringe);
2) outflow from the sample base (measured by a computer controlled piston);
3) the pressure at the sample base (controlled by the piston, which is set to maintain a constant 'back' pressure, while changing volume);
4) the fluid pressure across the sample (which is measured by a diaphragm pressure gauge connected in parallel with the sample).

Parameters measured in these tests were;

1) the supported stress at a constant strain rate;
2) the difference between the fluid pumped in for an interval and that exiting the sample, that is, the extra storage during any one interval;
3) the fluid pressure difference between the top and base of the sample, which gives the pore fluid pressure at the top of the sample (given the back-pressure).

Because the sediment response changes as its microscopic structure develops, thin sections were prepared from the samples after straining (examined in Chapter Seven).

Tests should be run with confining pressures greater than 600 kPa to prevent leakage between the sample and its rubber sleeve (which would render the tests 'fully drained'). The back pressure is usually run at half the confining pressure or less for the same reason. A number of tests (*Table 6.2*) were run prior to this becoming apparent and should, therefore, have a pore fluid pressure constantly at the back pressure throughout the tests. This is not the case, so it seems that leakage was either partial or non-existent.

The strain rate was chosen such as to take around two days to reach ~25% strain. This rate was chosen on the basis of the equipment, constraints on lab time, the maximisation of any pre-leak record, and as falling near glacial velocities (equipment constraints limited the closest strain rates to ~3 m a^{-1} ice velocity). The inflows used ranged between 0.001 and 0.004 ml min^{-1} (464.71 mm a^{-1} to 2323.57 mm a^{-1} melt). This influx rate was the lowest possible when the tests began. The rate is a little high for basal melt rates (~100 mm a^{-1}), however, it falls between basal melt and flux through a small subglacial channel. The temperature of the apparatus used could not be lowered to subglacial levels, so the material was not tested in a frozen state.

Test	Confining pressure (kPa)	Starting back pressure (kPa)	Sample interval (s)	Fluid inflow (mm^3 m^{-1} / m a^{-1} melt)	Deformation rate (mm m^{-1} / m a^{-1})
D1	Equipment failed to record				
D2	500	300	174	1 / 0.52	4.14x10^{-3}/ 2.18
D3	500	325	144	4 / 2.08	5.97x10^{-3}/ 3.15
D4	Sleeve punctured at test start				
D5	660	330	87	2 / 1.04	6.85x10^{-3}/ 3.61
D6	660	330	44	1 / 0.52	6.11x10^{-3}/ 3.22

Table 6.2 Conditions of triaxial test runs.

Samples were pressurised to the confining pressure (though the material was too dry to respond) then fluid was pumped in at both ends to give an ‘effective’ confining pressure. Initial saturation of each sample took approximately two days. Saturation is determined to have occurred when the sample reaches a constant back pressure. Throughflow was then instigated and the material’s pore space allowed to come into equilibrium with the throughflow and confining pressure. Equilibrium is marked by a halt in size change of the sample, measured by the difference between the fluid flowing in and that flowing out. Equilibrium took approximately six hours for these samples.

During saturation and equilibrium the sediment may be expected to have passed through the pressures between the initial confining pressure and the ‘effective’ confining pressure. The data presented by Boulton and Dobbie (1992; their figure 16-b) suggests the samples have previously been consolidated under pressures between 500 kPa and 600 kPa (‘*preconsolidation pressures*’). These figures are gained (here) by assuming the site was subjected to an overburden between Boulton and Dobbie’s maximum at 1 m above sea level, (in a lower till unit at their location), and the overburden 4 m below the top of their Skipsea layer. The latter gives a minimum by assuming the top of the section at Skipsea was the top of the Skipsea till. Sediments undergoing *fully-drained* tests have a smaller porosity change with stress than expected up to their preconsolidation pressure. Given these values, it is more than likely that the Skipsea material will pass through its preconsolidation pressure while saturating, then become normally consolidated as the pore pressure reaches the backpressure. It is unknown what effects may be inherited from the overconsolidated state when the pore-fluid levels are altered in the sample.

6.3 Results

6.3.1 Stress response

Stress - strain diagrams are presented below for the four successful test runs in Figure 6.6. The initial strain at low stress values is an artefact of the equipment adjusting to the irregular surface of the samples. Unimodal, normally consolidated material usually responds to strain by reaching a level stress plateau after 5-7%. Features to note are;

1) the increase in stress supported with confining pressure (in line with *Equation 3.1*) - other factors also affect this relationship (see below), for example compare D2 and D3, both run at ~300 kPa effective confining pressure;
2) the large difference between D5 and D6, despite identical confining pressures.
3) supported stress drops in tests D2 and D3 at <2.5% strain;
4) supported stress drops in tests D2, D5 and D6, and a stress plateau followed by rise in D3 between 6 and 8%;
5) strain hardening (starting around 7%) intensifying in D3 (at 9.5%), D5 (at 11.5%) and D6 (at 14.5%). In samples D5 and D6 this supported stress profile is stepped, with periods of constant stress.

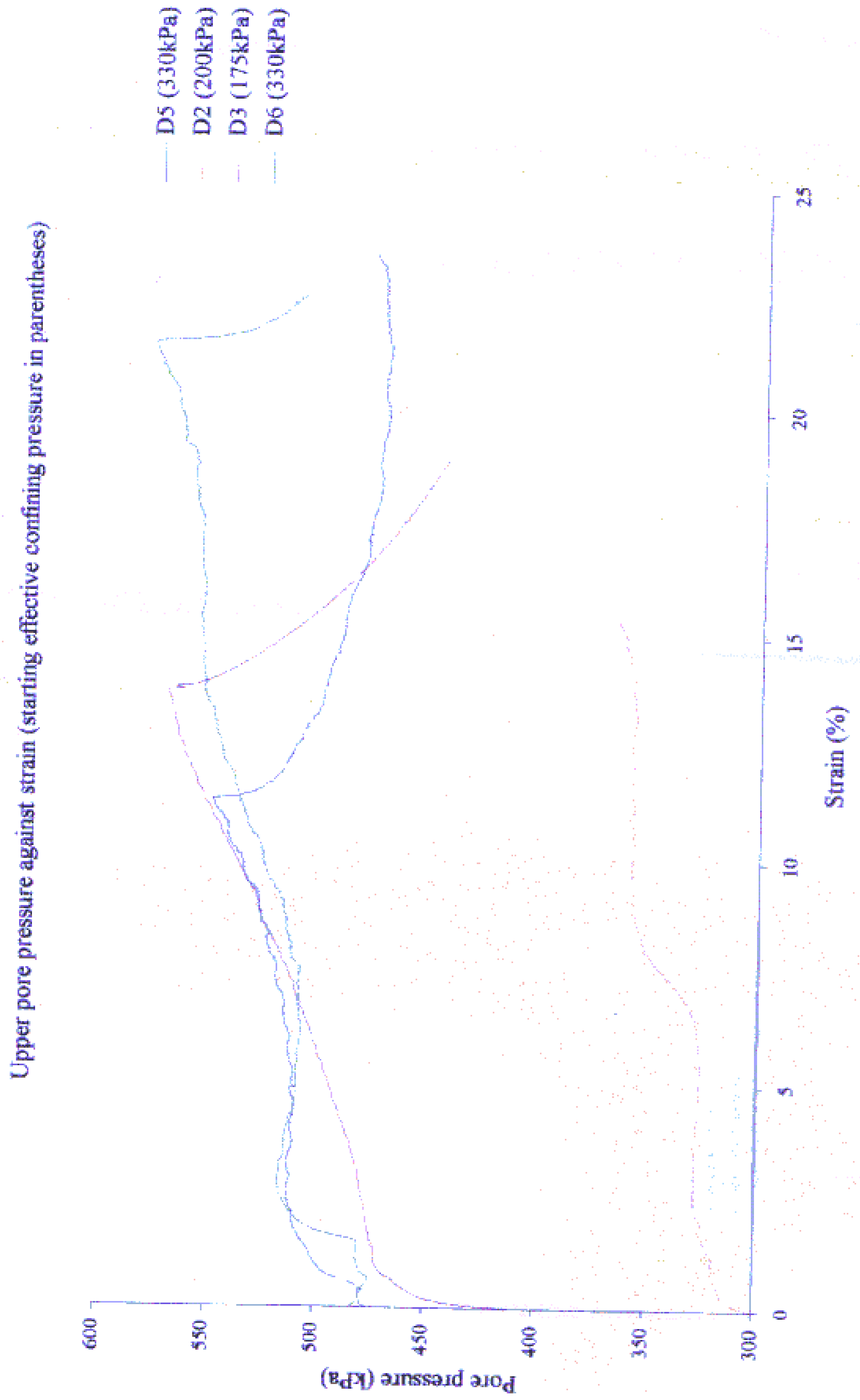

Figure 6.6 Stress-strain records for the triaxial tests.

6.3.2 Storage response

The storage response of the sediments is presented in Figure 6.7. The difference in signal variation for each test is considered to be a consequence of the change in equipment between tests D2 and D3, and D5 and D6. During these intervals the method of converting the signals from the fluid inflow and outflow pumps to signals suitable for recording on a computer was changed. The signal fluctuations are regular for tests D3 and D5 (wavelength of ~1% strain) between 12 and 15% strain. Test D3 has a response suggestive of at least two different wavelengths (~1% and ~12% strain). Both the short term regularity and longer term variation suggest the variations are instrument noise The change is probably due to a change in the signal processing between the input syringe and computer between the two tests. Thus, only the broad changes are regarded as experimentally useful and there is some suspicion that these mimic the temperature of the laboratory in D3, which may have varied during this particular test.

While none of the tests have an identical response, similarities exist.

1) In tests D2 and D5 the storage increased during the initial rise in stress up to 5 to 6.5% strain, then fell temporally to net expulsion as the stress dropped (at 6.5% for D2, and at 8 and 11.5% for D5). In both cases storage fell off at high strains.

2) Cumulative storages over the whole of the tests were (as percentages of the sample volumes) 0.616 % (D2), 0.278% (D5), 6.072% (D6), 20.477% (D3). The latter figure is far too large a porosity change. Given that most of the samples had a porosity (gained during the saturation of the sample from a air dried state) of ~40%, an extra 20% would leave cylinder D3 near its liquid limit at atmospheric pressure. However, at the end of test D3 the sample was still stiff enough to remove from the rig without deformation. This observation, in combination with the wave-like form of the storage response at least two scales, suggests the signal is a total artefact and is dismissed for D3. The signal for D6 appears more genuinely to vary with the other measured parameters, however, follows an opposite trend to D2/5 up to the end of the test, when a supported stress drop is matched by a drop in the net storage, possibly suggestive of expulsion.

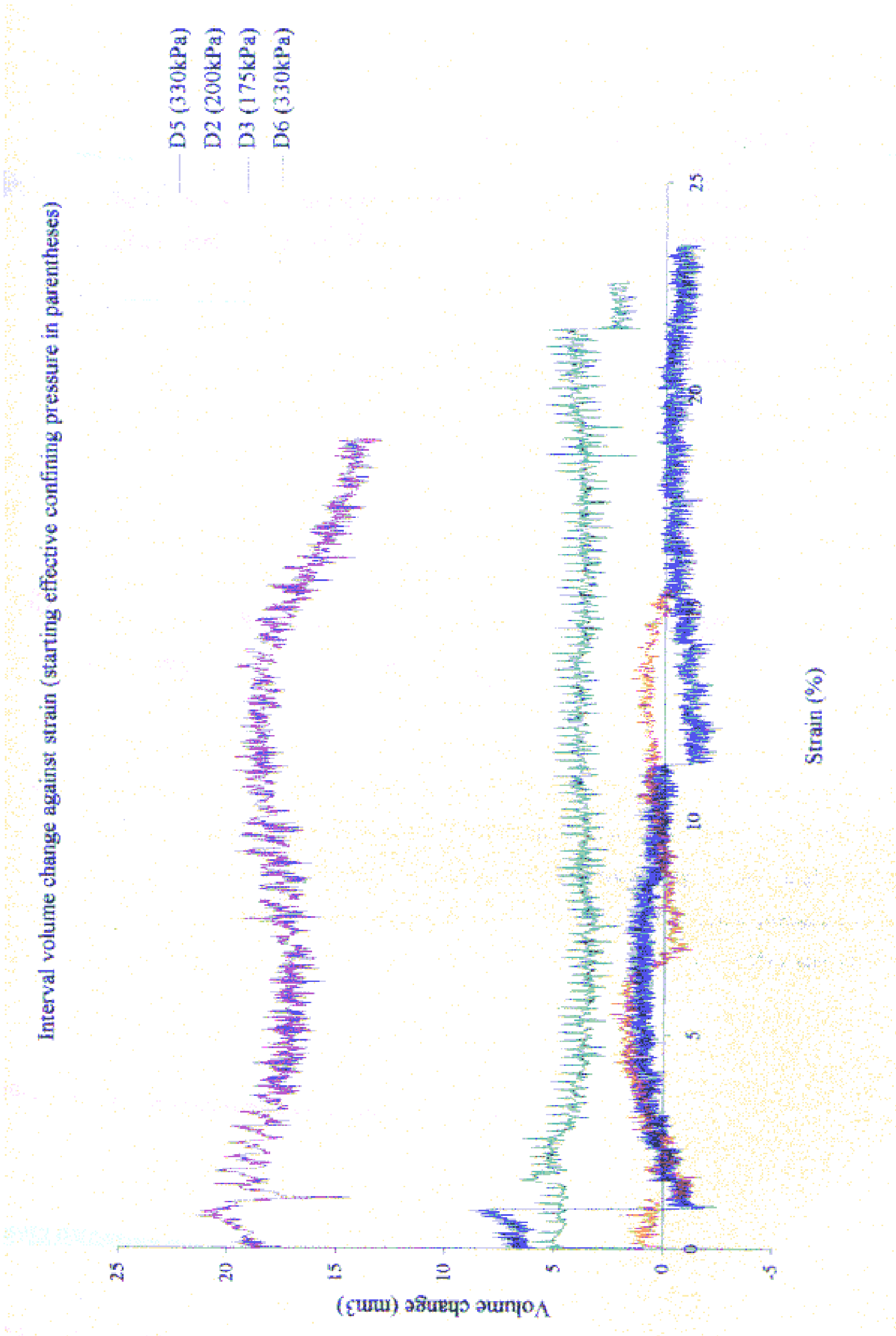

Figure 6.7 Storage records for the triaxial tests.

6.3.3 Upper pore pressure response

The upper fluid pore pressure (*Figure 6.8*) is allowed to equilibrate prior to the stress being applied, thus the initial ramping of pressure is not a machine artifice. There are a number of important features of the experimental records to note.

1) The initial rise in pressure of ~50 kPa in all the tests. These rises begin when stress starts to register for test D5 and D6, and slightly before for tests D2 and D3. As the conditions during adjustment to straining are unknown the latter results could still be due to stress application.
2) The steady *drop* of pressure (~10 kPa) to a new plateau (still higher than the start pressure) in tests D5 and D6. This is not matched in test D2, which simply reaches a plateau without falling. Test D3 never reaches a steady level, but does decline in slope.
3) The later ramping of pressure to a higher plateau (~50 kPa added) in samples D2 (at 7%) and D6 (at 8%). In both cases this is synchronous with a stress drop and fluid expulsion not seen in the two other samples. A lesser example of this behaviour is also seen at 2% strain in D2.
4) The rapid rise in pressure to a maximum for each sample followed by a rapid pressure drop to approximately the starting level. Each rise is synchronous with a stress drop or temporary plateau in stress, though in the case of D3 the drop is not that associated with the onset of work-hardening as in the other cases. The rapid fluid pressure drop would appear to accentuate the work-hardening, as one might expect from a greater effective confining pressure. However, fluid pressure changes cannot be responsible for the increase rate of hardening seen in D3 (at 9.5%) and D6 (at 14.5%).

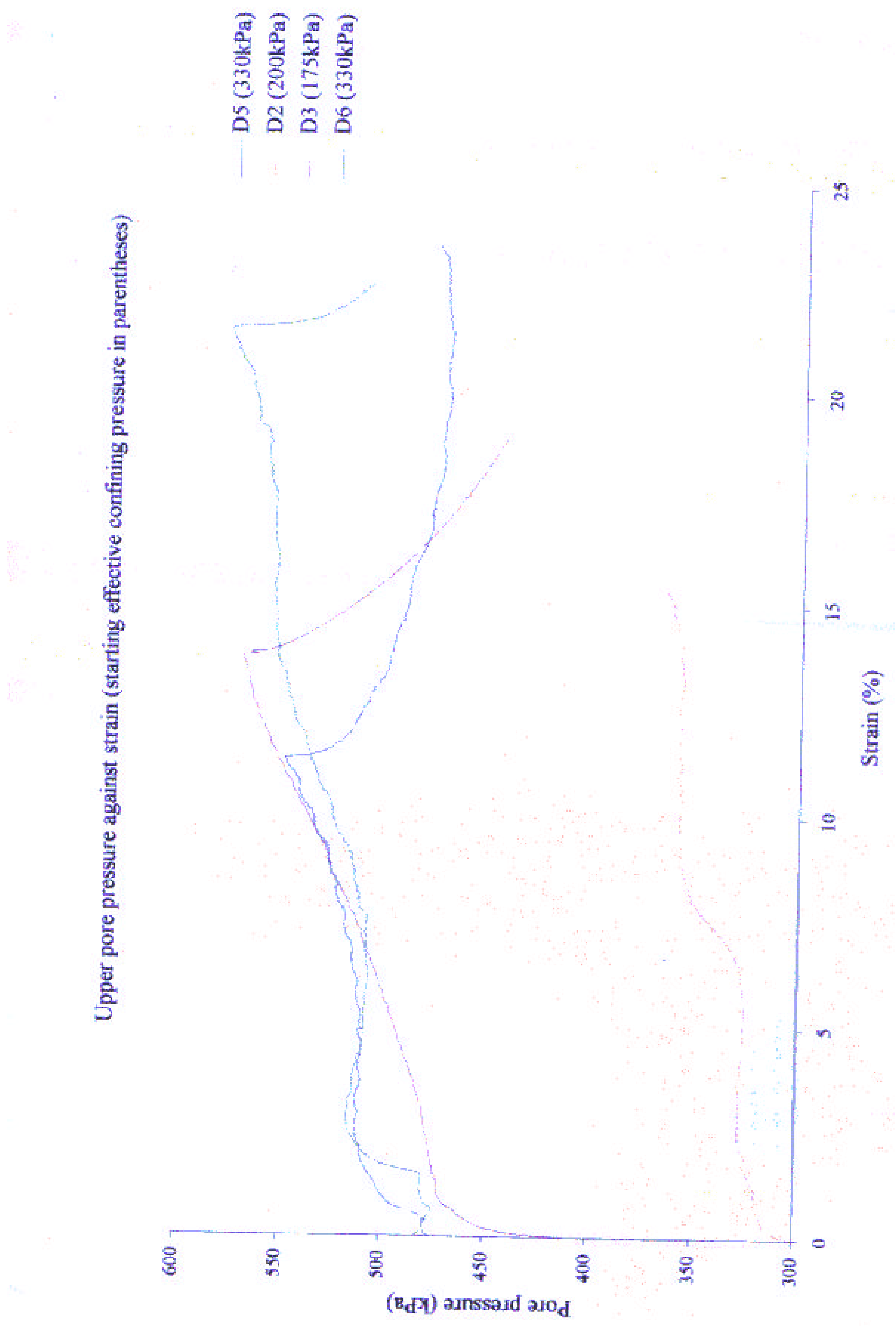

Figure 6.8 Upper pore fluid pressure record for the triaxial tests.

6.3.4 Stress paths

The average stress (p), average effective stress (p¢) and deviatoric stress (q) are defined (Jones, 1994) as

$$p = \frac{\left(s_a + 2s_c\right)}{3}$$

$$p' = \frac{\left(\left(s_a - P_p\right) + 2\left(s_c - P_p\right)\right)}{3}$$

$$q = \frac{\left(s_a - 2s_c\right)}{3}$$

where s_a is the supported stress measured on the proving ring and s_c is the confining pressure. There is no difference between the deviatoric stress and an effective deviatoric stress which might take pore fluid pressure into account. The stress paths of the samples in p-q and p¢-q space are given in Figure 6.9. The difference between p and p¢ is the pore fluid pressure.

In each case the stress behaviour is different, though D5 and D6 are most similar. The average applied stress path is typical for a drained sample (Jones, 1994, fig. 2.25). The effective stress paths, however, trend towards a critical state line (cf. Jones, 1994, fig. 2.25 and 2.28), but then move back to paths with gradients similar to those early in the tests. There is no clear yield line from which to gain Mohr-Coulomb parameters.

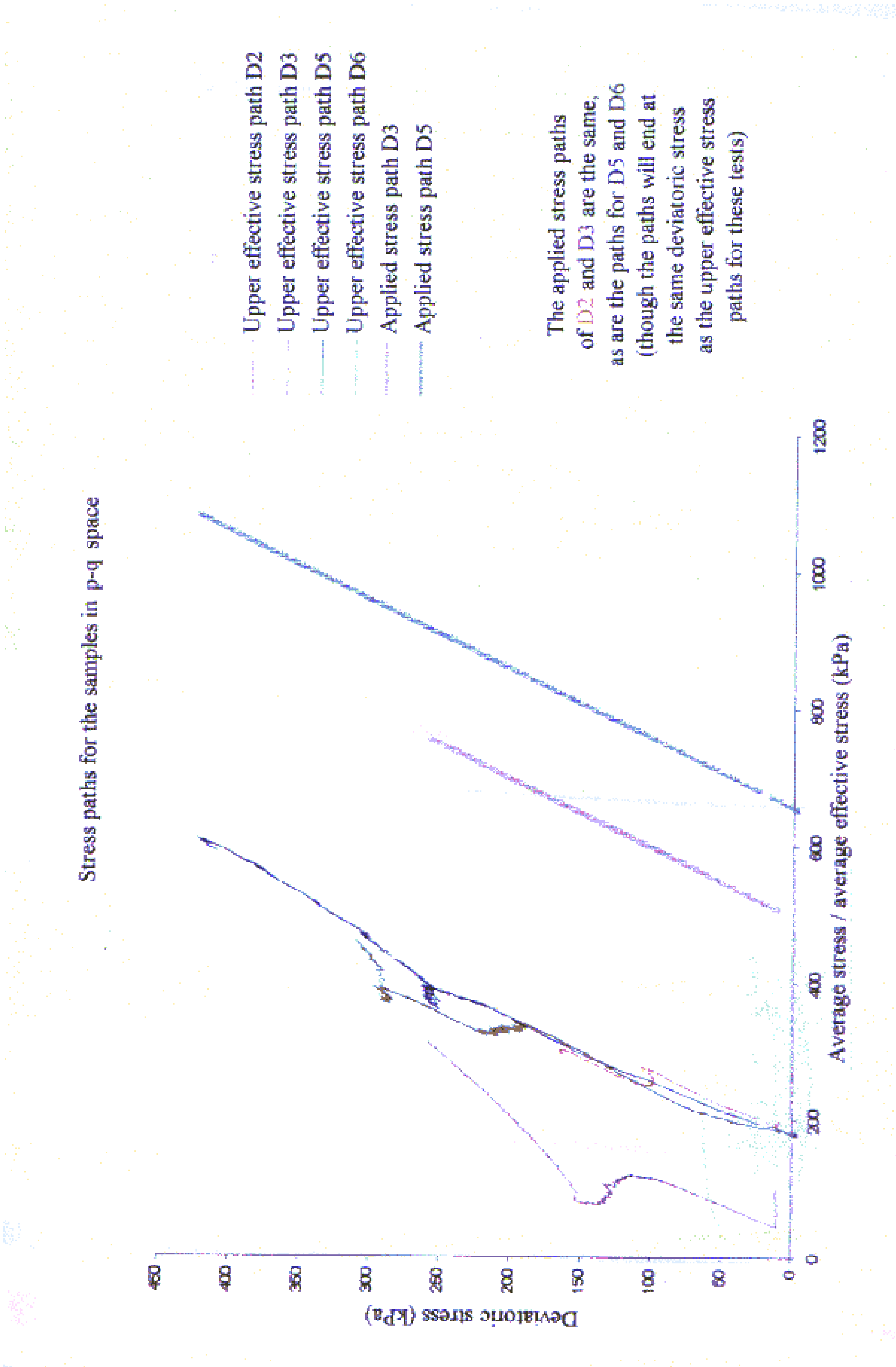

Figure 6.9 p-q space records for the triaxial tests

6.3.5 Visual scale deformation features

After deformation the samples were stiff enough to remove from the test rig without further damage. The samples were seen to have developed dislocation planes, above which the samples were shifted outwards and downwards (*Figure 6.10*). These shear planes also separated lower areas of deformation that appeared pervasive on the visual scale from upper areas that did not appear to have undergone as much destruction. Original features of sample preparation could be seen in the upper areas, whereas these were obliterated on the smoother surface of lower areas. Despite the dislocation planes and the preservation of features in the upper halves of the samples, almost all movement was by pervasive barrelling, and mostly above the shear planes.

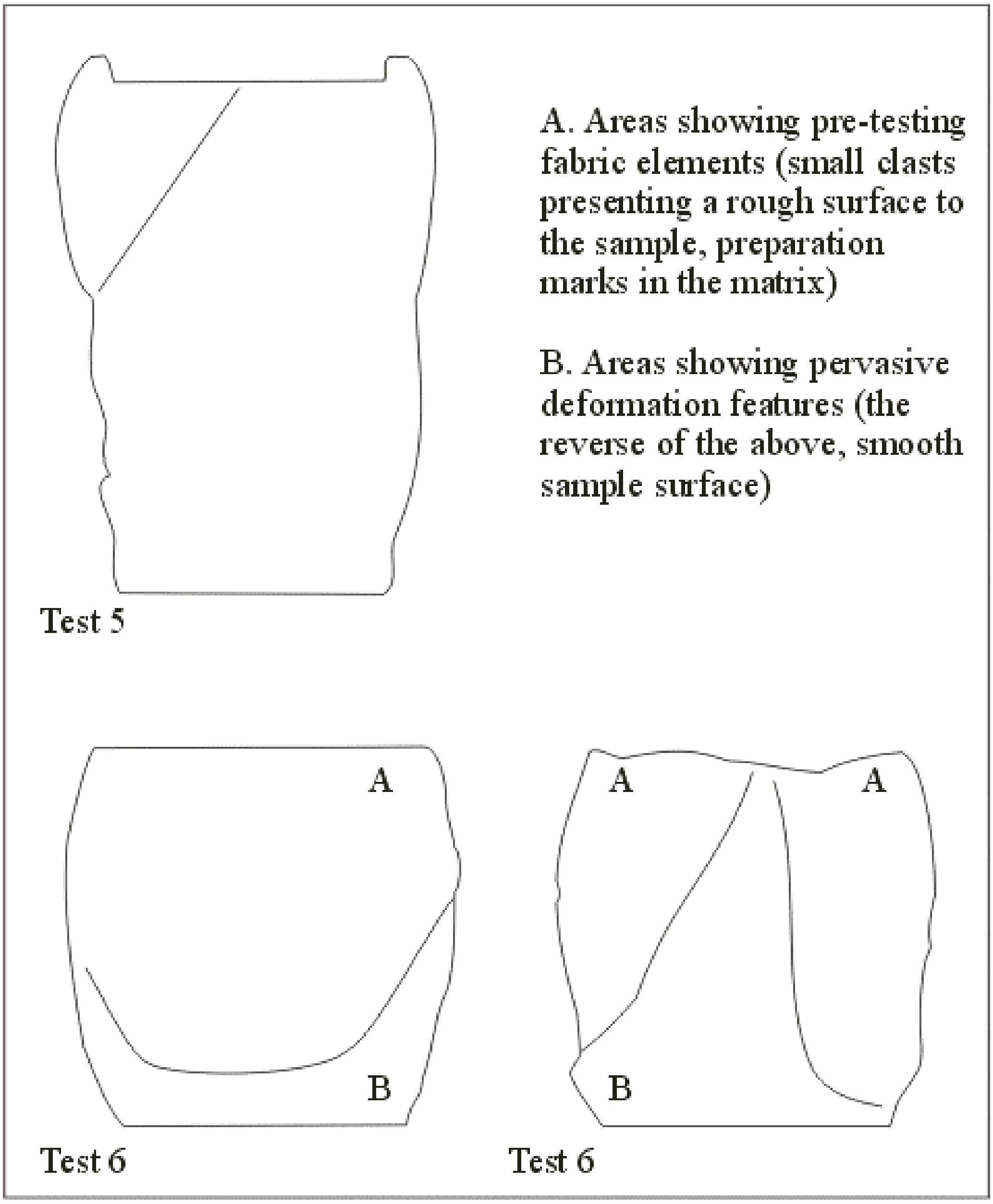

Figure 6.10 Visual scale appearance of two test samples. Test 5; cross section showing shear dip, drawn during sectioning for thin section samples. Test 6; showing outer surface after tests. Note the two dislocation planes.

6.3.6 Summary of results

The following features need explanation. They are given in their order of development.

1) Initial strain hardening of the samples coincident with a build up of pore pressure and increase in the storage of fluid (for D2 and D5) (0 to ~5%). Also, the small drops in supported stress at <2.5% strain for two samples.
2) The slowing of the fluid pressure rises without a change in the stress build-up or storage increase (between 2.5 and 7%).
3) The slowing of the stress rises, with a temporary fluctuation in stress and a simultaneous fluid *expulsion* in two samples (at ~5%).
4) The association, with this set of stress fluctuations or one prior, with a renewed increase in fluid *pressure* to a new plateau.
5) A stress fluctuation and simultaneous pore pressure increase which is followed by an equally rapid fluid pressure decline (D3 at 8%; D5 at 11.5%; D6 at 20%). There is no consistency in which stress fluctuation initiates this fluid pressure increase, though the first fluctuation always initiates either a stable (see 4, above) or unstable rise. The fluid pressure at which the rapid drop occurs is similar for similar confining pressures.
6) The work-hardening in samples (between 11 and 14%), unrelated to the fluid pressure, and its stepped profile.
7) The large variation in the responses of samples.
8) The pore fluid storage response of sample D6, which is at odds to the other reliable tests, despite showing similar responses in the other variables.

6.4 Discussion of results

This section outlines a self-consistent model of the processes based on the results above; which are often paradoxical at first sight. The events are interpreted in order of development. These interpretations are tested through comparison with the micromorphology of the test samples in Chapter Seven and related to ‘natural’ examples in Chapter Eight.

6.4.1 Initial stress and upper pore fluid pressure build up with dilation

Work by numerous authors (Chapter Three) suggests the early stress build-up in triaxial tests occurs because the sediment fabric is not optimal for strain, that is, shear zones have not yet developed. A micromorphological examination of the samples used in the triaxial tests (presented in the next chapter) indicates that they are unorientated and heterogeneous on a microscopic scale before deformation, suggesting the fabrics were not optimally arranged for stress dissipation. It should be remembered that there was no outcrop scale evidence for prior strain at the sampling location such as horizons of dilation or shear. Strain resistance due to this lack of uniform structure *may* be enhanced in the cases reported here by the increase in pore size indicated by the net storage in the samples. This dilation may result from the rising pore-fluid pressure, which will enlarge pores. However, the storage signals of both D2 and D5 are better matched by the *stress* response later in the tests. Similarly, in D6, storage does not reflect the fluid pressure signal; reduced storage changes appear where predicted on the basis of the fluid pressure, but the rises are muted. These facts indicate that dilation caused by the inflow of fluid is overprinted by the dilation caused by the applied (differential) stress. Early in the tests it appears that the dilation could be driving the pore fluid pressures' equalisation. However, this proposition does not hold up later in the tests.

The fact that dilation is not proportional to the strain shows that a large proportion of the strain is achieved without changing the samples overall volume and is undrained. The dilation appears proportional to the *increase* in supported stress at any given time. This relationship suggests that the *proportion* of volumetric deformation (dilation and compression) is related to the stress *magnitude*.

Work in other subject areas (Chapter Three) suggests that the stress-strain relationship changes because of changes in the grain orientation of the sediment, and the rise in pore-fluid pressure. The pore fluid pressure is in equilibrium prior to sample deformation, therefore, the increase in pore fluid pressure must be due to microstructural changes, which will be considerable in this previously unorganized material.

The strength of sediments is thought to be related to their effective confining pressure (*Equations 3.1* and *6.1*). The pore-fluid pressure gradient will, therefore, create a deformation gradient across the sample. This matches the form of sample D5, which showed a more marked barrelling in the upper half of the sample (*Figure 6.10*). In this situation dilation is more likely in the upper half of the sample where the fluid pressure is highest (though it is pointed out, above, that the effect of stress appears to be greater that that of fluid pressure in the sample taken as a whole).

The rise in pore-fluid pressure suggests a *reduction* in permeability, often associated with reduced pore size (discussion in Chapter Three). This contradicts the dilation implied by the storage signal. There are four possible explanations for this contradiction. In the first two, the permeability variation is between the base and top of the sample. In the third, the permeability variation is between local dilatant shear zones and the generally compressed mass of the rest of the sample. As we only record the *difference* between compression and dilation we cannot gauge the absolute size of these areas. The fourth explanation centres on tortuosity.

1) Excess pore-fluid pressure will dissipate more easily at the freely draining sample base, allowing greater stress to be transferred to the skeleton and causing pore collapse. This will decrease the permeability nearer the sample base. Under this scenario the permeability is controlled by the minimum pore neck size on the drainage path, as storage shows the bulk porosity to be increasing.

2) Prior to stress application the fluid pressure gradient across the sample is in equilibrium with the pore size down through the material. If compression occurs evenly throughout the sample, and the permeability is related to the porosity through a linear factor >1, or by a positive power law (Chapter Three), the permeability of the small pores lower down will be decreased to a greater extent than the upper ones. This will feedback as the pore pressure rises at the top of the sample. Under this scenario, the permeability, again, must be limited by the minimum pore neck size on the drainage path.

3) The dilatant areas may be incipient shear zones separated from a generally compressed mass with reduced permeability. Such incipient shears would have to be hydrologically

inactive or only active along limited pathways. This shear hypothesis accords with later events (at 7.5% and 12.5%+) which suggest the action of fully developed shears, and the presence of visual scale shear zones. If this hypothesis is true, it seems likely that such shears propagate from the high fluid pressure regions.

4) The above interpretations follow naturally from the inference that compression is responsible for the raised pore pressure. The alternative to this model is that sample tortuosity increases while dilation occurs to give net storage (tortuosity is discussed in greater detail in Chapter Three). However, it will be shown (below) that this is unlikely.

It is likely, in reality, that compression is more active lower in the sample, but that dilatant shears propagate from high in the sample and affect the throughflow. The low strain shears seen on several of the samples after testing (*Figure 6.10*) reached their lowest point of intersection with the sleeved boundary at least a third of the way up from the base platen. In fully drained or undrained tests, shears usually pass through the whole length of the sediment. This appears to confirms that shears developed in a zone *above* a lower stronger area, possibly compressive, and that the preservation of pre-test features in the upper part of the samples after testing is not a result of strength differences. These hypotheses will be examined further in a thin section study of the tested material in Chapter Seven.

Summary: The early response of the sediment to deformation is a result of the previously unorientated and heterogeneous material undergoing the transformation to a structure optimal for stress and fluid dissipation. Storage indicates dilation (which appears to vary in proportion to stress rather than raised pore fluid pressures), but pore fluid pressure suggests compression. Four possible explanations are put forward to account for this contradiction, including compression near the base of the sample and/or storage of fluid in incipient shears higher in the sample. In these hypotheses the pore fluid pressure is controlled by compression low in the sample and/or limited dilatant paths.

6.4.2 Slowing of the stress increase, storage fluctuations, and associated pore fluid pressure rises

In all of the tests there is a minor stress drop between 6 and 8% followed by a stress rise. In D2 the storage drops and returns at this point. Work by other authors comparing micromorphology and test responses (Chapter Three) suggests this event represents the opening of a fluid throughflow channel, probably a shear. The drop in the storage curves for D2 and D5 (for a similar event at 11.5%) suggests the fluid discharge through these features has a maximum of ~3.5 mm^3 per sample interval (~0.5 to 1.5 min see *Table 6.2*). A similar drainage event occurred in test D6 at 22% (and has a similar pore fluid pressure effect; see below). There is a stress fluctuation in test D6 at 8%, but this is synchronous with *increased* storage. Here the small stress drop, and more apparent stress rise may indicate greater dilation involved in the formation of a shear zone which subsequently collapsed. A similar stress record occurred for D3 at 7%.

As these stress events end, the upper pore fluid pressure increases in D2, D5 and D6 (in D3 it keeps rising). This change backs up the hypothesis that the events represent the formation and collapse of shears, as this process has been shown to lead to decreased permeability normal to the shear strike (see review of studies in Chapter Three).

The fact that the possible collapse of dilatant shear areas does not reduce the net storage to zero may seem to go against the hypothesis that dilation is occurring in incipient shears discussed in the last section. However, such a response is in line with studies showing that shear zones are surrounded by areas of material which have undergone pervasive reorientation that do not fail (Morgenstern and Tchalenko, 1967; Tchalenko, 1968; reviewed in Chapter Three). Thin sections from the visual scale shear areas found after the tests are examined in Chapter Seven, where the hydrological effect of potential shears is further discussed.

The potential shear collapse events outlined above allow some stress release, however, this is rapidly overprinted by work-hardening, despite the higher pore-fluid pressure (cf. Equation 6.1). Unimodal sediments usually respond to shear formation by becoming weaker (see Maltman, 1994, for a review).

Summary: A number of indicators of shear formation found by other authors (Chapter Three) were witnessed during the tests. These indicators suggest that shear zones open and release some of the supported stress. There are examples of both high and low levels of prior dilation.

These shears may then have collapsed, explaining expelled fluid and the decreased permeability of the samples.

6.4.3 Catastrophic pore fluid pressure releases, and work hardening

None of the samples reach a stable supported stress, instead each work-hardens. Stress increases from ~12.5% at much the same rate as during the pervasive pre-yield movement (~<7%). The start of the hardening is not synchronous with changes in fluid pressure, infact work-hardening in D6 begins during *rising* fluid pressure in contradiction to Equation 6.1. However, hardening does *accelerate* at the same time as fluid pressure drops in three samples (D3 at 14%; D5 at 11.5%; and as fluid pressure equalises for D6 at 14%). This indicates that while pore-fluid pressure cannot initiate hardening, a drainage caused component of the hardening cannot be ruled out.

Work hardening of sediment can be attributed to areas of either dilation or compression, dependent on the packing of the sediment. These areas can be in the form of shears, for it is not necessary that shears move to release stress once they form. Shear interference by clasts may explain the lack of stress release during the main drainage events of the tests. The mass of small shears active in the pervasive deformation of fine-grained sediments (Maltman, 1987) would probably not develop strain in this sediment as they would inevitably end abutting sand grains and larger clasts (see description of sample preparation and *Table 6.1*). Movement of the material would thus have to be by the compression of the sediment matrix between clasts, and the redevelopment of any shears at inefficient orientations. These shears, again, would quickly lock as they propagated. This hypothesis of locked shears is backed up by the low strain (throws of ~2 mm) across shears seen in the samples after the tests (*Figure 6.10*). The samples strained mainly by 'pervasive' barrelling. This indicates that continuous shears could form, but were limited in their movement.

The tests show some similarities with tests on bonded rocks that have been pervasively pre-fractured (cf. Jones, 1994, p.59). However, the clarity of the material when thin sectioned (Chapter Seven), and the evidence for pervasive movement, dictates against concretion (for further information on thin sections, see Chapter Seven). The stress supported by the sediments is higher than that usually associated with subglacial sediments tested without clasts (50-100 kPa). However, there is a small shear event early in the stress/storage records of tests D2, D3 and D6 (between 1.5% and 2.5%, also fluid discharge in D5 which may be associated with shear development) which matches the traditional yield strength of such material.

The cause of the stress plateaux in samples D5 and D6 is not understood. Alternation between work hardening and softening is a feature of cataclastic fault gouges, similar materials to tills. However, the process is not understood in this environment either (Chapter Three). As such 'stick-slip' behaviour is not found in unimodal clay or silt tested under low confining pressures, it seems likely that it is due to clast interactions with other clasts or shear zones. This hypothesis is in line with the suggestion of Simamoto and Logan (1981) that such behaviour only develops in cataclastites when the confining pressure is high enough to convert areas of the material into rock, and with the suggestion of Nasuno *et al.* (1997) that stick-slip at a higher strain frequency is due to the formation and collapse of grain-grain bridges which interrupt shear development.

The final fall in pore fluid pressure in each sample (at 14% strain for D3, 11.5% for D5, and 22% for D6), and the synchronous drop in storage for all these samples (though D3 is unreliable) suggests a drainage pathway opening. Equation 3.2 suggests that the instantaneous hydraulic conductivity of the sediments changed from 4.90×10^{-12} to 1.02×10^{-11} m s^{-1} as the drainage paths opened. *Short term* stress fluctuations during these events in tests D5 and D6 suggest some shear movement. However, the hardening after this point dictates that any movement is limited. This lack of movement dictates against the drainage being along moving shear zones, instead implying two possibilities:

1) That the fluid leaked between the sample and rubber sleeve. However, the fluid discharge through the features was similar to that potentially associated with shears above, and the fluid pressure falls were not instantaneous (D5 took a day to equilibrate to a lower fluid pressure level). The final fluid pressure was also less than that at which drainage started. These facts indicate a threshold at which channels opened and then slowly closed. An elastic response, with similar opening and closure periods would be expected for a rubber

sleeve around a perfectly smooth sample, though it is possible that the translocation of particles during drainage opened channels down the sample side.

2) That dilatant channels opened and the fluid pressure adjusted to the presence of these over time. Such dilation need not have swamped the net expulsion seen in the records. In hard rock mechanics, the opening of joints without a coincident stress release is associated with hydraulic fracturing. The fact that drainage is initiated in tests D3 and D6 at the same fluid pressure suggests hydraulic fracturing. However, the minimum effective principle stress never moves into the tensile regime during these tests (*Figure 6.9*). This means hydraulic fracturing is not occurring, unless there are small-scale tensile areas in the heterogeneous stress field of the clast-rich sediment. Instead it is likely the deviatoric stress is causing the dilation of 'shear' zones. The lack of movement indicated by the low stress release suggests particle rotation and collapse do not occur in such zones.

The stress paths for the tests (*Figure 6.9*) indicate that the thresholds mentioned above are not associated with pre-consolidation. Given that the hydraulic channels are dilatant shears, they may be those which were suggested to have collapsed earlier in the tests. This would match the above interpretation that the collapsed shears provide a barrier producing the initial raised fluid pressure. Unfortunately this hypothesis cannot be confirmed from the data.

The storage in D5 recovers from the drainage event between 15 and 20%. The record for this test suggests that an initial ~1.5 mm^3 $interval^{-1}$ change in storage brings about a 75 kPa change in pore fluid pressure before closure. This pore pressure change is not replicated in D2 at 7.5% suggesting that the fluid discharged from D2 moved through the sediment behind a dilation front, the fabric collapsing afterwards. This would cause discontinuous drainage during the event, and the effect of the drainage on the permeability would be overprinted by the permeability decrease due to the fabric collapse.

The material, thus, follows a collapse → decreased permeability → fracture → drainage cycle identical to that seen in clays by Brown and Moore (1993), and similar to the sequence suggested for the cyclic drainage of the Nankai accretionary prism (Moore, 1989; Bryne *et al*., 1993; Maltman *et al*., 1993b; Chapter Three). However, the range of responses from this material is far wider than those from their unimodal or mixed silt/clay sediments. This suggests the behaviour of the material is strongly affected by the quantity and size of the clasts in it. Clasts larger than 10% of a sample width are considered to significantly alter the stress field in triaxial tests (Vickers, 1983). No clasts of this size were found in samples after testing. Thus, it is the clasts, their concentration in the sediment by collision, and their relationship with microstructures that probably give the material its wide range of responses. It is, perhaps, surprising that there is not a *wider* range of responses. The above formulation of a general response which tests vary around, provides hope that continued tests, particularly on till analogues, can further elucidate the rheology of subglacial sediments.

Summary: Work-hardening occurs, probably because clasts render any shear zones, (found in most deformed sediments), immobile. However, shear opens hydraulically active channels. These open channels are maintained, possibly because the immobility of the shears prevents collapse, or possibly because stress heterogeneities allow some hydraulic fracture. Proposed earlier shears must have propagated with collapse occurring shortly after dilation. The processes producing stick-slip behaviour of the material undergoing work-hardening may match those producing the effect in cataclastic shear zones.

6.4.4 Summary of discussion

Thus, it can be seen that the following situations develop as the material is strained:

1) The material must have initially responded with a mix of compression and dilation to give a rise in pore fluid pressure at the same time as a rise in fluid storage. Theoretical considerations suggest compression will be greater towards the sample base, while work in other fields suggests incipient shears develop early in deformation, and these might be the fluid storage areas.
2) The material undergoes a fluid expulsion associated with a minor release of supported stress. Comparison with other studies suggests that this is due to shears propagating through the material by dilation, followed almost immediately by collapse. This hypothesis is further confirmed by the fact that the pore fluid pressure rises after these events, that the variations of these events between samples can all be explained by the shear model, and by the presence of shears on a visual scale after the test. Continued dilation has little affect on the fluid pressure.

3) The pore fluid pressure of the sediment rises each time the events described in (2) occur. The work-hardening continues. As this is not seen in fine-grained sediments, the most likely reason for the work-hardening is the particle size distribution. It is possible that the movement of clasts into the shear fabrics, usually responsible for weakening sediments, causes hardening.
4) The upper pore fluid pressure eventually reaches a threshold value at which drainage channels are forced open. These open pathways are maintained. It seems likely these open pathways are either shears immobilised by clasts, or hydrofracture areas caused by tensile areas within the heterogeneous material. The drainage is only coupled to the stress response in so far as a number of stress relieving events described in (2) appear to raise the fluid pressure. The two are not coupled in any predictable way as the permeability effect of each event (2) is not certain.

There are a number of hypotheses based on the results which can be examined by looking at the microscopic evolution of the sediment as strain continues:

1) Yield events involve the (limited) development of shear zones.
2) Shears are destroyed by the multi-modal nature of the till, leading to work-hardening and a spreading of the shear strain in broad zones and/or various directions.
3) Through-flow channels are present in the sample, possibly in the form of hydraulic fractures or inactive shears.

Chapter Seven presents evidence for or against such situations from the test samples themselves, and then unaltered examples from the Skipsea Till showing the ‘natural’ response of the sediments are examined in Chapter Eight.

6.5 Conclusions and implications for glacial deformation

Glacial sediments respond to deformation in a number of ways. Multi-modal tills under pure shear respond by work-hardening. This opposes the work-softening seen by Kamb (1991) in *size-truncated* multi-modal sediments under simple shear with a forced shear zone. This finite-strain hardening may be representative of the initial deformation of sediment, but cannot be maintained to a steady state given the deforming beds seen by various workers (Boulton and Hindmarsh, 1987; Blake 1992). Therefore, it is supposed that the till will eventually expel clasts from some areas allowing shear like that envisaged by Kamb to occur locally. This may have been the reason for the horizontal weakness experienced during the preparation of the sediment (above).

In Kamb's (1991) view there is no possibility of deforming beds maintaining any stress, however, there is another interpretation of his results. It is implicit in his constant strain tests that the stress representing the boundary between the two deformational behaviours *can* be supported and cause strain at the finite rates found for ice streams. This fact justifies the use of the term 'residual strength' for this value, rather than 'yield strength' as used by Kamb. Basal stress may drop down to this value under ice masses (1.5 kPa) (cf. Boulton and Jones, 1979). The potential strain rates are much lower than those predicated using $n \approx 100$ in Equation 6.1.

Such a shear stress may seem low compared with modern glaciers (~ 50 to 100 kPa), however, it may not have been such for the Dimlington ($\delta^{18}O$ Stage 2) ice sheets over Britain. The ice lobe that moved down the East coast depositing the Skipsea Till is considered to have been thin, as it originated from the relatively low altitude Cheviot Hills some 250 km to the North (*Figure 6.3*). If the 'drift' limit of Kendall (1902) is taken to represent the surface slope of the ice mass as recorded against the North York Moors (assumed flat based at sea level), the basal shear stress can be calculated as varying between 8.96 kPa at Robin Hood's Bay to 5.12 kPa at Scarborough (*Figure 6.5*). This surface slope would give a surface altitude of 1203 m over The Cheviots. The presence of ice in this area is well constrained by radiocarbon dates. Arctic mosses in silts under the tills at Dimlington (*Figure 6.5*) have been dated to a minimum of 18.01 ka B.P. (Rose, 1985) and postglacial organics in the Lake District (*Figure 6.3*) date the end of production of erratics found in the East Coast tills to ~14.3 ka B.P. However, even if the snout of the ice is considered to have left the Cheviots at 18.01 ka B.P. and 50% of the remaining period is allowed for ice degeneration, the needed advance rate is only 134.77 $m\,a^{-1}$ (for a more realistic 10% deglaciation this becomes 74.87 $m\,a^{-1}$). This movement is well within the range of shear rates which produced Kamb's finite residual strength (32 $m\,a^{-1}$ to 1903.2 $m\,a^{-1}$) and it is unnecessary to introduce perfect plasticity in the sediment to explain it. Thus the deformational structures produced in the East Coast tills can still be hypothesised to be of a non-meltout, deformational origin. In Chapter Eight it will be shown that ice movement due to bed deformation in this area was supplemented by decoupling between the ice and its bed.

However, as most present ice masses *are* calculated to have basal shear stresses above Kamb's threshold figure it is necessary to look more closely at the results presented above. Two processes may lead to a stiffer sediment than that maintained by Kamb:

1) Work hardening will occur. The residual state of till will probably be a mix of areas experiencing work hardening, and those with a Kamb rheology. Work-hardening will lead to increased 'Weertman (1957) sliding' at the till surface with increased regelation melt deposition against lodging boulders (Chapter Five), giving 'constructive deposition' (Hart *et al.*, 1990). This hypothesis is testable in that the sediment's strain should vary with clast density. It should be reiterated that the work of Rutter *et al*. (1986) (see Chapter Three) shows that tails of material strung out from clasts by strain are due to clasts interfering with shears, and that it is implicit in their findings that the clasts support some of the stress the material is subjected to. The shear strength of strung-out sandstone and chalk clasts found in tills is considerably larger than that of clays and silts at subglacial effective pressures, so clast fracturing cannot be envisaged unless the clays and silts undergo work-hardening, probably because the clasts obstruct shear areas in the sediment.

2) Stress is uncoupled from the hydraulic response. The material can drain with no stress release. This leads to a stiffer sediment, without the concomitant weakness one would expect if the drainage paths were moving shear zones. The maximum discharge through such features during the tests was only 1.4897×10^{-6} m^3 day^{-1}. However, this was 52% of the potential discharge (the fluid input during this period). The instantaneous hydraulic conductivity (Chapter Three) of the sediment changed from 4.90×10^{-12} to 1.02×10^{-11} m s^{-1} as the drainage paths opened. In traditional rock mechanics hydraulic fracture occurs perpendicular to the minimum principle stress. In these samples this direction will have been complicated by the heterogeneous stress field and/or the shear component necessary for fracture. However, subglacial hydrofracture will probably be in the direction of maximum applied stress under a pure shear geometry, and the shear stress elsewhere, ie. approximately horizontally. This will facilitate flow to the front of the glacier. Such a process

is likely to increase fluid flow in the direction of the resultant hydraulic gradients produced by the glacier profile and the fluid pressure in major channels.

It has been shown that events reduce the permeability of the sediment in the direction of the maximum applied stress. In the glacial case of stress between clasts, this would be horizontal. The permeability need not be reduced in the direction of the *minimum* applied stress (vertical glacially), provided the changes are due to tortuosity variations (Arch, 1988; Chapter Three) rather than pore size variations. If the permeability variation results from pore size changes the variation will be locally isotropic. The wider effect of the repacking will depend on the shear area facing the direction of fluid flow.

Thus, fluid pressure build-up will be accelerated subglacially. Such a rise will, however, be buffered by the channelling described above. This will lead to a dryer and stronger sediment than might be expected. It can therefore be seen that fabric collapse and dilation in subglacial sediments appears to drive their fluid pressure towards a buffered midpoint. In these tests this gave an effective confining pressure of ~200 kPa.

This chapter has examined the hydraulic and stress response of natural multi-modal glacial sediments under conditions representative of subglacial environments. The material follows a collapse → decreased permeability → fracture → drainage cycle identical to that suggested to occur in oceanic accretionary prisms. In the next chapter the interpretation of the test results are examined by looking at the micromorphology of the test samples. These results are then used to determine the stress and hydrological history of the glacier depositing the Skipsea Till and other sediments in Chapter Eight.

7. The Development of Micromorphology in Laboratory Tests

7.1 Introduction

Material from the cliff of Skipsea Till at Skipsea (*Figure 6.5*) was tested for its strength and hydrological response under deformation (Chapter Six). The material from two of the tests (tests 2 and 5) was thin sectioned to determine the microscopic structure. This gives information on the formation of various microstructures which will be used to interpret naturally occurring examples in Chapter Eight. The microscopic structure also illuminates the test results, and a number of the interpretations outlined in Chapter Six.

7.2 Methodology

Samples were removed from the cliff at Skipsea and tested such that the analogous applied stress on the samples in their 'natural' location would have been vertical. This was due to the difficulty in sampling such that the stress could be analogous to that applied horizontally (see Chapter Six). A confining stress was applied horizontally. Details of the test conditions and results are given in Chapter Six. Thin sections were prepared in vertical planes. The two test samples were selected to give a range of strains (test 2 went to 15% strain, test 5, 25%). Unaltered samples of Skipsea Till are examined in Chapter Eight. As the upper half of the sediments deformed to a greater extent than the lower half, sections were taken from both halves to give a larger strain range (these are denoted below as, for example, 15%- and 15%+). The thin sections from the upper halves of the samples were removed such that their planes were either across or with the strike of shears visible after the tests (for examples, see *Figure 6.10*). The samples were also selected to illuminate the rheological tests, particularly the unexpected high strength of the sediments and two contrasting hydraulic events:

1) Early hydrological events during deformation in which fluid was expelled locally from the samples and the overall permeability of the samples decreased;
2) Late hydrological events where fluid was expelled and these events were followed by a dramatic rise in the sample permeability.

Test 2 only passed through the former event, Test 5 suffered the only the latter.

Thin sections were blind-tested, that is, initially described without knowledge of their original sample or strain.

7.3 Results

The descriptions of the slides are given in Table 7.1. Descriptions are in terms of the general fabric of the diamict, and the fabrics in and around any inclusions such as clay bands. Skelsepic fabrics are where fine, 'matrix', particles (F) and/or sand grains (G) are parallel to the edges of larger grains. Lattisepic fabrics are those where areas of fabric exist in two orthogonal directions, either pervasively or in a lattice of separate bands. An omnisepic fabric is where a large proportion of the sample has a single fabric direction. 'SDF area' refers to a Single Direction Fabric area. This is an area of material which has a consistent internal direction but is not large enough to qualify as omnisepic. Multiple SDF areas may be arranged in one or more directions or may be randomly aligned (RA). It is felt the term 'domain' implies clays and a consistent sub-rectangular form. The term domain has also been applied to various sizes of fabric orientation, often under the impression it is unique to that scale. Other terms are defined in Chapter Two and the Glossary of fabrics.

Shears were seen on an unaided visual scale after the tests (*Figure 6.10*). The relationships of the sample plane to these shears are noted, as is the likely presence of such a shear within the thin section. Shears and more pervasive fabrics are given in terms of their dip angle. If the thin section plane is parallel to the shear dip '120° out' indicates a fabric falling at 120° outwards from the sample centre. If the thin section crosses the sample centre or runs parallel to the shear strike '120° right' indicates a fabric falling at 120° right if looking towards the sample centre. The sample centres are denoted by a 'c' on the small diagrams given to help the reader compare orientations with shear features etc. (these are only meant to convey an impression of orientations). Photographs of the more important features are provided in the section where the results are interpreted. The variation in strain between the upper and lower halves of samples means that the local strain falls either above or below the net sample strain. This difference is not calculable with the present equipment. The strain for each sample is therefore denoted as positive or negative in relation to the net strain.

Strain / position	**Sample No. / diagram**	**General fabric**	**Inclusions**
In plane of strike. Shear within section. 15%+	T27 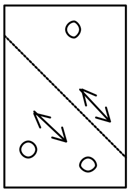 Key: c Omnisepic fabric Skelsepic Shear	Skelsepic fabric within other fabrics. Weak Omnisepic (135° out) fabric (100% of slide). Patches of intensity in Omnisepic fabric where skelsepicism (F+some G) increases. Most intense fabrics are on sample outer side at top. No large cracks not associated with clasts. Clasts well distributed but many clast rich patches. Clasts only locally aligned.	Clay patches (<1% total slide) with internal fabric at 135° ‘out’. Clays contain heavy mineral fragments and other fine sand grains.
In plane of strike. Shear within section. 15%+	T22 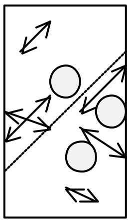 c Key: Large clast Lattisepic fabric	Almost no skelsepic fabric, though (G+F) around some clasts. Three large clasts (<7x7mm in 90° triangle) control fabric directions parallel to their sides, but these fabrics are not skelsepic (ie. carry on in same direction after clasts end). Fabric greatly variable but large SDF areas in two directions (120° ‘in’, 72% of slide, 130° ‘out’, 20%). Lattisepic fabric in one area (3%) and unorganized in another (5%). Clasts poorly distributed in clast rich patches. Considerable cracking in area between large clasts at 130° ‘out’ even where surrounding fabric at 120° ‘in’.	Clay patches (~2% total slide), at least two of which may be a brecciated clay band. Fabric the same as that surrounding them. Clays contain heavy mineral fragments.
In plane of strike. Away from shear. 25%-	T52 c 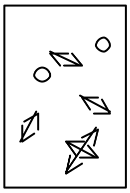	Skelsepic (G+F) within other fabrics & areas with just this fabric (12% of slide). Large SDF areas in two directions (115° right, 69%, 160° left, 8%). Fabric weak in patches especially at 160° left. Lattisepic (6%) and unorganized (5%) areas. Clasts generally well distributed but with clast rich patches. No cracks not associated with edge of clays.	Considerable clay bands (8%) showing finite strain on the order of 50% shortening. Fabric generally at 115° right, but cut by shears at 170°, 130° and 90° left. These shears were synchronous with the main fabric development (can be seen moving out of bands into surrounding material). Clays contain heavy mineral fragments.
Across strike. Away from shear. 25%-	T54 c 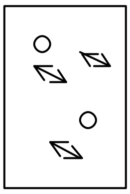	Skelsepic (G+F) within other fabrics & areas that are only this fabric (20% of slide). Omnisepic fabric (125° right, 72%). Fabric weak in patches. Unorganized areas (8%). Clasts well distributed but with occasional clast patches. Cracks exist not associated with large clasts.	Sample has large clast (13x11+mm) in section and had two large clasts closer than 7mm to the sample plain found during preparation. No silt or clay concentrations.
In plane of strike. Shear within slide. 25%+	T51 c 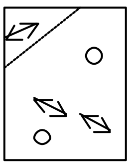	Skelsepic (G+F) within other fabrics. Large SDF areas in two directions (120° right (95% of slide), 120° left where shear crosses (5%)). Small amount of local clast alignment, but not in any one direction. Clasts well distributed. Considerable cracking.	No silt or clay concentrations.
Across strike. Shear within slide. 25%+	T53 c 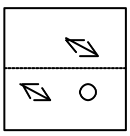	Skelsepic (G+F) within other fabrics. Omnisepic fabric (113° right, 100% of slide). Small amount of local clast alignment, but not in any one direction. Clasts well distributed. Some cracking.	One large clast (10x6mm) in section. Silts are concentrated around large clasts. Otherwise no silt or clay concentrations.

Table 7.1 The micromorphology of the triaxial test samples. Strain increases towards base of table.

7.4 Interpretation

There is a progression in three fabrics as the strain increases:

1) the material becomes more evenly distributed with strain and unimodal clay patches disappear, particularly after 25% strain;
2) the skelsepism of the samples increases, especially in the 25%- samples;
3) the sample undergoes greater crack development (away from material heterogeneities which are likely to cause cracking during sample preparation).

There is also a less plain progressive development of omnisepic fabrics from the relatively weak fabric of T27 to the stronger fabrics of later tests. In discussing this it is essential to distinguish between thin sections across the plane of strike and those parallel to the dip of the shears recorded on a visual scale, as shear has been implicated in the formation of these fabrics (Chapter Two). In the former, the omnisepic fabric in the shear direction increases from 72% of the slide area for 25%- strain to 100% of the slide area for 25%+ strain. In the case of sections parallel to the shear dips, the omnisepic fabric varies from a weak 100% or stronger 20% fabric at 15%+ strain, to 69% of the slide area at 25%- strain, and only 5% at 25%+ strain. However, the figure for 25%+ hides the fact that the omnisepic fabric in the direction of shear seen at a visual scale is heavily concentrated in the area where the shear was seen at the larger scale. Thus, there is some evidence that omnisepic fabrics are a shear strain feature. There is also evidence for the intensification of omnisepic fabrics with the overall shear strain, and intensification close to areas that have been seen to have sheared on a larger scale.

It will be shown that the fabric development suggests the processes by which high stresses are supported by the sediment during deformation, and the way the sediment hydrology responds to deformation.

7.4.1 Sample history

The low strain samples (<25%) have numerous unorientated areas and clay/sand patches (*Figure 7.1*). These decrease with strain suggesting that they are the natural fabric of the sediment. During the tests omnisepic strain fabrics become stronger, both in the direction of visible scale shears where they cross the samples, and in the conjugate direction away from such shears. This development to a well mixed and orientated sediment with mild strain indicates that only low strain occurred in the samples prior to the tests. It cannot, however, be said that prior to the tests the strain in the material was less than 25% as the strain alignment direction may have differed during the sediment's deposition and/or deformation, and the brecciated clay bands in the samples confirms the samples *did* suffer strains greater than 25% before the tests were initiated.

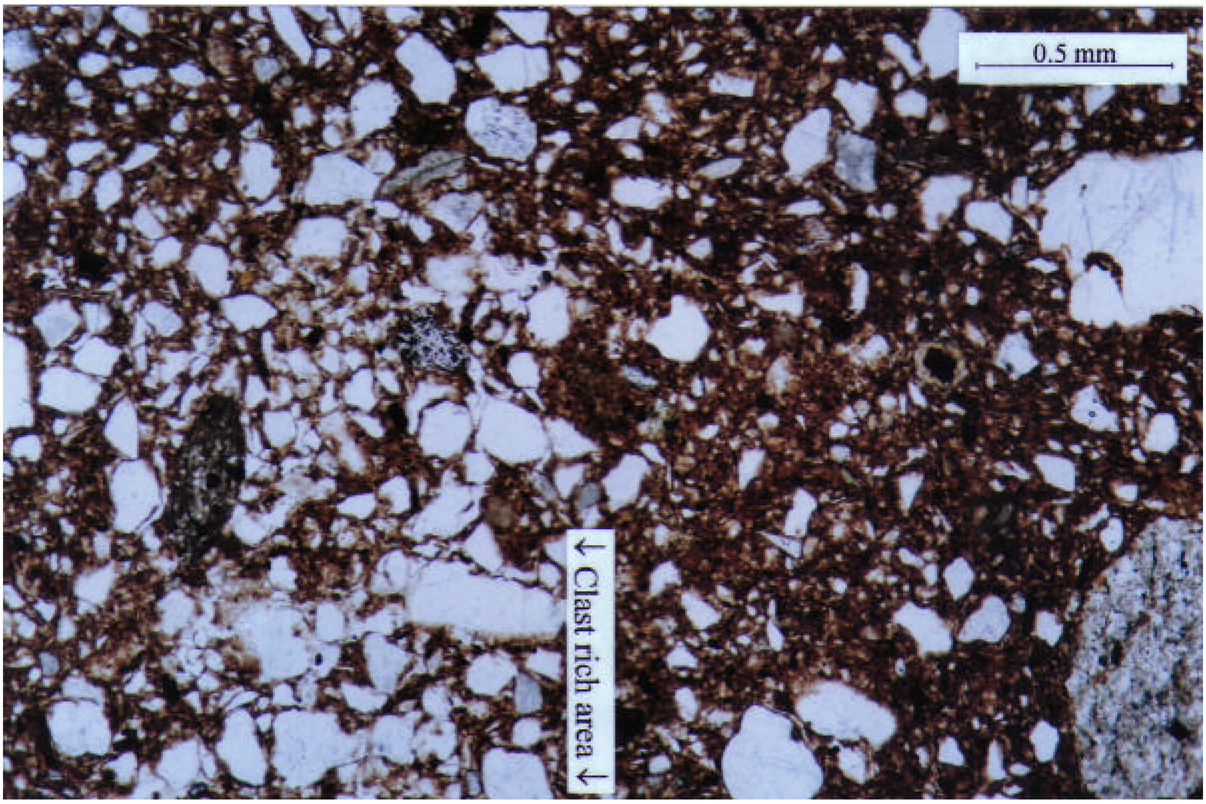

Figure 7.1 Photomicrograph of a clast rich patch from slide T22. Unpolarized light conditions.

7.4.2 Strength and fabric relationships

It will be remembered that Chapter Six posed two hypotheses relating to sediment strength;

1) yield events involve the (limited) development of shear zones, which were identified from their hydrological response and visual scale presence;
2) shear movement is limited by the multi-modal nature of the till, leading to work-hardening not seen in fine grained unimodal sediments, and a spreading of the shear strain in broad zones and/or various directions.

The omnisepic fabrics in the thin sections match the direction of the shear zones visible by eye at the end of the tests in slides T27 and T51. In T22 the orientations are reminiscent of conjugate shears, one orientation matching the direction of the visual scale shearing, the other close to orthogonal to it. These relationships suggest that the omnisepic fabric is formed by shear, and that omnisepic fabrics can be used as an indicator of local shear strain direction. Work by numerous authors (Chapter Three) shows that in *unimodal* sediments, deformation usually results in discrete shears. The development of a wider, omnisepic, shear fabric during the tests on the diamict therefore confirms that discrete shear development is prevented by clasts (Chapter Six). The shear of thick areas of sediment was shown by Logan *et al*. (1992) to require a longer strain period than thinner depths of material. This fact, plus the fact that discrete shear fabrics are an important component of the yield and weakening of unimodal sediments (Chapter Three), lends indirect evidence to support the hypothesis that clast disruption of shears causes the test samples to work-harden. It is still possible, however, that the presence of clasts affects work-hardening, but their shear disruptive action is completely separate.

Lattisepic fabrics are only found in the slides with large patches of internally uni-directional fabric in two different orientations (*Figure 7.2*). This suggests lattisepic fabrics form where conjugate shear areas abut each other. In T22 shears in these abutment zones can be seen forming by extending from clast sides. These sides are in the two approximate directions expected for conjugate shears (quasi-orthogonal shears mirrored around the applied stress, see Chapter Three). The clasts must provide stress concentrations that aid the initiation or rotation of the shear fabrics. Clasts close to each other also transform simple shear geometry conditions between them to pure shear geometries, and force the intermediate fabric at 90° to the overall simple shear direction (*Figure 7.3*). This alignment is so close to the usual conjugate shear direction that these areas may be exploited by shear in the conjugate direction.

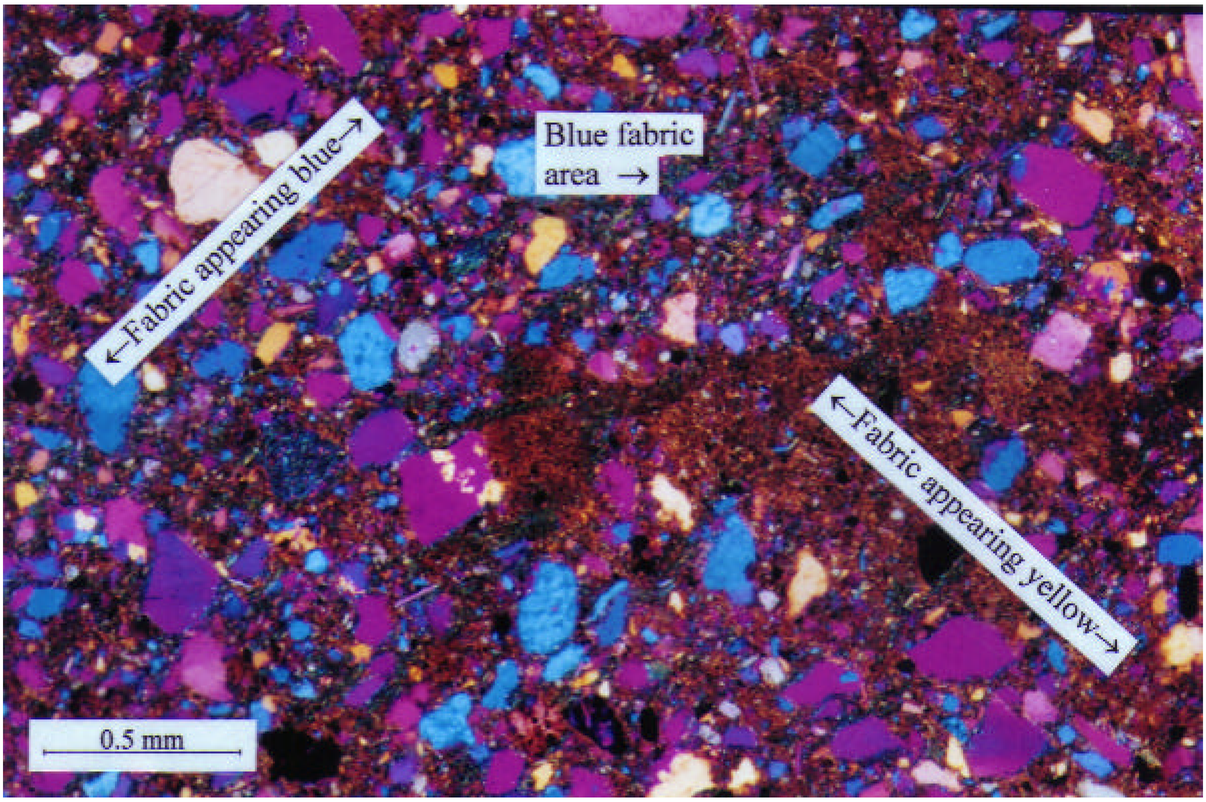

Figure 7.2 A pervasive lattisepic fabric photomicrograph from T22. Cross polarised light with a tint plate. Yellow areas of matrix are orientated in one direction, blue areas are aligned in another direction, along with some other thin grains.

Thus, lattisepic fabric represents a nascent shear fabric which develops in areas of conflicting shear alignment. Such a fabric is expected to development under pure shear geometries, where there is more likely to be several dominant shear directions; a situation that may also be encouraged by the clast obstruction of shears. Very local development of lattisepic fabric is expected under simple shear geometries when propagating shears interact during the development of complex décollements (Chapter Three). The increase in omnisepic fabric between strains < 25% and > 25% suggests one fabric or the other will come to dominate the material with greater strain in most cases.

It should further be noted that lattisepic fabric formed from conjugate shears in one vertical plane will probably appear as omnisepic in a vertical plane cut at 90°. Such a development can be seen in the samples described above (*Table 7.1*). Those thin sections cut parallel to the dip of the visual scale shears have two or more fabric directions (though one is often dominant), whereas those sections cut across the strike of shears are completely omnisepic.

The orientation of sand sized grains might have been expected given the development of other fabrics, but did not occur (though note the one example in sample T27). This suggests greater strains are necessary for sand alignment if it occurs. Some authors have suggested skelsepic fabrics indicate clast rotation (Chapter Two). The experiments throw some light on the formation of skelsepic fabrics, though the information is not conclusive. Two facts point towards shear rotation of clasts and the cohesion of clay grains to them as the origin of skelsepic fabrics. Firstly, in sample T27 the most intense skelsepic fabric is associated with the edge of the most intense omnisepic shear fabric. Secondly, clays and silts are often found concentrated around clasts in 'halos' with less sand grains (*Figure 7.4*). Cohesion may be initiated onto clays trapped in irregularities in the clast surface. Their size means that clays are

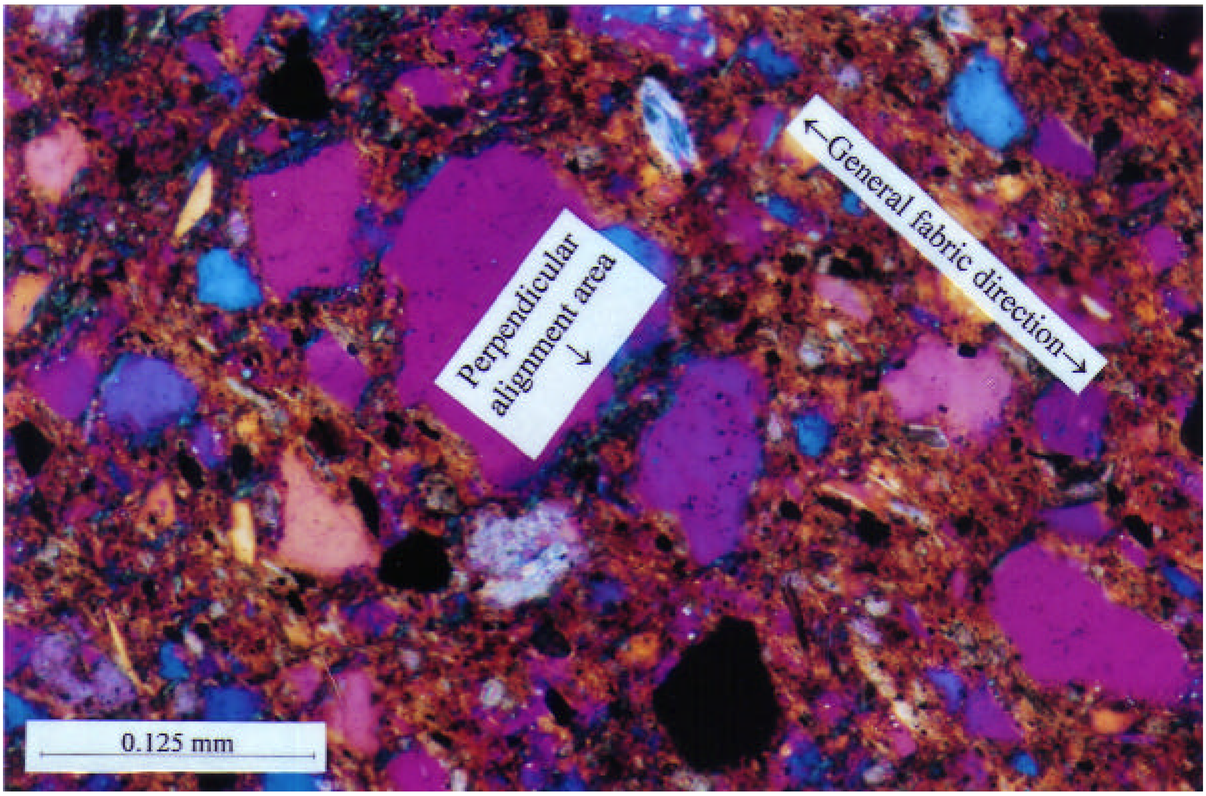

Figure 7.3 Photomicrograph of clasts within a sheared fabric that have developed an fabric parallel to their sides between them. Unpolarized light, Slide T22.

less likely to be removed from the surface of large clasts by abrasion against other grains that they rotate past. While silts have little cohesion of their own, silt grains trapped in cohesive clays would be less likely to be pushed away from a rotating clast than large sand grains. If this hypothesis is correct, skelsepic fabrics would vary with clay content and strain. There is insufficient clay variation to test this here.

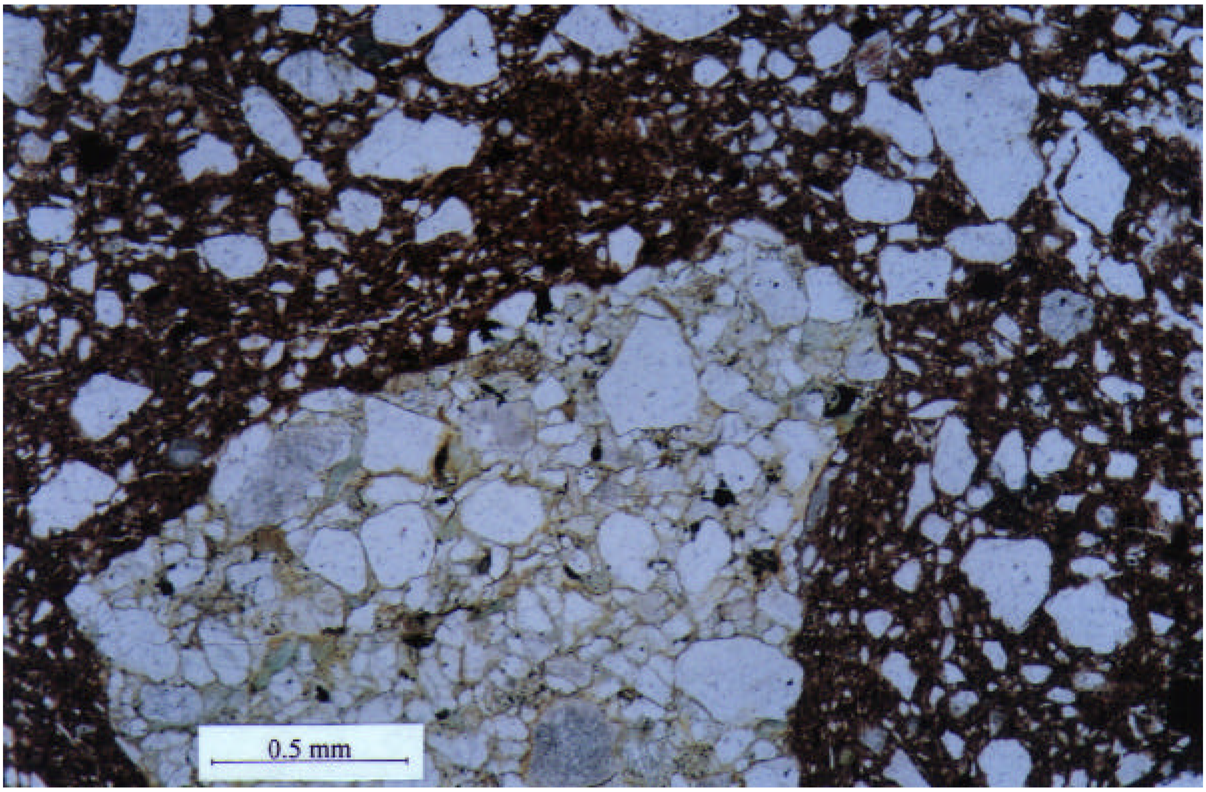

Figure 7.4 Photomicrograph of clay/silt concentration around a clast. Unpolarized light, slide T22.

7.4.3 Changes in hydrology during deformation

During the tests the samples underwent fluid expulsion events while developing higher fluid pressures, and other expulsion events during which permeability in the samples dropped (Chapter Six). The following interpretation was given;

'through-flow channels are present in the sample, possibly in the form of hydraulic fractures or inactive shears'.

The fabric development illuminates the nature of these throughflow channels. The pervasive fabric indicates that the collapse of discrete shear networks was *not* responsible for the events in which fluid was expelled and permeability rose. The absence of discrete shears despite the characteristic 'shear-like' stress, fluid expulsion, and permeability signals suggests the omnisepic fabrics acted locally as broad shear or dilatant zones, and this may explain the high volume of fluid expelled. Alternative suggestions, such as a dilation-collapse wave travelling across the whole sample would have to coordinate fabrics with differing orientations and, therefore, frictional properties, which is physically unlikely.

The pervasive fabric also suggests throughflow and an organised fabric can coexist. The mixing of randomly orientated fabric patches with a single internal orientation and completely disorientated fabric has been attributed to throughflow disruption (Menzies and Maltman, 1992). Strains of less than 25% removed the disorientated areas in the tests reported here. This suggests that fluid disorientation cannot withstand synchronous or subsequent strain, or alternatively, that lower effective pressures than the minimum seen in these tests (~100 kPa) and/or greater throughflow rates are necessary to disrupt fabrics during deformation.

Hydrofractured throughflow channels were predicted to exist in Chapter Six on the basis of large, permanent falls in pore fluid pressure as the tests proceeded. Microscopic cracks *are* found in the samples (*Figure 7.5*). However, before suggesting the cracks developed during the tests, it should be noted that cracks are often seen in thin sections and are usually dismissed as being due to sample preparation; particularly sample drying. On top of this, there is some cracking in the sample that was only taken to 15% strain and never underwent a permanent increase in permeability (test 2). However, two points should be noted:

1) The cracking increases in the sample that experienced a permanent pore fluid pressure fall (test 5), and at the top of that sample, where additional strain dilation is considered to be highest and could have contributed to opening channels (Chapter Six).
2) The cracks are modally vertical (*Figure 7.6*), which is the direction one would expect if they developed by hydraulic fracture parallel to the minimum effective pressure (Price and Cosgrove, 1990). None of the other sample fabrics are vertical. This modal crack direction points to tensile hydrofracture as the confining pressure was released at the end of the tests. However, the average direction of cracking belies the fact that the crack morphologies vary from straight to kinked (*Figure 7.5*). This morphology suggests the exploitation of areas of the shear fabric and possibly implicates shear weakening and/or dilation in the crack

formation. If hydraulic fracturing occurred along such lines of weakness, it is possible they were also exploited by fluid during the tests in local tensile stress regions.

Thus there is contradictory evidence as to whether the cracks were responsible for the pore fluid pressure drops, and it is safest to leave the matter open. The most parsimonious scenario is that weaknesses set up during the tests were exploited during the sample removal from the equipment.

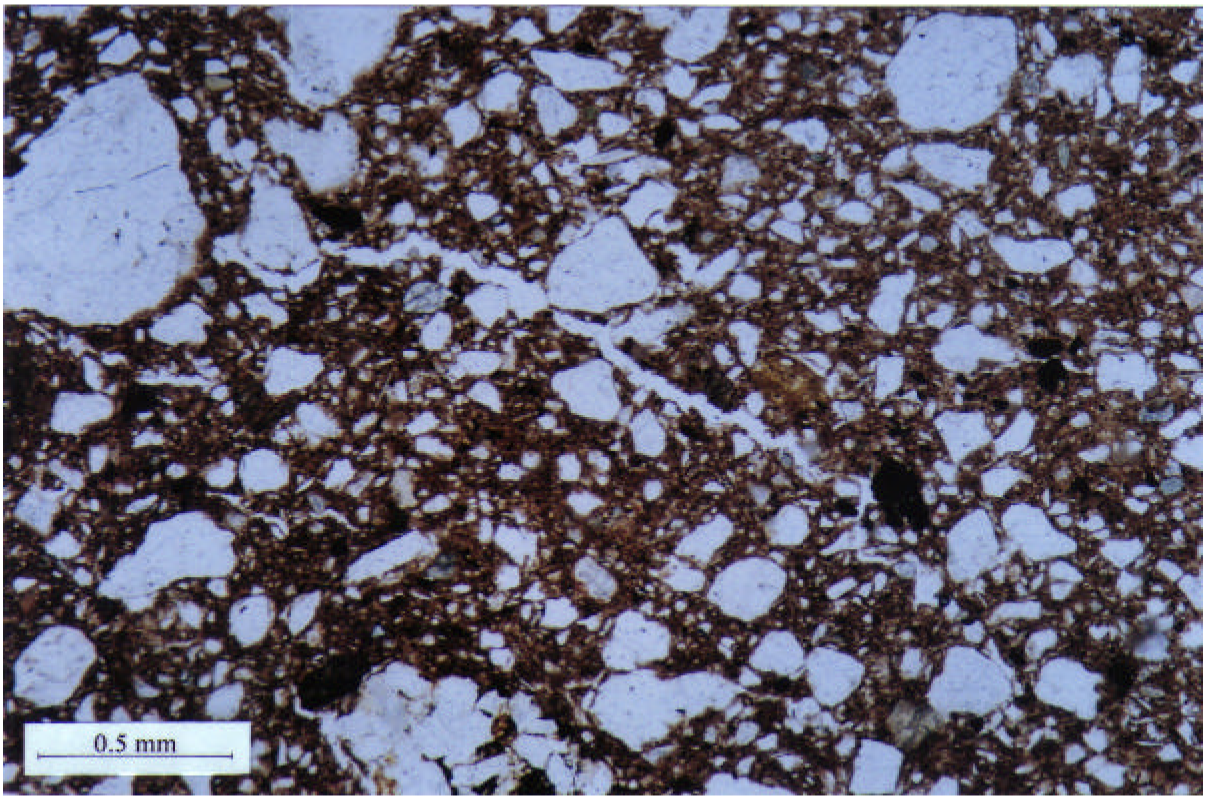

Figure 7.5 Cracking in thin section T51. Note the straightness of the cracking despite the heterogeneity of the material. Unpolarized light.

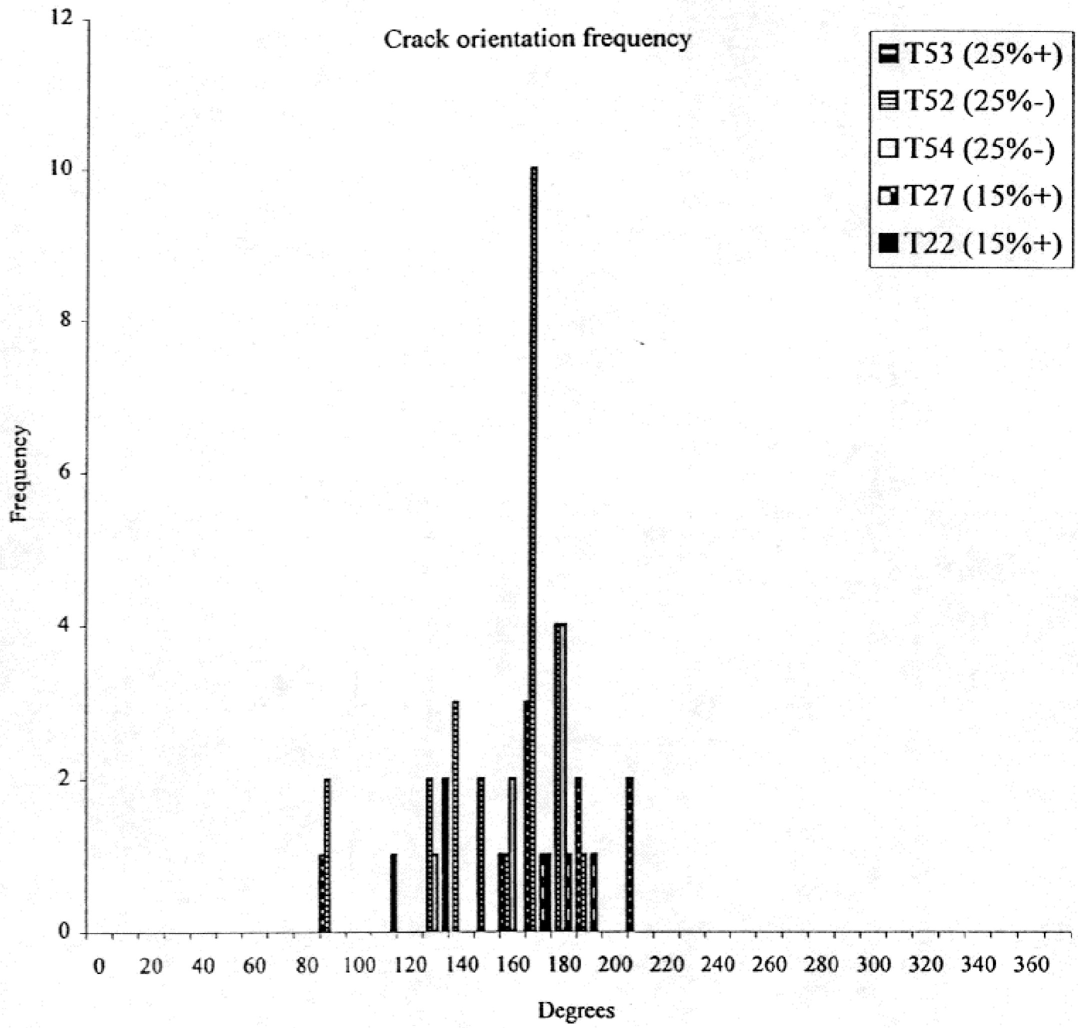

Figure 7.6 Crack orientations for the cracking in the thin sections prepared from the test samples. Measurements were taken in the range 90° to 270°, and the results are categorised in 10° bins.

7.5 Conclusions

Skipsea Till samples were subjected to triaxial testing (Chapter Six) and then thin sectioned for micromorphological study. The low strain prior to the sediments being used in the triaxial tests invalidates the experiments as an analogue of subglacial deformation at this particular site. However, the sediment tested here broadly matches that expected in the region as a whole, and subglacial sediments generally. In this sense the experiments provide a reasonable analogue for other localities that may have experienced higher strain. The triaxial sections show that omnisepic fabrics are formed by local simple shear, and that omnisepic fabrics can be used as an indicator of local simple shear deformation direction. Unimodal sediments develop weak discrete shears at low stresses after which their deformation is enhanced. The high strength of the test samples may result from the absence of such shears, which seem to have been disrupted by the presence of clasts. The triaxial tests also suggest lattisepic fabrics represent nascent shear fabrics developing in areas of conflicting shear stress directions. Clasts limit fabric directions between themselves to those which are suitable for the exploitation by, and development into, conjugate shears. It is likely that propagation of one of the conjugate shear sets will occur with greater strain and lead to an omnisepic fabric.

There is some evidence from the thin sections that skelsepic fabrics are formed by shear rotation and the cohesion of clay grains to clasts. If this is the case we would expect skelsepic fabrics to vary with clay content and strain and this could be tested triaxially.

The triaxial tests underwent fluid expulsion events associated with decreased permeability, and a reduction in supported stress. Such a response is usually attributed to discrete shearing (see Chapter Three). However, the samples failed to show such discrete shears, suggesting that the broad omnisepic fabrics found can also act in a similar manner.

The triaxial samples also underwent catastrophic and permanent *increases* in permeability during the tests, associated with fluid expulsion events. There is contradictory evidence from the thin sections as to whether hydraulic fracturing aided by shear dilation is responsible for such increases, and it is safest to leave the matter open. It is probable that weaknesses set up and exploited during the tests were further opened during sample preparation.

It is apparent from the tests that throughflow removal of fabrics is not possible if there is syn- or post-throughflow deformation without higher throughflow rates or lower effective pressures than the minimum seen in the test samples (~100 kPa). It is, however, worth noting that the randomization of fabrics can occur for several reasons and the individual sequence of events at any given site must be examined to draw out the processes acting to produce the fabric.

The following chapter uses the above discussion, and the results developed in prior chapters, to analyse the sediments deposited by the Devensian glaciers of the Yorkshire coast.

8. The application of microstructural analysis to macroscale forms: the dynamics of the East Coast Late Devensian Glaciers

8.1 Introduction

In the Late Devensian ($\delta^{18}O$ stage 2) ice extended from Scotland down the North Sea coast of the UK. These glaciers left a suite of sediments, largely diamicts, that can be traced from the Cheviot Hills just south of the Scottish Border (NT 3865) to Hunstanton in East Anglia (TL 567341) (*Figure 8.1a*). Individual sediment units can be traced for distances on the order of a hundred kilometres (Madgett and Catt, 1978; Evans *et al.*, 1995), and have been studied for more than a hundred years (Wood and Rome, 1868), giving an excellent region-wide appreciation of their form and content. The sequence of sediments is best exposed along the Yorkshire coast.

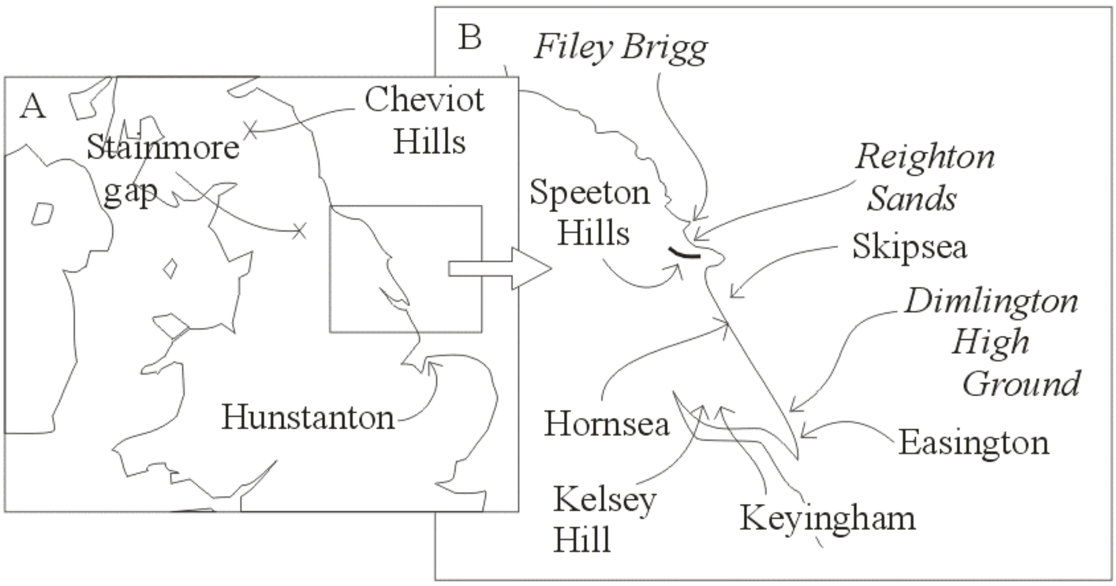

Figure 8.1 A) Map of locations discussed in the text. B) Location of sites on the East Yorkshire coast discussed in the text. Sample sites discussed in this chapter are in italics.

The diamicts of Yorkshire are probably subglacial tills (Evans *et al.*, 1995; Eyles *et al.*, 1994). They include rafts of older marine clays and sands (Catt and Penny, 1966), and soft clasts, some of which have been strung out into bands indicating shear deformation (*Figure 8.2*). Given this evidence the diamicts have been defined as deformation tills (Evans *et al.* 1995; Eyles *et al.*, 1994). This definition backs the seminal claims of the early soft bed modellers (Boulton and Jones, 1979; Boulton *et al.*, 1985) that till deformation was responsible for the extension of east coast glaciers so far from their small, and relatively low altitude, accumulation areas. The homogeneous diamict around the obviously deformed material is widely believed to be the same sediments mixed by high strain (Hart and Boulton, 1991; Eyles *et al.*, 1994).

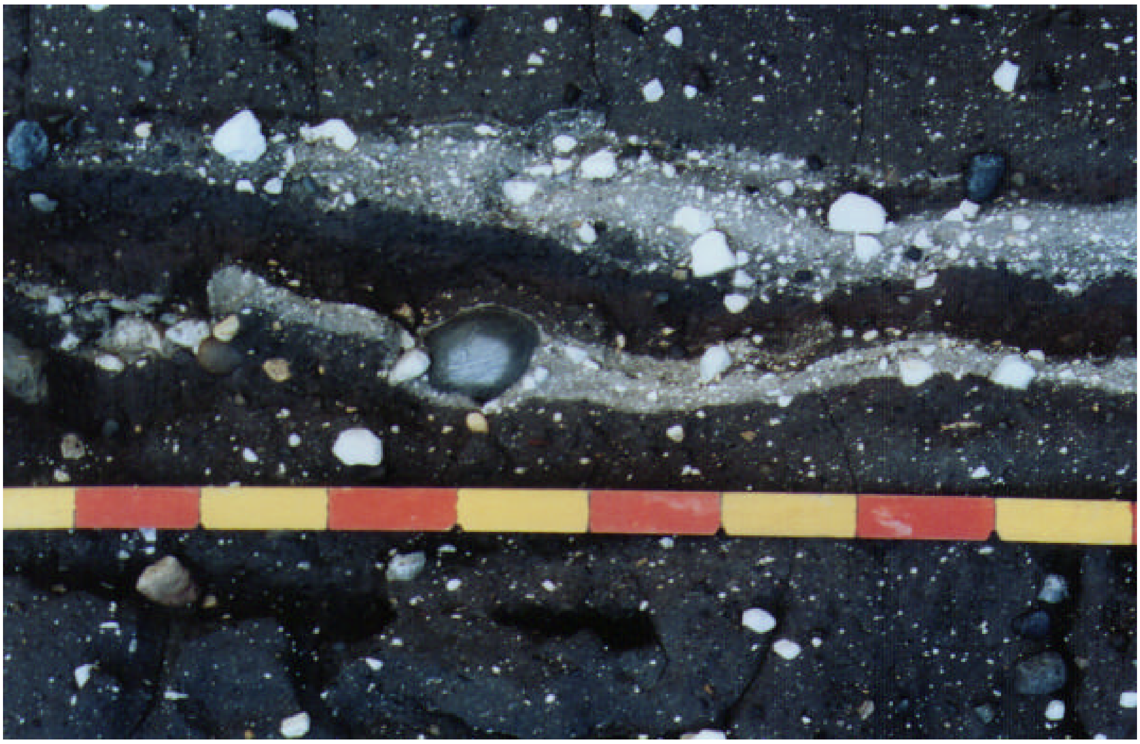

Figure 8.2 Shear extended chalk material at Hornsea, East Yorkshire Coast. Ruled divisions are 10 cm.

The Yorkshire sediments were deposited on flat marine plateaux (Kendall and Wroot, 1924; Valentine, 1952; Straw, 1961), and the flow of the glacier from its head to the terminus was relatively uninterrupted by topography. This means that any till deformation will have occurred under as near to 'textbook' conditions as one could hope for in an illiterate world. The sediments of the Yorkshire coast therefore provide an excellent suite of materials with which to examine;

1) the definition of the sediments on the basis of outcrop scale structural work;

2) the dynamics of the Late Devensian North Sea glaciers;

3) the potential processes and effects of deforming beds generally.

With this in mind, sediments were sampled from the 'Skipsea Till' in Yorkshire and its boundaries with the other local sediments. The Skipsea Till diamict, probably with a largely Scottish provenance, overlies a diamict known as the 'Basement Till' in Holderness, and bedrock further to the north. It, in turn, is overlain by the 'Withernsea Till' diamict, probably with a Lake District provenance (Kendall and Wroot, 1924; discussion in Madgett and Catt, 1978), between Easington (TA 403200) and Hornsea (TA 212472) (*Figure 8.1b*). The upper two diamicts were deposited by ice flowing down the east coast. Ice from Scotland was either superseded or superimposed (Carruthers, 1948; Madgett and Catt, 1978) by ice crossing the Pennines from the west at the Stainmore gap (*Figure 8.1a*).

Fluvial sand, silt, and gravel inclusions are found throughout the Skipsea and Withernsea Tills in the region. Two models have been proposed to account for the deposition and deformation of the sediments;

1) a single ice mass including ice streams of varying positions and velocities, depositing and deforming the diamicts, with the sands deposited from subglacial streams (Evans *et al.*, 1995);

2) a set of glaciers oscillating due to climatic variations or undergoing true surging across proglacial water-lain deposits (Eyles *et al*., 1994), some of which undergo partial disruption to form diamicts.

Sampling was therefore also carried out to investigate the nature of the fluvial events with the hope of distinguishing between the potential ice histories.

8.2 Methodology and sampling

Sediments were sampled from coastal cliffs after the removal of between 50 and 100 cm of surface material, following the techniques outlined in Chapter Three. Sample locations (Reighton Sands, Dimlington and Filey) are given on Figure 8.1b.

The boundary between the Withernsea Till and the Skipsea Till is largely inaccessible because of its height. This boundary may also represent a change in englacial sediment that has melted out, and therefore may not reflect subglacial conditions (Carruthers, 1948; Madgett and Catt, 1978). For these reasons, the boundary between the Basement Till and the Skipsea Till was chosen for sampling. Eyles *et al.* (1994) have shown that the Basement Till is Late Devensian, and thus that the Skipsea Till is a readvance unit. The boundary between the Basement and Skipsea Tills therefore gives information on the processes of readvance during the main glacial phase; a phase that may have been characterised by short-lived readvances or true surge type behaviour (Eyles *et al.*, 1994). The boundary between the diamicts varies in character, and this variety was accounted for in the sampling strategy. The different boundary morphologies sampled are summarised in Table 8.1.

Sample Site	Skipsea Till type and situation	Sub-Skipsea material	Lower Skipsea boundary nature
Filey Brigg (TA 125816)	Till homogenous. Suffered considerable overriding by glacier.	Jurassic Limestone	Homogeneous and sharp with bedrock.
Dimlington (TA 390218)	Till homogeneous. Suffered considerable overriding by glacier.	Basement Till and laminated silts.	Sharp 'shear' appearance.
Reighton sands (TA 145763)	Till homogeneous. 100m up ice from terminal moraine.	Sands.	Finite strain folding.

Table 8.1 Sample locations, diamict character, nature of lower boundary and the underlying material at the sample sites.

Material was also sampling from higher in the sequence at Filey Brigg to give information on the homogeneous areas of diamict, and the nature of the fluvial deposition events.

The microstructures from each of the three sites are detailed below, and conclusions drawn for each in turn in terms of processes and history. Information from the triaxial tests on the Skipsea Till (Chapters Six and Seven) is used in this interpretation. Finally, the chapter concludes with a review of the conclusions for each site, and the implications for the dynamics and history of the ice mass as a whole.

8.3 Filey Brigg

8.3.1 Introduction

Material was sampled from the coastal cliff at the inland southern end of a small peninsula known as Filey Brigg (TA 125816), just north of the main town of Filey (*Figure 8.1b*). The Brigg sediments (*Figure 8.3, Figure 8.4* and *Figure 8.5*) have been correlated with the Skipsea Till further south (Evans *et al.*, 1995). The area has been extensively studied on an outcrop and S.E.M. scale by Evans *et al.* (1995). However the authors failed to gain satisfactory thin sections for optical examination because of the very low permeability of the sediments (D.Roberts, pers.comm., 1994). Considerable information can be revealed at this intermediate level. Therefore success with similar sediments, and the otherwise complete prior work, dictated this sequence as the most suitable site for a detailed thin section investigation of the Skipsea Till.

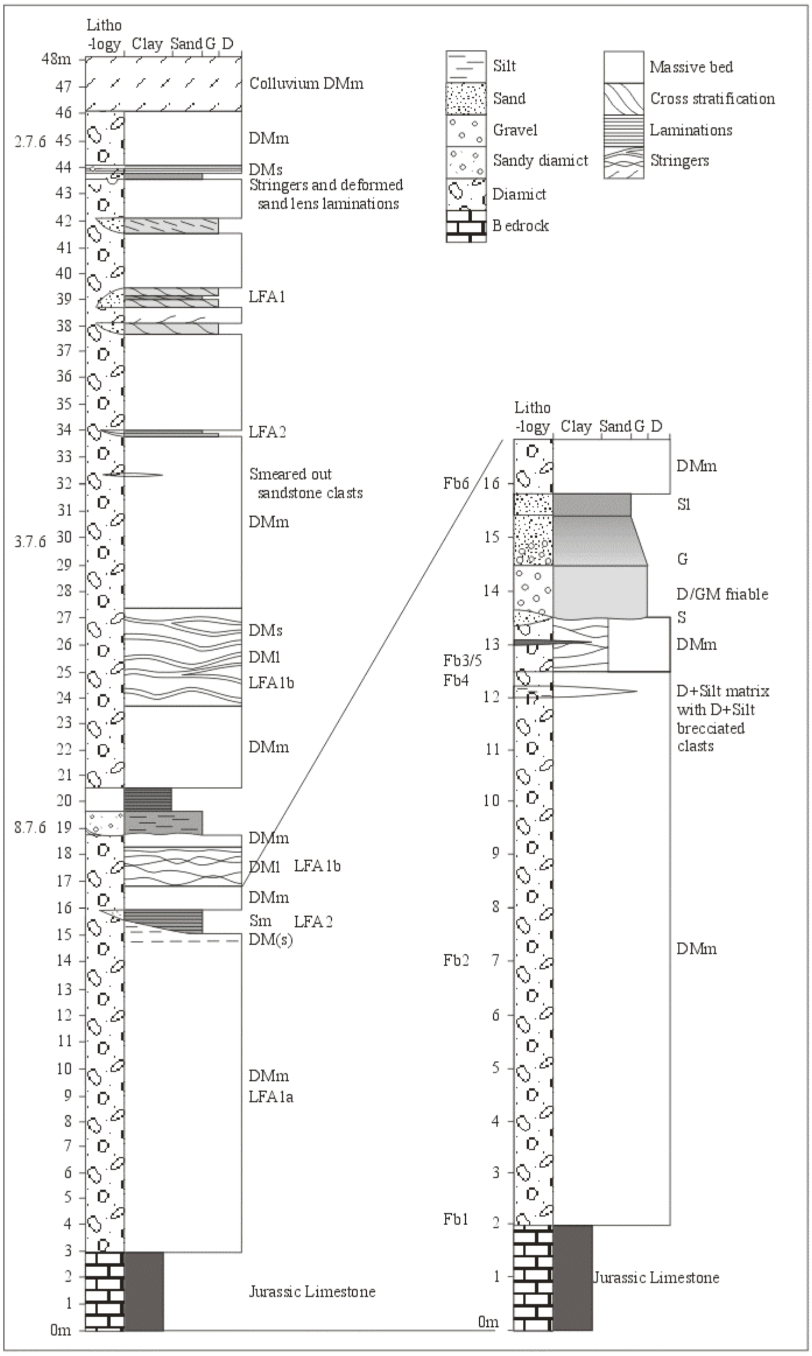

Figure 8.3 Sediment sequence at Filey Brigg, East Yorkshire coast. Compound sequence for the whole Brigg area from Evans et al., 1995, also showing the positions of their S.E.M.thin section samples 2.7.6, 3.7.6 and 8.7.6. Sequence on right is the stratigraphy at the sample site discussed in this chapter with heights of samples (Fb1 to 6) (after an original diagram by S.Church, 1996, unpub.).

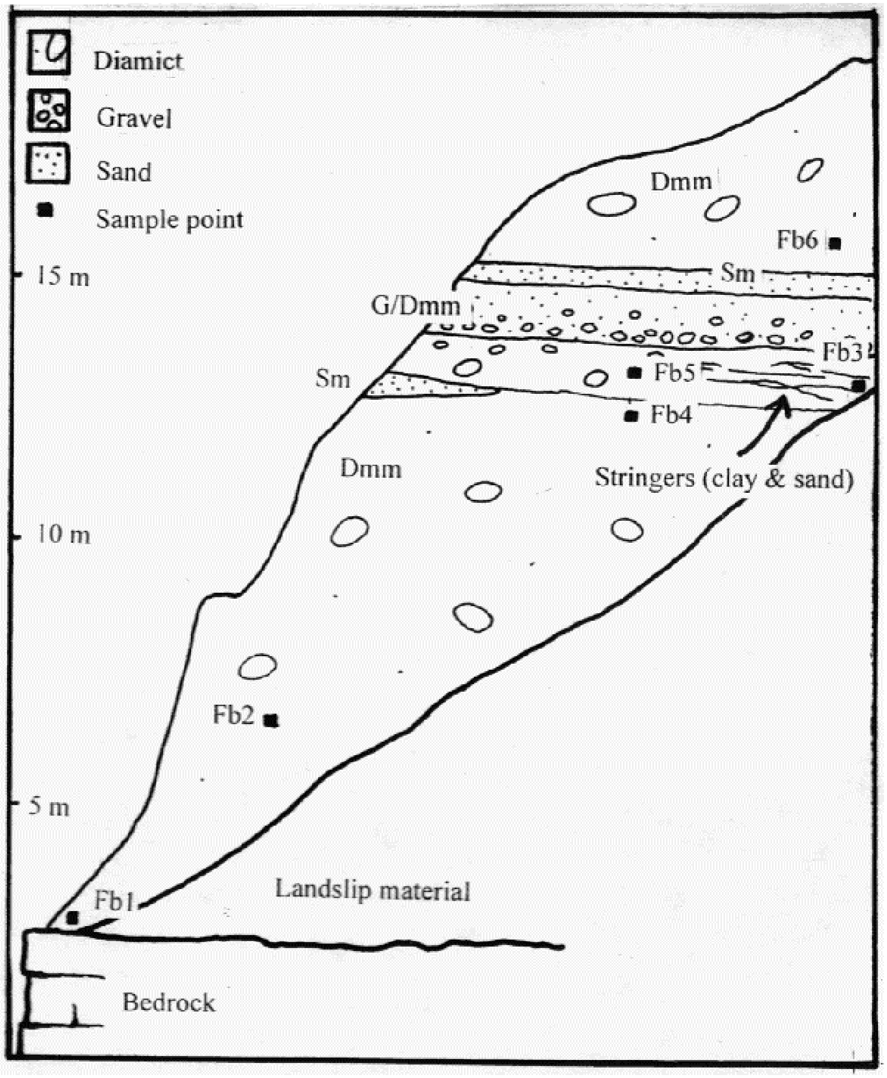

Figure 8.5 Sketch of the two dimensional form of the sampled sediments.

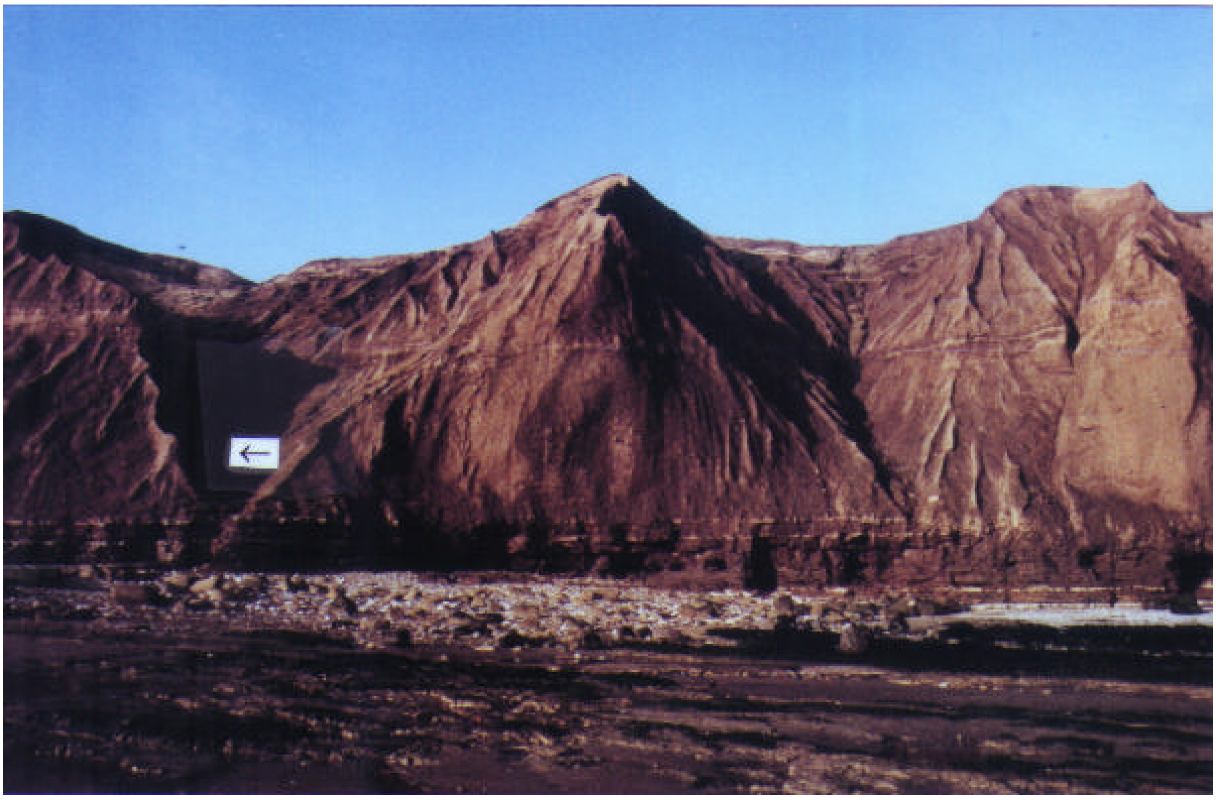

Figure 8.4 Photograph of Filey Brigg showing sampling site.

Evans *et al.* (1995) split the sequence into two alternating diamicts. The majority of the sequence is one massive diamict (lithofacies association 1a [LFA 1a]) (*Figure 8.3*) with an number of sub-angular clastic layers, smeared sandstone clasts, and a generally up-sequence coarsening of the particle size (Evans *et al.*, 1995). The S.E.M. revealed microstructure of the diamict as found by Evans *et al.* (1995) is of moderately aligned silts with occasional sand grains. In their sample 3.7.6 (*Figure 8.3*) the fabric is skelsepic around the sands and there is some silt bridging. There are also microshears (dipping west) and coarse grain silt areas. Their samples 8.7.6 and 2.7.6 are more strongly aligned, but again 8.7.6 has coarse silt patches with a lower alignment. Evans *et al.* (1995) suggest this is a deformation till showing a variable strain or rheological conditions.

The second till (LFA 1b) is split into two separate layers; one has laminae of clay which anastamose around diamict blocks. The S.E.M. revealed microstructure of the diamict again has areas of silts and sands, but with a highly varied grain size and alignment. They suggest this is a meltout till disrupted by high pressure fluids or differential strain. The other exposure of LFA 1b is of thin bands of diamict of various colours. They implicitly define this as having the same origin as the former exposure.

The upper level of diamict LFA 1a is bisected by sands. Evans *et al.* (1995) have suggested that these were deposited in subglacial 'canals' of the type outlined by Walder and Fowler (1994). 'Canals' are shallow, broad based, anastomosing streams with a bed of deforming sediment that is constantly inflowing and being removed. The alternative interpretation, that of Eyles *et al.* (1994), is that the sand bodies are proglacial and the diamicts subglacial, indicating oscillation of the ice front over the area.

8.3.2 Sampling

At the sampling location the fluvial events are represented by up to 4m of sediments. Several sand lenses, showing low strain, mark the base of a gravelly diamict. This diamict has a distinct boundary with gravels above which merge with laminated sands with height, above which diamict deposition is again resumed. It should be noted that sand lenses are not found lower in the sequence, and would, therefore, appear to be associated with the event ultimately responsible for the larger sand layer. Below the boundary with the gravelly diamict is a horizon of diamict which has, on one side of the exposure, layers of discontinuous and anastomosing clay (2 to 30 mm thick) and sands (~5 mm thick). Elsewhere on this horizon and below is homogeneous diamict.

The interdigitation of the sand stringers, sand lenses, clays, and diamicts points towards concurrent, very localised, formation within a single environment. This observation rules out the simple ice front oscillation over a sandur proposed by Eyles *et al.* (1994). Further evidence against Eyles *et al*.'s model as a general explanation for the sediments of the Yorkshire coast is given by Carruthers (1948) and Catt and Penny (1966), both of whom describe blocks of Withernsea Till within the sands and gravels of Kelsey Hill and Kirmington (*Figure 8.1b*). These sediments were regarded by Eyles *et al*. as those most likely to be 'proglacial' (ie. pre-Withernsea Till deposition). These blocks abut bedding in the water-lain deposits with little or no disruption, indicating syndepostion of the diamict and the sands/gravels. Thus, it is unlikely that the model of Eyles *et al.* is applicable as widely as they stated. However, there is an alternative proglacial explanation for the interdigitated sediments of Filey Brigg. As the sediments show only low to moderate strain, the diamict between must have suffered only moderate strain *after* their deposition (though the sediments may have been deposited into high strain material). The low strain indicates three possible depositional origins for the diamicts.

1) They are subglacial tills formed by deformation advection of material. The material may have been non-glacial, frozen or unfrozen, and was possibly partially decoupled from the ice in this area to give low strain. Any such lateral movement, however, would have to have been very low (metres on the basis of macroscale strain).
2) The diamicts are proglacial or subglacial diamicts reworked by mass movements, that is, they are 'flow tills'.
3) The diamicts are subglacial meltout tills, with the ice above moving or stagnant.

To resolve the problem diamict samples (*Figure 8.3* and *Figure 8.4*) were taken from;
1) in the diamict immediately above the laminated sands,
2) between the sand and clay bodies in the diamict below the sand lens horizon,
3) in the homogeneous diamict at the same height as '2',
4) immediately below sample '2' in the homogeneous diamict that extends to bedrock.

The main body of the diamict at Filey is homogeneous. When there is local evidence that deformation has occurred, such material is usually considered to have been mixed by infinite strain. The homogeneous material was sampled to examine this hypothesis.
The positions of the samples examined below are detailed on Figure 8.3. The samples were thin sectioned in north-south planes.

8.3.3 Results

The descriptions of the slides are given in Table 8.2, and this is directly followed by a summary. Descriptions are in terms of the general fabric of the diamict, and the fabrics in and around any inclusions such as clay bands or diamict pebbles. Skelsepic fabrics occur where matrix particles (F) and/or sand grains (G) are parallel to the edges of larger grains. Lattisepic fabrics are those where areas of fabric exist in two orthogonal directions, either pervasively or in a lattice of shear zones. An omnisepic fabric is where a large proportion of the sample has a single fabric direction. 'SDF area' refers to a Single Direction Fabric area. This is an area of material which has a consistent internal direction but is not large enough to qualify as omnisepic. Multiple SDF areas may be arranged in one or more directions or may be randomly aligned (RA). It is felt that the term 'domain' implies clays and a consistent sub-rectangular form. The term domain has also been applied to various sizes of fabric orientation, often under the impression it is unique to that scale. 'Bands' of material are taken to have a length to width ratio of greater than four; below this ratio, bodies are described as pebbles (distinct boundary with surrounding material) or patches (diffuse boundary). Other terms are defined in Chapter Two and the Glossary.

Shears and more pervasive fabrics are given in terms of their dip angle. Samples were cut in north-south and east-west planes so that shears and other fabric elements are given in terms of their dip angle downwards in a cardinal direction (N,S,E,W). The dip angles are means, often of very small populations. It is impossible to reliably assess the errors involved, however, the variation was $^{+}/_{-}$ 5° before the angles were taken to be different.

Position	Sample	General fabric	Inclusions
Diamict above the laminated sands.	Fb6a and b	Some Skelsepic (G+F) overprinting. Generally Omnisepic (a; 124° E, b; 115° N) , with occasional RA SDF areas. Both samples have intense SDF areas in the main fabric direction. Two shear sets in E-W sample (a) which developed synchronously. A major set at 124° E and another at 151° W. These cross the clay band.	7 clay rich bands through E - W sample (a) (low strained, 0.5 to 0.75mm thick in an area ~3mm thick). Strong fabrics in direction of sample fabric. 7+ Diamict pebbles (0.75 to 2mm) within these bands are skelsepic (F) near their clasts with RA SDF areas away from them. Some pebbles may be flow noses (often surrounded on only three sides by clays). 4 clay patches. 1 clay pebble.
Diamict at same level as clay/sand stringers.	Fb5a and b	(a) Some skelsepic (F+G) (2% of slide + overprinting). Non-organised (22%). Two sets of omnisepic fabric broadly split between the upper south half at 125°S (30%) and lower north (39%) which varies between 160°N and 160°S. (b) Skelsepic overprinting (G+F). Omnisepic at 130° E with intense SDF areas this direction.	(a) One clay band, originally omnisepic, now broken so that fabric in two halves at right angles. (0.5 x 0.5mm).
Diamict from within area of clay and sand stringers.	Fb3a and b	Some skelsepic overprinting (F+G). Patchy omnisepic fabrics. Sample (a) has intense SDF areas in the main fabric direction (113° E). In (b) the fabric is aligned with shears in the clay patches (150° S)	(b) 5 Clay patches + 3 pebbles and 5 clay bands (all 0.5 to 1mm long) with internal fabrics in the general fabric direction. One pebble with a skelsepic/RA SDF internal fabric. (a) 2 clay patches + 1 pebble. Internal fabric in general fabric direction.
Diamict from below the horizon containing clay and sand stringers.	Fb4a and b	Diamict patches of 3 types. 1) No clear fabric (a;13% of slide, b; 25%) 2) Skelsepic (G+F) (a;26%, b;17%) Both samples had intense SDF areas (0.1 to 0.6mm) in two direction. In (a) these were at 138° W (32%) and 128° E (29%). In (b) 100° S (28%) and 130°S (25%). Some evidence in (a) of slump noses covered in sand grains.	Numerous clay areas with single direction or RA SDF fabrics. 3 clay pebbles, 2 in (a) and 1 in (b) which contained a sand layer (all ~0.5 x 0.4mm). (a) 4 Clay bands (0.1mm thick, ~2.3mm long) finitely strained. These are associated with patches (layers?) of fine grained sand (0.5mm thick) with a horizontal fabric prior to straining. (a) Two shear sets in the clays at 138° W and 128° E. These developed synchronously and are in direction of local clay fabrics.
5m above rock bed	Fb2 a and b	Some skelsepic (F+G) round clasts. Largely structureless but with faint traces of SDF areas (too faint to gain directions).	
Just above limestone / sandstone	Fb1a and b	Small amount of skelsepic (F+G) behaviour. Structureless with no preferred orientation, though some faint RA SDF areas in (b) - (a) is too thick to tell. Matrix supported, but many clasts.	2 Clay inlyers (3 and 1.5mm) with sharp boundaries and fabrics of RA SDF areas. Long axis of few clasts in clays align parallel to walls.

Table 8.2 Summary of the micromorphology of samples taken from the sediments at Filey Brigg, East Yorkshire. The table is arranged such that the samples are in their stratigraphic position. The samples from the base of the sequence are lowest in the table.

Samples Fb4a/Fb6a (the diamict at 12.3 m and the diamict at 16 m, *Figure 8.3*) show small numbers of rhythmic alterations between of sandy layers and clay bands within the generally silt-clay matrix. Some of these alterations have the form of small clay slurry flows into the sandy material. Fb6a contains diamict pebbles with skelsepic fabrics within the clay bands, however there is no evidence of such features in the surrounding matrix. Along with these clay bands and others (width to length ratio of >4) the samples from higher than 12 m contain numerous clay pebbles (defined as having distinct borders) and patches (diffuse borders).

Samples from the homogeneous diamict at 5 m above the bedrock (Fb4a/b) have a skelsepic fabric, with no clay patches. Higher diamicts (12.3 m plus) have some skelsepic fabric, but this is not the dominant fabric. The external form of the clay areas in these higher diamicts indicate low strain deformation that varies across single samples, however, this low strain deformation has been overprinted by a more pervasive fabric which has aligned the internal fabric of the clay areas. This overprinting is strongest above the main sand body (ie., above 15.75 m, Fb6a/b) where it produces an omnisepic fabric. Below the main sands (ie., below 13.5 m) the fabrics are more varied within the slides, however, there are local fabrics in the same direction as the strong omnisepic fabric above 15.75 m. There is only one sample above 12 m that has no overprinted in its clay areas, and that is sample Fb5a.

Close to the bedrock (Fb1a/b) the skelsepic fabric of the material 5 m higher is replaced by a more random fabric with clay rich areas.

8.3.4 Interpretation

The fluvial deposits and surrounding diamicts

It has been shown above that, because of the interdigitation of the sands and diamicts, the only proglacial features that could explain the Filey deposits are flow tills. All the samples from around the laminated sands (Fb4a/b upwards) contain microscopic scale clay bodies that have suffered low strain deformation (*Figure 8.6*). These clay bands indicate either;

1) low strain reworking of local clay deposits (compatible with a subareal flow till);

2) the washing in of clay material by fluid moving through the sediment;

3) a meltout origin for the clay and maybe the diamict, possibly involving particle sorting.

None of the materials match the more heterogeneous sediment and porous character attributed to flow tills by Owen and Derbyshire (1988) and van der Meer (1993). In addition to this fact, there are no extensive unimodal clay bodies to rework in this part of the sequence, making a flow till origin for the clays unlikely. This dismissal is backed up by the similarity of the diamict fabric between the sand lenses and that in the *massive* diamict above the main sand body, which is probably too thick and homogeneous to be a subaerial flow till, and the wide variation

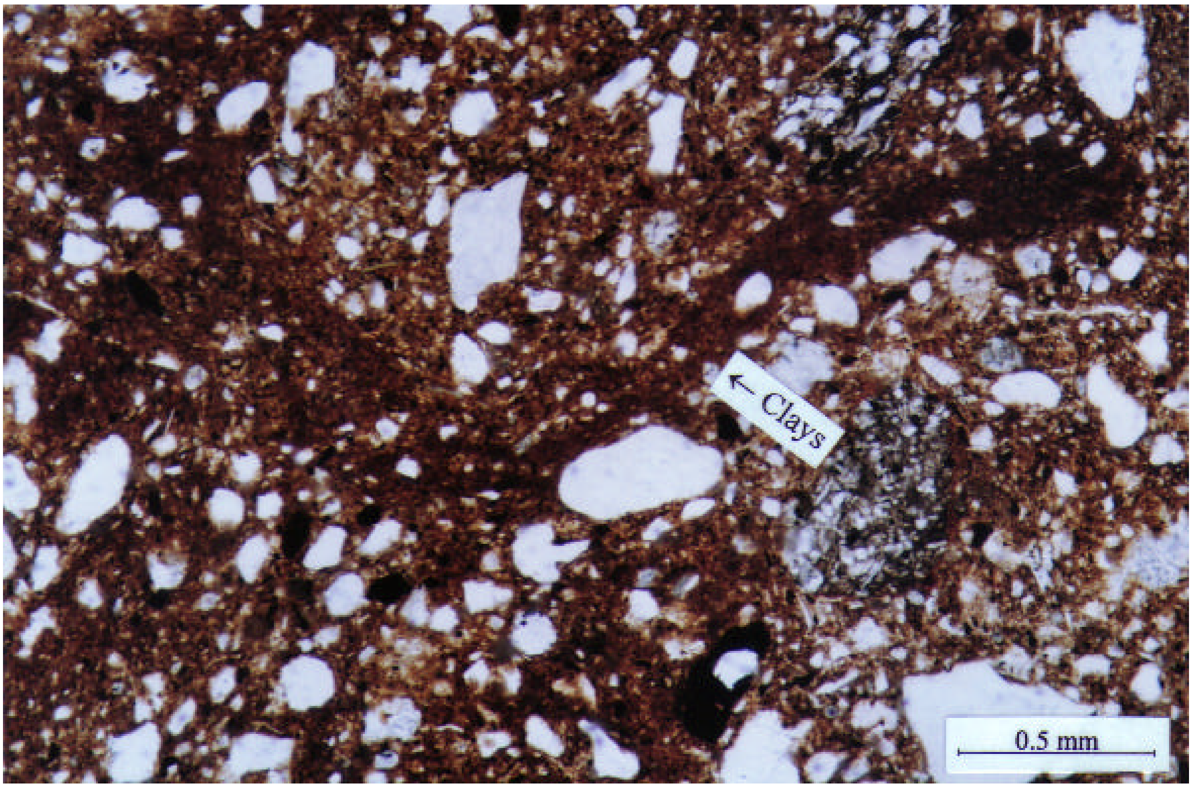

Figure 8.6 Photomicrograph of a clay body from sample Fb6a showing low strain deformation. Unpolarized light conditions.

in strain seen on a sub-millimetre scale in the slides, which may dictate against flow in a single body. When combined, these four lines of evidence place serious doubt on the proposed proglacial origin for the sands (Eyles *et al.*, 1994) by suggesting the intimately interbedded diamicts and clays are not proglacially reworked.

The rhythmite or microscale mass movement nature of the clays in sample Fb4a/Fb6a precludes the internal translocation cause for the clays. In addition to this suggestion, there are none of the more certain fluid through-flow features which might be expected, such as areas of more porous material (see Chapter Two). These facts suggest internal translocation reworking of the diamict is not responsible for the clays. However, the diamict pebbles in the clay band of Fb6a has the same fabric (skelsepic and randomly aligned patches) as the main diamict body deeper in the sequence (samples Fb2a and b). This may indicate the main diamict body *has* been reworked by water in some manner to produce the clays.

It seems highly unlikely that the clays could have been deposited by melt or water into a diamict forming by reworking of other local deposits, and suffer only low strain at this scale. This may suggest that *both* the diamict and clays melted out of the ice. The meltout origin hypothesis implies heterogeneous material is being supplied (diamict and unimodal clays) and cannot, alone, explain the diamict pebble in the clays of sample Fb6a. However, a meltout origin for the diamict, with small ice-sediment interface streams (microscale) producing the clays, explains the material without contradictions. It is worth noting that such a model does not assign any ultimate origin to the diamict, simply that this area was one of melt-off of the material from the base of the ice.

Meltout into a ephemeral subglacial stream environment explains all the features of the sediments. The presence of diamict pebbles in the clays of sample Fb6a but not the surrounding diamict shows that the conditions of clay deposition were different from those of the surrounding diamict and involved reworking. The possible sand-clay couplets seen in samples Fb4a/Fb6a may suggest a rhythmic depositional environment. This could be a subaerial lake, however, a subglacial possibility also exists in the form of subglacial cavity ponds (Van der Meer, 1987b; Owen and Derbyshire, 1988), activated repeatedly and flooded with new sediment. There is also some evidence of small scale material slumping in slide Fb4a and Fb6a (*Figure 8.7*), which would not be expected in material formed by the deformation of other beds or the deposition of large scale proglacial flow tills.

Such a model of mixed meltout and overflow matches the clay rich, laminated, sediments of LFA 1b (Evans *et al.*, 1995), which, in this model, can be seen to be of the same environment as LFA 1a, but possibly with a greater melt rate producing greater overflow activity and/or less subsequent deformation. Alternatively, the deposits of LFA 1b may represent the same melt rate as LFA 1a, with less diamict being produced because the ice had less sediment in it per unit of meltwater produced. As the area of diamict showing macroscale clay and sand stringers would appear to be at the transition between LFA1a and LFA1b, if not fully part of LFA1b, we can investigate the strain and melt/ice-sediment difference between the two LFAs in a quantitative manner.

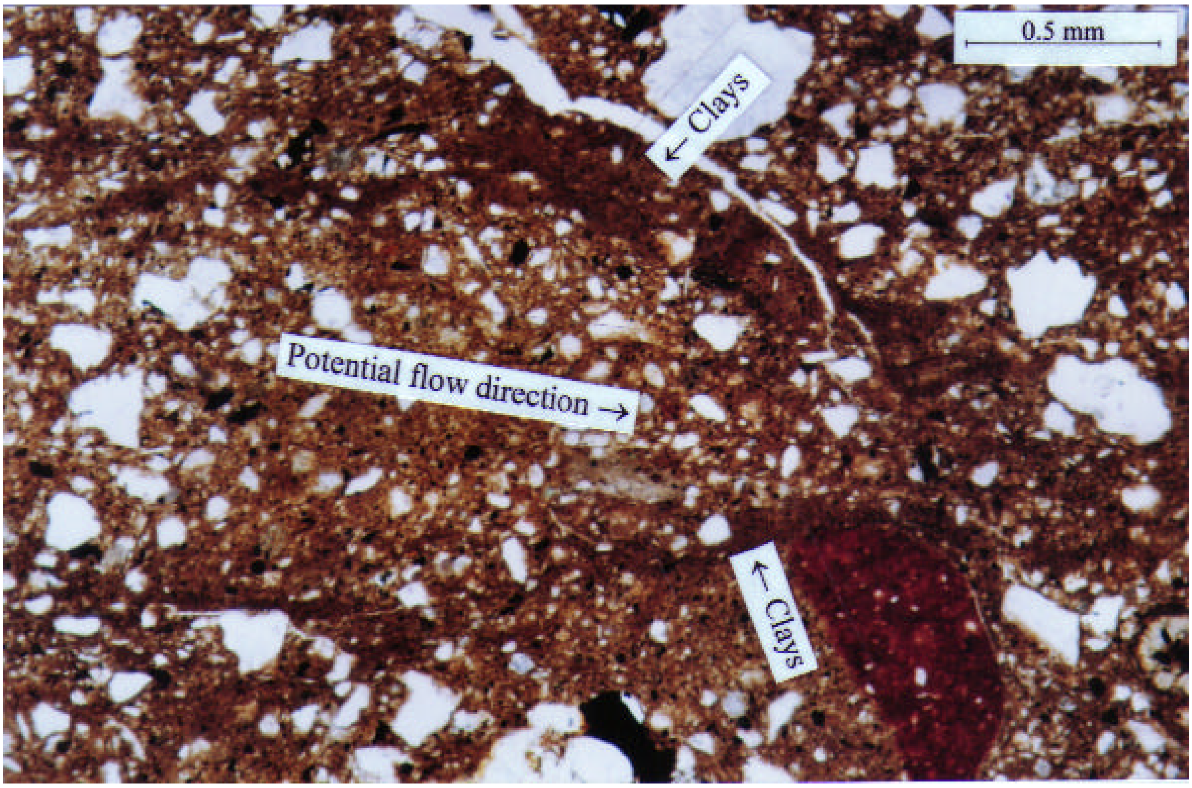

Figure 8.7 Potential small scale 'mass movement' deposit. Note how the clays are folded around an area that might have 'flowed' into them in a semi-coherent mass. Sample Fb6a, unpolarized light conditions.

A greater strain *or* a melt/ice-sediment variation may be causing the absolute difference in the number of clay areas between the two LFAs. However, the meltout variation can be normalised for, if we assume that the clay bands are formed by meltout and that, with strain, the bands break up into pebbles (with a distinct boundary with the diamict) and patches (with a diffuse boundary). Making these assumptions we can give an estimation of bulk strain without any dependence on the meltout. This is achieved by normalising the number of such pebbles and patches using the number of bands, to give a 'disruption value' representing the strain. These values are given in Table 8.3.

Sample area	Patches with graded boundaries with diamict	Pebbles - distinct boundaries with diamict	Bands - length to width ratio > 4:1	Disruption value
Diamict above sands	4	1	7	0.71
Diamict with stringers	7	4	5	2.20
Homogeneous diamict at the same height as diamict with stringers	0	0	1	1
Diamict below stringer level	3	0	4	0.75

Table 8.3 Clay body distribution in the uppermost samples taken at Filey Brigg. The table does not include patches of clay around large clasts, which may be concentrated during deformation (see Chapter Seven).

Thus, there is evidence (although the population sizes necessarily make this weak) that the diamict with the stringers has suffered the greatest strain during deposition, indicating that the greater presence of clay features within it may have been due to a melt and/or ice-sediment variation. Unfortunately the number of clay features in the diamict at the same level as that with the stringers is too small to justify any comparison between the two, which were presumably deposited synchronously.

There is no evidence as to the geometry of the 'microstreams' which deposited the clays, or why they formed. They may, for example, be part of an extensive ice-sediment interface water layer. However, it may be hypothesised that such water bodies will form when the melt rate is faster than the drainage into the sediment, in line with the development of larger (sand carrying) streams. This drainage will largely be controlled by the diffusivity of the diamict and the pressure-flux relationship in surrounding channels. While the largest sand bodies are at the top of one of the diamicts in question, the 'microstreams' were probably active as diamict was deposited near this upper boundary, and smaller sand bodies exist within the diamict.

The combination of the ice-interface water layer and larger streams indicates that the larger streams did not rapidly draw fluid from the surrounding ice-sediment interface. This suggests that the streams were at atmospheric pressure or had a *positive* hydraulic pressure to discharge relationship. In the case of a *negative* pressure-flux relationship large streams have a lower pressure than small ice-interface fluid layers, and rapidly draw water from them (Weertman, 1972). A positive pressure-flux relationship is one of the unusual features of Walder-Fowler canals (Walder and Fowler, 1994), and this evidence goes some way to confirming their calculations for soft bedded channels and Evans *et al.*'s (1995) interpretation of the sediments at Filey. However, the caveat must be given that the ice-bed boundary is not the ideal often envisaged in hydraulic models, and the above deposits may be possible under other water systems.

The appearance of these materials in the sequence may suggest a progressive rise in fluid availability. The final products of this increase may have been the gravelly diamict, which under this model would be left by winnowing of the diamict during or after deposition, and the laminated sands. An increase in fluid with height in this area matches Evans *et al's*. (1995) discovery that the sequence slightly coarsens upwards. There are two possible explanations for this increased fluid; an increase in melt rate or the increased amount of impermeable material between any given horizon and the potentially permeable limestone at the base of the sequence.

Deformation after deposition

As noted above, the clay bands in the sediments near the sand bodies have suffered low strain deformation. This strain varies within each slide, indicating the deformation is unlikely to have been synchronous across the whole slide. This should be contrasted with the strong omnisepic deformational fabric which cuts across the highest slides (Fb6a and b), including the internal clay bands (*Figure 8.8*), indicating post-depositional deformation has occurred overprinting the whole sample at once. The strength of this fabric suggests the overprinting occurred subglacially.

This omnisepic fabric contrasts with the skelsepic nature of the main diamict body further from the sand bodies (samples Fb2a/b). As expected with such overprinting, the samples between these two heights in the sequence (samples Fb5a/b and Fb4a/b) are semi-skelsepic and semisheared in the same directions. The samples from below the sand lens horizon (Fb4a/b) also show overprinting of clay bands. The fact that the overprinting spans the sand bodies suggests it occurred after their deposition (*Figure 8.8*). Thus, it seems likely that the low strain deformation occurred approximately synchronously with deposition of the material, whereas the omnisepic overprinting may have occurred after the sands were deposited.

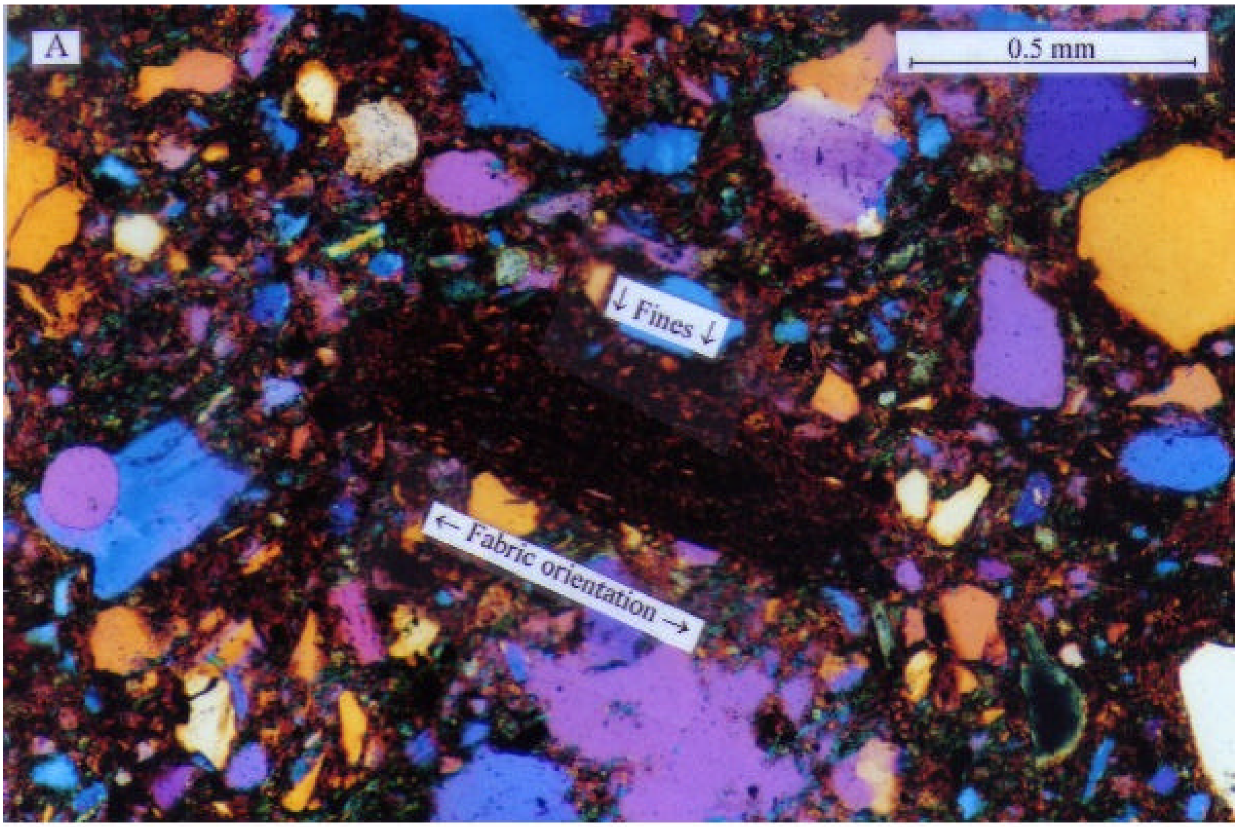

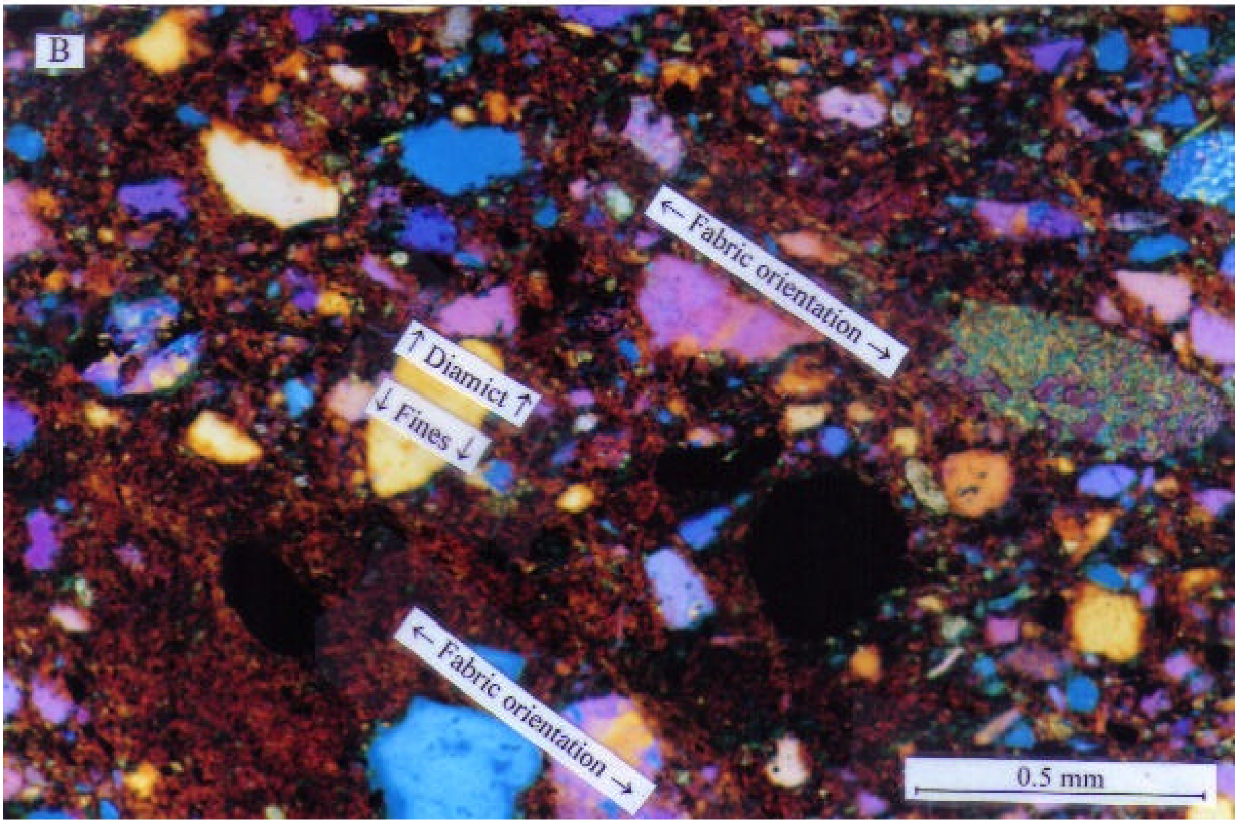

Figure 8.8 Photomicrographs of clay bands showing overprinting. a) Sample Fb6a. b) Sample Fb4a. Picture taken under cross polarized light with a tint plate.

While the strong fabrics of the samples suggest subglacial deformation, the overall strain as suggested by the clay bodies, is low. The ice depositing these sediments extended at least as far as a morainic system on the Speeton Hills (*Figure 8.1*), suggesting the materials underneath should exhibit high strain if well-coupled to the ice base. The low strain of the sand lenses and clays therefore indicates a rapidly rising deformation layer of low strain, or only low coupling between the ice and sediment. Three factors may have contributed to these situations;

1) drainage stiffening of the sediment, and the resultant enhansed regelation which will have lead to meltout deposition (though there was not enough drainage to initiate discrete shear);
2) a high melt rate (note the unusually large (> 50 m) amount of material deposited in this area over 4 ka (see Chapter Six for dating details);
3) the separation of the ice from the sediment, as implied by the clay bearing micro-streams suggested above (probably incompatible with the regelation deposition in '1', above).

In the case of the latter hypothesis, clay bands and patches may give a semi-quantitative estimate of the separation of the ice and sediment where low strain conditions can be quantified through the whole sequence.

The triaxial tests outlined in Chapter Six showed that, under the test conditions, diamicts supported higher stresses than those usually associated with unimodal clays. If the unimodal clays seen here had a different strength from the diamict they may have protected diamict pebbles within them, for example, in the diamict above the sands (Fb6a) where skelsepic diamict pebbles within some of the clays have not been overprinted (*Table 8.2*).

The overprinting of the samples after the deposition of the sands appears to have affected all but one omnisepic clay area. The single clay area in the homogeneous diamict at the same level as the diamict with the macroscale sand and clay stringers (sample Fb5a) does not show omnisepic overprinting in the same direction as the diamict in the slide (*Figure 8.9*). This difference could be due to variations in the resistance of the material to realignment (see intense patches described in the triaxial sediments, Chapter Seven). However, there is another, less probabilistic, explanation.

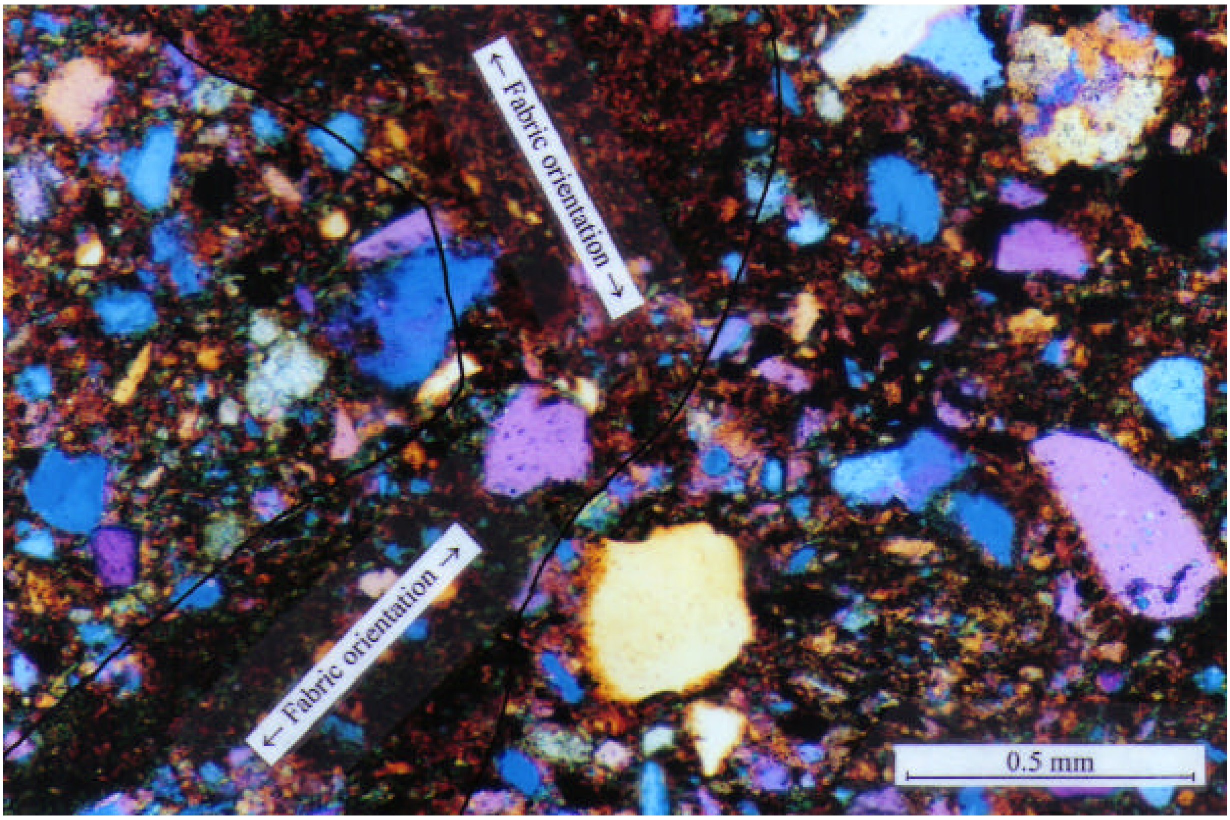

Figure 8.9 Photomicrograph of clay band from sample Fb5a. Note that the internal fabric of the clay has not been overprinted after the band's deformation.

A model explaining the microstructural variation can be developed based on the relative strengths of the sediments at different effective pressures. The strength of sediments is reasonably well modelled using the Mohr-Coulomb equation (*Equation 3.1*), which gives strength as a function of a constant cohesion and a pressure dependent internal friction term. Generally clays have a high cohesivity but do not gain strength rapidly with increased effective pressures because of their small angle of internal friction. At Filey, however, the diamict contains silts, sands, and larger clasts, and will probably have a lower cohesivity and a higher angle of internal friction. As can be seen from Figure 8.10, because of these differences, there may be a point at low effective pressures where clays will be stronger than diamicts.

The micromorphology of the samples suggests the combination of shear stress and effective pressures moved from conditions where all the material was deforming to give an omnisepic fabric, to a situation where, in the material with the inconsistent clay fabric, only the diamict was deforming internally. The two stress paths that could have produced this situation are given in Figure 8.10. It should be noted that a shear stress variation between the two sample points is unlikely on this scale (Kamb and Echelmeyer, 1986), and we would expect all the material to suffer the same stress changes. Therefore, the difference in behaviour is attributed in these models to the material with the inconsistent fabric having a higher effective pressure than elsewhere. This suggests a drainage potential variation in the sediment on a scale of metres.

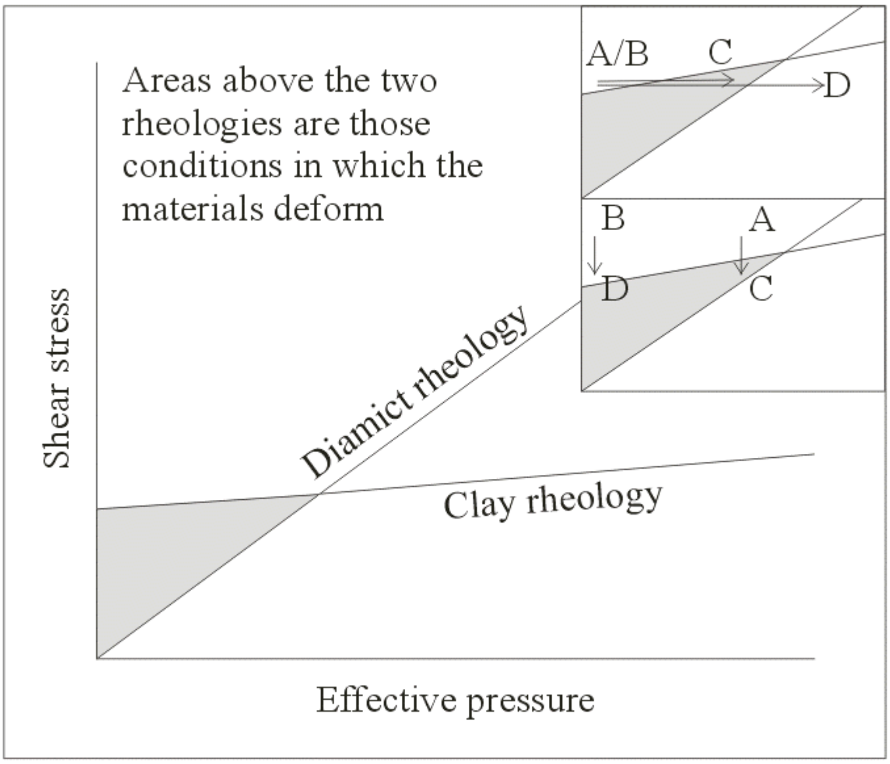

Figure 8.10 Hypothetical shear stress - effective pressure paths accounting for the microstructures observed in the upper part of the sequence at Filey Brigg, East Yorkshire coast. Main diagram shows the suggested rheologies of the material. The inset diagrams are paths which may have produced the strain evidence presented in the text. A and B are the starting conditions for the material with the inconsistent fabric and elsewhere respectively. C and D are their respective final conditions.

The homogeneous diamict

The main body of the Skipsea Till is skelsepic (Fb2a/b, at 7m in Figure 8.3). In three dimensions this probably accounts for the randomly orientated patches of fabric seen in two dimensions. Comparison with the low grade deformation fabrics in rhythmites at Dimlington (below) suggest that the skelsepic fabric is produced by strains of greater than 2%. We cannot say that the strain here was too low for an omnisepic fabric to develop as the development of an omnisepic fabric might be controlled by clast density and/or ice thermal regime. The absence of clay patches in these sections may be due to a lower melt rate than that discussed above or greater ice coupling. A lower meltout rate reduces the rate at which the deforming layer rises, and any given horizon will suffer greater strain. On the basis of the triaxial test samples (Chapter Seven) the strain would probably have had to be greater than 25% to remove the clays if present.

The more random fabric of the till close to the bedrock (Fb1a/b) cannot be attributed to any specific cause (contrast with the fabrics at Dimlington, below). However, given the presence of clay patches here, their absence in the homogeneous area of the till body (Fb2a/b), and the discussion above on the nature of the sediments at the top of the sequence, it might be suggested that this material is undeformed meltout material that has been protected by the irregularity of the bedrock surface and/or drainage into the potentially permeable bed.

Summary: The clay bands in the sediment indicate its origins. Flow tills are dismissed as the micromorphology is dissimilar to other flow tills, there are no clay bodies in the area to rework, and the fabrics are continuous across macroscale units that show no flow till bedding. The interdigitation of sands, clays, and diamicts on two different scales suggests the diamicts have not been deposited over proglacial water lain deposits in the simple manner suggested by Eyles *et al.* (1994), though this cannot be refuted absolutely for the large laminated sand body at this site. The rhythmic nature of some of the clay bands dictates against the deposition of the clays within the diamicts by translocation. A model of diamict meltout into an environment of intermittently active micro-streams that rework older diamict into clay rich units seems to explain the sediments without contradiction. This situation matches the discharge-pressure relationships suggested for canals by Walder and Fowler (1994). These clays suffered syndepositional deformation, shown by variable strains within each slide. This material was then overprinted with an omnisepic fabric after the deposition of the sands. Earlier sediments were probably initially protected from deformation by bedrock irregularities or drainage into the bedrock, however, in the middle of the sequence the absence of clay bands seen at the top and base of the sequence suggests higher strain.

8.4 Dimlington

8.4.1 Introduction

Samples were taken from the coastal cliff at Dimlington High Land (TA 390218, *Figure 8.1b*). The sedimentology, petrology and structure of the area has been studied by Catt and Penny (1966), Madgett and Catt (1978), and Eyles *et al.* (1994). Sampling was carried out to reveal the processes at work in the advance (Madgett and Catt, 1978) or readvance (Eyles *et al.*, 1994) of ice over the area.

The lowest material exposed in the sequence at Dimlington (*Figure 8.11*) is the 'Basement Till' which rests on a marine platform at approximately -34m O.D. (Catt and Digby, 1988). This diamict is overlain by the 'Dimlington Silts'; organic, rhythmic, freshwater deposits (*Figure 8.11*). This boundary was sampled with the hope of deriving information on the nature of high strain till fabrics through comparison with the low strain silts. The upper part of the Basement Till and the remnants of the silts have been gently folded into basins by the ice depositing the overlying Skipsea Till. The Skipsea Till truncates the silts. The geometry of the basins suggest that the ice moved from the north east (Madgett and Catt, 1978).

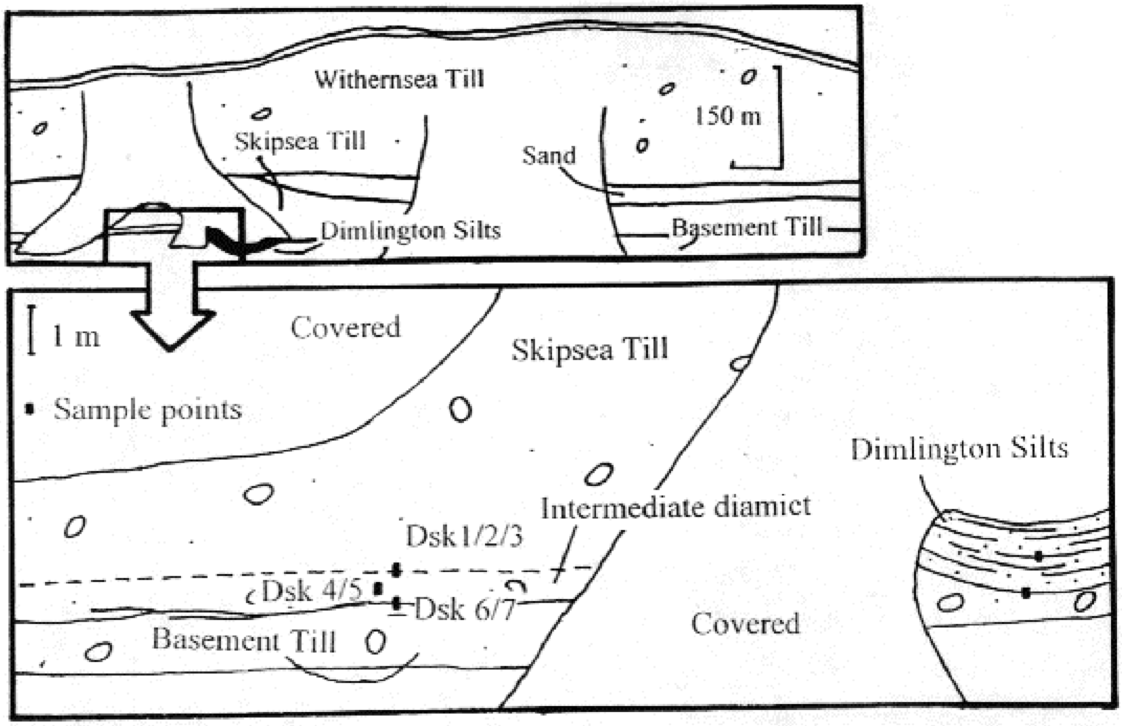

Figure 8.11 Sediment sequence at Dimlington High Ground, East Yorkshire coast. Inset shows the position of the sample site at the scale of Catt and Penny's (1966) survey of the area (though note that the area's structure has changed because of coastal retreat).

The silts have been seen picked up into the lower Skipsea Till (Eyles *et al.*, 1994), however the top of the silts presently exposed at Dimlington is obscured by landslide material, therefore it was not possible to sample this boundary. However, samples *were* taken from where the Basement Till and higher diamict are in direct contact (*Figure 8.11* and *Figure 8.12*). At these places the Basement Till has a sharp contact with the higher diamict. In areas the boundary is formed of thin (mm) resistant layers, continuous on the order of metres, with slightly undulating lengths (m wavelengths, mm amplitudes), and *en échelon* areas of greater resistance within them. Such forms are often described as 'shear zones' by researchers. There has been no micromorphological work to confirm that such features are formed by shear.

Above these so-called 'shear zones' at Dimlington, there is a 1m thick layer of diamict intermediate in colour to the two main tills, but also similar in colour to the Dimlington Silts; the stratigraphic position of which it occupies (*Figure 8.12*). This material has a sharp boundary with the overlying 'true' Skipsea Till, and the boundary does not appear to have a 'shear' morphology. This material is regarded as a sub-unit of the Skipsea Till and will be referred to as the 'intermediate diamict' in the discussion below, thereby distinguishing it from the main body of the Skipsea Till. The Skipsea Till is broken up by Eyles *et al.* (1994) into numerous such sub-units, which they suggest are deformed blocks of older material. They either imply that grouped together, such sub-units represent a recession-transgression cycle of ice movement, or that each unit is itself representative of such a cycle. Which they are suggesting is not clear from their discussion as it implies all sands with undeformed bedding may be proglacial, and that such sands form sub-units within the Skipsea Till, while suggesting the Skipsea Till as a whole is the product of a single cycle. Samples were taken from the boundaries between the Basement Till, the intermediate sub-unit and the main body of the Skipsea Till, as well as from the body of the sub-unit and the main body of the Skipsea Till.

Figure 8.12 Photograph of the sediments sampled at the boundary between the Skipsea Till and the Basement Till at Dimlington High Ground, East Yorkshire coast. Open ended sample boxes are in the approximate sample positions.

8.4.2 Results

The descriptions of the slides are given in Table 8.4 in terms of the general fabric of the diamict and the external and internal fabrics associated with any inclusions such as clay bands or diamict pebbles. The nomenclature used is that of Table 8.2. Shears and more pervasive fabrics are given in terms of their dip angle downwards in a cardinal direction (N,S,E,W). Samples were cut in north-south and east-west planes. Other terms are defined in Chapter Two and the Glossary. A summary of the chief results is given after the table.

Position	Samples	Fabric	Inclusions
Skipsea Till just above boundary with intermediate diamict	Dsk1	Some grain skelsepic behaviour. Largely a faint ($CaCO_3$ stained?) omnisepic fabric (140° W but variable).	
Intermediate diamict - Skipsea Till boundary	Dsk2 / 3	Broadly omnisepic fabric (2; 117° E, 3; 96° N but variable outside intense patches in latter) over... An area (5mm thick) of clay bands (0.5mm max. thickness) over... A coarser material with a fabric of RA SDF areas, these areas possibly have a modal direction in Dsk2 (*Figure 8.13*).	Band of clays with a faint horizontal fabric (also in patches of diamict between bands) disturbed in areas by a finite strain of < 5%. Sharpness of boundary is independent of strain local to it.
Intermediate diamict between Basement Till and Skipsea Till	Dsk4 and 5	(5) Some skelsepic (F) on the order of 2-3 grains around some clasts. One wide clay rind found around a large clast. Strong omnisepic fabric (85° S). (4) Fabric in two directions (130° W / 160° E - latter more widespread) Both slides have intense SDF areas in the prominent fabric direction.	
Boundary between basement Till and intermediate diamict.	Dsk6 and 7	Diamict with an omnisepic fabric (6;106° S) over... Diamict with fabric of SDF areas (~5mm) over... A 16mm layer of sand / matrix with a skelsepic fabric. The upper boundary of this is sharp in one sample and diffuse in the other. The sandy material is almost clast supported. The lower boundary of this sandy horizon is sharp. This is over... Basement Till with SDF areas in two directions and cracking (6; 180° NS / 92° S, 7; 106° W / 140° E).	The sand/matrix layer contains lenses of clean sand in the E-W plain (horizontal 6.4 x 1mm and 3 x 0.31mm). The Basement Till has shears in both the directions of the fabric patches. These end at the sharp but irregular boundary with the sands where they hit grains. A mature, discrete, shear (‘A’) is found just below the boundary where development of such a feature could first have formed without interference from the irregular boundary.
Dimlington silts	Ds1 and 2	Couplets of sands/matrix and silts/clays. Strong horizontal fabric. Two shear sets (1; 133°S and 164°N, 2; 150°W and 120°E). Lattisepic fabric around sand grains.	Some sand layers contain diamict pebbles.
Boundary between silts and Basement Till	Ds8, 9 and 10	Sand/matrix (~0.5mm) and clay/silt (~0.15mm) couplets over a thick clay layer. All have strong horizontal fabric and one shear set (9; 130°W, 10; 167°W, 8; none). These are over... A 10mm layer of mixed diamict pebbles, diamict and sand with sand layers over... Diamict.	The upper Basement Till is exclusively diamict pebbles, but these merge with depth to form a matrix with pebbles in it. These finally disappear at the base.

Table 8.4 Summary of the micromorphology of samples taken from the sediments at Dimlington High Ground, East Yorkshire coast. The table is arranged such that the samples are in their stratigraphic position. The samples from the base of the sequence are lowest in the table

The Skipsea Till (sample Dsk1) shows an off-horizontal omnisepic and skelsepic fabric. Its boundary with the underlying Intermediate diamict (Dsk2/3) is marked by a series of slightly buckled clay and diamict bands with a faint horizontal fabric. Under these bands the diamict becomes coarser, with a fabric in numerous directions, possibly with two modal off-horizontal angles (*Figure 8.13*). Further away from this boundary (Dsk4/5) the fabric of the Intermediate diamict gains a strong horizontal alignment in the north-south plane, and this fabric is seen to be comprised of two high angle fabric directions when sectioned east-west.

The boundary between the Intermediate diamict and the underlying Basement Till (Dsk6/7) is marked by a sand rich layer which is almost sand grain supported. The sand layer has diffuse and sharp boundaries with the Intermediate diamict (which has a more random fabric at the boundary) and a sharp boundary with the lower Basement Till. The layer contains lenses of clean sand with no matrix. Below this layer the Basement Till includes a mature, discrete shear (denoted as shear ‘A’ below) which is continuous across the sample, and which has developed in the highest area that such a shear could form without interference from sand grains. The Basement Till also shows less well developed shears in at least two directions in both thin section planes. There are also broader fabric patches in both shear directions in each thin section plane.

Thin sections from the Dimlington Silts (Ds1 and 2), show them to be composed of rhythmic couplets of clay with silts and sand with silts, each with a strong horizontal fabric. The clay-silt layers have shears in two high angle directions, which become more pervasively lattisepic in the sandy layers. The boundary between the Dimlington Silts and the underlying Basement Till (Ds8, 9 and 10) is marked by a 10 mm layer of mixed diamict pebbles and sand rich layers, which coalesce into diamict with depth.

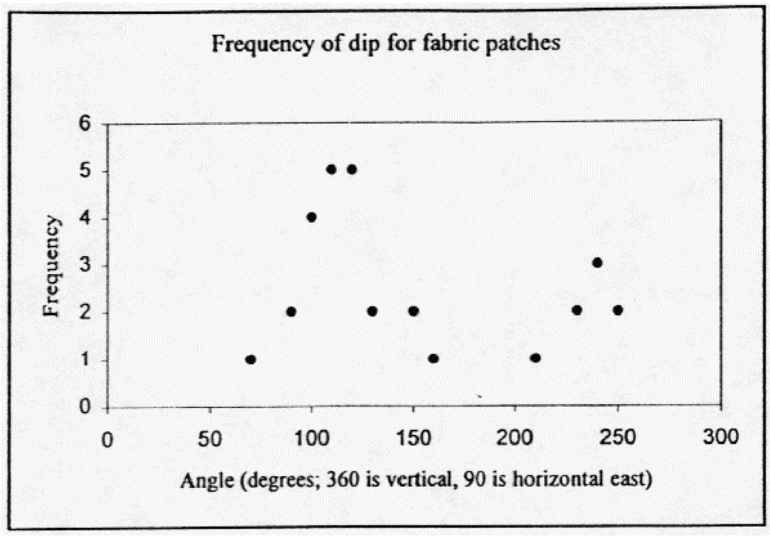

Figure 8.13 Frequency of dip angles found in Dsk2. This slide contained the only SDF orientation for which there was uncertainty as to whether the fabric was aligned or random on the basis of a visual interpretation of frequency data. The fabrics appear to be in two directions, however, the fabrics are random in the north-south plain as seen in Dsk3. This figure is referred to within Table 8.4.

8.4.3 Interpretation

The boundary between the Basement Till and intermediate diamict

The material at the boundary between the Basement Till and the intermediate diamict (Dsk6/7) progresses up from the Basement Till, through a very sand rich diamict layer containing clean sand lenses (*Figure 8.14*), to a zone of intermediate diamict with disturbed fabric, and finally, to omnisepic intermediate diamict. The Basement Till has a complex fabric, which may be a result of overprinting in front of, and under, the ice depositing the Skipsea Till (see Filey Brigg, above). Table 8.5 outlines the shear fabric change through the whole sequence.

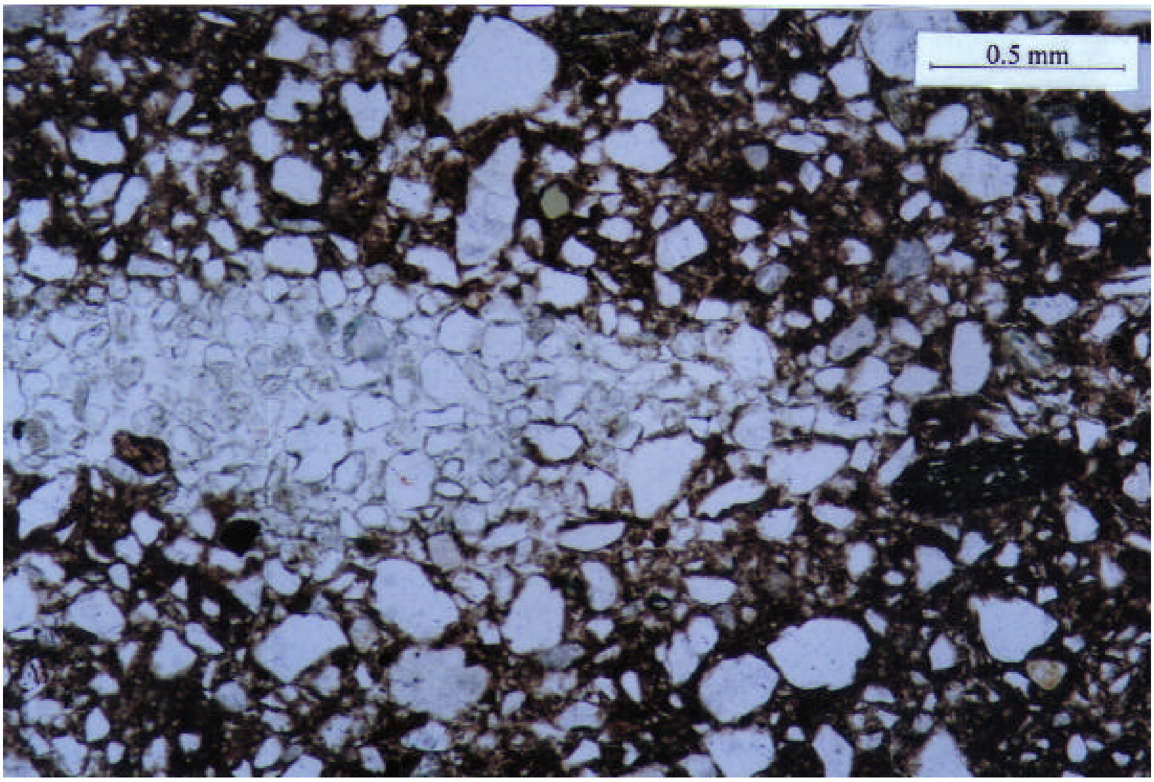

Figure 8.14 Photomicrograph of clean sand lenses in sample Dsk7. Unpolarized light conditions.

Sample	**East-west plane**	**North-south plane**
Skipsea Till above intermediate diamict	117°E	
Intermediate diamict	130°W 160°E	~ 90°
Dimlington Silts	150°W 120°E	133°S 164°N
Dimlington Silts near Basement Till	167°W 130°W	
Basement Till under intermediate diamict	106°W 140°E	~90° 180°
Basement Till under Dimlington Silts	157°W 147°E	Sample too shallow to see unpebbled fabric

Table 8.5 Shear fabrics measured in the thin sections from Dimlington High Ground (in order of height in the sequence, top down).

This gives contradictory evidence for and against overprinting, and without a greater understanding of the different rheologies it will be impossible to decide the matter. That some overprinting has occurred is indicated by the presence of a well developed single shear 'A' at the top of the Basement (*Figure 8.15*). This formed by avoiding the sand rich material where such material encroaches on the Basement Till, indicating shear *after* the sands were deposited.

The fact that the top of the Dimlington Silts rise above the height at which, elsewhere, the Skipsea and Basement Tills are in direct contact (*Figure 8.11*) indicates that the silts were removed from these direct contact areas. The order of development must have been; the removal of the silts, then the formation of the sand rich material, and then décollement along the single shear ‘A’. The sand/matrix mix is unlikely to be loess or proglacial sands. Loess has been found below, and lacustrine sands above, the Dimlington Silts (Eyles *et al.*, 1994), but neither were seen on the outcrop scale at the time of sampling. It is unlikely that proglacial sands would survive the truncation of the sequence in such a thin layer, and therefore the sand rich material must be associated with the intermediate diamict.

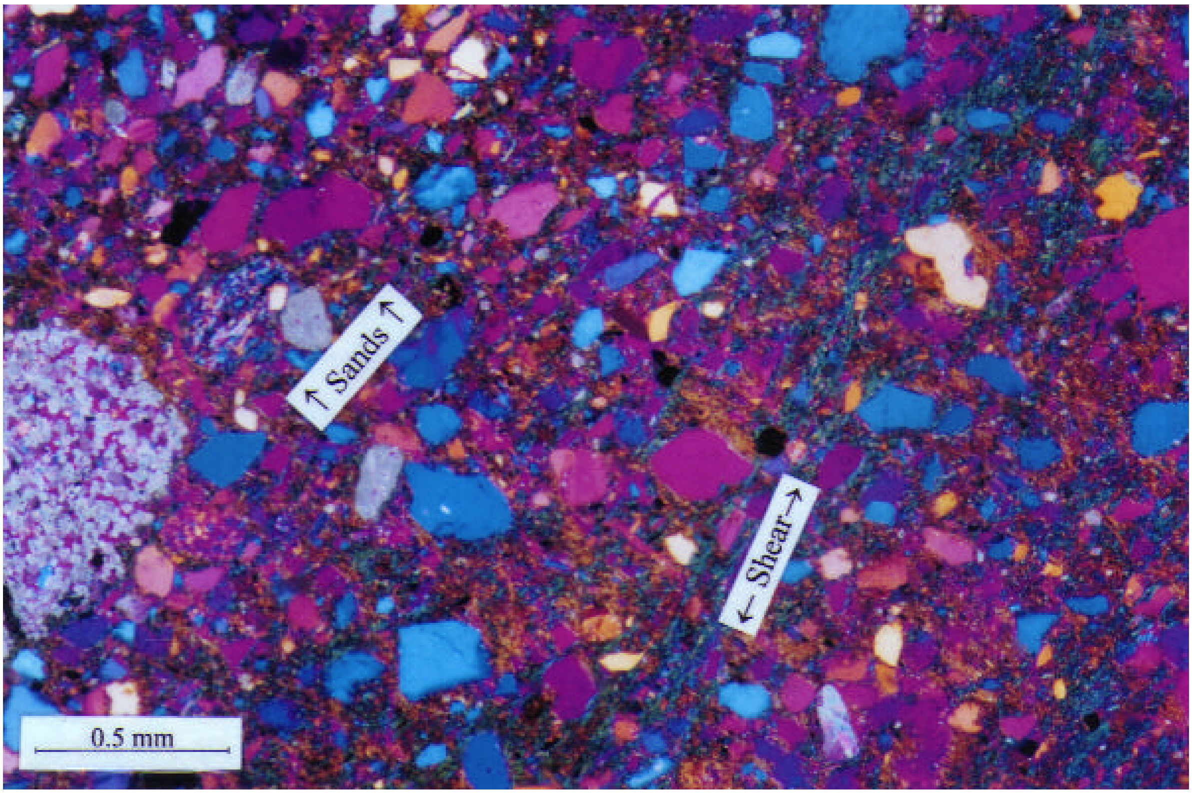

Figure 8.15 Photomicrograph of shear ‘A’ at the top of Basement Till. The orientation of the sheared fabric gives it a green colour. Sample Dsk6, under cross polarized light with a tint plate.

It is simplest to explain the sands as subglacially concentrated and deposited. The clean sand lenses within the sand rich diamict probably attest to fluid throughflow (for a theoretical basis see Clarke et al., 1984 and Clarke, 1987). This throughflow will have winnowed out the matrix and weakened the rest of the material allowing it to mix. It is unlikely that there was a subaerial escape route for the fluid which forced its way through this material. It is also unlikely that the sand lenses are buried subaerial channels, as this would imply they had been left clean while the deposition of sand mixed with matrix continued around and above them.

The throughflow winnowing hypothesis is tested by comparing the long axis size of the sand grains in the intermediate diamict, the sand/matrix material, and the clean sand lenses. The sand sizes are also compared with the same sediments in the alternative sampling plane to eliminate grain rotation as a factor as far as possible. The sizes were compared using the 'Student's t' test (Hoel, 1984, sample size of twenty five). It is to be expected that the sand grains in the proposed throughflow areas will be the same size or larger than those in the diamict under the throughflow hypothesis. Variations in sand source or deposition might be expected to show up as a grain size variation. The 't-scores' are presented in Table 8.6. Values for the 't-scores' of over 1.316 or under -1.316 would have shown the samples to be significantly different at 90%.

Grains sampled	**Clean sand lenses E-W plain**	**Sand rich material E-W plain**	**Intermediate diamict E-W plain**	**Sand rich material N-S plain**
Intermediate diamict N-S plain	0.048507	-0.28134	-0.79552	-0.56268
Sand rich material N-S plain	-0.36865	-0.63059	-1.13507	
Intermediate diamict E-W plain	-0.15522	-0.50447		
Sand rich material E-W plain	-0.310446			

Table 8.6 't-scores' showing that the sands in the intermediate diamict, the sand rich material, and the clean sand lenses, are from the same grain population. Only grains larger than 0.01 mm were measured. There were no clean sand lenses in the north-south plain. Note that none of the comparisons rise above the 90% significant.

None of the compared samples are significantly different at the 90% or higher confidence levels. There is no statistical difference between the material in the clean sand lenses and the other areas. This suggests that only particles smaller than the smallest measured grains (0.01mm) were removed by throughflow. The intermediate diamict is 64.5% matrix, whereas the matrix content of the sand rich material is 44.5% (100 sample point-counts; averages of both sampling planes - there was only 1% difference between each). Thus 31% of the matrix was removed by throughflow erosion. Given the thickness of the sand-rich layer this is 0.0046 m^3 for each metre squared of ice-bed interface. The size of this figure is revealed when recalculated for a glacier 400 km long and 50 km wide (as may have been the case on the east coast). The sediment lost to the proglacial environment through this mechanism is then $9.3x10^7$ m^3, though it is likely the event was much more localized than this in reality.

The clay layers above the intermediate diamict at its boundary with the main body of the Skipsea Till (Dsk2/3) would, at some time, have been an aquitard between the ice, which was presumable supplying fluid if it was warm bedded, and the intermediate diamict. The absence of sand lenses at the boundary with the main body of the Skipsea Till therefore suggests the throughflow of fluid had stopped winnowing the sediment before this aquitard was deposited.

Given that throughflow is responsible for the sand concentration at the boundary between the Basement and intermediate diamicts, the disturbed nature of the fabric immediately above the sand rich material can also be attributed to this mechanism. The simple overriding of the rough surface of the sands is not necessarily enough to disturb the fabric of this material (see the Reighton Sands samples, below). The triaxial tests (Chapter Seven) suggest that throughflow rearrangement is overprinted at even low strains, therefore the fabric may have been disturbed *after* the overlying omnisepic fabric stopped forming. However, given that the unorientated material has transferred stress across itself without aligning at some point, it is possible the omnisepic fabric formed after the sands were concentrated, the unorientated material not orientating because it was strengthened by drainage into the clean sand lenses.

A drainage event between the sand's concentration and formation of shear 'A' is also indicated by two other lines of evidence:

1) The proposed translocation concentrating the sands implies that the material forming the sands was saturated, and therefore probably had little strength. It is more likely to have been able to transfer stress to the underlying material after a drainage event.

2) The discrete nature of the shear 'A', which suggests a high effective pressure (see Chapter Three).

Three possible scenarios account for any drainage event:

1) The throughflow channels proposed above, maintained open by the clean sand grains within them, drained the sediment.

2) The till layer built up, allowing a greater drainage area through the main diamict body (though it is impossible to know how much material there was above the sand rich layer when it formed).

3) The high melt rate or fluvial event supplying the pore fluid necessary for the proposed translocation ended.

The combination of discrete shear in the top of the Basement Till and an unorientated layer in the intermediate diamict also suggests that the intermediate diamict could not strain as effectively as the underlying finer grain sediments. Thus, these fabrics may provide more weight of evidence for the sediment responding to stress by a mix of work-hardening and localised discrete shear (work-softening) as outlined in Chapters Six and Seven.

The sequence reflects the manner in which microstructures buffer the pore fluid pressure of tills, providing a stabilising effect. The above diamict may have responded to higher fluid pressures with an increased number of channels containing cleaned sands. The sequence also indicates that the resistant and shear-like nature of the sediment on an outcrop scale is not due to the décollement shear zone (which is only a few grains thick), but the winnowed sand rich layer. Other 'shear zones' interpreted from an outcrop scale may, in fact, represent depositional permeability discontinuities exploited by fluid.

The intermediate diamict and Skipsea Till

The intermediate diamict is only present where the Basement Till and Skipsea Till are not separated by the Dimlington Silts. Given that there are no rhythmites in the intermediate diamict, and we have no idea how much the Basement Till was truncated, it is impossible to determine the origin of the material in the intermediate diamict using micromorphology, though the material is *likely* to be a mix of the three other sediments at the boundary.

The intermediate diamict has an omnisepic fabric with intense patches suggesting that shear stress could not be released through the production of narrow shear zones, probably because of the presence of clasts (Chapters Six and Seven). The development of fabrics under triaxial deformation (Chapter Seven) suggests that the sub-horizontal omnisepic fabric was formed strain under a sub-horizontal simple shear geometry. This is the only case in the samples examined in this research of the simple shear ('shear-box') geometry suggested by Boulton and Hindmarsh (1987) to be representative of subglacial deformation. This may point to greater coupling with the ice, or sediment, above with no irregularities projecting into the sampled horizon. The absence of the clay patches seen at the two other locations in this chapter may point to shear destruction or, alternatively, less water flow between the ice and sediment (that is, greater coupling between the two, which would probably result in greater strain as well).

The boundary between the intermediate diamict and the main body of the Skipsea Till is marked by a clay band. Below this is disturbed or possibly bi-directional intermediate diamict (*Figure 8.13*). Above the clay band is aligned Skipsea Till from the main Skipsea Till body. Comparison with the fabrics at the base of the intermediate diamict suggests that the disturbed nature of the diamict immediately below the clay band indicates fluidization of the diamict, possibly during deposition of the clays, though the justification for this comparison is limited, especially given the possible bi-directional fabric. The boundary between the clays and the overlying material is diffusely mixed in areas, and this is unrelated to later low strain buckling of the clays, backing up the fluidization hypothesis.

Because the clay layers here may be horizontally continuous we cannot refute the possibility that these clays are proglacial (in contrast to Filey where the sediments were seen to be interdigitated on a metre to sub-millimetre scale). It seems unlikely that such a thin layer would escape destruction from the marginal compression seen at the front of the same ice mass at Reighton Sands (below) and in the folding of the Dimlington Silts, however, the possibility exists that equally thin sand layers *have* survived at Reighton Sands (below). Nor can Eyles *et al.*'s (1994) implication that the sub-units in the Skipsea Till are blocks of older material be refuted, as the clays may have been deposited in a hydraulic fracture line between the two materials. It must, therefore, only remain a *possibility* that the clays reflect water flow at the ice-sediment interface. Because of this uncertainty over the origins of the clays, no definite statement can be made regarding the origin of the Skipsea Till material here (contrast with

Filey Brigg diamicts, and also note that there are no macroscale structures in the Skipsea Till at this site to aid in an interpretation).

Dimlington silts

The Dimlington silts are formed from layers of sand in matrix in couplets with clay/silt layers. The clay/silt layers have a strong fabric, probably due to the combination of a prior horizontal fabric and consolidation (the bedding of the material has not been lost through extensive shearing which might otherwise have caused the fabric). That such a horizontal fabric can develop may suggest some of the horizontal fabric of the intermediate diamict is due to consolidation. The sand and matrix layers in the rhythmites have responded differently to the low strain than the clay/silt layers. While the clay/silts show two discrete conjugate shear sets, the sand and matrix layers have developed a pervasively interlaced lattisepic fabric. Such a fabric was predicted to develop under these conditions in Chapter Seven. The lack of skelsepic fabric in the sand and matrix layers suggests this fabric type does not form at less than 2% strain, although grain density and effective pressure may have an effect.

The fabric at the boundary between the Dimlington Silts and the Basement Till (Ds8/9/10) is dominated by the presence of diamict pebbles of various sizes, and sand-rich layers (*Figure 8.16*). Both fall off in frequency with distance below the boundary. The fabric away from these features is similar to that at the top of the Basement Till directly under the intermediate diamict (Dsk6/7). The absence of the pebbles below the intermediate diamict suggests that the Basement Till below the intermediate diamict must have been at some depth below its original upper surface. In both the sets of slides the Basement Till displays a broadly lattisepic fabric, both also having intense patches of fabric in the two lattisepic shear directions (*Figure 8.17*). This suggests a similar history. Such a history may have influenced the formation of the pebbles.

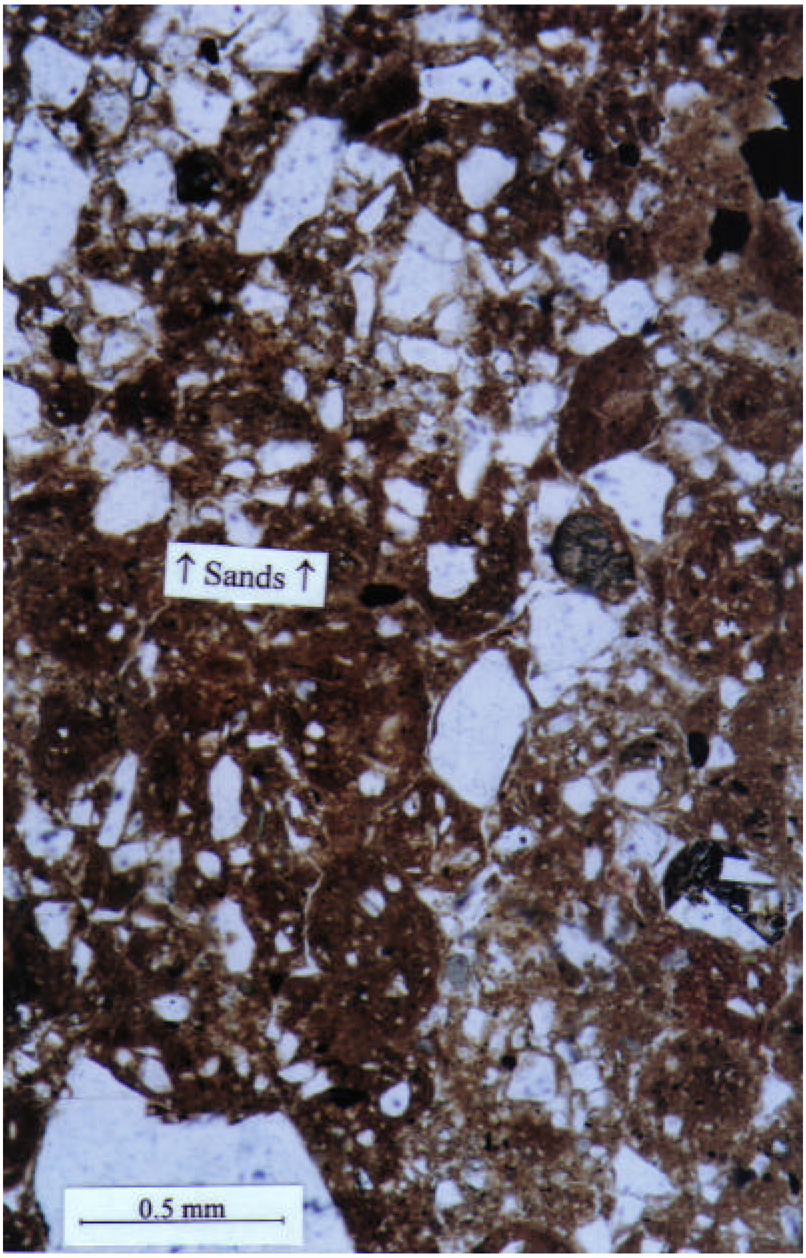

Figure 8.16 Photomicrograph of diamict pebbles in the sands and diamict at the top of the Basement Till under the Dimlington Silts. Sample Ds9, under unpolarized light conditions.

The interior material of the pebbles strongly resembles the material around and below them, suggesting that the pebbles are of Basement Till, rather than Skipsea Till washed into a proglacial environment. As was noted above, there is little evidence either way that the shears were not present before the Dimlington Silts were deposited. It is shown in Chapter Six and Seven that shear zones *may* be sites of weakness under tensile effective stresses, or low compressive stresses when associated with shear dilation. On top of this, shears are, by definition, weak areas under shear stress at some point in their history. Given these facts, the hypothesis is put forward that the shears influenced the formation of the pebbles. Two potential processes can be envisaged;

1) the shears weakened the material along their length and their lattisepic layout demarcated areas which became pebbles;

2) the shears strengthened the material in the intensely sheared patches by increasing face-face clay contacts, and these patches became the pebbles.

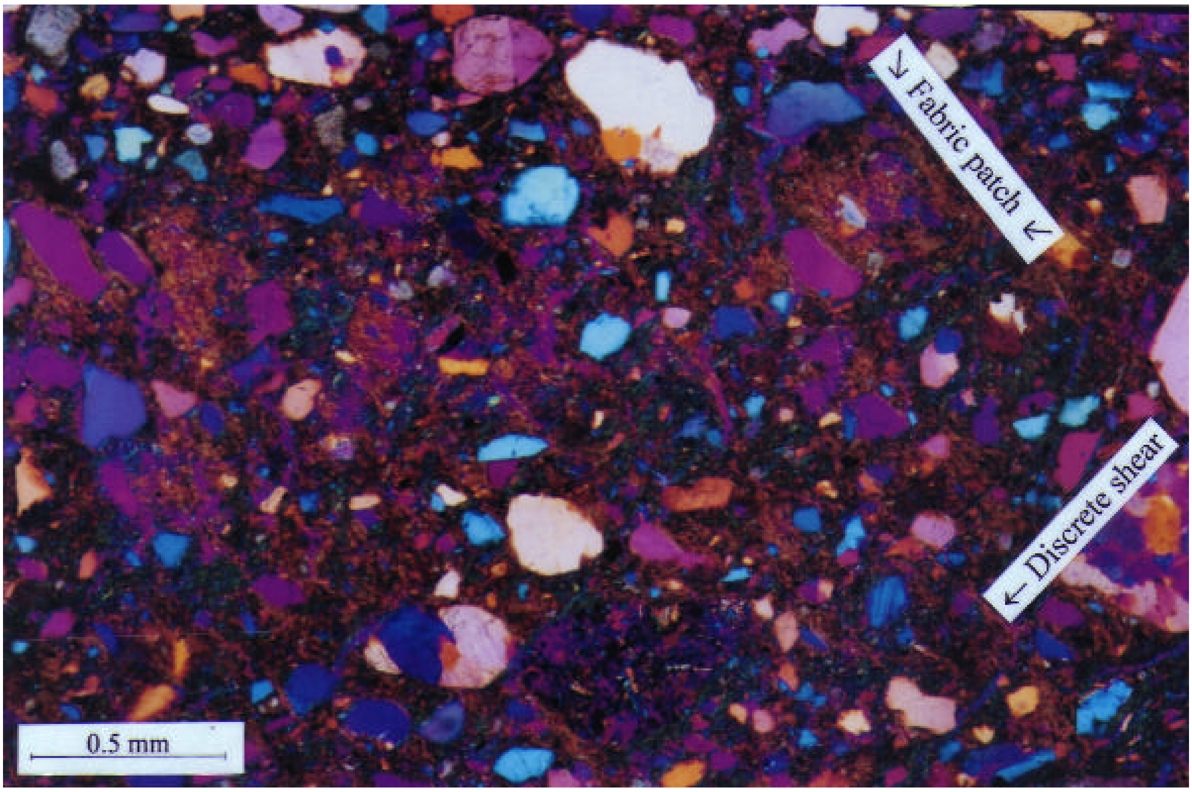

Figure 8.17 Photomicrograph of slide Dsk6, showing the Basement Till. Note the discrete shears and patches of shear aligned material. Cross polarized light conditions with a tint plate.

The former hypothesis is based on that suggested by van der Meer (1993), the latter is an alternative suggested by the micromorphology. The hypotheses were tested by statistical comparison of the micromorphology.

It was plain that the pebbles found just below the surface of the Basement diamict (in the upper low-sand layer) are probably larger than could be produced by the shear fabrics that were found lower in the sequence in either hypothesis. To test this probability, the long axes of this pebble population alone was compared with the shear data from the top of the Basement Till under the intermediate diamict using the Rank Sum test (Hoel, 1984, p.342 - sample size 30). The shear zone data is twofold; the distance between shears transverse to the shear direction, and the length of intense patches in the shear direction (always the longest axis of such patches). Linear shears with widths of less than 10 grains, were ignored in the measurement of the intense patches as being unlikely to form the ovoid pebbles through hardening (these shears are discrete from the intense patches in practice). The data from each sampling plane is compared with the other plane to eliminate as far as is possible the potential the pebbles have rotated. The results are presented in Table 8.7 as the probability that the tested pair of sizes are the same. Those not significantly different at 10% significance are in bold.

The strong difference between all the tested features in the north-south plane and the pebbles in the same plane indicate that the shear features cannot be determining the pebble size without some rotation. The distance between the shears is also not responsible for the pebble size, whatever the rotation. The only variable tested that could be responsible is their development from the shear patches probably followed by the rotation of the fabric/pebbles. It should be noted that the lack of similarity between the pebbles and patches in the north-south plain, but their similarity in the east-west plain is not contradictory as pebbles may have their form

	North - South Plane pebbles	**East - West Plane pebbles**
North-South Plane shears...		
Patch along shears at 92	0.0035	**0.119**
Patch along shears at 180	0.0052	0.0681
Between shears at 92	0.001	0.0401
Between shears at 180	0.001	0.001
East-West Plane shears...		
Patch along shears at 106	**0.3669**	**0.2709**
Patch along shears at 140	**0.102**	**0.3669**
Between shears at 106	0.0021	0.0721
Between shears at 140	0.001	0.0274

Table 8.7 Probabilities that shear fabrics could be controlling the size of the diamict pebbles at the top of the Basement Till. Those probabilities that are in bold are those for which the hypothesis is possible given a 10% significance as a cut of point for the hypothesis being unmaintainable.

determined by the fabrics in one direction and rotate into two preferred orientations. Given the results presented in Table 8.7 we can dismiss the suggestion that shears weaken the sediment and are exploited to produce pebbles. The opposite, however, may still be hypothesised; that shear alignment strengthens the sediment along the shears and the removal of the surrounding areas leaves the sheared patches as pebbles.

The statistical evidence *in favour* of sediment strengthening is weak (note significances), and this should be held as a possibility rather than a probability on the strength of the above data. Alternative controls may be found. The potential for pre-determining a sampling strategy to continue such a validation is limited by our lack of understanding of the depositional constraints on pebbles.

It will be noted that no environmental origin has been given for the pebbles yet. As the pebbles have formed at the top of lake-covered diamict, the pebblization process may have occurred within the diamict or under fluvial shear. Whichever origin is true, these pebbles point to low effective pressure conditions, for this would seem necessary for the survival of the pebbles under rotation/shear. This location provides the *only* environmental evidence associated with diamict pebbles. There may, of course, be more than one process forming them. If pebbles reflect high fluid pressures, they may be important in maintaining the buoyancy of clasts in the low strength diamict (contrast with Clark, 1991 on the origin of clast pavements by fluidization of tills). The diamict pebbles will act as clasts do in a clast-supported diamict at a larger scale, building up a supportive skeleton within the diamict.

Summary: The deposits at Dimlington High Ground were sampled to investigate the readvance mechanisms of the Skipsea Till depositing ice, and the nature of low strain deformation. It has been suggested that the truncation of the pre-glacial Dimlington Silts was followed by the deposition of the intermediate diamict. This was then disrupted by fluid throughflow, which created a set of clean sand microchannels. It is unlikely that there was a subaerial escape route for the fluid which forced through the resulting high-friction, sediment clogged sandy diamict. It is also unlikely that the pure sand lenses are buried subaerial channels, as this would imply they had been left clean while the deposition of sand mixed with matrix continued around and above them. Thus, the micromorphology of the material changed to buffer high pore fluid throughflow. At some point after this, the material drained and stress was transferred to the top of the Basement Till, which underwent discrete shear. Also at some point after this, a clay band was deposited at the top of the intermediate diamict. The intermediate diamict deposited between the depositional times of the two boundaries suffered horizontal simple shear of the type suggested by Boulton and Hindmarsh (1987). Examination of the Dimlington Silts backs up the proposal in Chapter Seven that lattisepic fabrics form in areas of conflicting conjugate shear fabrics. The lack of skelsepic fabric in the sand and matrix layers suggests this fabric does not form at less than 2% strain, though clast density and effective pressure may effect this. Comparison between diamict pebbles at the top of the Basement Till and shear fabrics from deeper in the sequence refutes the hypothesis that the pebbles formed when shear-caused weaknesses were exploited. However, the same analysis cannot refute an alternative hypothesis; that shear alignment strengthened the material in patches and these stronger patches were released to become diamict pebbles.

8.5 Reighton Sands

8.5.1 Introduction

Material was sampled from the top of the coastal cliff (TA 147757) just North of the morainic Speeton Hills (*Figure 8.1b*). The sequence has been studied by Lamplugh (1881), Melmore (1935), and Catt and Penny (1966). Coastal retreat will have significantly changed the structural appearance of the location since these studies. The structure and sedimentology of the sample site is given in Figure 8.18 (see also *Figure 8.19*). The local structure is ever changing and complex, but broadly one of low strain folding and the possible rafting of pre-glacial sediment units. The visible sequence at the sample site starts at ~25 m O.D. and is of a shell and sand lithofacies (the 'Speeton Shell Bed') (lithofacies E) overlain by faintly laminated sands (lithofacies D), above which is a grey diamict unit (lithofacies A) (variously ascribed on the basis of colour and geology to the Withernsea, Skipsea and Basement Tills; Melmore, 1935). The boundary between the diamict and sands is diffuse to sharp with patches of recumbently folded chalk gravel (lithofacies C). The diamict also overlies a brown diamict which takes the place of the chalk gravel (lithofacies B) and has a sharp boundary with the surrounding lithofacies.

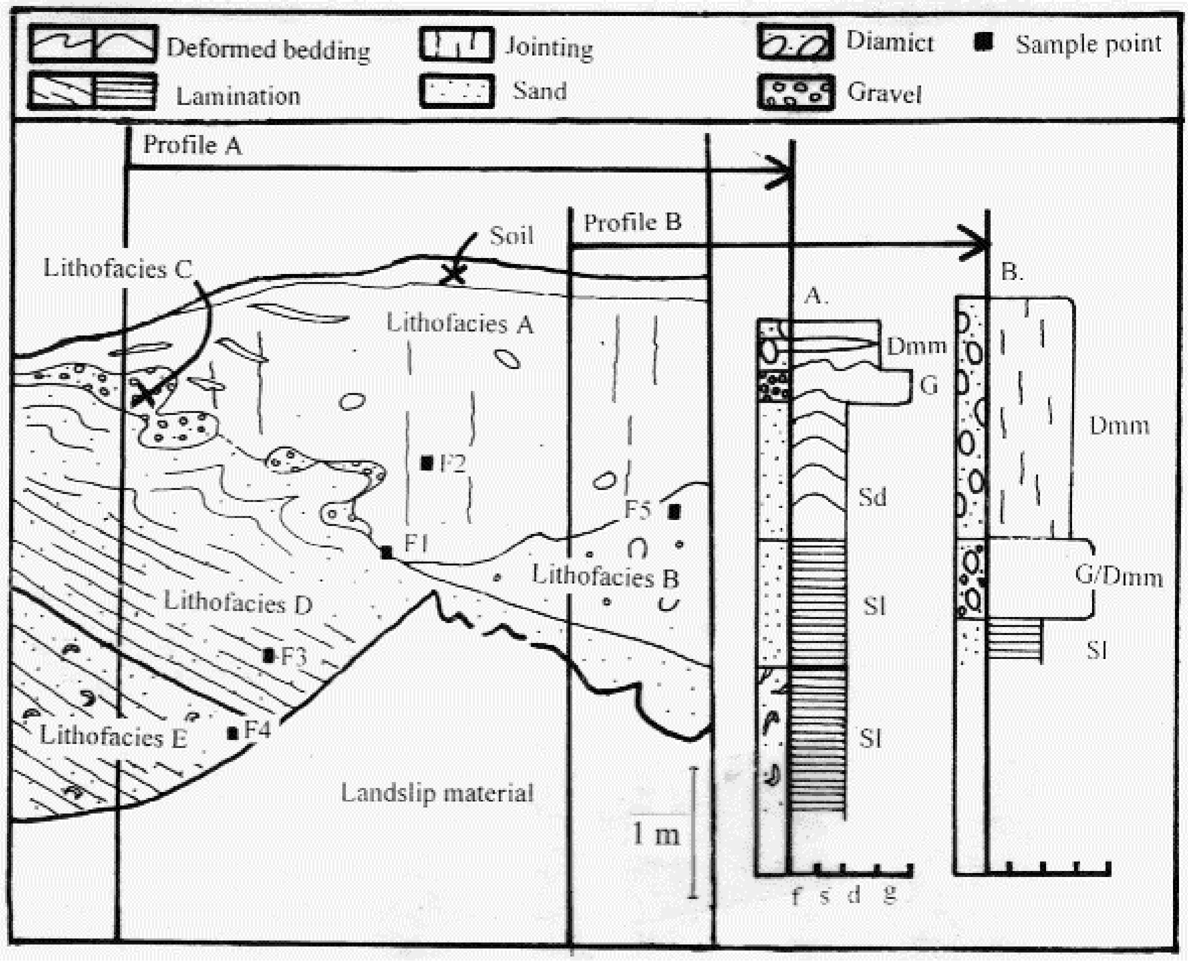

Figure 8.18 Sediment sequence at Reighton Sands, East Yorkshire coast. The visible sequence starts at ~25 m O.D. Lithofacies A) Grey diamict. B) Brown diamict. C) Chalk gravel. D) Faintly laminated sands. E) Massive shells and sands.

Figure 8.19 Photograph of the sample site at Reighton Sands.

Samples were taken to elucidate the nature of the diamict formation and low strain deformation fabrics. Samples were taken from lithofacies E and D, the boundary with the blue-grey diamict (lithofacies A) where sharp and uninterrupted, the body of lithofacies A, and lithofacies B (*Figure 8.18*).

8.5.2 Results

The descriptions of the slides are given in Table 8.8 in terms of the general fabric of the diamict and the external and internal fabrics associated with any inclusions such as clay bands or diamict pebbles. The nomenclature used is that of Table 8.2. Shears and more pervasive fabrics are given in terms of their dip angle downwards in a cardinal direction (N,S,E,W). Samples were cut in north-south and east-west planes. Other terms are defined in Chapter Two and the Glossary. A summary of the chief results follows the table.

Position	Sample	Fabric	Inclusions
3.5m above sands; lithofacies B	F5a	Diamict (~33% of sample) with patchy Omnisepic fabric at 90°. Many shears but three dominant sets (90°, 140°N, 135°S) which cross into the surrounding material.	Clay bands (~22%) in couplets with distinct and diffuse bodies of silt and long iron minerals (~45%). Fabric of these bodies parallels their outer form as they have contorted in low strain shear (<10%). Concentrated glauconitic sand bodies.
3.5m above sands (A)	F2	Identical to F1, though less shears.	
Diamict above sands; lithofacies A	F1b and a (part of slide furthest from sands)	Very strong grain and fabric alignment. In sample (b) this is in three areas. Two areas (20% and 30% of slide) orientated in approximately the same direction (41° N and 33° N - but very confused in the latter), separated by a third at 48° S (but variable). Shears in the first two areas are at 48° S and include 'mature' (infinite strain) shears. (a) Broad fabrics at 305° NNW and 240° NWW. (a/b) High porosity of two types; 1) small patches (on the order of ~0.5mm) of porous fabric; 2) linear areas (>3mm x <0.5mm).	Many clay rich blocks (~4 mm^{-2}), often, but not exclusively, iron stained on the outside. These are of two sorts… 1) omnisepic bands of various orientations (~0.5 to 0.1 thick, up to 3mm long); 2) smaller rounded pebbles with interior fabric paralleling exterior surface. The borders with the matrix are sharp for both sorts, though inclusions of the matrix occur. Shears in the blocks splay at the borders, but only enter the matrix for a few grains length.
Boundary between sands and till; lithofacies A and D	F1a (part of slide nearest sands)	Diamict over sands. Fabric matches the sand boundary close by, but becomes omnisepic further away (~0.5mm) to 240° NWW. The sands are heavily iron stained and not orientated.	
Boundary between sands and till - below boundary; lithofacies A and D	F1c	A matrix and sand mix with a poor horizontal orientation over... A layer of large quartz and chalk grains (~1mm thick), then fine grains over... Large grains again and then low matrix small sands (~4.5mm thick) with an irregular boundary over... Matrix rich sand with a mild (but stronger than above) horizontal fabric and grain orientation.	The material contains glauconite, heavy minerals, and iron-rich laminated clays. Also, the upper most material includes iron stained blocks of mixed sand and matrix.
Sands; lithofacies D	F3a/b	Very angular to rounded sands, very well sorted (~ 0.1mm diameter), homogeneous, in a clay matrix. Sub-horizontal sand fabric.	One lense (0.75 x 3+mm) of disrupted chalk.
Shells and sands; lithofacies E	F4a/b	Glauconitic sand. Wide size range but < 0.5mm diameter, except for long (~1mm+, length:width ratio ~7) grains rich in heavy minerals. Some unfabriced clay matrix with sands in (~1cm thick) lenses showing low strain.	

Table 8.8 Summary of the micromorphology of samples taken from the sediments at Reighton Sands, East Yorkshire coast. The table is arranged such that the samples are in their stratigraphic position. The samples from the base of the sequence are lowest in the table

The boundary between the sands of lithofacies D and the diamicton lithofacies A (sample F1c) is marked by alternating layers of sand rich silt matrix and large sand grains, including chalk layers (in the same stratigraphic position as the chalk rubble lithofacies C). The large grained layers are partially iron cemented. The diamict directly above these layers has a fabric that parallels the perimeter of the nearest sand grains (F1a). This fabric becomes largely omnisepic within 0.5 mm of the boundary, however, this omnisepic fabric is disrupted by broad areas orthogonal to it. These broad areas match the direction of more discrete shears within the omnisepic fabric. This material is also highly porous in patches and linear areas (both on the order of 0.5 mm wide). The material also contains clay bands with omnisepic internal fabrics in a variety of directions, and clay pebbles with an internal fabric paralleling their exterior form. The clays areas have been iron stained (unlike the surrounding diamict), and sheared synchronously with the surrounding material. Sample F2 suggests lithofacies A is less sheared away from the boundary with lithofacies D, but is otherwise unchanged with height.

Lithofacies B (F5a) is a melange of interlayered clay-silt units, glauconitic sands, and diamict. The internal fabrics of the silt-clay units parallel their exterior form, and they have undergone low (<10%) strain. The glauconitic sands match those of lithofacies E (F4a/b). The diamict has a weak omnisepic fabric which has been disrupted by shear that was synchronously with the deformation of the other materials in the melange.

8.5.3 Interpretation

The boundary between the sands and lithofacies A is sharp (Sample F1a). The uneven upper surface of the matrix rich sands is directly overlain with diamict. The fabric of the diamict initially mirrors the surface of the sands, but gains a distinct single alignment away from the boundary (*Figure 8.20*). Just below this boundary (F1c) the matrix rich sand alternates in layers that are cleaner and have larger grains. The stress conditions at the boundary of the diamict must at some point have been suitable enough to force the diamict fabric parallel to the sands, but not to set up a shear zone at the boundary or move the sands. This may indicate that the sediment was saturated and weak, or the boundary fabric is due to consolidation rather than the shear seen higher in slide F1a. A highly fluid situation is also implied by the higher lithofacies A material (samples F1a/b and F2). Sample F1b has a wide shear zone with indicators of fluid throughflow in the form of porous zones (see Chapter Three for details of how shear geometries reflect the effective pressure).

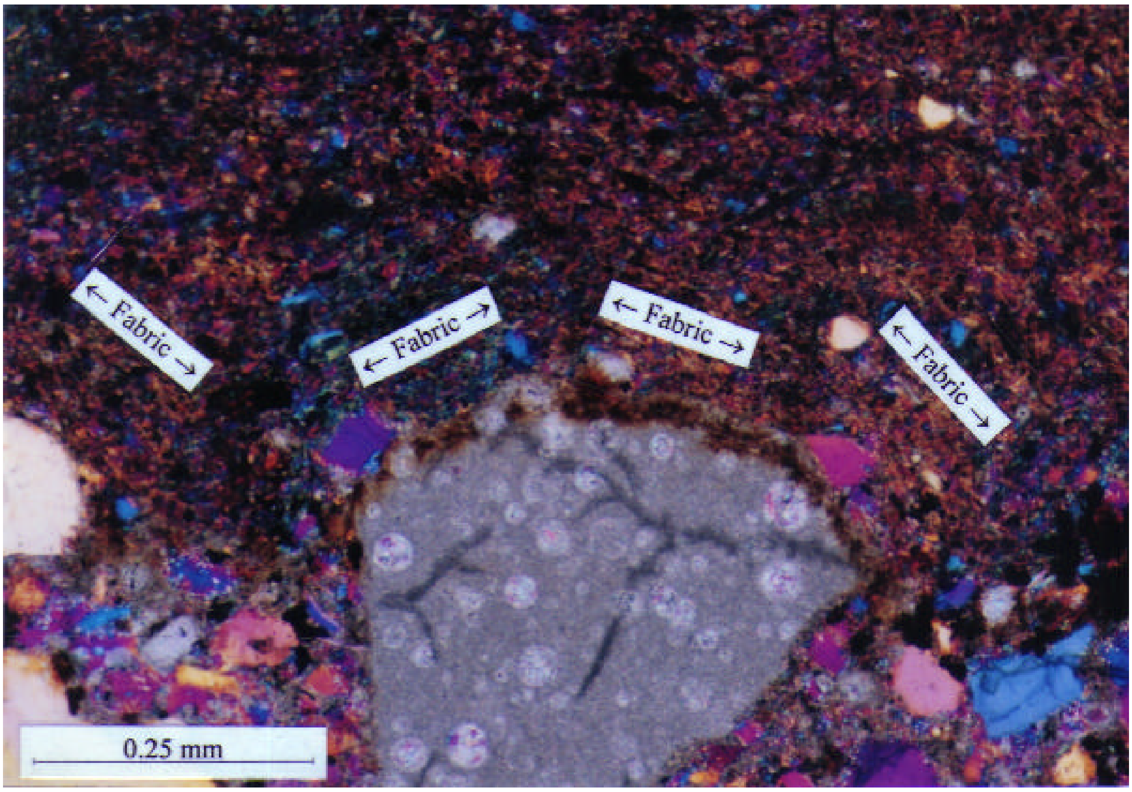

Figure 8.20 Photomicrograph of fabric following the sands at base of lithofacies A, the long axes of the long dark grains follow the general fabric direction. Sample F1a, under cross polarized light with a tint plate.

The clay patches in lithofacies A (samples F1a/b and F2) may be meltout products or throughflow translocation deposits (both matching the high fluid content of the diamict). The origin of the diamicts, therefore, cannot be determined (contrast with Filey Bay, where there were no other throughflow microstructures). However, the clays' strong orientation and the fact that some of the pebbles show fabrics paralleling their outer surfaces points to material that has been sheared and possibly consolidated, subglacially or proglacially.

Proglacial deformation of the sequence could have been responsible for the consolidation and throughflow. However, the various orientations in the clays in F1 a/b and F2 suggests that they had a fabric prior to their breaking up and being mixed into the diamict, thus the following sequence is necessary (*Figure 8.21*);

1) the clays are suspended in throughflow fluid within the diamict (fluid moving faster than the skeleton and eroding fines from it; see Clarke, 1987, for background theory),
2) the clays are deposited again in the diamict (fluid moving slower than the skeleton),
3) the clays are consolidated/sheared to give them a fabric (fluid moving faster than the skeleton but not fast enough to winnow),
4) the clays are broken up in a matrix that is being winnowed (fluid moving faster than the skeleton and eroding).

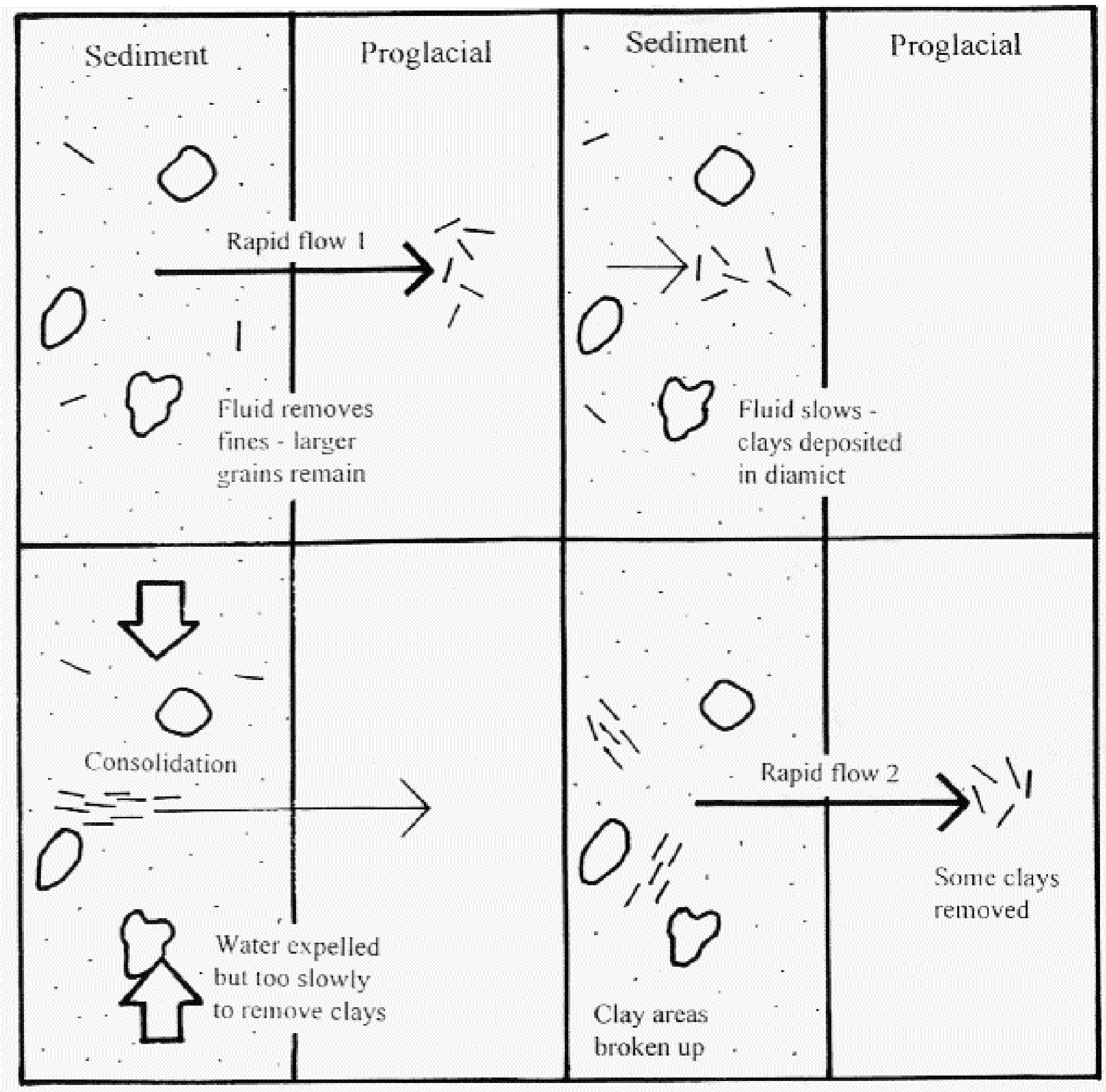

Figure 8.21 Potential fluid-flow / deformation history for lithofacies A.

This sequence implies a two part throughflow sequence. A two advance formation for the material, with the fabric development and throughflow being forced proglacially is more complex than a single advance with intermittent throughflow and deformation subglacially. However, the former interpretation matches Eyles *et al.*'s (1994) multiple-surge hypothesis for the formation of the material.

The low strain in sample F5a allows us to see that on the microscale lithofacies B is a melange being produced by the incorporation of heterogeneous materials (*Figure 8.22*). The silts and clays may be in couplets, though strain makes this difficult to confirm. If they are in couplets, these rhythmites may be from a proglacial lake or deposition in intermittently active subglacial ponds, both of which may have contributed to the sediments saturation.

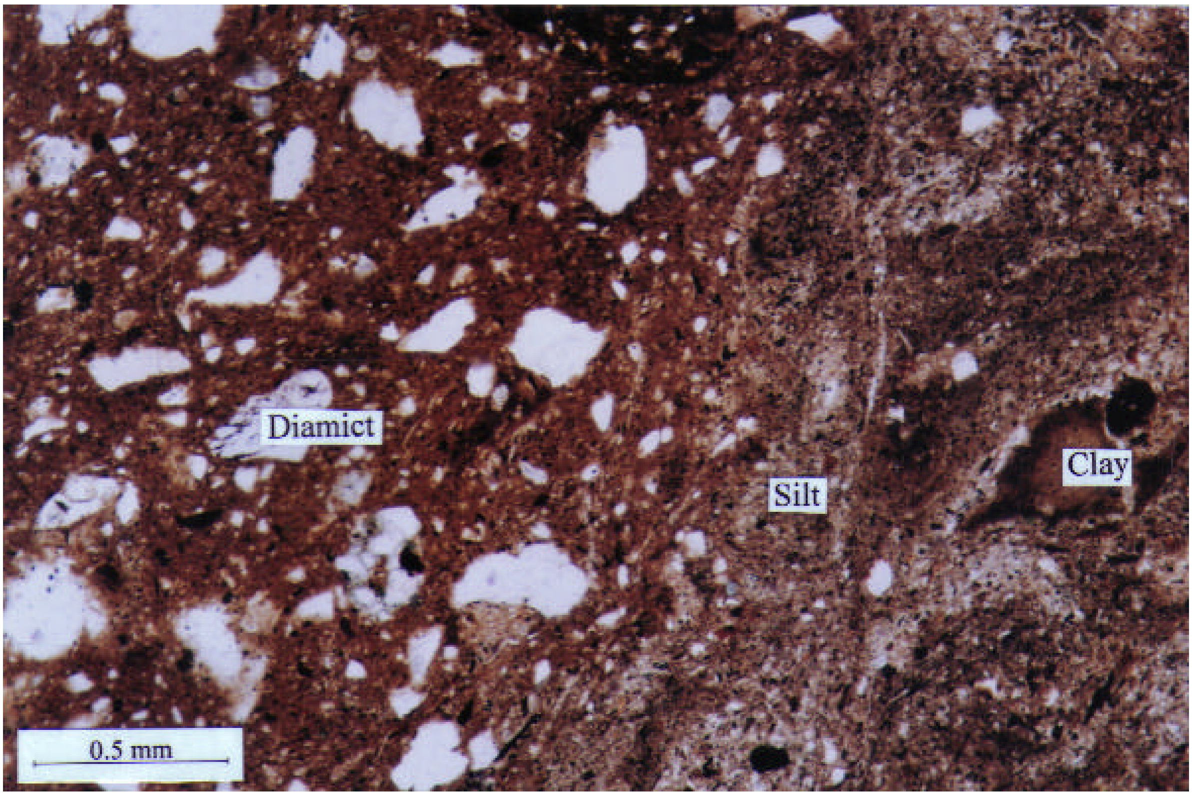

Figure 8.22 Photomicrograph of the melange of diamict, silts and clays that makes up lithofacies B which appears to be a diamict on an outcrop scale. Sample F5a, under unpolarized light conditions.

The highly fluid nature of lithofacies A indicated by its microstructures can be compared with the diamicts overriding the lake-deposited rhythmites at Dimlington, which appear to have been, relatively, drier. On the basis of such a comparison it might be tempting to dismiss lacustrine conditions as the cause of the sediments saturation at Reighton and invoke a high marginal melt rate. This would match the potential meltout origin of the diamicts and the possible throughflow described above. However, the sands overridden at Reighton may have stored a far greater amount of fluid than the Dimlington Silts, and this could have been expelled into surrounding sediments during deformation.

Summary: The micromorphology of the Reighton Sands sediments suggests two alternative sets of conditions, which, unfortunately, match exactly with the two models proposed for the whole region. The rhythmitic sediments, sheared diamicts and clay rich patches seen in the sequence may either suggest a series of multiple advances of ice up to, or over, the area through a proglacial water body, or a single advance with a high basal melt rate and water ponding at the ice-sediment interface. Unfortunately the present macroscale morphology is consistent with either explanation. Equally, past research in the area has concentrated (with only controversial results) on whether the Speeton Shell Bed has been thrust into its present position, and on regional diamict correlations (Lamplugh, 1881; Melmore, 1935; Catt and Penny, 1966). These studies offer no evidence that can be used to elucidate the specifics of the glacial history of the diamicts. Both models may therefore be regarded as likely in this marginal ice position.

8.6 Conclusions

8.6.1 Sediment strength and fabric development

The above interpretations provide additional information to that provided in Chapters Six and Seven on the manner in which subglacial materials strain and develop small scale structures.

At Dimlington High Ground an omnisepic fabric developed in the intermediate diamict, but this development was followed by the transferral of stress to the boundary with the underlying basement sequence where a discrete shear developed. This suggests the omnisepic fabric was ineffective in releasing stress and discrete shears formed where they could. This backs up the rheology suggested in Chapter Six after the discovery of work-hardening behaviour in laboratory-deformed Skipsea Till.

However, there is evidence that discrete shear décollement did *not* occur during the deposition of the main body of the Skipsea Till at Dimlington. Here the layers of the sequence expected to be weakest (unimodal clays) did not show discrete shear deformation (though note that conditions may have existed at Filey in which clays were stronger than diamicts, and the clays may have formed *after* the diamict aligned). It should also be noted that examination of the 'shear' fabric at the boundary between the intermediate diamict and Basement Till at Dimlington suggests many 'shears' identified at an outcrop scale may be areas of fluid exploitation due to permeability changes, and do not necessarily represent strain.

There is also evidence from the micromorphology of the area that lattisepic fabrics do not aid the formation of diamict pebbles by weakening the material relative to areas between the shears. However, there is still a possibility that shear strain strengthens the sediment by locally aligning cohesive clay grains, and these stronger areas form pebbles. Further evidence is given that pervasive lattisepic fabrics form where conjugate shears interact in clast rich material.

8.6.2 Glacial hydrology

The micromorphology of the samples reflect the hydrological system at the ice base. The deposits on Filey Brigg are probably formed by melting of ice with a variable sediment content into an environment of sand depositing streams. The ice was probably separated from the sediment by thin, clay depositing, fluid layers, which reworked the previously deposited diamict. The combination of an ice interface water layer and larger streams indicates that the streams did not rapidly draw fluid from the surrounding ice-sediment interface. This suggests that the streams were at atmospheric pressure or had a *positive* hydraulic pressure to discharge relationship, one of the features of Walder-Fowler canals (Walder and Fowler, 1994).

The massive sand bodies high in the sequence at Filey Brigg suggest that the streams depositing the sands finally became dominant over the deposition of the diamict. The rise in available water suggested by the sands, if not the ice interface clays, is probably due to an increase in the melt rate and/or the increased amount of impermeable material between any given horizon and the potentially permeable limestone at the base of the sequence. Following deposition of the massive sands *all* the sediments were subjected to further low strain deformation. The sediment was possibly deforming under a low effective pressure and the strain may have been dependent on the heterogeneous drainage potential of the material. This low strain overprinting may indicate that low effective pressures are associated with deep deforming layers.

At Dimlington, higher levels of fluid than could drain through the sediment did not immediately result in a water layer between the ice and bed. Here the boundary between the active diamict and the basement sequence was exploited by the translocation of fines and the formation of sand filled channels. Some 31% of the local matrix was removed in this event (0.0046 m^3 for each metre squared of ice - bed interface). That a fluid layer did not form may suggest that the interface between ice and sediment was more coupled than at Filey because of its geometry.

8.6.3 Low sediment strain: ice - sediment coupling

Ice interface fluid was inferred to exist at Filey through the deposition of clays. This water may explain why the subsequent strain, which brecciated the clays, was so low. Such a water layer would have decoupled the ice and sediment. Clays deposited at the ice and sediment interface could give a semi-quantitative estimate of the separation of the ice and bed, but only where the strain is quantifiable through the whole of the sequence. In higher strain areas the mixing in of clays could occur without greater ice-sediment coupling if the deforming layer rises slowly, for example, and if the meltout rate is lower. Under such conditions there will be increased strain in any one horizon and less preserved clay bodies despite potentially weak coupling.

The hypothesis of greater coupling across the ice-sediment interface at Dimlington than elsewhere in the area matches the development of a strong, sub-horizontal, simple shear fabric in the ‘intermediate’ diamict. There is equivocal evidence, but it seems likely that at some stage deposition like that at Filey (across a decoupled ice-sediment interface) took over at Dimlington. Clays are deposited higher in the sequence than the sub-horizontal fabric, and the strain may be lower (the sediment has not developed a horizontal omnisepic fabric, probably the only potential infinite strain fabric). This change could have been due to the increasing mass of impermeable sediment between the ice and the exploited boundary with the basement sequence (where the clean sand lenses drained fluid). This aquitard build up could have lead to fluid at the ice boundary, and the submergence of roughness important in transferring stress to the bed (similar to the thickening of the sequence at Filey, above).

8.6.4 Low sediment strain: meltout of the diamicts

Low strain is seen in the upper units at Filey, and possibly the Skipsea Till at Dimlington and the Skipsea Till from Skipsea examined in Chapter Seven. The extension of diamicts far inland from these points suggests a potential for high strains, whether the glacier remained over the sediments (Evans *et al.*, 1995) or repeatedly surged inland (Eyles *et al.*, 1994). The lack of such high strain therefore suggests a rapid rise in the deformation layer and/or decoupling of the ice or higher sediment. Decoupling may have been due to ice-sediment interface fluid and/or discrete shear in the sediments (as discussed above).

A rise in the deforming layer may be attributable to a high meltout rate. This hypothesis matches the proposed meltout nature of the diamicts at Filey, as well as the water logging of the sediments at Reighton Sands. The sediments used in the triaxial tests in Chapter Six have a similar microstructure to the deposits at Filey, but include sand rich patches and have been deformed in the laboratory, and therefore no definitive origin can be ascribed to them.

A high meltout rate may have been characteristic of this glacier, the majority of which lay below present day sea level, probably in the local ablation zone. The supply of ice would have to have been maintained by having several accumulation areas, a high accumulation rate, or true store-and-purge surge behaviour (as opposed to climatically induced movements). In the case of the Skipsea Till at Dimlington, and the material around the sands at Filey, melting could have been enhanced by increased drainage stiffening the sediment and enhancing regelation, although this may be incompatible with models of greater coupling between the ice and bed.

8.6.5 The nature of glaciogenic sediments in the area and the ice mass depositing them

The glacial history and deposition in the area is reflected in the microstructures and their interrelationships. In many ways, the results of this study resolve the dialectic battle between the previous interpretations for the area, and explain the contradictions in the outcrop scale evidence. Evans *et al.*'s (1995) model of a single ice mass with subglacial channels is verified by this study for the Filey field site, at least for the smaller sand lenses. The regional low strain conditions used as evidence by Eyles *et al.* (1994) are explained in this context as being due to decoupling between the ice and bed, and possibly within the bed itself. On top of this, the high melt rates may have increased this decoupling, and raised the deformation layer by adding more material, reducing the strain in any one horizon. Doubt is cast on the idea that the diamicts of the area are advected older deposits which have not been incorporated into the ice at some point. However, the overriding of proglacial lacustrine areas and shallow water bodies proposed by Eyles *et al.* is still possible at Reighton and Dimlington and surge-type behaviour may have been necessary to maintain the ice presence under a high melt rate.

9. Conclusions

The aim of this thesis was to investigate how glacial microstructures might reflect the processes and conditions forming them, and how these microstructures might then affect the situations they develop within. It is hoped that, on a more general level, this thesis has shown the immense amount of useful information glaciogenic microstructures might contain. This information is an essential adjunct to information collected at other scales. While each chapter of this thesis explores one particular area or process, it is hoped that in combination these studies provide information on the formation of some of the 'classic' glacial microstructures, and their effect on the materials in question.

9.1 The development of microstructures

9.1.1 Omnisepic fabrics and discrete shear

Thin sections from triaxial tests (Chapters Six and Seven) showed that omnisepic fabrics develop at low strain (15 to 25%), and that the grain orientation matches the direction of discrete shears seen at a larger scale. There was no evidence of discrete shear in the thin sections so it seems likely any higher strain areas are impossible to distinguish within the omnisepic fabric. This may not be important if we are examining the mechanics of the material in question, as the discrete shears appear to be very low strain features that have locked after their formation. It is not certain how such ambiguous strain features would appear in the field. Chapter Eight provided another example of an apparent high strain 'discrete shear', which, on the microscale appears to largely be the result of fluid removal of the diamict and the concentration of sands. Thus, discrete shear seen in the field need not represent high strains, however, as was discussed in Chapter Six, it seems likely that at some stage in subglacial deformation discrete shears must develop (below).

9.1.2 Lattisepic fabrics

The thin sections from the triaxial tests (Chapters Six and Seven) showed that lattisepic fabrics formed in areas of conflicting shear strain in two directions. This suggestion was confirmed by field evidence in Chapter Eight, where discrete and widely separated shears in two directions in the clay/silt beds of the Dimlington Silts were seen to be replaced by a pervasive lattisepic fabric in the more sand rich layers. Evidence was given from the thin sections from the triaxial tests (Chapter Seven) that the formation of lattisepic fabrics is aided by the alignment of grains between clasts trapped at different levels in a medium that is shearing in one direction. The dominance of omnisepic fabrics in thin sections from higher strain tests suggests lattisepic fabrics are eventually replaced by a single direction fabric.

9.1.3 Microscopic melanges

The formation of microscopic melanges appears to reflect coupling levels at the ice-bed interface. It was suggested (Chapter Five) that mixes of pre-consolidated material, silt beds, and unimodal sand beds, in high strain flow bodies formed as material melted out of the ice pushing against a lodging clast and pre-consolidated material flowed from the sides of the ploughing gouge. This interpretation is backed up by the overall geometry of the deposit in question (the thickness of the melange unit increases towards the clast), and a model of the processes which predicted reasonable ice-till properties and the correct thickness of material.

Melanges of diamict, clay bands with reworked diamict pebbles, and sands were examined in Chapter Eight. Here there is no evidence for consolidation prior to the material being placed in its present position (except in the pebbles which show a potentially high-strain fabric), and little evidence for coherent flow bodies. The combination of low strain in the clay bands, the presence of reworked material within them, and the bands morphology, suggests that these are water lain features. The interdigitation with the surrounding diamict suggests the materials were deposited synchronously. Thus, it is suggested that the sediments represent diamict meltout from the ice into a region of small, flowing, water bodies. Where the strain in the sediments can be quantified, such fabrics could give quantitative information about the level of coupling between the ice and the bed.

9.1.4 Skelsepic fabrics and till pebbles

Indicators were found in the thin sections examined in this research of the processes forming till skelsepic fabrics and diamict pebbles, however, the evidence is not conclusive and needs further investigation.

Skelsepic fabrics appear to form at low strains (<15%) within areas of shear strain in a single direction (Chapter Seven). There is evidence for the cohesion of clays to clasts (Chapter Seven), and this may initiate skelsepic fabrics by trapping silt and sand sized material which is then orientated by rotation of the clast against free material. Further investigation is needed of these processes, and could proceed in the laboratory by the deformation of materials with varying clay contents and clasts within a shear box.

Evidence from Dimlington High Ground (Chapter Eight) suggested that diamict pebbles do not form through the exploitation of shear weakened areas within tills, however, the features may still form through the removal of material leaving shear *hardened* areas. Shear hardening of material may occur where a random alignment is replaced by the orientation of grains in a single direction with an increase in face-face contact between clay grains. In the case of the pebbles at Dimlington, they appear to have formed at the base of a water body. A greater amount of statistical and environmental evidence is needed before a formation process can be attributed to diamict pebbles, and it is unfortunate that this evidence can only be collected when such features are fortuitously discovered within sediments. Even when diamict pebbles are found, it is rare that appropriate collaborative evidence is present.

9.1.5 Multiple fabrics within sediment bodies

The presence of multiple sets of superimposed fabrics, and information on how the form of fabrics change with stress and hydraulic conditions (Chapter Three) allows the reconstruction of the stress and hydrological history of the deposits. Examples are presented in Chapter Four for a single sediment bed at Criccieth in North Wales, and in Chapter Eight for Filey Brigg, Dimlington High Ground and Reighton Sands in Yorkshire. Such a methodology gives us important information on the response of the sediments to the surrounding conditions, and how these responses affect those conditions. This information has been supplemented in this research with laboratory tests to give details of how the ice is coupled to soft beds, the conditions at the interface between the two, and the response of the sediment to stress and hydraulic conditions. This information is reviewed in the next sections.

9.2 Ice-bed coupling

In Chapter Five it was shown that the microstructure of the sediments allows the production of a model of the ploughing and lodgement of clasts initially trapped in the base of the ice. This model predicted reasonable ice velocities (~20 to 60 m a^{-1}) and till residual strengths (~20 to 50 kPa) for the ice at Criccieth in North Wales when meltout material was assumed to have little effect on the decoupling of the ice from the clast. The model gave similar order of magnitude results when the meltout material was assumed to have an effect. The model thus appears reliable, and can be used to predict the time until lodgement of clasts, the force on the clasts during the period they are decoupling from the ice and coupling to the bed, and the associated meltout material levels which will go to produce the matrix of the lodgement till. Example results for clasts with diameters of 0.01 m, 0.11 m, and 1 m were given in Chapter Five.

Future model developments will look at reducing the number of potential ice velocities and till residual strengths at Criccieth by constraining the model to produce the same proportions of meltout material and pre-consolidated material that can be seen in the thin sections. It is also hoped to develop the model into a full, multisize, multiclast, bed model in which the ice responds to the process of clast lodgement. This may be achievable by relating the clast decoupling length of the model given in Chapter Five to the decoupling length used in the basal shear stress model of Kamb and Echelmeyer (1986).

At Filey Brigg (Chapter Eight), the micromorphology was seen to imply decoupling between the ice and its sedimentary bed. The presence of a fluid layer, or set of micro-streams between the ice and the bed may explain the low strain in the material. To this explanation may be added the fact that the meltout nature of the material at Filey, and possibly Reighton Sands, may have led to low strains being recorded in any one horizon, if the meltout accumulation rate was high enough. The presence of thin sand bodies, and possibly rhythmites, within the sequences of the Yorkshire coast may suggest both water flow and ponding occurred at the ice-sediment interface. The juxtapositioning of larger sand bodies and this ‘decoupled ice’ micromorphology at Filey Brigg *may* reflect a positive flux / fluid pressure relationship in the water bodies responsible for the large sands beds, though given the imperfect nature of the ice-sediment interface this is far from definite.

9.3 Till response to stress and fluid build-up

Laboratory tests on the Skipsea Till presented in Chapter Six indicated that when the material was deformed under a pure shear geometry it responded by undergoing work-hardening with stick-slip behaviour. While shear events *did* occur, the strain along them appeared to be low. Thin sections taken from the samples indicated that the discrete shears usually seen in unimodal sediments did not form in this material, which has a broad grain size range. Thus, it appears that the larger grains in the material disrupted the propagation of the discrete shears which are suspected as being responsible for work-softening in unimodal sediments. Such disruption may be related to the work-hardening response of the Skipsea Till. It has been suggested that stick-slip behaviour seen in other environments may be due to the interaction of harder areas of the materials with shears (Chapter Three). The work-hardening seen in the Skipsea Till may be contrasted with the more unimodal till that the clast ploughed through at Criccieth (above). Here the ploughing model suggests a low residual strength for the till, and this matches the more discrete shear seen in thin sections from below the ploughing trace.

However, the profile of the ice along the Yorkshire coast suggests that the shear stress at the base of the ice was less that 10 kPa over the area the triaxial and thin section samples were taken from (Chapter Six). As this is an order of magnitude lower than the stresses supported in the triaxial tests, other processes than work-hardening deformation must have been responsible for the shallow profile of the ice. Evidence for two such processes was outlined in Chapter Eight; the decoupling of the ice from its bed by fluid bodies (above), and the presence of discrete shears in areas where they can form with less disruption. The latter matches with the presence of horizontal weaknesses in the material used in the triaxial tests (Chapter Six). Thus, it is suggested that tills respond to stress with a mix of work-hardening in areas under a pure shear geometry, for example, between two clasts, but that discrete shear may occur in some areas to work-soften the material. Further research is needed to build this information into a semi-quantitative estimate of how such materials respond to varying their size distribution.

The laboratory tests suggest that tills may buffer fluid pressure increases, strain in the material leading to increasing fluid pressures until a threshold is reached and hydraulic fracture occurs or the fluid is released down immobile shear features, such as areas of omnisepic fabric (Chapters Six and Seven). In the tests this led to a stabilisation of the pore fluid pressure at ~470 kPa, approximately 100 kPa lower than the upper threshold. The instantaneous hydraulic conductivity of the material changed from ~$4x10^{-12}$ to $1x10^{-11}$ m s^{-1} during these drainage events.

The results in Chapters Six and Seven represent the first combined stress and hydraulic testing of real, undisturbed, glacial sediments in a triaxial rig. It is seen that the mixed size of the material in these tests leads to a response which follows a distinct model of development, but in a manner which makes it impossible to quantify when, or if, certain elements of the model will occur. This makes examining these events difficult. Future triaxial tests will aim to recreate real sediments, but in a more controlled way. It is hoped to carry out experiments looking at the response of mixed clay-silt-clast materials, using neutrally buoyant clast replacements. This will allow a quantitative estimate of the effect of varying clast density on the rheology of the material and the development of microstructures.

Field evidence is also presented for other buffering mechanisms which would prevent fluid pressure building up in the Skipsea Till. At both Reighton Sands and Dimlington High Ground there is evidence for the removal of fine material by throughflowing water. At Dimlington, the whole of the sequence that has been eroded can be measured within one thin section, allowing the calculation of the amount of material eroded. This was shown to be 0.0046 m^3 for fines for each m^2 of ice base, or, for the extremely unlikely event of this occurring under the whole glacier, a sediment volume on the order of $1x10^8$ m^3.

The build up of fluid and the stress response of the till under the Yorkshire ice may have been determined by variations in the geometry of the ice-bed interface and at Dimlington, the response of the diamict was shown to have changed over time, possibly reflecting the variation of this boundary. It is worth noting that in the situation where the fluid flow occurred through the sediment at Dimlington, the diamict was seen to show discrete shear and a horizontal omnisepic fabric suggesting the sediment deformed to lower the supported stress. This may be compared with the results from Filey, where fluid flow could occur at the ice-bed interface and decouple the ice, and there was seen to be non-horizontal and low strain fabrics, perhaps suggesting that work-hardening in the diamict was allowed to continue because the supported stresses were lowered by the decoupling.

Thus, this thesis hopes to account for the origin of omnisepic and lattisepic fabrics, microscopic melanges and some clay banding features (*Figure 9.1*). It also investigates the formation of till pebbles and skelsepic fabrics (*Figure 9.1*), though can make no definitive statements on their origin. The development of micromorphology in sediments in the field and laboratory allows the rheology of subglacial diamicts to be outlined. In addition this thesis has examined how micromorphology reflects the coupling/decoupling processes between the ice and the sediment under it (*Figure 9.2*). It is hoped that this thesis contributes to the continuing process of understanding the ice-bed interface and how microstructures reflect and affect the conditions at this interface.

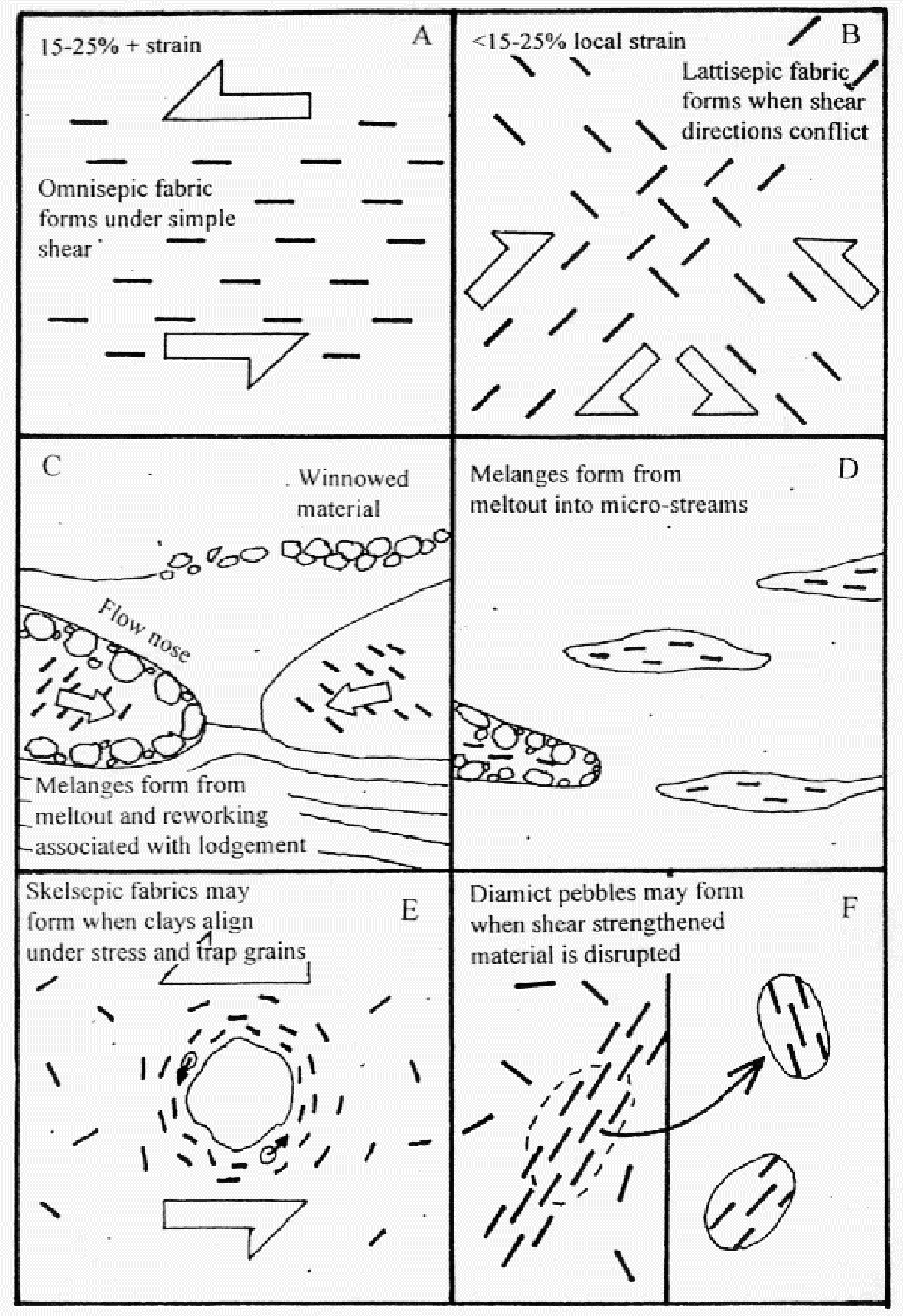

Figure 9.1 Summary of the main conclusions on the origin of microstructures in this thesis. For further information, see the following chapters; A) Chapter seven, B) Chapters seven and eight, C) Chapter four, D) Chapter eight, E) Chapters seven and eight, F) Chapter eight.

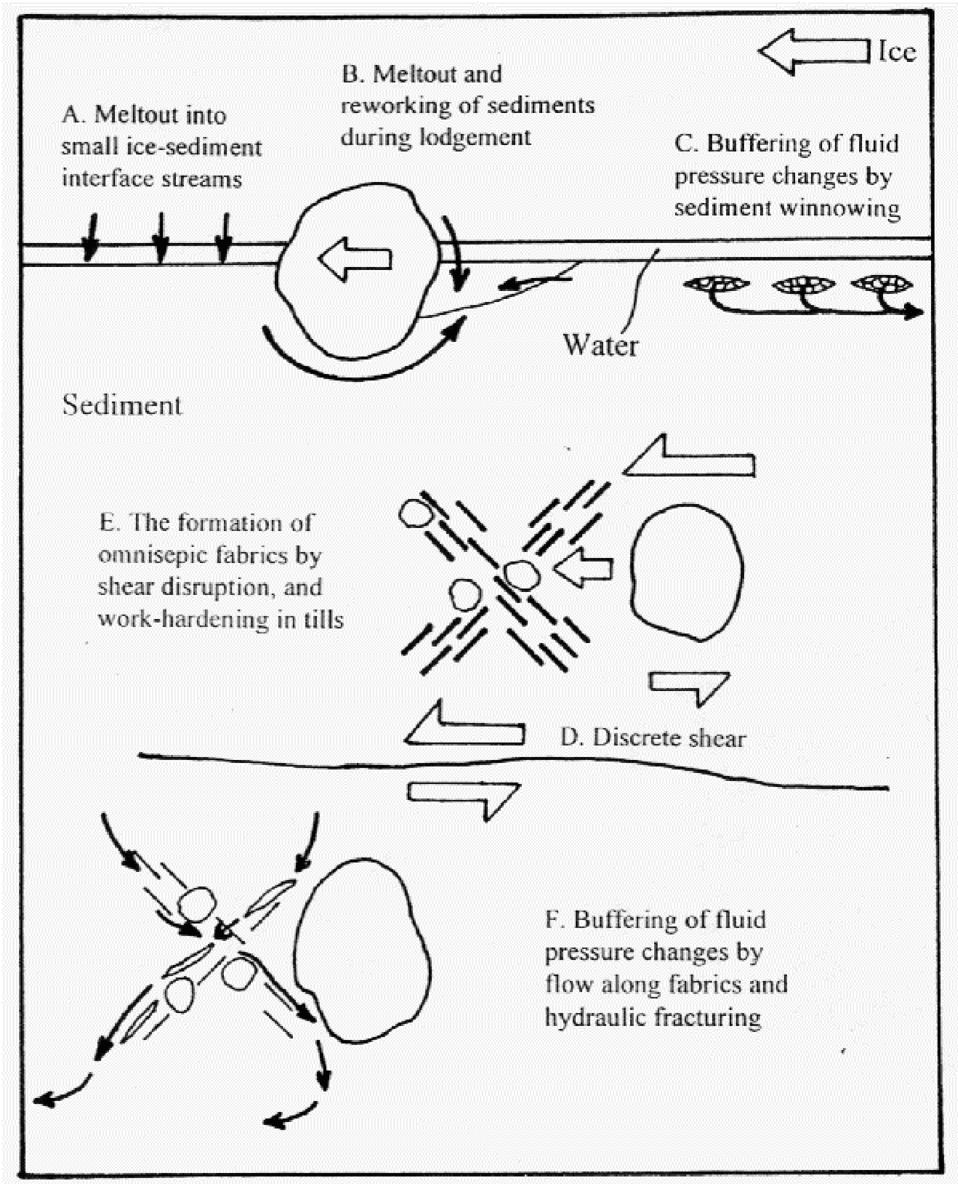

Figure 9.2 Summary of the main conclusions on the processes acting at the ice-sediment interface and below. For further information, see the following chapters; A) Chapter eight, B) Chapter five, C) Chapter eight, D) Chapters six, seven and eight, E) Chapters six, seven and eight, F) Chapters six and seven.

Appendix A : Glossary of fabrics

Bands: In this thesis, used to describe bodies that have a different sediment constitution from the surrounding material, with a length to width ratio of four or greater. They may have a diffuse of distinct boundary with the surrounding material, however, the former is rare as these features are usually found in low strain situations.

Bimasepic fabric: The microscopic orientation of silt and clay grains such that their long axes are arranged in two directions, the angle between which may be anything. The term is used interchangeably for a pervasive mix of grains in two directions and the presence of two discrete sets of bands in two directions with other fabrics between them. See lattisepic and masepic.

Crenullated fabric: Microscopic orientation of grains of any size such that the fabric sharply undulates over a wide area. Not associated with shears. Contrast with kink fabric.

Kink bands: Microscopic orientation of grains of any size such that the fabric sharply undulates. Usually associated with shear fabrics. Kinking usually undulates parallel to the direction of a nearby shear zone. Contrast with kink fabric.

Lattisepic fabric: The microscopic orientation of silt and clay grains such that their long axes are arranged in two directions, the angle between which is 90°. The term is used interchangeably for a pervasive mix of grains in two directions and the presence of two discrete sets of bands in orthogonal directions with other fabrics between them. See bimasepic.

Masepic fabric: Microscopic orientation of grains of silt and clay such that bands of grains have their long axes in one direction. Between the bands are other fabrics or, more usually, random grain orientations.

Omnisepic fabric: Microscopic orientation of grains of silt and clay such that most of the visible grains have their long axes in one direction.

Patches: In this thesis, used to describe bodies that have a different sediment constitution from the surrounding material, but a diffuse boundary with the surrounding material, and a length to width ratio of less than four. Contrast with pebbles and bands.

Pebbles: Areas of material that appear to form rounded bodies distinct from the surrounding material. These are usually seen because of a difference in material constitution, cracking around their edges, or fabric changes across the boundary. They have a length to width ratio of less than four. Contrast with patches and bands.

Shears (Riedel, Thrust, Principle Displacement): Areas of grains of any size that have been lined up by the application of stress on a large depth of a sedimentary body (as opposed to depositional features where the stress only acts on the depositing grains). These areas are in the form of bands. Principle Displacement shears form in the direction of maximum strain. Riedel shears form obliquely to these, against the slip direction, whereas Thrust shears form oblique to the direction of maximum strain, but in the slip direction. The order of formation is usually Riedels, Thrust shears then Principle displacement shears. Shears are also referred to as shear 'bands', and multiple shears make up a shear 'zone'

Skelsepic fabric: Microscopic orientation of any size of body such that their long axes are arranged parallel to the outside of a larger body.

Unistrial fabric: Not used in this thesis. Used interchangeably with masepic fabric.

Appendix B Programs used in Chapter Five

The following programs are written in Borland Turbo Pascal for PC Windows.
Lodge1 calculates the ploughing length, supported force and meltout associated with variable sized clasts and variable residual strengths for the till. Lodge2 takes the geometry of the features at Criccieth and calculates the potential residual strengths for the tills and potential ice velocities.

```
program lodge1;
uses WinCrt;                              {Allows the program to draw windows}

const
 densityice = 900; {kg per m cubed}
 gravity = 9.81; {m s-1 s-1}

var
 filename : string;
 outfile : text;
 time : integer;
 temp : char;                             {Number of model iterations of one hour}
 continuing : boolean;                    {Continuing to plough}


 {physical parameters of boulder}
 clastwidth : real;
 clastheight : real;
 conductivity : real;                     {Thermal conductivity of the rock}
 clasttillcontactheight : extended;
 clasticecontactheight : extended;

 {physical parameters of till}
 residualstrength : extended;
 internalfriction : real;
 bedslope : real; {in radians}            {Local bedslope in radians}

 {lodgement parameters}
 movementtotal : extended;                {Total ploughing path}
 movedistance : extended;                 {Distance moved so far}
 strain : extended; {for this unit time}
 stresstransfered : extended;
 forcefromresidualstrength : extended;
 shearstress : extended;
 dragwhenlodged : extended;
```

```
 fill : extended;                       {Inflow of till from infront}
 coeffofheight : extended;
 volume : extended;
 oldfillheight : extended;
 volumetotal : extended;

 {ice parameters}
 icevelocity : real;
 debrisfraction : real; {vol of debris / vol of ice}

{-----------------------procedures and functions------------------------------}

{-----------------------read in variables-------------------------------------}

procedure entervars;

begin
{physical parameters of boulder}
writeln ('Enter clast width (= depth downice also) ');
readln (clastwidth);
writeln ('Enter clast height ');
readln (clastheight);

{physical parameters of till and ice }
writeln ('Enter till residual strength ');
readln (residualstrength);

{set parameters}

conductivity := 429.92244;{per hour}   {0.1194229 joules per degree C per sec
                                        per cm, then divided by 100 for path
                                        length increase from cm to m,
                                        and x 10000 for area increase }

{physical parameters of till and ice}
internalfriction := 22; {in degrees - converted to radians later}
bedslope := 5; {in degrees - converted to radians later}
{ice parameters}
icevelocity := 0.002276867;{per hour} {0.00000063246m/s} {20m a-1}
debrisfraction := 0.20; {vol of debris / vol of basal ice}


{convert degrees to radians}
bedslope := bedslope * (Pi/180);
iceslope := iceslope * (Pi/180);
internalfriction := internalfriction * (Pi/180);

end;
```

```
{----------------------calculate drag when lodged---------------------------}

procedure calcdrag;                    {Calculated from the Weertman, 1957, equations}

begin
 if (clastwidth=0.01) then dragwhenlodged := 214.7;
 if (clastwidth=0.1) then dragwhenlodged := 2147.98;
 if (clastwidth=1.75) then dragwhenlodged := 37583.037;
end;

{----------------------check for lodgement----------------------------------}

function lodged : boolean;

begin
 if (forcefromresidualstrength >= dragwhenlodged) or (clasticecontactheight <= 0) then
  begin
   lodged := true;
   writeln ('lodged')
  end
 else
  begin
   lodged := false;
  end;
end;



{--------------------calc shear stress melt and creep-------------------------}

function stresseffect (stress : extended) : extended;

const
 C = 0.0742; {degrees Celsius per Pa}
 heatoffusion = 333333.333; {joules per kg}
 heatloss = 1; {proportion}
 B = 1.98e-20; {per hour, 5.5e-15 s-1 kpa-1 from Glen's law.
                  Value from Paterson, 1981, table 3.1 zero Celsius}
 n = 3; {from Glen's law}

var
 actiondistance : extended;           {Weertman's distance of creep action}
 meltdistance : extended;
 creepdistance : extended;
```

```
begin

 meltdistance := ((heatloss*C*stress*conductivity)/(heatoffusion*densityice*clastwidth));
 actiondistance := clastwidth; {as used by Weertman}
 creepdistance := ((2/9)*B*actiondistance*(exp((n)*ln(stress))));
 stresseffect := (meltdistance + creepdistance);

end;

{---------------------------clast movement-----------------------------------}

procedure calcclastmovement;

begin

 movedistance := (icevelocity -
                    (stresseffect (stresstransfered)));
 if (movedistance < 0) then movedistance := 0;
 movementtotal := movementtotal + movedistance;

end;


{------------------calc meltout sediment volume------------------------------}

function fillheight : extended;

const
 C = 0.0742; {degrees Celsius per Pa}
 heatoffusion = 333333.333; {joules per kg}
 heatloss = 1; {proportion}

var
 meltvolume : extended; {per unit time}
 force : extended;
 volume : real;
 sedimentlength : real;

begin

 force := forcefromresidualstrength;
 meltvolume := ((heatloss*C*force*conductivity)
                                /(heatoffusion*densityice*clastwidth));
 volume := (meltvolume * debrisfraction);
 volumetotal := volumetotal + volume;
 sedimentlength :=
```

```
  (exp((1/2)*ln((2*volume)/((sin(internalfriction))/(cos(internalfriction))))));
  oldfillheight := fill;
 if (sedimentlength > movedistance)then fill := ((volume/sedimentlength)+
  ((oldfillheight*(sedimentlength-movedistance))/sedimentlength))
  else fill := (volume/sedimentlength);
 fillheight := fill;

end;

{------------------calc new clast and till variables-------------------------}

procedure calcnewvars;

var
 coverdistance : extended; {distance until clast covered}
 tillinflow : extended;
 extra : extended;

begin
 coverdistance := (clastheight/((sin(bedslope))/(cos(bedslope))));
 clasttillcontactheight := clastheight - (((coverdistance)-
 (movementtotal))*((sin(bedslope))/(cos(bedslope))));


 extra := (0.5*(movedistance))*((movedistance)*((sin(bedslope))/(cos(bedslope))));
 tillinflow := (movedistance * clasttillcontactheight) + extra;
 if (movedistance <= 0) then clasticecontactheight := (clasticecontactheight - (fillheight))
                                                {accounts for lack of till inflow and dividing by zero}
 else clasticecontactheight := (clastheight - ((fillheight) + ((tillinflow)/(movedistance))));

end;

{--------------------calc force of till on clast------------------------------}

procedure calcresidualforce;

begin

 forcefromresidualstrength := (clasttillcontactheight*clastwidth*residualstrength);
 stresstransfered := forcefromresidualstrength/(clastwidth*clasticecontactheight);

end;


{---------------------------main program-------------------------------------}

begin
```

```
repeat

entervars;                                                      {Calls function}
volumetotal := 0;
movementtotal := 0;
clasttillcontactheight := 1e-12;
clasticecontactheight := clastheight - 1e-12;
forcefromresidualstrength := 1e-12;
stresstransfered := 1e-12;
time := 0;
writeln ('Enter name of output file ');
readln (filename);
assign (outfile,filename);
rewrite (outfile);

calcdrag;
continuing := true;
fill := 0;

while not lodged and continuing do                    {Calls function ‘lodged’}

begin
 time := time + 1;
 write (outfile,time);
 calcdrag;{drag changes with ploughdepth}                       {Calls function}
 write (outfile,dragwhenlodged);
 calcclastmovement;                                             {Calls function}
 write (outfile,movementtotal);
 calcnewvars;                                                   {Calls function}
 calcresidualforce;                                             {Calls function}
 write (outfile,forcefromresidualstrength);
 write (outfile,stresstransfered);
 write (outfile,clasttillcontactheight);
 write (outfile,clasticecontactheight);
 writeln (outfile,fill);
 if (movedistance <= 0) then continuing := false;
end;


 close (outfile);
 writeln ('Done');
 write ('volume of sediment = ');
 writeln (volumetotal);
 writeln ('do you wish to run another test?');
 readln (temp);

until temp = 'n';
```

```
end.
```

```
program lodge2;
uses WinCrt;                              {Allows the program to draw windows}

const
 densityice = 900; {kg per m squared}
 gravity = 9.81; {m s-1 s-1}

var
 filename : string;                       {For the name of the output file}
 outfile : text;
 time : extended;                         {Number of model iterations of one day}
 continuing : boolean;                {Continuing to plough}

 {physical parameters of boulder}
 clastwidth : real;
 clastheight : real;
 conductivity : real;                     {Thermal conductivity of the rock}
 clasttillcontactheight : extended;
 clasticecontactheight : extended;

 {physical parameters of till}
 residualstrength : extended;
 internalfriction : real;
 bedslope : real;                              {Local bedslope in radians}

 {lodgement parameters}
 movementtotal : extended;                     {Total ploughing path}
 movedistance : extended;                      {Distance moved so far}
 stresstransfered : extended;
 forcefromresidualstrength : extended;
 dragwhenlodged : extended;
 fill : extended;                         {Inflow of till from infront}
 coeffofheight : extended;
 volume : extended;
 oldfillheight : extended;
 volumetotal : extended;
 loopresidual : integer;
 loopicevelocity : integer;
 maxforce : extended;                     {Maximum force supported on clast}

 {ice parameters}
 icevelocity : real;
 debrisfraction : real; {vol of debris / vol of ice}
```

```
{-----------------------procedures and functions------------------------------}

{-----------------------read in variables-------------------------------------}

procedure entervars;

begin

 {physical parameters of boulder, till and ice}
 conductivity := 10318.13856;{per day}          {0.1194229 joules per degree C per sec per
                                                 cm, then divided by 100 for path length
                                                 increase and x 10000 for area increase }
 internalfriction := 22;
 bedslope := 5;
 debrisfraction := 0.20; {vol of debris / vol of basal ice}
 clastwidth := 1.75;
 clastheight := 1.0;

 {convert degrees to radians}
 bedslope := bedslope * (Pi/180);
 internalfriction := internalfriction * (Pi/180);

end;

{-----------------------calculate drag when lodged----------------------------}

procedure calcdrag;                 {Drag calculated using the Weertman, 1957, equations
                                        rearranged for force}
var
 A : extended;
 B : extended;

begin
 A := (2.66805e17*icevelocity)+(6930*(exp((1/2)*ln(3.68505e27+(1.48225e27*
 (exp((2)*ln(icevelocity))))))));
 B := (exp((1/3)*ln(A)));
 dragwhenlodged := ((500/231)*B)-(1.21523e12/B);
end;

{-----------------------check for lodgement-----------------------------------}

function lodged : boolean;

begin
 if (forcefromresidualstrength >= dragwhenlodged) or (clasticecontactheight <= 0) then
  begin
   lodged := true;
  end
```

```
 else
  begin
   lodged := false;
  end;
end;


{--------------------calc shear stress melt and creep-------------------------}

function stresseffect (stress : extended) : extended;
                                                      {Calculated using the Weertman, 1957,
                                                         equations}
const
 C = 0.0742; {degrees Celsius per Pa}
 heatoffusion = 333333.333; {joules per kg}
 heatloss = 1; {proportion}
 B = 4.752e-19; {per day, 5.5e-15 s-1 kpa-1 from Glen's law. Value from Paterson, 1981,
  table 3.1 zero Celsius}
 n = 3; {from Glen's law}

var
 actiondistance : extended; {Weertman's, 1957, distance of creep action}
 meltdistance : extended;
 creepdistance : extended;


begin
 meltdistance := ((heatloss*C*stress*conductivity)/(heatoffusion*densityice*clastwidth));
 actiondistance := clastwidth;                              {as used by Weertman, 1957}
 creepdistance := ((2/9)*B*actiondistance*(exp((n)*ln(stress))));
 stresseffect := (meltdistance + creepdistance);

end;

{---------------------------clast movement------------------------------------}

procedure calcclastmovement;

var sheareffect : extended;

 begin

 movedistance := (icevelocity -
                       (stresseffect (stresstransfered)));
 if (movedistance < 0) then movedistance := 0;
 movementtotal := movementtotal + movedistance;

end;
```

```
{------------------calc meltout sediment volume------------------------------}

function fillheight : extended;

const
 C = 0.0742; {degrees Celsius per Pa}
 heatoffusion = 333333.333; {joules per kg}
 heatloss = 1; {proportion}

var
 meltvolume : extended; {per unit time}
 force : extended;
 volume : real;
 sedimentlength : real;

begin
 force := forcefromresidualstrength;
 meltvolume := ((heatloss*C*force*conductivity)
                                    /(heatoffusion*densityice*clastwidth));
 volume := (meltvolume * debrisfraction);
 volumetotal := volumetotal + volume;
 sedimentlength :=                                                {Calc. inflow distribution}
(exp((1/2)*ln((2*volume)/((sin(internalfriction))/(cos(internalfriction))))));
 oldfillheight := fill;
 if (sedimentlength > movedistance)then fill := ((volume/sedimentlength)+
  ((oldfillheight*(sedimentlength-movedistance))/sedimentlength))
 else fill := (volume/sedimentlength);
 fillheight := fill;

end;

{------------------calc new clast and till variables--------------------------}

procedure calcnewvars;

var
 coverdistance : extended; {distance until clast covered}
 tillinflow : extended;
 extra : extended;

begin
 coverdistance := (clastheight/((sin(bedslope))/(cos(bedslope))));
 clasttillcontactheight := clastheight - (((coverdistance)-
(movementtotal))*((sin(bedslope))/(cos(bedslope))));

 extra := (0.5*(movedistance))*((movedistance)*((sin(bedslope))/(cos(bedslope))));
```

```
 tillinflow := (movedistance * clasttillcontactheight) + extra;
 if (movedistance <= 0) then clasticecontactheight := (clasticecontactheight - (fillheight))
  {accounts for lack of till inflow and dividing by zero}
 else clasticecontactheight := (clastheight - ((fillheight) + ((tillinflow)/(movedistance))));

end;

{--------------------calc force of till on clast------------------------------}

procedure calcresidualforce;

begin

 forcefromresidualstrength := (clasttillcontactheight*clastwidth*residualstrength);
 if (forcefromresidualstrength > maxforce) then maxforce := forcefromresidualstrength;
 stresstransfered := forcefromresidualstrength/(clastwidth*clasticecontactheight);

end;


{----------------------------main program-------------------------------------}

begin

 filename := 'testres.dat';
 assign (outfile,filename);
 rewrite (outfile);
 writeln ('started');

 icevelocity := 0;

 for loopicevelocity := 1 to 200 do
  begin
   residualstrength := 0;
   icevelocity := (((icevelocity*366) + 10)/366);{per day in 10 m pa steps}
    for loopresidual := 1 to 50 do
      begin
        residualstrength := (residualstrength + 1000);
        entervars;                                               {Calls function}
        volumetotal := 0;
        maxforce := 0;
        clasttillcontactheight := 1e-12;
        clasticecontactheight := clastheight - 1e-12;
        forcefromresidualstrength := 1e-12;
        stresstransfered := 1e-12;
        time := 0;
        movementtotal := 0;
        oldfillheight := 0;
```

```
        calcdrag;                                                              {Calls function}
        continuing := true;
        fill := 0;

         while not lodged and continuing do

          begin
            time := time + 1;
            calcdrag;{drag changes with ploughdepth}                           {Calls function}
            calcclastmovement;                                                 {Calls function}
            calcnewvars;                                                       {Calls function}
            calcresidualforce;                                                 {Calls function}
            if (movedistance <= 0) then continuing := false;
          end;


         if (movementtotal > 10) and (movementtotal < 11) then
          begin
            icevelocity := (icevelocity*366);
            write (outfile,icevelocity);
            icevelocity := (icevelocity/366);
            write (outfile,residualstrength);
            write (outfile,movementtotal);
            write (outfile,volumetotal);
            writeln (outfile,maxforce);
          end;


        end;
      end;
    close (outfile);
   writeln ('finished');
end.
```

References

Ahuja, L.R., D.K.Cassels, R.R.Bruce and B.B.Barnes, 1989. Evaluation of spatial distribution of hydraulic conductivity using effective porosity data. Soil Science, v.148 (6), p.404 - 411.

Allen, J.R.L., 1977. The possible mechanics of convolute lamination in graded sand beds. Journal of the Geological Society of London, v.134 (1), p.19 - 31.

Alley, R.B., 1989. Water-pressure coupling of sliding and bed deformation: II velocity-depth profiles. Journal of Glaciology, v.35 (119), p.119 - 129.

Alley, R.B., 1991. Deforming-bed origin for southern Laurentide till sheets? Journal of Glaciology, v.37 (125), p.67 - 76.

Al-Tabbaa, A. and D.Muir Wood, 1987. Some measurements of the permeability of kaolin. Géotechnique, v.37 (4), p.499 - 503.

Al-Tabbaa, A. and D.Muir Wood, 1991. Horizontal drainage during consolidation: insights gained from analyses of a simple problem. Géotechnique, v.41 (4), p.571 - 585.

Åmark, M., 1986. Clastic dikes formed beneath an active glacier. Geologiska Föreningens i Stockholm Förhandlingar, v.108 (1), p.13 - 20.

Arch, J., 1988. An experimental study of deformation microstructures in soft sediments. unpublished Ph.D. thesis, University of Wales, Aberystwyth. 387pp.

Arch, J. and A.Maltman, 1990. Anisotropic permeability and tortuosity in deformed wet sediments. Journal of Geophysical Research, v.95 (B10), p.9035 - 9045.

Arch, J. and A.Maltman, 1993. Reply to “Comment on “Anisotropic Permeability and Tortuosity in Deformed Wet Sediments” by Arch, J. and A.Maltman” by Brown, K.M. and J.C.Moore. Journal of Geophysical Research, v.98 (B10), p.17865 - 17866.

Arch, J., A.J.Maltman and R.J.Knipe, 1988. Shear - zone geometries in experimentally deformed clays: the influence of water content, strain rate and primary fabric. Journal of Structural Geology, v.10 (1), p.91 - 99.

Athy, L.F., 1930. Density, porosity, and compaction of sedimentary rock. Bulletin of the American Association of Petroleum Geologists, v.14 (1), p.194 - 200.

Atkinson, J.H. and D.Richardson, 1987. The effect of local drainage in shear zones on the undrained strength of overconsolidated clay. Géotechnique, v.37 (3), p.393 - 403.

Awadallah, S.A., 1991. A simple technique for vacuum impregnation of unconsolidated, fine grained sediments. Journal of Sedimentary Petrology, v.61 (4), p.632 - 633.

Aydin, A., 1978. Small faults formed as deformation bands in sandstone. Pure and Applied Geophysics. v.116, p.913 - 930.

Baas-Becking, L.G.M., M.I.R.Kaplan and D.Moore, 1960. Limits of the natural environment in terms of pH and oxidation-reduction potentials. Journal of Geology, v.68 (3), p.243-284.

Baker, D.W., K.S.Chawla, and R.J.Krizek, 1993. Compaction fabrics of pelites: experimental consolidation of kaolinite and implications for analysis of strain in slate. Journal of Structural Geology, v.15 (9/10), p.1123 - 1137.

Bardet, J.P. and J.Proubet, 1992. Shear - band analysis in idealized granular material. Journal of Engineering Mechanics, v.118 (2), p.397 - 415.

Barron, R.A., 1948. Consolidation of fine-grained soils by drain wells. Proceedings of the American Society of Civil Engineers, v.113, p.718 - 754.

Bell, C.M., 1981. Soft-sediment deformation of sandstone related to the Dwyka glaciation in South Africa. Sedimentology, v.28 (3), p.321 - 329.

Benn, D.I.,1995. Fabric signature of subglacial till deformation, Breidamerkurjökull, Iceland. Sedimentology, v.42, p.735 - 747.

Benn D.I. and D.J.A.Evans, 1998. Glaciers and Glaciation. Arnold. 734pp.

Blake, E.W., 1992. The deforming bed beneath a surge-type glacier: measurement of mechanical and electrical properties. unpublished PhD thesis, University of British Columbia. 179pp.

Bolton, M., 1979. A guide to soil mechanics. MacMillan Press, London and Basingstoke. 439 pp.

Boulton, G.S, 1976. The origin of glacially fluted surfaces - observation and theory. Journal of Glaciology, v.17 (76), p.287 - 309.

Boulton, G.S, 1977. A multiple till sequence formed by a late Devensian Welsh ice-cap: Glanllynnau, Gwynedd. Cambria, v.4, p.10 - 31.

Boulton, G.S, 1979. Processes of glacier erosion on different substrata. Journal of Glaciology, v.23 (89), p.15 - 38.

Boulton, G.S., 1987. A theory of drumlin formation by subglacial sediment deformation. In, Menzies, J. and J.Rose (eds.), 1987. Drumlin Symposium. Balkema. p.25 - 80.

Boulton, G.S. and K.E.Dobbie, 1993. Consolidation of sediments by glaciers: relations between sediment geotechnics, soft-bed glacier dynamics and subglacial ground-water flow. Journal of Glaciology, v.39 (131), p.26 - 44.

Boulton, G.B. and R.C.A.Hindmarsh. 1987. Sediment deformation beneath glaciers: rheology and geological consequences. Journal of Geophysical Research, v.92 (B9), p.9059 - 9082.

Boulton G.S., and A.S.Jones, 1979. Stability of temperate ice caps and ice sheets resting on beds of deformable sediment. Journal of Glaciology, v.24 (90), p.29 - 43.

Boulton, G.S., D.L.Dent and E.M.Morris, 1974. Subglacial shearing and crushing, and the role of water pressures in tills from South-east Iceland. Geografiska Annaler, v.56 (A), p.135 - 145.

Boulton, G.S., G.D.Smith, A.S.Jones and J.Newsome, 1985. Glacial geology and glaciology of the last mid-latitude ice sheets. Journal of the Geological Society of London, v.142 (3), p.447 - 474

Bouma, J., A.G.Jongmans, A.Stein, and G.Peek, 1989. Characterizing Spatially Variable Hydraulic Properties of a Boulder Clay Deposit in The Netherlands. Geoderma, v.45, p.19 - 29.

Brewer, R., 1976. Fabric and mineral analysis of soils. Krieger, Huntington. 482pp.

Broecker, W.S. and G.H.Denton, 1990. The role of ocean-atmosphere reorganisations in glacial cycles. Quaternary Science Reviews, v.9 (4), p.305 - 341.

Brown, K.M. and J.C.Moore, 1993. Comment on “Anisotropic Permeability and Tortuosity in Deformed Wet Sediments” by J.Arch and A.Maltman. Journal of Geophysical Research, v.98 (B10), p.17859 - 17864.

Brown, K.M., D.N.Dewhurst, M.B.Clennell and G.K.Westbrook. Permeability anisotropy in consolidated and sheared kaolinite. In press.

Brown, N.E., B.Hallet, and D.B.Booth. 1987. Rapid soft bed sliding of the Puget glacial lobe. Journal of Geophysical Research, v.92 (B9), p.8985 - 8997.

Bruce, V. and P.R.Green, 1990. Visual perception; physiology, psychology and ecology. Laurence Erlbaum Associates, Hove and London. 431pp.

Byerlee, J., V.Mjachkin, R.Summers, and O.Voevoda, 1978. Structures developed in fault gouge during stable sliding and stick-slip. Tectonophysics, v.44, p.161 - 171.

Bryne, T., A.Maltman, E.Stephenson, W.Soh and R.Knipe, 1993. Deformation structures and fluid flow in the toe region of the Nankai accretionary prism. In, Hill, I.A., A.Taira, J.V.Firth et al., 1993. Proceedings of the ocean drilling program, scientific results, v.131, p.83 - 101.

Carruthers, R.G., 1948. The secret of the glacial drift (I/II). Proceedings of the Yorkshire Geological Society, v.27 (3), p.129 - 173.

Catt, J.A. and P.G.N.Digby, 1988. Boreholes in the Wolstonian Basement Till at Easington, Holderness, July 1985. Proceedings of the Yorkshire Geological Society, v.47 (1), p.21 - 27.

Catt, J.A., and L.F.Penny, 1966. The Pleistocene deposits of Holderness, East Yorkshire. Proceedings of the Yorkshire Geological Society, v.35 (3), p.375 - 420.

Clark, P.U., 1987. Subglacial sediment dispersal and till composition. Journal of Geology, v.95 (4), p.527 - 541.

Clark, P.U., 1991. Striated clast pavements: Products of deforming subglacial sediment? Geology, v.19 (5), p.530 - 533.

Clark, P.U., and A.K.Hansel, 1989. Clast ploughing, lodgement and glacier sliding over a soft glacier bed. Boreas, v.18 (3), p.201 - 207.

Clarke, G.K.C., 1987. Subglacial till: a physical framework for its properties and processes. Journal of Geophysical Research, v.92 (B9), p.9023 - 9036.

Clarke, C.K.C. and T.Murray, 1991. Effect of deformation on permeability of glacial till. EOS, v.72 (44), p.158.

Clarke, G.K.C., S.G.Collins and D.E.Thompson, 1984. Flow, thermal structure, and subglacial conditions of a surge-type glacier. Canadian Journal of Earth Sciences, v.21 (2), p.232 - 240.

Coutard, J.P. and H.J.Mücher, 1985. Deformation of laminated silt loam due to repeated freezing and thawing cycles. Earth Surface Processes and Landforms, v.10 (4), p.309 - 319.

Cowan, D.S., 1982. Origin of “vein structure” in slope sediments on the inner slope of the Middle America trench off Guatemala. DSDP, v.67, p.645 - 649.

Cowan, D.S., 1985. Structural styles in Mesozoic and Cenozoic mélanges in the western Cordillera of North America. Bulletin of the Geological Society of America, v.96 (4), p.451 - 462.

Daintith, J. and R.D.Nelson (eds.), 1989. The Penguin dictionary of mathematics. 350pp.

Delage, P. and G.Lefebvre, 1984. Study of the structure of a sensitive Champlain clay and of its evolution during consolidation. Canadian Geotechnical Journal, v.21, p.21 - 35.

Dewhurst, D.N., M.B.Clennell, K.M.Brown, and G.K.Westbrook. Mechanical behaviour and permeability anisotropy of consolidated clays. In press.

Dowdeswell, J.A. and M.Sharp, 1986. Characterization of pebble fabrics in modern terrestrial glacigenic sediments. Sedimentology, v.33 (5), p.699 - 710.

Dreimanis, A., 1988. Tills: their genetic terminology and classification. In, R.P. Goldthwait and C.L.Matsch (eds). Genetic classification of glaciogenic deposits. Balkema, Rotterdam. p. 17 - 84.

Echelmeyer, K. and W.Zhongxiang, 1987. Direct observation of basal sliding and deformation of basal drift at sub-freezing temperatures. Journal of Glaciology, v.33 (113), p.83 - 98.

Evans, D.J.A., L.A.Owen, and D.Roberts, 1995. Stratigraphy and sedimentology of Devensian (Dimlington-stadial) glacial deposits, East Yorkshire, England. Journal of Quaternary Science, v.10 (3), p.241 - 265.

Evenson, E.B., 1971. The relationship of Macro- and Microfabric of Till and the Genesis of Glacial Landforms in Jefferson County, Wisconsin. In, R.P.Goldthwait (ed). Till: a Symposium. Ohio State University Press, Ohio. p.345 - 364.

Eyles, N.and A.M.McCabe, 1989. The late Devensian Irish Sea Basin: the sedimentary record of a collapsed ice sheet margin. Quaternary Science Reviews, v.8 (4), p.307 - 351.

Eyles, N., C.H.Eyles and A.D.Miall, 1983. Lithofacies types and vertical profile models; an alternative approach to the description and environmental interpretation of glacial diamict and diamictite sequences. Sedimentology, v.30 (3), p.393 - 410.

Eyles, N., A.M.McCabe and D.Q.Bowen, 1994. The stratigraphic and sedimentological significance of Late Devensian ice sheet surging in Holderness, Yorkshire, U.K. Quaternary Science Reviews, v.13, p.727 - 759.

Fearnsides, W.G., 1910. The Tremadog slates and associated rocks of S.E.Carnarvonshire. Quaterly Journal of the Geological Society of London, v.LXVI, p.142 - 188.

Fischer, U.H., 1995. Mechanical conditions beneath a surge-type glacier. unpublished Ph.D., University of British Colombia, 100 pp.

Fitzpatrick, E.A., 1984. Micromorphology of soils. Chapman and Hall, London. 433pp.

Freeser, V., 1988. On the mechanics of glaciotectonic contortion of clays. In, Croot (ed.), Glaciotectonics: Form and processes, Balkema. p.63 - 76.

Garrels, R.M. and C.L.Christ, 1965. Solution, minerals, and equilibria. Harper and Row, New York, Evanston, and London. 450pp.

Goodyear, J., 1962. X-ray examination of some East Yorkshire boulder clays. Clay Minerals Bulletin, v.5 (27), p.43 - 44.

Glen, J.W., J.J.Donner and R.G.West, 1957. On the mechanism by which stones in till become orientated. American Journal of Science, v.255 (10), p.194 - 205.

Grant, A., 1990. Magnetic and sedimentological studies of glacigenic and related sediments in the Lleyn peninsula, North Wales. Unpublished M.Phil. thesis. Uninversity of Wales, Aberytwyth. 161pp.

Gravenor, C.P and W.A.Meneley. 1958. Glacial flutings in central and Northern Alberta. American Journal of Science, v.256 (10), p.715 - 728.

Hallet, B., 1979. A theoretical model of glacial abrasion. Journal of Glaciology, v.23 (89), p.39 - 50.

Hallet, B., 1981. Glacial abrasion and sliding: their dependence on the debris concentration in basal ice. Annals of Glaciology, v.2, p.23 - 28.

Harrison, P.W., 1957. A clay-till fabric: its character and origin. Journal of Geology, v.65 (3), p.275 - 308.

Hart, J.K., 1989. Proglacial glaciotectonic deformation and the origin of the Cromer Ridge push moraine complex, North Norfolk, England. Boreas, v.19 (2), p.165 - 180.

Hart, J.K., 1994. Till fabric associated with deformable beds. Earth Surface Processes and Landform, v.19 (1), p.15 - 32.

Hart, J.K. and G.S.Boulton, 1991. The interrelation of glaciotectonic and glaciodepositional processes within the glacial environment. Quaternary Science Reviews, v.10, p.335-350.

Hart, J.K., R.C.A.Hindmarsh and G.S.Boulton, 1990. Styles of subglacial glaciotectonic deformation within the context of the Anglian ice-sheet. Earth surface processes and landforms, v.15 (3), p.227 - 241.

Hart, J. K. and D. H.Roberts, 1994. Criteria to distinguish between subglacial glaciotectonic and glaciomarine sedimentation: I - Deformational styles and sedimentology. Sedimentary Geology, v.91, p.191 - 214.

Hoel, P.G., 1984. Introduction to mathematical statistics. Wiley, Chichester. 436pp.

Hooke, R.LeB., and N.R.Iverson, 1995. Grain-size distribution in deforming subglacial tills: role of grain fracture. Geology, v.23 (1), p.57 - 60.

Hubbard, B.P., M.J.Sharp, I.C.Willis, M.K.Nielsen and C.C.Smart, 1995. Borehole water-level variations and the structure of the subglacial hydrological system of Haut Glacier d'Arolla, Valais, Switzerland. Journal of Glaciology, v.41 (139), p.572 - 583.

Iverson, N., 1990. Laboratory simulations of glacial abrasion: comparison with theory. Journal of Glaciology, v.36 (124), p.304 - 314.

Iverson, N.R. and D.J.Semmens, 1995. Intrusion of ice into porous media by regelation: A mechanism of sediment entrainment by glaciers. Journal of Geophysical Research, v.100 (B7), p.10219-10230.

Iverson, N.R., T.S.Hooyer and R.LeB.Hooke, 1996. A laboratory study of sediment deformation: stress heterogeneity and grain-size evolution. Annals of Glaciology, v.22, p.167 - 175.

Jansson, P., 1995. Water pressure and basal sliding on Storglaciären, northern Sweden. Journal of Glaciology, v.41 (138), p.232 - 240.

Jones, M., 1994. Mechanical principles of sediment deformation. In. A.J.Maltman (ed.). The geological deformation of sediments. Chapman and Hall, London. p.37 - 71.

Kamb, B., 1991. Rheological non-linearity and flow instability in the deforming bed mechanism of ice stream motion. Journal of Geophysical Research, v.96 (B10), p.16585 - 16595.

Kamb, B. and K.Echelmeyer, 1986. Stress-gradient coupling in glacier flow I: longitudinal averaging of the influence of ice-thickness and surface slope. Journal of Glaciology, v.32 (111), p.267 - 284.

Kemmis, T.J., 1981. Importance of the regelation process to certain properties of basal tills deposited by the Laurentide ice sheet in Iowa and Illinois, USA. Annals of Glaciology, v.2, p.147 - 152.

Kemp, R.A., 1995. Distribution and genesis of calcitic pedofeatures within a rapidly aggrading loess-paleosol sequence in China. Geoderma, v.65, p.303-316.

Kemp, R.A., E.Derbyshire, X.M.Meng, F.H.Chen, and B.T.Pan, 1995. Pedosedimentary reconstruction of a thick loess-paleosol sequence near Lanzhou in north-central China. Quaternary Research, v.43, p.30-45.

Kendall, P.F., 1902. A system of glacier-lakes in the Cleveland Hills. Quaterly Journal of the Geological Society, v.LVIII, p.471 - 571.

Kendall, P.F. and H.E.Wroot, 1924. The geology of Yorkshire. Published by the authors. 995pp.

Kirkbride, M.P., 1995. Processes of transportation. In, Menzies, J. (ed.). Modern glacial environments; processes, dynamics and sediments. Butterworth-Heinemann, Oxford. p.261 - 292.

Kluiving, S.J.,1994. Glaciotectonics of the Itterbeck - Uelsen push moraines, Germany. Journal of Quaternary Science, v.9 (3), p.235 - 244.

Kluiving, S.J., M.Rappol and F.M.van der Wateren, 1991. Till stratigraphy and ice movements in eastern Overijssel, The Netherlands. Boreas, v.20 (2), p.193 - 205.

Korina, N.A. and M.A.Faustova, 1964. Microfabrics of modern and old moraines. In, A. Jongerius (ed.). Soil micromorphology. Elsevier, Amsterdam. p.333 - 338.

Lafeber, D., 1964. Soil fabric and soil mechanics. In, A. Jongerius (ed.). Soil micromorphology. Elsevier, Amsterdam. p.351 - 361.

Lamplugh, G.W., 1881. On a shell-bed at the base of the drift at Speeton near Filey, on the Yorkshire coast. The Geological Magazine, New Series, Decade II, v.VIII, p.174 - 180.

Lawson, D.E., 1979. A comparison of the pebble orientations in ice and deposits of the Matanuska Glacier, Alaska. Journal of Geology, v.87 (6), p.629 - 645.

Logan, J.M., C.A.Dengo, N.G.Higgs and Z.Z.Wang, 1992. Fabrics of experimental fault zones: their development and relationship to mechanical behavior. In, Evans, B. and T-f Wong (eds.). Fault mechanics and transport properties of rocks, Academic press. p.33 - 67.

Lowe, D.R., 1975. Water escape structures in coarse-grained sediments. Sedimentology, v.22 (2), p.157 - 204.

Madgett, P.A. and J.A.Catt, 1978. Petrography, stratigraphy and weathering of Late Pleistocene tills in East Yorkshire, Lincolnshire and North Norfolk. Proceedings of the Yorkshire Geological Society, v.42 (1), p.55 - 108.

Maltman, A.J., 1977. Some microstructures of experimentally deformed argillaceous sediments. Tectonophysics, v.39, p.417 - 436.

Maltman, A.J. 1987. Shear zones in argillaceous sediments - an experimental study. In, M.E. Jones and R.M.F. Preston (eds.). Deformation of sediments and sedimentary rocks, Geological Society of London Special Publication, v.29, p.77 - 87.

Maltman, A.J., 1988. The importance of shear zones in naturally deformed wet sediments. Tectonophysics, v.145., p.163 - 175.

Maltman, A.J., 1994. Introduction and overview. In, Maltman, A.J. 1994. (ed.) The geological deformation of sediments. Chapman and Hall, London. p.1 - 35.

Maltman, A., T.Byrne, D.Karig, S.Lallemant and Leg 131 Shipboard Party, 1992. Structural geological evidence from O.D.P. Leg 131 regarding fluid flow in the Nankai prism, Japan. Earth and Planetary Science Letters, v.109, p.463 - 468.

Maltman, A.J., T.Byrne, D.E.Karig, S.Lallemant, R.Knipe and D.Prior, 1993a. Deformation structures at site 808, Nankai accretionary prism, Japan. In, Hill, I.A., A.Taira, J.V.Firth et al., 1993. Proceedings of the ocean drilling program, scientific results, v.131, p.123 - 133.

Maltman, A.J., T.Byrne, D.E.Karig and S.Lallemant, 1993b. Deformation at the toe of an active accretionary prism: synopsis of results from O.D.P. Leg 131, Nankai, S.W. Japan. Journal of Structural Geology, v.15 (8), p.949 - 964.

Matley, C.A., 1936. A 50ft. coastal terrace and other late-glacial phenomena in the Lleyn peninsula. Proceedings of the Geological Association, v.47 (3), p.221-33.

May, R.W., 1980. The formation and significance of irregularly shaped quartz grains in till. Sedimentology, v.27 (3), p.325-331.

McCabe, A.M. and G.F.Dardis, 1994. Glaciotectonically induced water-throughflow structures in a Late Pleistocene drumlin, Kanrawer, County Galway, western Ireland. Sedimentary Geology, v.91, p.173 - 190.

McCarroll, D. and C.Harris, 1992. The glacigenic deposits of Western Lleyn, North Wales: terrestrial or marine? Journal of Quaternary Science, v.7 (1), p.19 - 29.

McConnachie, I., 1974. Fabric changes in consolidated kaolin. Géotechnique, v.24 (2), p.207 - 222.

Meer, J.J.M. van der, 1987a. Field trip ‘Tills and end moraines in The Netherlands and N.W.Germany’. In, Van der Meer, J.J.M. (ed), Tills and glaciotectonics. Balkema, Rotterdam. p.261 - 268.

Meer, J.J.M. van der, 1987b. Micromorphology of glacial sediments as a tool in distinguishing genetic varieties of till. Geological Survey of Finland Special Paper, v3, p.77 - 89.

Meer, J.J.M. van der, 1993. Microscopic evidence of subglacial deformation. Quaternary Science Reviews, v.12 (7), p.553 - 587.

Meer, J.J.M. van der, M.Rappol and J.N.Semeijn. 1985. Sedimentology and genesis of glacial deposits in the Goudsberg, Central Netherlands. Mededelingen van de Rijks Geologische Dienst, v.39 (2), p.1 - 29.

Melmore, S., 1935. The glacial geology of Holderness and the Vale of York. T.Buncle & Co. 96pp.

Menzies, J., 1986. Inverse-graded units within till in drumlins near Caledonia, southern Ontario. Canadian Journal of Earth Science, v.23 (3), p.774 - 786.

Menzies, J., 1990. Brecciated diamictons from Mohawk Bay, S.Ontario, Canada. Sedimentology, v.37 (3), p.481 - 493.

Menzies, J. and A.J.Maltman, 1992. Microstructures in diamictons - evidence of subglacial bed conditions. Geomorphology, v.6 (1), p.27 - 40.

Mesri, G. and R.E.Olson, 1971. Mechanisms controlling the permeability of clays. Clays and Clay Minerals, v.19, p.151 - 158.

Moore, C.J., 1989. Tectonics and hydrogeology of accretionary prism: role of the décollement zone. Journal of Structural Geology, v.11 (1/2), p.95 - 106.

Moore, D.E., R.Summers and J.D.Byerlee, 1986. The Effects of Sliding Velocity on the Frictional and Physical Properties of Heated Fault Gouge. Pure and Applied Geophysics, v.124 (1/2), p.31 - 52.

Morgenstern, N.R. and J.S.Tchalenko, 1967. Microscopic structures in kaolin subjected to direct shear. Géotechnique, v.17 (3), p.309 - 328.

Mücher, H.J., 1985. Micromorphological study of the Terrace Sands (unit 4) and "loams" (unit 5) and their paleosols in the Belvédère pit near Maastricht, Southern Limbourg, the Netherlands. Mededelingen Rijks Geologische Dienst, v.39 (1), p19 - 29.

Mühlhaus, H.-B. and I.Vardoulakis, 1987. The thickness of shear bands in granular materials. Géotechnique, v.37 (3), p.271 - 283.

Murray, T., 1990. Deformable glacier beds: measurement and modelling. Unpublished PhD thesis, University of Wales, Aberystwyth. 321pp.

Murray, T., in press. Conditions at the glacier bed: assessing the paradigm shift.

Murray, T. and J.A.Dowdeswell, 1992. Water throughflow and the effects of deformation on sedimentary glacier beds. Journal of Geophysical Research, v.97 (B6), p.8993 - 9002.

Nasuno, S., A.Kudrolli, and J.P.Gollub. 1997. Friction in granular layers: hysteresis and precursors. Physical Review Letters, v.79 (5), p.949 - 952.

North, F.J., 1943. Centenary of the glacial theory. Proceedings of the Geologists' Association, v.LIV (1), p.1 - 28.

Nyborg, M.R., 1989. A model for the Relationship between the hydraulic Conductivity and Primary Sedimentary Structures of Till. Nordic Hydrology, v.20 (3), p.137 - 152.

Ostry, R.C. and R.E.Deane, 1963. Microfabric analyses of till. Bulletin of the Geological Society of America, v.74 (2), p.165 - 168.

Owen, L.A. and E.Derbyshire, 1988. Glacially deformed diamictons in the Karakoram Mountains, northern Pakistan. In, D.G.Croot (ed.) Glaciotectonics: Forms and Processes. A.A.Balkema, Rotterdam. p.149 -176.

Paré, J.-J., N.S.Verma, A.A.Loiselle and S.Pinzariu, 1984. Seepage through till foundations of dams of the Eastmain - Opinace - La Grande diversion. Canadian Geotechnical Journal, v.21, p.75 - 91.

Paterson, W.S.B., 1981. The physics of glaciers (second edition). Pergamon Press, Oxford. 385pp.

Paterson, W.S.B., 1994. The physics of glaciers (third edition). Pergamon Press, Oxford. 480pp.

Paul, M.A. and N.Eyles, 1990. Constraints on the preservation of diamict facies (meltout tills) at the margins of stagnant glaciers. Quaternary Science Reviews, v.9 (1), p.51 - 69.

Philip, J.R.,1980. Thermal fields during regelation. Cold Regions Science and Technology, v.3, p.193 - 203.

Platt J.P., and R.L.M.Vissers, 1980. Extensional structures in anisotropic rocks. Journal of Structural Geology, v.2 (4), p.397 - 410.

Porter, R.P., 1997. Glacier surging: subglacial sediment deformation and ice-bed coupling. Unpublished Ph.D. thesis, University of Leeds. 210pp.

Porter, P.R., T.Murray and J.A.Dowdeswell, 1997. Sediment deformation and basal dynamics beneath a glacier surge-front: Bakaninbreen, Svalbard. Annals of Glaciology, v.24, p.21 - 26.

Price, N.J. and J.W.Cosgrove. 1990. Analysis of Geological Structures. Cambridge University Press, Cambridge.

Rieke, H.H., III. and G.V.Chilingarian. 1974. Compaction of argillaceous sediments. Developments in Sedimentology. 16. Elsevier, Amsterdam. 424pp.

Ronnert, L. and D.M.Mickelson, 1992. High porosity of basal till at Burroughs glacier, southeastern Alaska. Geology, v.20 (9), p.849 - 852.

Roscoe, K.H., 1970. The influence of strains in soil mechanics. Géotechnique. v.20 (2), p.129 - 170.

Rose, J., 1985. The Dimlington Stadial/Dimlington Chronozone: a proposal for naming the main glacial episode of the Late Devensian in Britain. Boreas, v.14 (3), p.225 - 230.

Rutter, E.H., R.H.Maddock, S.H.Hall and S.H.White, 1986. Comparative Microstructures of Natural and Experimentally Produced Clay-Bearing Fault Gouges. Pure and Applied Geophysics, v.124 (1/2), p.3 - 29.

Sammis, C., G.King and R.Biegel, 1987. The kinematics of Gouge Deformation. Pure and Applied Geophysics, v.125 (5), p.777 - 812.

Saunders,G.E., 1968. A reappraisal of glacial drainage phenomena in the Lleyn peninsula. Proceedings of the Geologists Association, v.79 (3), p.305 - 324.

Sheppard, J.A., 1957. The medieval meres of Holderness. Transactions of the Institute of British Geography, v.23 (1), p.75 - 86.

Shimamoto, T. and J.M.Logan, 1981. Effects of Simulated Fault Gouge on the Sliding Behavior of Tennessee Sandstone: Nonclay Gouges. Journal of Geophysical Research, v.86 (B4), p.2902 - 2914.

Shoemaker, E.M., 1988. On the formulation of basal debris drag for the case of sparse debris. Journal of Glaciology, v.34 (118), p.259 - 264.

Simpson, C. and S.M.Schmid, 1983. An evaluation of criteria to deduce the sense of movement in sheared rocks. Bulletin of the Geological Society of America, v.94 (11), p.1281 - 1288.

Sitler, R.F. and C.A.Chapman, 1955. Microfabrics of till from Ohio and Pennsylvania. Journal of Sedimentary Petrology, v.25 (4), p.262 - 269.

Sole-Benet, A., M.A.Marques and E.Mora, 1964. Injection features in mid-altitude Mediterranean soils. In, A. Jongerius (ed.). Soil micromorphology. Elsevier, Amsterdam. p.227 - 233.

Stephenson, E.L., A.J.Maltman and R.J.Knipe, in press. Fluid flow in actively deforming sediments: "Dynamic permeability" in accretionary prisms.

Straw, A., 1961. The erosion surfaces of East Lincolnshire. Proceedings of the Yorkshire Geological Society, v.33 (8), p.149 - 172.

Summers, R. and J.Byerlee, 1977. A note on the effect of fault gouge composition on the stability of frictional sliding. International Journal of Rock Mechanics, Mining Science and Geomechanics (abstracts), v.14(3), p.155 - 160.

Talbot, C.J. and V.von Brunn., 1987. Intrusive and extrusive (micro)melange couplets as distal effects of tidal pumping by a marine ice sheet. Geological Magazine, v.124 (6), p.513 - 525.

Tchalenko, J.S., 1968. The evolution of kink-bands and the development of compressional textures in sheared clays. Tectonophysics, v.6 (2), p.159 - 174.

Tchalenko, J.S., 1970. Similarities between shear zones of different magnitude. Bulletin of the Geological Society of America, v.81 (6), p.1625-1640.

Thomas, G.S.P., 1984. The origin of the glacio-dynamic structure of the Bride Moraine, Isle of Man. Boreas, v.13 (3), p.355 - 364.

Tucker, M.E., 1991. Sedimentary petrology. Backwell Scientific, London. 260pp.

Valentin, H., 1957. Glazialmorphologische Untersuchungen in Ostengland. Abhandlungen der Geographische Institut der Freien Universitat, Berlin, v.4, p.1 - 86.

Vickers, B., 1983. Laboratory work in soil mechanics. Granada Publishing, London. 170pp.

Walder, J.S. and A.Fowler, 1994. Channalized drainage over a deformable bed. Journal of Glaciology, v.40 (134), p.3 - 15.

Wateren, F.M. van der, 1986. Structural geology and sedimentology of the Dammer Berge push moraine, FRG. In, Van der Meer, J.J.M. (ed), Tills and glaciotectonics. Balkema, Rotterdam. p.157 - 182.

Weertman, J., 1957. On the sliding of glaciers. Journal of Glaciology, v.3 (21), p.33 - 38.

Weertman, J.,1964. The theory of glacial sliding. Journal of Glaciology, v.5 (39), p.287 - 303.

Weertman, J.,1972. General theory of water flow at the base of a glacier or ice sheet. Reviews of Geophysics and Space Physics, v.10 (1), p.287 - 333.

Weertman, J.,1979. The unsolved general glacier sliding problem. Journal of Glaciology, v.23 (89), p.97 - 115.

Whalley, W.B., 1996. Scanning electron microscopy. In, J.Menzies (ed). Past glacial environments, sediments, forms, and techniques. Butterworth-Heinemann, Oxford. p.357 - 375.

White, S.H., S.E.Burrows, J.Carreras, N.D.Shaw, and F.J.Humphreys, 1980. On mylonites in ductile shear zones. Journal of Structural Geology, v.2 (1/2), p.175 - 187.

Wood, S.V. and J.L.Rome, 1868. On the glacial and postglacial structure of Lincolnshire and south-east Yorkshire. Quaterly Journal of the Geological Society of London, v.24, p.146 - 184.

Znidarcic, D. and S.A.Aiban, 1988. Discussion on “Some measurements of the permeability of kaolin.” by Al-Tabbaa, A. and D.Muir Wood. Géotechnique, v.38 (3), p.453 - 454.